eman ta zabal zazu
Universidad del País Vasco
Euskal Herriko Unibertsitatea

Blocking ATP Signaling and ROS Generation Preserves Neurogenesis and Network Activity In Epileptogenesis In Hippocampal Organotypic Slice Cultures

Ane Rodríguez Bodero

DOCTORAL THESIS

2023

Doctoral thesis opting for PhD degree at the University of the Basque Country

Faculty of Medicine and Nursery, Department of Neurosciences

Supervised by:

Dr. Juan Manuel Encinas Pérez

Dr. Jan Tønnesen

This doctoral thesis has been performed thanks to the usage of a UPV/EHU fellowship for the hiring of predoctoral researchers during 2019-202

TABLE OF CONTENTS

LIST OF ABBREVIATIONS

AAV	Adenoviral Vector
AD	Alzheimer's Disease
ADP	Adenosine diphosphate
AEDs	Antiepileptic Drugs
AMPA	α-amino-3-hydroxy-5-methyl-4-isoxazolepropionic acid
ANPs	Amplifying Neural Progenitors
ATP	Adenosine-5'-triphosphate
BBB	Blood-brain barrier
BSA	Bovine Serum Albumin
Ca^{+2}	Calcium Ion
$CaCl_2$	Calcium Chloride
CaM	Calmodulin
$Ce^{+3/+4}$	Cerium Ions
CeO_2	Cerium Oxide
CeO_2NPs	Cerium Oxide Nanoparticles
CNO	Clozapine-N-oxide
CNS	Central Nervous System
CNT	Control
CM-H2DCFDA	2',7'–dichlorofluorescein Acetate
CO_2	Carbon Dioxide
DAPI	4′,6-diamidino-2- phenylindole
DCF	Dichlorofluorescein
DCX	Doublecortin
DG	Dentate Gyrus
DIV	Days *In Vitro*
DNA	Deoxyribonucleic Acid

DPI	Days Post Injection
DREADDs	Designer Receptors Exclusively Activated by Designer Drugs
DS	Dravet Syndrome
eATP	Extracellular ATP
EE	Enriched Environment
EEG	Electroencephalography
FWHM	Full Width at Half Maximum
GABA	γ–amino Butyric Acid
GCamp6f	Genetically Encoded Calcium Indicator
GCL	Granule Cell Layer
GCs	Granule Cells
GFAP	Glial Fibrilary Acidic Protein
GFP	Green Fluorescent Protein
GSI	Global Synchronization Index
HBSS	Hank's Balanced Salt Solution
HD	Huntington's Disease
HEPES	4-(2-hydroxyethyl)-1-piperazineethanesulfonic Acid
HIHS	Heat Inactivated Horse serum
hOTCs	Hippocampal Organotypic Slice Cultures
H_2O	Water
H_2O_2	Hydrogen Peroxide
HS	Hippocampal Sclerosis
Hz	Hertz
IF	Instantaneous Firing Rate
IL	Interleukin
IPCs	Progenitor Cells
IR	Infrared
KA	Kainic Acid
KCl	Potassium Chloride
KH_2PO_4	Monopotassium phosphate

kHz	Kilohertz
LED	Light Emitting Diode
LUT	Look-up Table
mACSF	Modified Artificial Cerebrospinal Fluid
MEA	Multi-Electrode Array
MEM	Minimum Essential Medium
MF	Mossy Fiber
$MgCl_2$	Magnesium Chloride
Mm	Millimeter
mM	Millimolar
Mn	Manganese
Ms	Millisecond
MTLE	Mesial Temporal Lobe Epilepsy
Na	Sodium
$NaHCO_3$	Sodium Bicarbonate
NaH_2PO_4	Sodium Dihydrogen Phosphate
NaOH	Sodium Hydroxide
NeuN	Neuronal Nuclear Protein
nM	Nanomolar
Nm	Nanometer
NMDA	N-methyl D-aspartate
NO	Nitric Oxide
NPs	Nanoparticles
NPCs	Neural Progenitor Cells
NSCs	Neural Stem Cells
NSs	Network Synchronizations
O_2	Oxygen
$O_2^{\cdot -}$	Superoxide Anion
$\cdot OH$	Hydroxyl Radical
OS	Oxidative Stress

PBS	Phosphate Buffered Saline
PD	Parkinosn's Disease
PFA	Paraformaldehyde
Prox1	Prospero Homeobox Protein 1
PSD	Power Spectral Density
PTFE	Polytetrafluoroethylene
PTX	Picrotoxin
PV	Parvalbumin
P2XR	Purinergic 2X Receptors
P2YR	Purinergic 2Y Receptors
RFP	Red Fluorescent Protein
RMS	Rostral Migratory System
ROS	Reactive Oxygen Species
ROI	Region of Interest
RT	Room Temperature
RV	Retroviral Vector
-S	Serum-free
+S	Serum-based
S100β	S100 Calcium-binding Protein β
SE	Status Epilepticus
SEM	Standard Error of the Mean
SGC	Subgranular Zone
SOD	Superoxide Dismutase
SOM	Somatostatin
SVZ	Subventricular zone
SYN	Synapsin
TBI	Traumatic Brain Injury
TLE	Temporal Lobe Epilepsy
TNF	Tumor Necrosis Factor
TNP-ATP	Triethylamonium Salt

TTX	Tetrodotoxin
TW	Time-bandwidth
UDP	Uridine diphosphate
UTP	Uridine triphosphate
UV	Ultraviolet
VGAT	Vesicular GABA Transporter
VIP	Vasointestinal Neuropeptides
WIV	Week *In Vitro*
WT	Wild Type
µl	Microliter
µM	Micromolar
µs	Microsecond

SUMMARY

Epilepsy stands as one of the most prevalent and severe neurological disorders, yet our understanding of epileptogenesis remains limited. In the context of temporal lobe epilepsy (TLE), the most common form of epilepsy, the focal epileptic center frequently resides within the hippocampus, where it is closely associated with gliosis and abnormal neurogenesis.

Our general objective is to evaluate and potentially mitigate the occurrence of abnormal neurogenesis in TLE. To assess and manipulate abnormal neurogenesis in epileptiform conditions, we have established an *ex vivo* model using hyperexcitable hippocampal organotypic culture slices (hOTCs). This model relies on the disruption of GABAergic synaptic transmission, using picrotoxin (PTX), and is complemented by the use of retroviral vector-based cell labeling for newborn neurons. We have validated that the epileptiform environment diminishes the density of newborn neurons, impairs dendritic arborization, and disrupts dendritic spine growth. Functionally, inhibiting newborn neurons preserved normal neuronal firing patterns and circuit synchronization, suggesting a connection between neurogenesis and neural network activity.

In our investigations, we targeted neuroinflammation during epileptogenesis by acting on ATP signaling pathways. First, we blocked purinergic receptors (P2XR), and later, we inhibited the excessive production of reactive oxygen species (ROS) through the introduction of cerium oxide nanoparticles (CeO_2NPs) known for their potent antioxidative properties. In both cases, we successfully recovered normal levels of cell survival, neurogenesis, and dendritic spine growth and structure. However, dendritic arborization exhibited similar recovery only in the case of P2XR inhibition, not in oxidative stress (OS) reduction. Regarding the activity of neural networks, modulating the ATP signaling pathway through P2XR inhibition preserved both single and pair-wise neural activity, along with circuit synchronization, successfully preventing the emergence of epileptiform activity. In conclusion, our research demonstrates the suitability of epileptiform hOTCs model for long-term studies and provides evidence that ATP and ROS play crucial roles in aberrant neurogenesis process.

1. INTRODUCTION

INTRODUCTION

3.1 Adult Neurogenesis in the Mammalian Brain

The process of neurogenesis, in which new neurons are generated and integrated into the central nervous system (CNS), continuously reacts in a variety of manners to changes in brain homeostasis, acting as a sensor that provides information about ongoing processes such as neuronal hyperexcitation or neuroinflammation. Between the hilus and the granule cell layer (GCL) of the dentate gyrus (DG), in a narrow and loose area called the subgranular zone (SGZ) a population of neural stem cells (NSCs) keeps generating neurons throughout adult life of most mammals[1]. Mounting evidence suggest that postnatal and adult hippocampal neurogenesis also take place in the human brain[2–4], as others forms of plasticity do[5], although further work is necessary to fully characterize its features and extent as some controversy still remains[6]. The most extensively studied neurogenic niches are the hippocampal DG and the subventricular zone (SVZ). The neurogenic process, in which we are going to focus on in this project, is the one that occurs in the hippocampal DG, where NSCs go through a complex activation and differentiation cascade to give rise to granule cells (GCs) that migrate shortly into the GCL and integrate into the hippocampal circuitry (Fig. I1B). The other well-characterized niche is the SVZ, in which the process is relatively similar, as progenitor cells differentiate into neuronal precursors that migrate rostrally, supported by astrocytes and thus forming the rostral migratory steam (RMS) towards the OB where they mature mostly into local interneurons (Fig. I1C). Finally, yet importantly, the generation of newborn neurons has also been described in the hypothalamus (Fig. I1D). Here, new neurons are derived from a subpopulation of tanycytes (hypothalamic SCs), which have been shown to display neurogenic characteristics and can generate precursors that commit to a neuronal phenotype and that move into the hypothalamic nuclei. Additionally, there is new experimental evidence showing neurogenesis in other parts of the brain. Certainly, progenitor cells have been observed to differentiate and mature into other brain regions including the prefrontal cortex[7,8], striatum[9,10], substantia nigra[11,12], and amygdala[13,14] (Fig. I1A).

Adult neurogenesis is an extra form of brain plasticity in which newborn neurons and astrocytes modify existing neural circuitry[15,16]. The properties of NSCs as well as the process of neurogenesis and gliogenesis are reshaped divergently by changes in neuronal activity and by different types of disease and damage. This richness of plastic responses identifies NSCs and newborn neurons as biosensors of the health state of the hippocampus, detecting and providing useful information about processes such as neuronal and network hyperexcitation, excitotoxicity, neurodegeneration, and neuroinflammation.

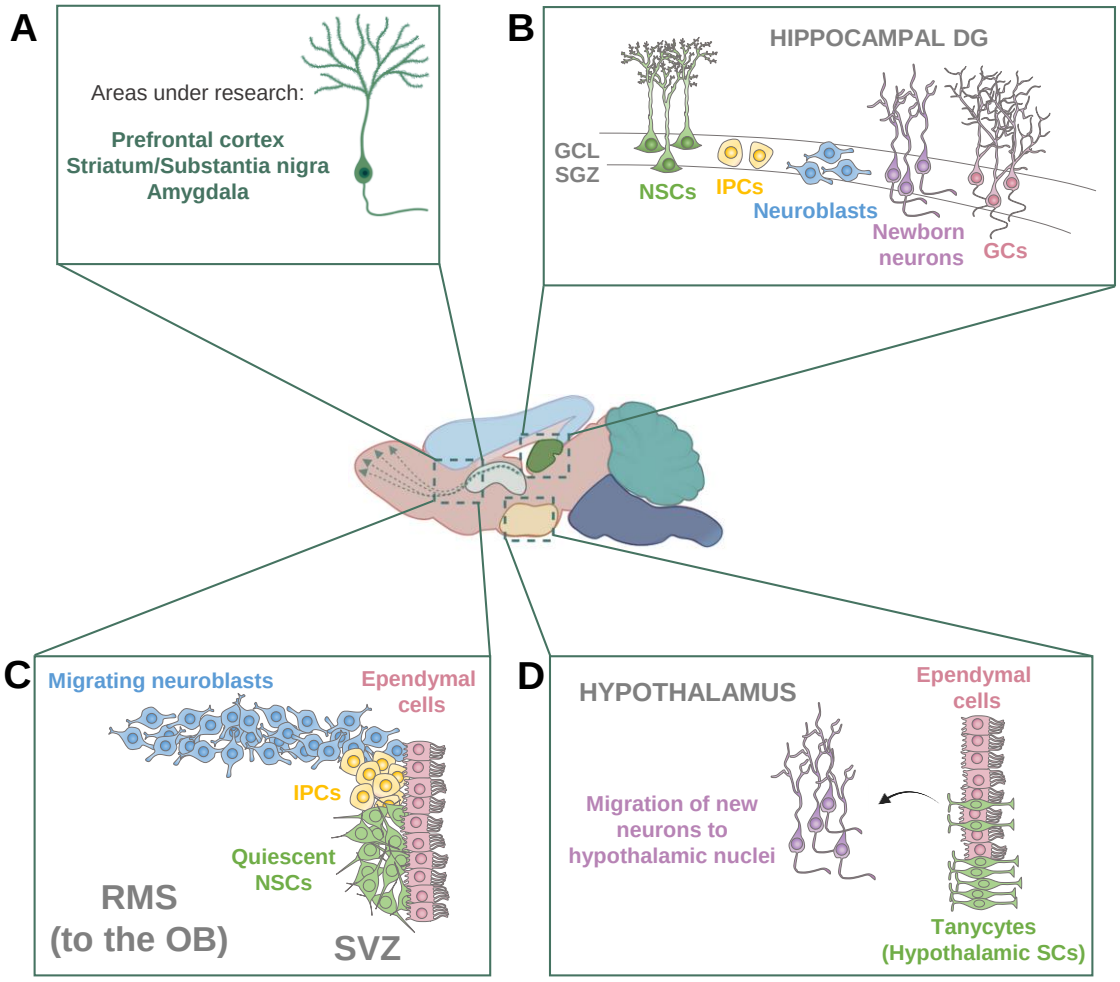

Figure I1. Niches of adult neurogenesis in different brain regions. The generation of new neurons from NSCs has been mainly described in the hippocampal DG and the subventricular zone (SVZ). **(A)** Experimental evidence has suggested that progenitor cells can deviate from the rostral migratory stream (RMS) and differentiate and mature in other brain regions including the prefrontal cortex, striatum, substantia nigra, and amygdala. **(B)** This scheme depicts the neurogenic cascade in the subgranular zone (SGZ) of the DG. Here, in the granule cell layer (GCL), the NSCs generate neural progenitor cells (NPCs), which amplify their number. Unless most of them die, the ones that survive become neuroblasts, that differentiate into immature neurons and finally granule cells (GCs) that are integrated into the brain circuitry. **(C)** Similarly, dividing progenitor cells (IPCs) in the SVZ can differentiate into neuroblasts and migrate through the RMS towards the OB. Besides these two regions, there is emerging evidence indicating that the tanycytes present neurogenic capacity **(D)**. (Modified from Jurkowski *et al*. 2020).

3.1.1 Hippocampal Neurogenesis

As previously mentioned, as we are going to fully focus on the hippocampal DG for the development of the present work, it is of utmost importance to gain a deeper insight into the details of the hippocampal neurogenesis process. Because of that, we present the following Figure 2, in which the process of hippocampal adult neurogenesis is summarized. The hippocampus stands out as a brain region abundant in plasticity, with newly formed cells playing a crucial role in enhancing one of its primary functions: converting experiences into memory traces. These imprints, in turn, facilitate the refinement of behavior through a phenomenon known as learning, while also aiding in the regulation of emotions[16–18]. This indicates the relevance of understanding the molecular mechanisms that control the development of these new neurons in the pre-existing hippocampal circuits. In the hippocampus, synaptic plasticity occurs as potentiation or depression of the efficacy of synaptic transmission. Synaptic plasticity in the DG is accompanied by another type of plasticity: neurogenesis, the generation of new neurons from NSCs[18] (Fig. I2).

Hippocampal neurogenesis is a multistep process in which quiescent NSCs (also called type-1 cells) are activated by entering cell division in a continuous manner, but with low frequency[19]. NSCs can divide asymmetrically giving rise to transient amplifying neural progenitors (ANPs or type-2 cells) which proliferate a few times for 2-4 days. Then, these progenitors either die by apoptosis, being removed by microglia[20], or they stop dividing and differentiate into post-mitotic neuroblasts that finally mature into new neurons[21]. Most of those NSCs that have entered the cell cycle divide several times (2-3 on population average) consecutively to yield neuronal progeny and then go back into quiescence and differentiate into astrocytes. Direct neuronal differentiation is also possible, but in both cases the consequence is the same, once NSCs get activated to generate neurogenic progeny, they differentiate, exiting the NSC pool which therefore diminishes over time[21,22]. Thus, the neurogenic cascade of the hippocampal DG comprises defined steps in which gliogenesis takes place in parallel to neurogenesis in the DG[23].

NSCs were initially termed radial astrocytes[24], which share similarities with radial glia, characterized by a single apical process extending towards the molecular layer[19]. These cells also exhibit protein expression patterns akin to astrocytes, as glial fibrillary acidic protein (GFAP). Notably, these cells are functionally characterized by a low rate of division (when considering the whole population), which can be quantitatively analyzed by thymidine analog 5-bromo-2′-deoxy-uridine (BrdU) pulse-and-chase tracing. BrdU is incorporated into the DNA undergoing mitosis during the synthesis phase (S-phase) because as a thymidine analog, when available it will be used in the same manner as thymidine by cells to duplicate their DNA[25]. Then BrdU can be easily recognized by specific antibodies and visualized by immunohistochemistry and microscopy. With only 2–5% cells labeled

with BrdU, radial glia or NSCs represent less than 10% of all BrdU-labeled cells after a short pulse[26]. Consequently, at the population level, they are predominantly considered quiescent, and most of the dividing cells are the ANPS or type-2 cells.

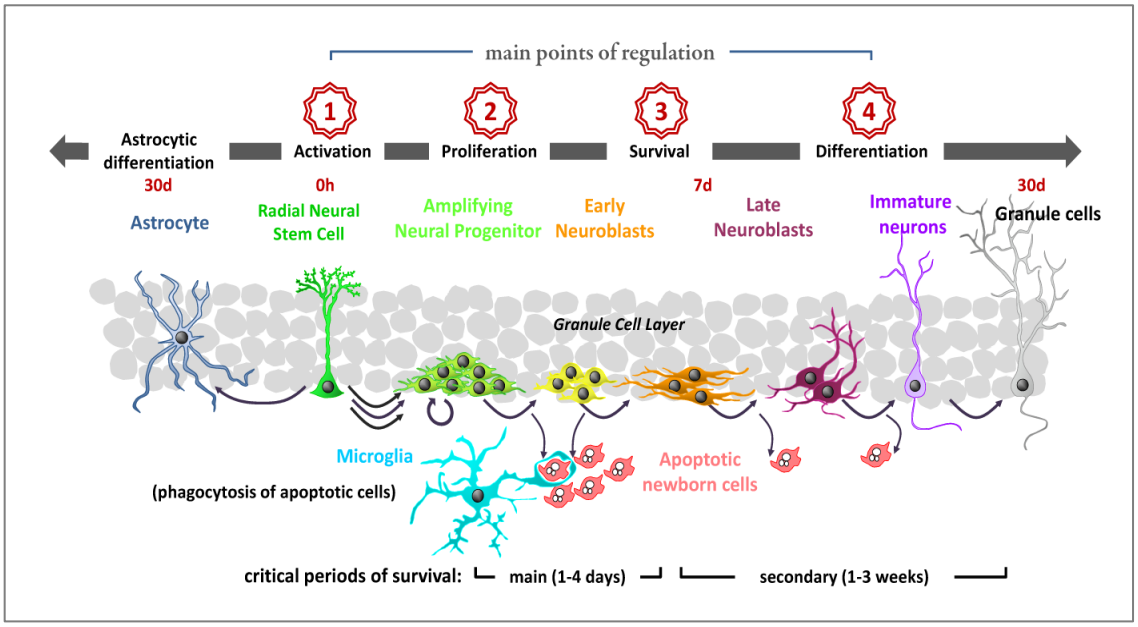

Figure I2. Model of hippocampal adult neurogenesis. In the DG, precursor cells located in the SGZ divide asymmetrically and give rise to ANPs that proliferate quickly before either undergoing apoptosis or slowly committing to a neuronal phenotype. These neuroblasts will eventually go through a stage of immature neurons before integrating into the existing hippocampal circuitries. The encircled numbers denote the main steps that define the amount of neurogenesis, or neurogenic output, and that are affected by aging. (Taken from Encinas and Sierra 2012).

Symmetric division could potentially compensate for the natural depletion of NSCs that is concomitant to their activation to generate neuronal progenitors, which takes place through direct differentiation into astrocytes or neurons[21,22]. However, symmetric division in normal conditions is just not abundant enough to compensate for depletion[21]. It is important to point out that the neurogenic cascade, there is not a synchronized neurogenic wave followed by an astrocytic one as during cortex development for instance, but rather NSCs are progressively getting activated in low numbers and the neurogenic and astrocytic cascade takes place continuously. Therefore, quiescent and activated NSCs, neural precursors, immature and mature neurons, and newborn astrocytes coexist as immediate neighbors in the hippocampal neurogenic niche in a strict and controlled environment that maintains the correct functioning of hippocampal neurogenesis[27].

Each of these steps in the hippocampal neurogenic cascade can be distinguished and quantitatively analyzed using a combination of cell-specific markers and morphological features. Markers in the neurogenic cascade are critical for understanding the various stages of neurogenesis, from the proliferation of NSCs to the differentiation of mature neurons. Starting with Nestin (neuroepithelial stem protein), a widely recognized marker for neural stem and progenitor cells. It is an intermediate filament protein that is highly expressed during neural development and is often used to identify

undifferentiated or early differentiating neural cells[28]. During neuro- and gliogenesis, Nestin is replaced by cell type-specific intermediate filaments such as neurofilaments (NF) in neurons and glial fibrillary acidic protein (GFAP) in glial cells. GFAP is a marker commonly associated with astrocytes, and is often used to identify both quiescent and activated NSCs.

Another marker used for neural progenitor cells (NPCs) is the sex-determining region Y-box 2 (Sox2), a transcription factor crucial for maintaining the pluripotency and self-renewal of NSCs that is expressed in the neural tube during embryonic development. However, Sox2 is also present in astrocytes and progenitors in the hippocampus. Furthermore, Prox1 is especially important for understanding the differentiation of newborn neurons into specific neuronal subtypes, as it is a transcription factor involved in neuronal differentiation and GC development in the DG[29]. Prox1 is useful because it labels postmitotic cells committed to the neuronal fate. Meanwhile, NeuN is crucial for distinguishing between newborn neurons and mature neurons in neurogenic studies[30], as it is expressed in the nuclei of post-mitotic neurons and therefore, is used to identify and quantify the number of mature, functional neurons. Prox1 is specific of the neurons of the GCL, but NeuN labels all neurons in the brain except for few exceptions. In these terms, another example would be NeuroD1 (neurogenic differentiation 1), a basic helix-loop-helix transcription factor associated with neuronal differentiation that is expressed in AMPs transitioning toward a more differentiated state[31].

In the course of this developmental process, newborn neuron markers such as doublecortin (DCX) play a crucial role in identifying and studying the process of neurogenesis in the DG[32]. DCX is a microtubule-associated protein highly expressed in immature or newborn neurons, but not typically found in mature neurons, making it an excellent marker for identifying recently generated neurons[33]. Its expression is especially prominent in regions associated with ongoing neurogenesis, such as the SVZ and the DG of the hippocampus. Additionally, its role extends beyond being a mere marker, as it actively participates in microtubule polymerization and stabilization, contributing to the dynamic cytoskeletal changes required for neuronal migration[34]. Its association with the microtubule network is crucial for the extension and guidance of neuronal processes, facilitating the developing neurons' journey to their final destinations.

There are also markers present in different neural cell subtypes, as is the case of S100β, a calcium-binding protein primarily found in astrocytes but also present in certain subsets of NPCs, but mostly during development. In the adult hippocampus, NSCs do not express S100β and therefore it is a very useful marker to identify them in combination with Nestin and GFAP. In neurogenesis studies, S100β is used to identify specific astrocytic subpopulations and their involvement in the neurogenic niche, and can also be indicative of interactions between astrocytes and newly generated neurons[35]. It is already known that the structural properties of the astrocytic cytoskeleton are maintained thanks to the intermediate filament network that is primarily composed of GFAP[36]. The expression of this protein is upregulated in brain injury and CNS degeneration and its upregulation is normally indicative of

gliosis[37]. In the context of neurogenesis, as abovementioned, GFAP is used to identify NSCs in combination with other markers[38].

In order to identify and study proliferation dynamics of cells, besides BrdU, Ki67 is a key nuclear marker due to its role in indicating active cell division, which is linked to the presence of NPCs actively dividing and contributing to neurogenesis[39]. It is expressed throughout the cell cycle, except during the G0 phase, making it a reliable marker for actively dividing cells, therefore its presence in the nucleus indicates that the cell is in an active phase of the cell cycle. Among the division markers, in the neurogenic process the aforementioned BrdU is frequently employed in studies involving cell proliferation, development, gliosis and neurogenesis, as longer-chase studies allow for addressing newborn cell differentiation[40]. Thus, it is especially valuable in tracing the fate of dividing cells over time, providing insights into the dynamics of cell turnover and differentiation. While Ki-67 provides a snapshot of the overall proliferation status of a cell population, BrdU allows for the tracking and fate mapping of individual dividing cells, offering a more dynamic perspective on cell division events.

These cell division markers enhance our ability to precisely label and track dividing cells, but there is also a tool that serve as efficient gene delivery systems introducing marker genes into the genome of actively dividing cells: retroviral vectors (RVs). RVs are powerful implements used in molecular biology and neuroscience to mark and study dividing cells, particularly in the context of neurogenesis where the generation of new neurons occurs through mitosis. These vectors are derived from retroviruses, a family of RNA viruses, and are modified for use in research as gene delivery systems[41]. They are employed to permanently label only dividing cells and track their fate, or in the case of the neurogenic cascade in the hippocampus, newborn neurons. The integration of their genetic material into the host cell's genome ensures stable, long-term expression of the marker gene in the dividing cells and their progeny, which enables birth-dating cells[42]. They are often engineered to carry a marker gene, such as a fluorescent protein (e.g., green fluorescent protein, GFP). As a result, cells actively undergoing division will express the marker gene and become labeled, permitting their subsequent imaging[43].

In neurogenesis research, RVs have been extensively used to study the generation of new neurons in the brain. These vectors can be injected directly into specific brain regions, and the labeled cells (often NPCs and their progeny) can be tracked over time to investigate their morphology, migration, differentiation, and integration into existing neural circuits. All the above are just some examples of the different ways of tracking the neurogenic cascade that we want to include in our studies, as they play an indispensable role in the process of neurogenesis, offering key insights into the different stages that occur within the brain's dynamic environment.

The different pathways involved in hippocampal neurogenesis should not be considered as isolated and irreversible, but as possible events that depend on both intrinsic and extrinsic properties, including those generated by disease and damage. The loss, disruption, or alteration of the hippocampal

neurogenic cascade arguably results in the impairment of the tasks in which the addition of new neurons in the DG plays an important role in the formation of new memories and learning[18,44]. Additionally, it affects responses to anxiety and fear[45,46], as well as a multitude of extrinsic stimuli key for cognition, behavior or brain repair[44,47]. Certainly, the pathological alteration of the hippocampal cascade has been related to different neurological and neurodegenerative diseases[2] such as epilepsy, Parkinson's disease (PD), Alzheimer's disease (AD), Huntington's disease (HD), or dementia, pathologies in which at least part of the symptoms could be potentially caused or favored by reduced or altered neurogenesis.

Consequently, NSCs present a differential fate in both healthy and diseased conditions (Fig I3). We have observed that hippocampal NSCs are not limited to produce neurons (I3.4), they can also give rise to astrocytes (I3.5), engage in symmetric division to create copies of themselves (I3.1), and even generate oligodendrocytes through gene manipulation (I3.6). However, in pathological conditions like epilepsy, abnormal neuroblasts are generated, exhibiting unusual migration patterns, dendritic branching, and dendritic spine density (I3.7). In more severe cases such as temporal lobe epilepsy (TLE) with hippocampal sclerosis, NSCs deviate from their neurogenic role and transform into reactive-NSCs (8). These reactive-NSCs no longer participate in neurogenesis but undergo massive activation, entering symmetric cell division to generate more reactive NSCs, ultimately differentiating into reactive astrocytes (9).

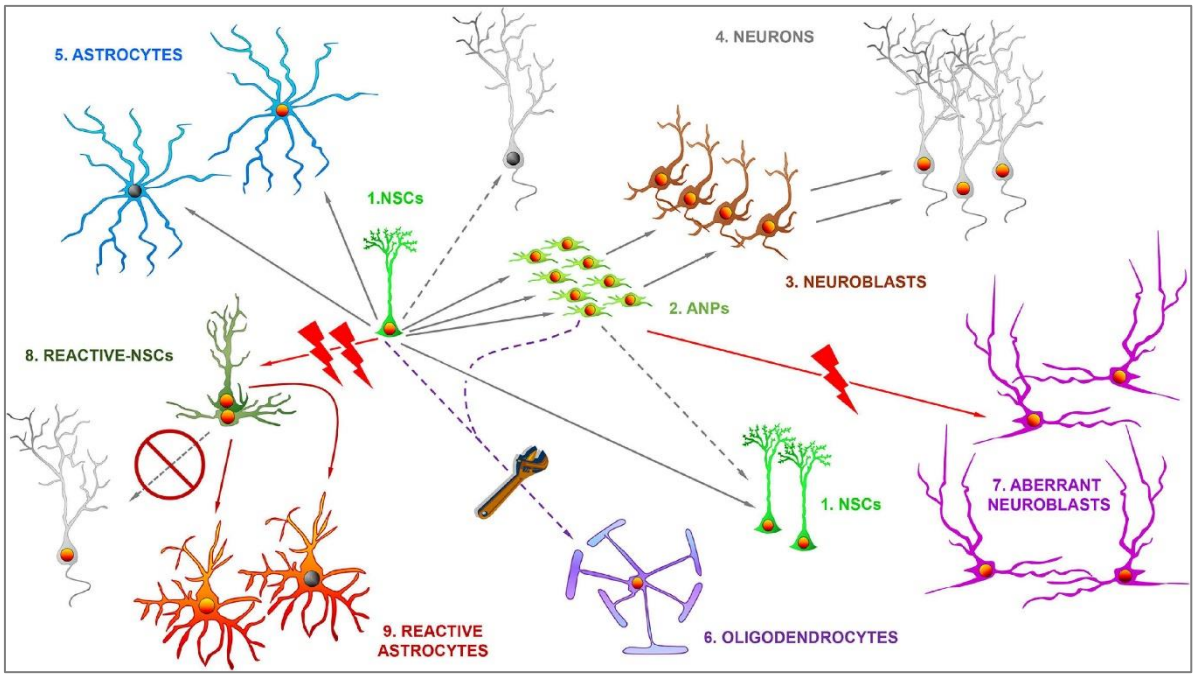

Figure I3. Schematic summary of the differential fate of multipotent adult hippocampal NSCs in health and disease. In normal conditions, the hippocampal NSCs (1) in the DG are activated at a low rate and divide asymmetrically to generate ANPs (2) which ultimately differentiate into immature neurons (3) and eventually become fully mature neurons (4) within the GCL. Some NSCs may also directly differentiate into neurons or generate astrocytes (5) through ultimate differentiation. Additionally, they can divide symmetrically to generate copies of themselves or by manipulating gene expression differentiate into oligodendrocytes (6). In pathological situations like epilepsy, NSCs can generate aberrant neuroblasts (7) characterized by abnormal migration, dendritic arborization and dendritic spine density. In more severe cases like temporal lobe epilepsy with hippocampal sclerosis, NSCs abandon neurogenesis and transform into reactive-NSCs (8). These reactive-NSCs no longer follow the neurogenic process but instead they massively get activated to enter symmetric cell division and ultimately differentiate into reactive astrocytes (9). (Adapted from Rodríguez-Bodero and Encinas-Pérez, 2022).

3.1.2 Newborn Neurons

Going further into detail, our main interest remains in one of the main characters in the neurogenic process: newborn neurons. As observed in the Figure 2 above, these newly born cells are continuously generated from NSCs located in the SGZ of the adult DG, where they integrate into pre-existing hippocampal memory circuits playing a role in several functions but specially in the codification of spatial memory[17,18]. The continuous addition of new neurons to the DG is a key component of the hippocampal circuitry and a structural element of the cognitive reserve[48], as a consequence, researchers have made strides in understanding how disease-specific genetic and environmental factors play crucial roles in determining which neurons succumb to degenerative processes. Certainly, newborn neurons, especially during their early stages as progenitors and neuroblasts, are highly sensitive to changes in their niche microenvironment. The niche, which refers to the local cellular and molecular environment that surrounds these developing neurons, plays a crucial role in regulating their survival, differentiation, and integration into existing neural circuits. Hence, several factors can influence the behavior of newborn neurons within the niche (Fig I3).

1. Neurotrophic Factors

The spectrum of potential biological roles for neurotrophic factors in the development and maturation of the nervous system continues to widen. These molecules are produced within the niche and provide critical signals for the proper development of newborn neurons[49]. During the critical early stages of newborn neurons, some of these factors, as is the case of the nerve growth factor (NGF), help prevent programmed cell death (apoptosis) and promote cell proliferation, ensuring that an adequate number of neurons are generated[50]. They are also involved in the differentiation of newborn neurons into specific cell types with distinct functions, just like neurotrophin-3 (NT-3), which influences the development of neuronal morphology, including the growth of dendrites and axons, the formation of synapses, and the establishment of neural circuits[51]. Indeed, these neurotrophic factors contribute to

the development of synaptic connections between newborn and other neurons, playing a role in synaptic plasticity. Neurotrophins like brain-derived neurotrophic factor (BDNF), for example, are known to enhance synaptic transmission and promote the formation of synapses, as well as support the survival and differentiation of neurons being particularly important in the growth and maturation of new neurons in the hippocampus[52]. Glial cell line-derived neurotrophic factor (GDNF) on the other hand, is an example of a neurotrophic factor that contributes to the functional integration of newborn neurons into existing neural circuits by influencing the establishment of appropriate connections and enhancing the responsiveness of newborn neurons to neurotransmitters and other signaling molecules[53]. Additionally, neurotrophic factors like insulin-like growth factor-1 (IGF-1) can be modulated by environmental enrichment, learning, and physical activity, increasing their expression and thus, promoting the survival and integration of newborn neurons[54], which highlights the role of neurotrophic factors in the brain's ability to adapt to changing conditions.

2. Cell-Cell Interactions

Within the neural niche, the behavior of newborn neurons is significantly influenced by complex cell-cell interactions. In the CNS, neurons, with their remarkable ability to interpret sensory signals and control cognitive functions, take center stage. However, the regulation of these newborn neurons' activity is a multifaceted process, reliant on their interactions with various CNS-resident cells like microglia, astrocytes, and oligodendrocytes[55].

a. Microglia

Microglia play a crucial role as specialized cells in the nervous system, impacting brain development, maintaining the neural environment, responding to injuries, and aiding in repair processes. They actively contribute to neuronal proliferation and differentiation, eliminate dying neurons through phagocytosis, remodel synapses, and clear debris and abnormal proteins[56]. Microglial cells promptly respond to environmental alterations through the release of various soluble substances, such as cytokines, chemokines, nitric oxide (NO), and reactive oxygen species (ROS)[57]. Microglia widely respond to different stimuli, from a simple variation of neural activity, to apoptotic cell phagocytosis in the neurogenic niche or even to neuroinflammation due to an injury[58–60]. These differential microglial responses to environmental disturbances have the potential to either harm or benefit the surrounding cells. Microglia selectively colonize the cortical proliferative zones and phagocytose neural precursor cells as neurogenesis nears completion[61]. As they age, there is a change in their morphology, leading to a diminished capacity for normal functions like migration, clearance, and the ability to transition from a pro-inflammatory to an anti-inflammatory state for regulating injury

and repair[62]. This alteration in microglial behavior may play a role in increased susceptibility and neurodegeneration associated with aging.

In terms of cell-cell connections, microglia could play a crucial role in newborn neuron regulation. By participating in processes such as synaptic pruning, they could help refine and sculpt the connections between neurons, essential for the formation of functional neural circuits[20,63,64], although this interaction has not been fully addressed in the hippocampal neurogenic cascade. Microglia actively survey their microenvironment through dynamic interactions involving motile microglial processes and constant engagement with neurons[65]. Microglial processes have been observed to establish specialized connections with the cell bodies of developing neurons throughout embryonic, early postnatal, and adult neurogenesis[66]. These early developmental connections closely resemble somatic purinergic junctions, crucial for microglia-neuron communication in the mature brain. These junctions are identified as interaction sites between neuronal cell bodies and microglial processes in mouse and human brain, which have a specialized nanoarchitecture optimized for purinergic signaling. They appear to function as communication sites that under physiological conditions, are present on most of the neurons in both mice and humans[66]. Microglia constantly monitor neuronal status through these somatic junctions, allowing neuroprotective actions to take place in a targeted manner. The early establishment of somatic purinergic junctions in development serves as a vital interface for microglia to monitor the status of immature neurons and regulate neurodevelopment.

b. Astrocytes

Astrocytes, on the other hand, are involved in regulating the chemical environment of neurons, including the balance of neurotransmitters[67,68]. Their influence on newborn neurons is significant as they contribute to the overall homeostasis and health of the neural environment. They are involved in promoting the proliferation and differentiation of NSCs into neurons while releasing various signaling molecules that support the survival and development of newborn neurons[69]. Among these molecules, they release growth factors such as BDNF and IGF[70,71], and cytokines like interleukin-6 (IL-6), that in the context of neurodevelopment, [72,73]. Astrocytes are also contributors to the formation and maturation of synapses, as the factors they release influence synaptic development, helping to establish functional connections between newborn and other neurons[74]. These are the cases of TGF-β (transforming growth factor-beta), which is involved mainly neuronal survival, differentiation, and synaptogenesis[75]; and TNF-α (tumor necrosis factor-alpha), a cytokine implicated in inflammatory responses as it plays a role in regulating neurogenesis and synaptic plasticity[76]. Indeed, astrocytes play a crucial role in regulating neurotransmitters in the synaptic cleft, as they are able to uptake neurotransmitters released by neurons, such as glutamate[77], helping to maintain the appropriate chemical environment for optimal neuronal communication.

Astrocytes can communicate with neurons through various signaling pathways. They participate in calcium signaling by generating calcium waves in response to neuronal activity, and these waves can trigger the release of gliotransmitters, affecting nearby neurons[78]. The gliotransmitters release includes ATP, D-serine, and glutamate, which act on receptors located on neurons[79]. For instance, the activation of purinergic receptors by the ATP released modulates neuronal excitability and synaptic transmission[80]. Indeed, neuronal excitability can be directly regulated by astrocytes, as they take up excess glutamate released during synaptic transmission[79]. If this is not done, the dysregulation of glutamate signaling can impact synaptic function and contribute to excitotoxicity. Therefore, astrocyte participation in neuroplasticity occurs through the release of factors that modulate synaptic strength and connectivity, allowing them to sense neuronal activity and, in turn, modulate synaptic function. The connection between astrocytes and blood vessels is established through a specialized structure known as the blood-brain barrier (BBB). Astrocytes extend fine processes known as end-feet that surround blood vessels in the brain, creating a physical connection between astrocytes and the vascular endothelial cells that form the blood vessel walls[81]. Simultaneously, it helps the passage of substances between the blood and the brain as well as ensures that regions of heightened neural activity, including those populated by migrating neuroblasts, receive an optimal blood supply, facilitating metabolic support[82,83].

c. Oligodendrocytes

Finally, oligodendrocytes are brain cells primarily responsible for myelinating axons in the CNS, providing insulation and improving the efficiency of signal transmission along axons[84]. Their function in myelin production covering neural axons allows for faster and more efficient transmission of electrical signals, making them crucial for ensuring that newborn neurons can integrate into existing neural circuits and communicate effectively with other neurons[85]. However, there is no direct evidence of a link between oligodendrocyte-mediated myelination and newborn neurons, as myelination is a process that occurs after neurons have differentiated and established functional connections[86].

3. Neuroinflammation and Immune Response

Inflammatory molecules like interleukins, interferons, and TNF-α can significantly reduce the proliferation of cells, activate NSCs, and hinder the production of new neurons[87]. However, the use of non-steroidal anti-inflammatory drugs, such as indomethacin or minocycline, has shown promise in restoring neurogenesis[88,89]. Neuroinflammation, characterized by the activation of the immune system in the brain, is a central player that links various factors like neurodegeneration, bacterial and viral infections, and aging, ultimately impairing the activity of NSCs. As individuals age, there is a notable shift from a state of rapid cell activity to a more conservative, slow-paced model, which is marked by

a deepening of NSCs quiescence. In early adulthood, NSCs begin to differentiate into at least the following two subpopulations: one that remains relatively unchanged, maintaining its usual behavior in terms of activation and neuron generation, and the other that experiences a decrease in the likelihood of activation[90]. Several factors contribute to this deepening quiescence, including increased expression of the glucocorticoid receptor[91], the interplay between ASCL1 and the E3 ubiquitin ligase HUWE1[92], and interactions involving nuclear lamina protein lamin B1 and SUN-domain containing protein 1 (SUN1) [93], as well as tyrosine-protein kinase Abl[94]. Notably, neuroinflammation emerges as a key factor influencing the transition toward deeper quiescence of NSCs. In specific brain regions like the hippocampus and the SVZ, increased signaling of interferons promotes the quiescence of NSCs[95,96]. Additionally, the balance between quiescence and activation of NSCs is linked to the levels of ROS, which are crucial in inflammatory processes[97].

Immune responses and signaling molecules released by immune cells within the brain[98] also regulate adult neurogenesis. Traditionally, immune activation, characterized mostly within the brain by microglial reaction with a strong component of cytokine release, has been perceived as detrimental[99]. However, the impact of immune activation on neural function is dependent upon the specific form of the immune response, as microglia and other immune-reactive cells in the brain can either strengthen or disrupt brain function based on their distinct phenotypes and behaviors[56,99]. For example, microglia exhibiting an inflammatory phenotype generally reduce cell proliferation, survival, and the overall function of newly formed neurons. These behaviors can be part of a defense mechanism against pathogens or injury but, when prolonged, may lead to neuroinflammation and tissue damage[100]. Previously, it was believed that microglial cells could have an active or inactive state. This simplified theory claimed microglia adopt an M1 phenotype in response to pro-inflammatory signals, in which they release inflammatory cytokines (such as IL-6, IL-1β, TNF-α) and ROS.. On the other hand, microglia displaying an alternative protective phenotype actively support adult neurogenesis[20,101]. This anti-inflammatory and tissue repair phenotype was referred to as M2, in which anti-inflammatory cytokines (such as IL-10 and TGF-β) are released promoting tissue healing and regeneration[100]. However, in 2005 an essential discovery contrasted this theory and proved microglial cells are highly active in their presumed resting state, continually surveying their microenvironment with extremely motile processes and protrusions[65], a premise that has been largely confirmed during the following years and continues nowadays[100,102]. They create a microenvironment that is conducive to neurogenesis by decreasing excessive inflammation, reducing oxidative stress (OS), and promoting supportive conditions for the survival and differentiation of NSCs.

4. Neuronal Activity and Electrical Signals

Electrical activity and specific molecular signaling pathways play a crucial role in promoting both neuronal survival and regeneration[103]. Activity-dependent mechanisms, such as the regulation of gene expression by calcium signaling, can enhance the synthesis of neuroprotective proteins that protect neurons from harmful stimuli[104]. Electrical activity influences the balance between pro-survival and pro-apoptotic factors, determining whether a neuron will undergo programmed cell death or persevere[105]. Within the DG, neural activity is fundamental for encoding and consolidating incoming sensory information into the hippocampal circuitry[106,107]. This heightened activity serves as a trigger for the mobilization of NSCs, initiating a cascade of events that lead to the production of new neurons[16,108]. Especially patterns associated with learning and memory tasks influence the activation of NSCs and the production of new neurons, which contribute to the encoding and integration of memories. Interestingly, neural activity in the DG is linked to pattern recognition and separation, enabling the discrimination between similar sensory inputs and ensuring that distinct neural representations are formed for each experience, as well as integrating these novel experiences into the existing neural circuitry[109]. Thus, electrical activity, including action potentials and synaptic signaling, is fundamental for the functional integration of newborn neurons into established networks[110–112]. Neurotransmitters released during electrical activity, such as glutamate and GABA, can impact both integration and development[113]. Glutamate, as the principal excitatory neurotransmitter, serves as a driving force for synaptic activity, promoting the formation of excitatory synapses and the elaboration of dendritic arbors[114]. In contrast, GABA, the principal inhibitory neurotransmitter, contributes to the delicate balance of excitation and inhibition, crucial for the refinement of neural circuits.

Following injury or damage, the function of neurons is attempted to be restored, as electrical activity provides the stimulus that triggers the activation of regenerative pathways. For instance, during axonal regrowth, electrical activity guides the extension of neurites and axons, facilitating the reconnection of damaged neural pathways. Additionally, it can influence the expression of molecules that enhance axon elongation and guide neurons toward their targets[115]. This phenomenon has been extensively studied in the context of mature neurons; however, it is not confirmed for newborn neurons although similar principles could be applied in terms of axonal growth and circuit integration. Certainly, the integration of newborn neurons into de existing neural network as well as their maturation is seems to be mainly guided by the synaptic inputs coming from surrounding neurons[111,116]. These synaptic inputs occur when newborn neurons extend processes (axons and dendrites) and form synapses with existing neurons[117,118]. They direct the structural refinement of dendritic arborizations contributing to the distinctive architecture that characterizes the newborn neurons' responsive zones within the neural network. This communication is crucial for the development of the neural circuitry,

and it highlights the importance of newborn neuron's capability of exhibiting intrinsic excitability, which in turn contributes to early stages of development, including migration and process outgrowth[119,120]. The mechanism involved in the translation of increased neuronal activity into modified neurogenesis are poorly understood, but as we will detail later, ATP could be a good candidate because it is known that in hyperexcitatory conditions there is an excess of extracellular ATP.

5. External Stimuli: Environmental Enrichment and Stress

Hippocampal neurogenesis is influenced by external stimuli, and the effects can vary depending on the nature of the stimuli, whether they are enriching (meaning complex and stimulating) or stressful (detrimental) thus affecting the development and resilience of newborn neurons. Enriching experiences, such as exposure to a stimulating environment, physical exercise, and cognitive challenges, have been associated with an increase in hippocampal neurogenesis, promoting the activation of NSCs, the production and survival of new neurons[121]. Enriched environment (EE) not only enhances normal neural development through reinforcing neuroplasticity at the cellular level but can also lead to heightened synaptic plasticity, influencing the strength and efficacy of synaptic connections. It plays a crucial role in nerve repair during CNS injury, a process that involves morphological, cellular, and molecular adaptations in the brain, promoting the restoration of functional activities[122,123]. On the contrary, stressful experiences, whether acute or chronic, have been linked to a reduction in hippocampal neurogenesis. Stress hormones, such as cortisol, can negatively impact the proliferation and survival of NSCs, leading to a decrease in the production of new neurons[124,125]. This stress can impede the survival and disrupt synaptic plasticity of newly generated neurons in the hippocampus, as the detrimental effects on neurogenesis are associated with increased apoptosis of developing neurons, limiting their integration into the existing neural circuitry[126,127]. Reduced generation of new neurons and their integration in the hippocampal circuits represents one of the mechanisms by which chronic stress translates into cognitive impairment, affecting specially to learning, memory, and behavior[128].

It is noteworthy that the effect of the environment on the nervous system varies at different stages of development after birth, as the developing brain exhibits varying degrees of responsiveness to environmental cues during its maturation process[129]. During the early stages of postnatal development, the nervous system is particularly susceptible to environmental influences, evident in the plasticity of neural circuits, where experiences and stimuli can profoundly shape the emerging architecture of the brain[130]. Environmental cues during this critical period can exert lasting effects on synaptic connections, neural networks, and even structural organization. As the brain progresses through subsequent developmental stages, its responsiveness to the environment undergoes obvious changes.

The interaction between genetic information and environmental factors becomes increasingly complex, influencing not only the structural network of the nervous system but also its functional capabilities. Environmental stimuli continue to sculpt and refine neural circuits, contributing to the establishment of cognitive and behavioral functions[131]. Actually, in addition to genetic information, environmental factors such as chronic stress or exposure to toxins exert a profound influence on the structure and function of the nervous system, as well as the occurrence and progression of certain nervous system diseases such as AD, PD, HD or even epilepsy[123,132,133].

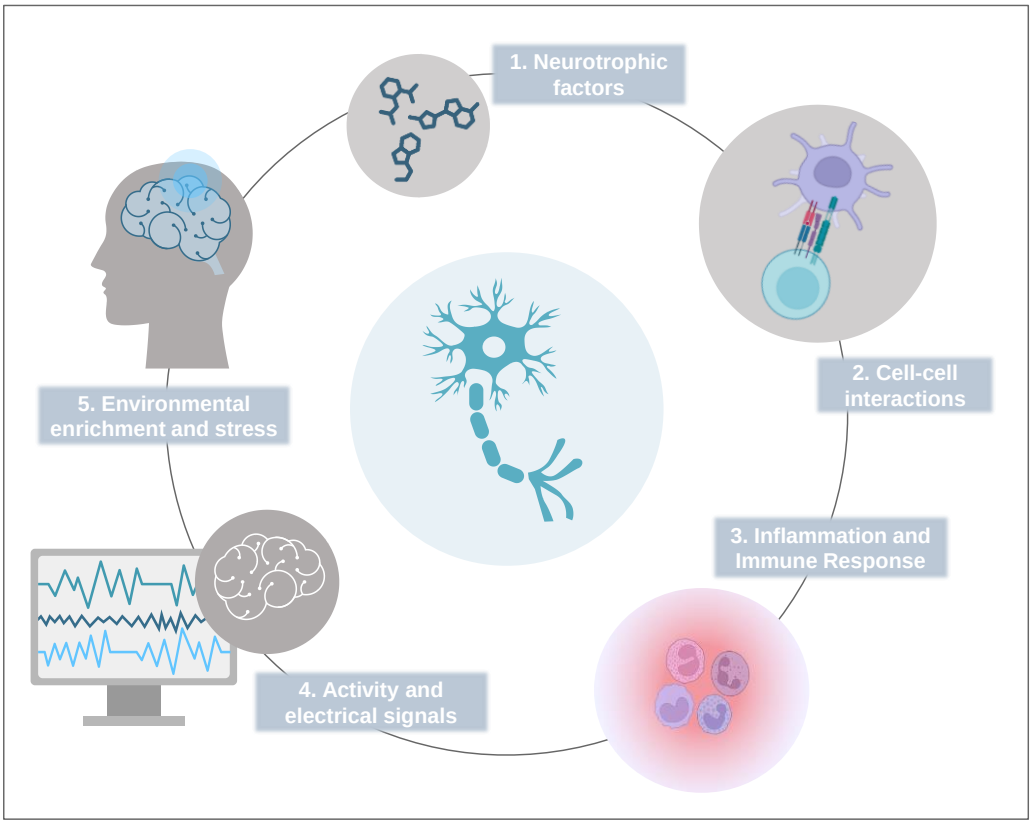

Figure I3. Schematic illustration of the factors influencing newborn neuron development. 1. The neurotrophins play diverse roles in the development and maturation of the nervous system, supporting the growth, survival, plasticity, and differentiation of neurons. 2. In the CNS, diverse cell types collaborate to maintain neuronal functions, as neurons decode sensory signals and regulate movement and cognition, with interactions involving microglia, astrocytes, and oligodendrocytes. 3. Adult neurogenesis involves immune responses where immune cells' diverse phenotypes determine support or disruption of brain function, making immune-neural interplay key in newborn neuron development. 4. Electrical activity and molecular signaling contribute to neuronal survival, regeneration, and integration. 5. Environmental factors, including enrichment and stress, profoundly influence neural development, function, and recovery.

3.2 Epilepsy

3.2.1 Introduction to Epilepsy

As mentioned above, neuronal activity is a major regulator of hippocampal neurogenesis. Therefore, it is expected that pathologies associated with neuronal hyperexcitation will course with modification of the neurogenic cascade which in turn may contribute to further alterations of circuits and neuronal network activity. Epilepsy is a major neurological disorder characterized by spontaneous bursts of synchronized neuronal hyperexcitation and subsequently represents a pathological framework of interest to study hippocampal neurogenesis. Epilepsy, comprising a constellation of varied epileptic syndormes, places a significant burden on public health, affecting an estimated 65 million people worldwide, while the developing countries are the most impacted areas[134]. Beyond its prevalence, epilepsy presents a major health concern due to its associated side effects, and more importantly, comorbidities such as cognitive impairment, depression, and psychiatric disorders[135]. These additional factors accentuate the significance of addressing epilepsy from a full perspective in healthcare. As a result, it is of utmost importance to better understand the mechanisms of epileptogenesis, which refers to the transformation of a normal brain into one that generates recurrent spontaneous seizures. Intracellularly, synchronous epileptic events occur as large, complex postsynaptic potentials with or without synchronous cell firing[136,137], involving both excitatory and inhibitory signalling[138]. The impaired balance of excitation and inhibition is the most conventional theory underlying interictal spike generation, and most of our knowledge about the cellular and network basis of cortical hyperexcitability comes from animal models[139].

Although the cellular properties underlying hyperexcitability have been widely explored in the human neocortex, little is known about how an impaired balance of excitation and inhibition of the neuronal network contributes to epileptic hypersynchrony in humans. Several risk factors contribute to the development of this disease, including genetic predisposition, traumatic brain injury (TBI), fever, tumors, brain infections, or neurodegenerative diseases[60]. Identifying and understanding these risk factors play a vital role in both early detection and target prevention strategies for this condition, as long as this neurological disease remains a challenging condition to treat effectively. The conventional drug-based approaches can only manage the symptoms but do not provide a definitive cure, in fact, despite advancements in the number of new drugs developed for epilepsy in the last decades, the efficacy of antiepileptic drugs (AEDs) has seen little improvement over the past 70 years[141]. Furthermore, a significant portion of epilepsy patients, approximately 30%, are considered pharmacoresistant or refractory to current pharmacological treatments, leading to worsened prognoses[142]. In some cases, the disease progresses, leading to an escalation in seizure frequency and

cognitive decline. Hence, a broad diagnostic evaluation is mandatory as many conditions could cause a new onset of status epilepticus (SE), which is complex and yet not fully understood, and not all epileptic patients respond equally to the same drugs[143,144]. Anti-epileptic medications present many pharmacologic profiles as they act on the different types of seizures against which they are most effective. A better understanding of the molecular effects of existing anti-seizure drugs as well as the development of new ones that act against novel targets is now a high priority[144,145].

Typically, epilepsy is diagnosed after an individual has experienced at least two seizures unrelated to any known medical conditions[135,146]. This diagnostic criterion helps medical professionals differentiate epilepsy from other potential causes of seizures, enabling more accurate and timely treatment for those affected. Epileptic seizures can lead to a wide range of symptoms that impair features such as movements (convulsions or uncontrollable jerking), levels of consciousness (loss of awareness or mental absence) and can even cause changes in behavior and feelings. Indeed, additional dysfunctional issues usually worsen this symptomatology due to the epileptic imprinting in the brain, which finally makes it a chronic disease[147,148]. In fact, epilepsy is defined by the recurring and unprovoked (spontaneous) seizures, which behave as chronic aberrant patterns due to abnormally excessive or synchronous neuronal activity in the brain. It can be classified into two main types: focal and generalized epilepsy, depending on the specific brain region where seizures originate[149] . Generalized seizures involve the entire brain and typically lead to altered consciousness, often accompanied by tonic-clonic spasms. On the other hand, focal epilepsy originates in a specific area of the brain, with symptoms reflecting the affected brain region's function[140].

The main impairments both in patients and animal models of MTLE have been observed in spatial navigation and memory[150,151], which are linked to hippocampal sclerosis (HS)[152]. HS is a condition characterized by the selective loss of neurons in the hippocampus, which is often associated with epilepsy and can be detected and studied using various neuroimaging techniques, including EEG (electroencephalography). EEG can provide insights into the abnormal electrical activity in the brain, especially in cases of epilepsy associated with HS[153]. The distinctive patterns observed in EEG recordings help identify and characterize epileptic activity, and each oscillation type is associated with specific brain states and functions.

In the case of the low-frequency oscillations, theta oscillations (4-8 Hz) are often associated with the hippocampus and are crucial for memory formation and spatial navigation[154]. Impairments in memory are associated with alterations in these oscillations[155,156], as their disruption has been suggested as a potential factor contributing to memory deficits[157]. In systemic rat models of MTLE, various alterations in theta characteristics have been documented in the literature. These changes encompass a decrease in theta rhythm coherence[158], as well as reductions in theta frequency and power[155,156]. The factors contributing to the decline in theta power, coherence, and phase-precession in epilepsy models

are complex, as any damage or temporary inhibition in the brain structure results in a significant reduction in hippocampal theta power and consequential spatial memory impairments[159,160].

Alpha oscillations (8-13 Hz) on contrary, are linked to a state of relaxed wakefulness[161]. These oscillations are prominent in the occipital and parietal areas and are often associated with an inactive or inhibitory state of the cortex[162]. Alterations in these oscillations have been observed in various neurological conditions, including epilepsy. These changes may manifest as a decrease in alpha power or a disruption in the typical rhythmicity of alpha waves[163,164]. Studies have shown that there can be abnormalities in alpha oscillations during interictal periods in individuals with epilepsy[165], and these abnormalities may be indicative of underlying network dysfunction. The functional implications of altered alpha oscillations in epilepsy are not fully understood, but they may be linked to disruptions in normal inhibitory processes in the brain and can affect information processing and contribute to cognitive impairments often seen in individuals with epilepsy.

In contrast, beta oscillations (13-30 Hz) are associated with active, alert, and attentive states[166]. They are particularly relevant to motor control, and alterations may be associated with motor symptoms[167]. While beta oscillations are generally considered a normal part of brain activity, alterations in their patterns have been observed in the context of epilepsy. Studies have shown that individuals with epilepsy may exhibit abnormal beta oscillations in both interictal (between seizures) and ictal (during seizures) periods, and have been implicated in the generation and propagation of seizures[168]. Some research suggests that alterations in beta oscillations may be associated with the development of hypersynchronous networks, which can promote the generation and spread of epileptic discharges[169].

On their part, gamma oscillations (30+ Hz) are involved in cognitive processes, including memory and perception[170]. They are typically observed during cognitive processes that involve the synchronous firing of neural populations. These fast oscillations are crucial for coordinating information processing and communication between different brain regions[171]. There are two types of gamma oscillations: low gamma oscillations (30 to 50 Hz) and high gamma oscillations (50 to 100 Hz)[172]. Low gamma oscillations are often associated with sensory processing, perception, and early stages of information processing. They play a role in the synchronization of neural activity within a specific brain region and are commonly observed in sensory areas of the brain, such as the visual cortex, being particularly important for processing sensory inputs, including visual stimuli[173]. High gamma oscillations are often linked to more complex cognitive functions, including memory, attention, and conscious awareness. They are thought to be involved in the integration of information across different brain regions, and are observed in various brain regions, including the hippocampus and prefrontal cortex[174,175]. The hippocampus, in particular, shows high gamma activity during memory-related tasks[174]. Both low and high gamma oscillations are part of the broader spectrum of brain rhythms that contribute to information processing and communication between neurons[173]. There is ongoing research into the role

of gamma oscillations in seizure generation. Although the precise mechanisms are not fully understood, some studies suggest that abnormal gamma activity may contribute to the initiation or propagation of epileptic seizures[176,177].

Finally, there are high-frequency oscillations (HFOs) in the brain, which are neural activities characterized by oscillatory patterns at frequencies higher than the typical gamma range (30-100 Hz). Two types of HFOs that are often studied in the context of neurophysiology and epilepsy. First, slow ripples (100-250 Hz) are associated with specific patterns of neural network activity, and are often linked to memory consolidation processes, being particularly observed in the hippocampus[178]. Moreover, they have been studied in the context of epilepsy, as abnormal increases in slow ripple activity have been observed in epileptic patients, suggesting a potential association with seizure generation[179]. Contrarily, fast ripples occur at even higher frequencies, typically between 250 and 600 Hz. They are thought to be related to pathological processes in the brain, particularly in the context of epileptogenic zones, and are often considered as potential biomarkers for identifying regions of the brain that are prone to generating seizures[180]. These are sometimes used as a diagnostic tool in epilepsy monitoring, as their presence in certain brain regions may indicate an increased risk of seizures[181].

3.2.2 Epilepsy and Neurogenesis

1. Neural Stem Cells as Biosensors of Neuronal Activity

Increased neuronal activity can stimulate NSCs activation, and GABAergic receptors play a crucial role in the process[182]. This mechanism becomes particularly significant in conditions of pathological neuronal hyperexcitation, such as epilepsy, where GABAergic transmission is impaired. The hippocampus is more vulnerable to neuronal hyperexcitation and excitotoxicity than other brain structures, making it a frequent focal point for seizures due to its recurrent circuits. This occurs especially in MTLE, the most common form of epilepsy. A main characteristic is that the hippocampus, or sometimes related structures such as the amygdala, are the focus of seizures[183]. Thus, studying NSCs in neurogenesis in MTLE has gained increased attention.

In experimental models of neuronal hyperexcitation, like induced seizures or electroshock, NSCs are reported to be overactivated[184–186]. It was initially expected that sustained hyperexcitation would boost neurogenesis due to increased NSC activation. However, ongoing hyperactivation may deplete the NSCs over time, impairing neurogenesis[22,187]. There is a possibility that symmetric division, where NSCs divide into identical cells, could increase to maintain the NSC pool and sustain higher levels of neurogenesis for longer periods. Nevertheless, the chronic impairment of neurogenesis has been linked

to an accelerated depletion of NSCs, potentially explaining observed declines in hippocampal neurogenesis in epilepsy patients over time[184,188].

Interestingly, around one third of MTLE patients do not respond to drugs and unilateral hippocampalectomy is the last therapeutic resort of choice to control seizures[183]. In these cases of severe hyperexcitation, patients present MTLE with hippocampal sclerosis (MTLE-HS), which is characterized by unilateral neuronal loss in CA, GCL dispersion and intense reactive gliosis and neuroinflammation, and a remarkable transformation occurs in NSCs. Instead of contributing to neurogenesis, these NSCs get massively activated as they become hypertrophic, multibranched, and migrate away from the SGZ. These NSCs are termed reactive (React-NSCs), and undergo symmetric division and abandon neurogenesis[184,189]. During a few weeks React-NSCs are different from NSCs, astrocytes and reactive astrocytes[190], but they ultimately differentiate into reactive astrocytes, although their functional contribution to gliosis is still ignored. In general, reactive gliosis associates with neuroinflammation, which depending on the type of insult or disease and the timing can be detrimental or beneficial. Reactive gliosis is often considered epileptogenic, impacting potassium buffering, GABA synthesis, and cytokine modulation among others, thus modifying neuronal activity[191].

An intriguing question emerges regarding the contribution of NSCs to epileptogenesis through reactive gliosis. Even if the conversion of NSCs into React-NSCs during reactive gliosis is prevented, it remains uncertain whether these NSCs could generate healthy neurons, especially when the neurogenic niche is severely disrupted, as is the case in MTLE-HS. Understanding these processes is crucial for unraveling the complex relationship between neuronal hyperexcitation, NSC behavior, and the potential consequences for neurogenesis in conditions like epilepsy.

2. Aberrant Neurogenesis

Examining the response of newborn neurons to changes in the niche is vital for revealing the mechanisms that underlie neural plasticity and the formation of functional neural circuits. This insight is essential for developing potential therapeutic strategies for various neurological conditions given their implications in neurodevelopmental disorders and neuro-regeneration. Typically, neuroinflammation provokes a reduction in cell proliferation (NSCs and precursors), but also the alteration of newborn neurons whose maturation in terms of dendritic arborization and synaptic connections is reduced and presents a dystrophic phenotype[192]. Dystrophic morphology can be interpreted as diminished maturation when dendrites are less elaborated and the density on dendritic spines is lower, as is the case in models of neuroinflammation and neurodegeneration[192,193]. However, the opposite effect, more developed dendritic arborization richer in dendritic spines has also been found, for instance in a model of glucocorticoid administration[194].

Nevertheless, this effect could be due not just to the levels of glucocorticoids, but also to the abolition of the changes and fluctuations of these levels. Selective knock-down of glucocorticoid receptors in newborn neurons also triggers an increase in dendritic arborization and higher density of dendritic spines[195], and modified morphology changes are accompanied by functional changes[16,195]. Several molecular mechanisms have been found to regulate the differentiation at least in terms of morphological development of newborn neurons[196–198], however, the role of these mechanisms and the involvement of others in disease-induced newborn neuron dystrophy remains to be fully explored. An aspect that is usually overlooked is whether these alterations are transient, lasting, or even permanent.

Our global picture in this project is to try to prevent epilepsy-derived aberrant neurogenesis, which we consider that is related to neuroinflammation and gliosis. Certainly, the dystrophic phenotype in newborn neurons can result from their abnormal formation under various conditions such as in neurodevelopmental disorders, neurodegenerative diseases, and after brain injury. In the case of epilepsy, seizures provoke dramatic alterations in the neurogenic niche. The increase in neurogenesis following neuronal hyperexcitation is a consistent outcome in epilepsy models, as Parent demonstrated in the pioneering experimental mesial temporal lobe epilepsy (MTLE) research, where a sharp surge in neurogenesis was shown to be triggered by seizures[199] (Fig I4A,B). However, the survival of these seizure-induced new neurons is diminished compared to normal conditions[2,200]. Additionally to increased cell proliferation, in rodent models of epilepsy, these alterations to adult hippocampal neurogenesis have shown other negative consequences, such as abnormal migration and formation of aberrant synaptic hippocampal connections that can initiate epileptic seizures[199,201]. In this context, neurons often exhibit morphological abnormalities, which are referred to as aberrant neurogenesis. This term is used to refer to newborn neurons that present irregularities such as altered dendritic arborization with frequent basal and lateral dendrites in addition to modified main apical dendrite[199,202] (Fig I4C-E).

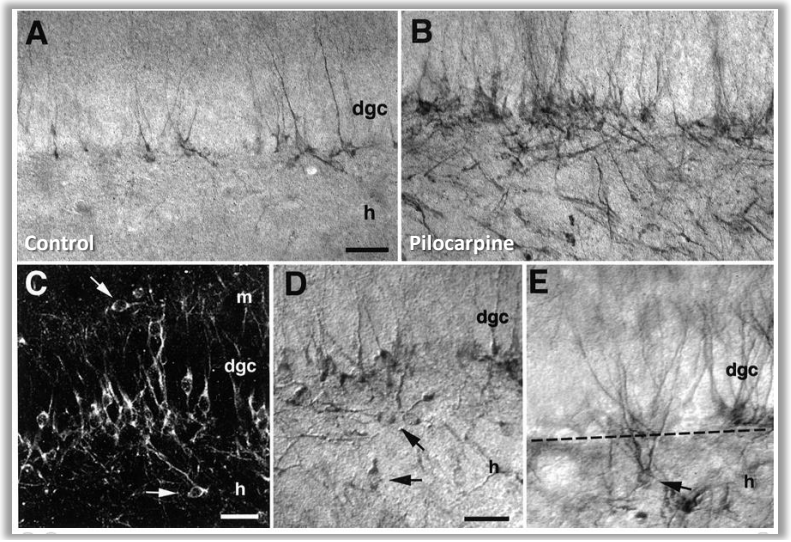

Figure I4. Aberrant neurogenesis shown in a pilocarpine model of epilepsy. (A,B) Images of differentiating neurons in the dentate granule cell layer (GCL, dgc in the image) of rats 28 days after saline (A) or pilocarpine (B) administration. (C–E) In pilocarpine-treated but not control rats, many immunolabeled cell bodies with the size and shape of granule cells were found in the inner molecular layer (arrow in C) or the hilus (arrows in C–E). (Adapted from Parent *et al.* 1997).

Aberrant newborn neurons are capable of contributing to epileptogenesis during a critical period of their maturation process, which is marked by their integration into the neural networks of the brain, as these alterations modify the connectivity of the DG[203,204]. This is an exceptionally relevant finding as it highlights how neurogenesis could be directly contributing to this pathology, as it does not only participate in the promotion of seizures but also in the associated cognitive decline[16,201]. However, despite the duration of aberrant neurogenesis remains unclear, evidence suggests that it may not be sustained for extended periods, both in experimental models[184,205] and human samples[206,207]. The level and quality of neurogenesis can be independently regulated, and aberrant neurogenesis can occur concurrently with decreased neurogenesis as in the MTLE model by injection of kainic acid (KA) in the amygdala[189]. However, neurogenesis is more commonly observed to be increased in models as in the aforementioned work of Parent[199] or in other conditions such as Dravet Syndrome (DS), a rare but devastating pediatric generalized epilepsy, or experimental TBI[208,209]. Notably, a small percentage of TBI patients develop seizures over time, raising the intriguing possibility that aberrant neurogenesis may play a role in seizure generation in DS or TBI, although this hypothesis has not been tested yet.

In the most prevalent form of epilepsy, MTLE, the increased cell proliferation may have a close relationship with the circuit that give rise to seizures being located in the temporal region of the brain, specifically in the hippocampus. Because here, seizures trigger an immediate overall proliferative response mediated by the activation of NSCs, and this increased proliferation of neuronal precursors consequently can lead to an increase in the generation of new neurons in the short term[204,210]. Interestingly, seizures appear to accelerate the maturation and integration of these newly born GCs, though the exact implications of this phenomenon remain unclear[211–213]. Newborn neurons show enhanced activity compared to mature GCs, making them a potential cellular source of neuronal hyperactivity. Silencing newborn neurons or suppressing neurogenesis have been shown to reduce seizure activity; however, these effects are transient, implying other cellular sources of modulators of neuronal hyperactivity during epilepsy progression[203,204,214]. One potential source could be reactive astrocytes generated from differentiating NSCs, whose contribution to epilepsy is not well defined[184].

3.2.3 Hyperexcitability and Epileptogenesis

The most widely accepted theory explaining the generation of interictal spikes highlights the disrupted balance between excitation and inhibition. Our understanding of the cellular and network mechanisms responsible for cortical hyperexcitability comes from insights obtained from animal

models[215]. Actually, this state in which neurons become more easily excited and fire action potentials more frequently than in a balanced or normal state results from various factors including imbalance in neurotransmitters, changes in ion channel activity or in neuronal connectivity[216,217].

Despite considerable research into the cellular properties responsible for hyperexcitability within the human neocortex, our understanding of how the disrupted equilibrium between neuronal excitation and inhibition contributes to epileptic hypersynchrony in humans remain limited. However, our understanding advanced when it was observed that synchronous population bursts are not just manifested at the cellular level, but also at the network level[218]. For this analysis of network hyperexcitability, epileptiform discharges were considered the best characterized clinical biomarkers, but there are also other promising indicators. For example, neurogenesis provides information about ongoing processes such as neuronal hyperactivity or neuroinflammation, as it is continuously modulated in response to changes in brain homeostasis. Indeed, this hyperexcitation stems from an imbalance, wherein excitatory neurotransmission, predominantly mediated by glutamatergic signaling, is increased, or inhibitory neurotransmission, mainly through γ-amino butyric acid (GABA) signaling, the major inhibitory neurotransmitter in the CNS, is diminished[219,220].

During this process, when neurons are excessively stimulated by neurotransmitters, particularly glutamate, excitotoxicity occurs. Excitotoxicity is a common feature in many neurodegenerative diseases, implicated in nerve cell damage or death through apoptosis or necrosis, depending on its intensity. It arises from a strong association with abnormal calcium ion (Ca^{2+}) influx caused by uncontrolled glutamatergic activity[223]. The over-activation of glutamatergic receptors leads to a substantial influx of Ca^{2+} into the cells[224] and this influx, in turn, triggers the activation of a cascade of enzymes that ultimately damage the cellular structure, membrane, and DNA, resulting in cell death[225]. The conventional understanding of this process points to a sustained disruption of Ca^{2+} homeostasis, primarily triggered by the overactivity of ionotropic N-methyl D-aspartate (NMDA) and α-amino-3-hydroxy-5-methyl-4-isoxazolepropionic acid (AMPA)/kainate receptors[226,227].

Consequently, this disruption sets in motion mitochondrial-dependent or independent cell death pathways and in this context, neural death is a consequence of an overwhelming burden on neuronal Ca^{2+} buffering systems, including the Ca^{2+}/calmodulin (CaM) signaling cascade[225,228]. Ca^{2+} is the main second messenger that helps to transmit depolarization status and synaptic activity to the biochemical machinery of a neuron. These features make its regulation a critical process in neurons, which have developed extensive and intricate Ca^{2+} signaling pathways[229]. Over the last decades, it is becoming obvious that the excess synchronization of neurons that is characteristic for seizures can be linked to various calcium signaling pathways, making it increasingly recognized as an important factor in epileptogenesis.

Epileptogenesis is associated with changes in various cellular and molecular processes, including neuronal death, neurogenesis, reactive astrogliosis, microglia activation, and the upregulation of inflammatory mediators[230]. While understanding epileptogenesis is critical for advancing epilepsy research, studying it in humans presents significant challenges due to the heterogeneity of epileptogenic injuries, long latent periods lasting months to decades, and the confounding effects of anticonvulsant treatment after the first spontaneous seizure. To overcome these limitations, animal models of epilepsy have proven indispensable in elucidating the physiological and behavioral changes associated with human epilepsy[231,232]. These models have also played a crucial role in the discovery of many AEDs. However, working with animal models of epilepsy requires a substantial number of animals, and data collection is often slow due to the extended latent period until seizures manifest[233].

3.3 Hippocampal Organotypic Slice Cultures (hOTCs)

For the development of our final objective and be able to preserve normal neurogenesis by acting on the neuroinflammatory response, we therefore discarded the direct use of animal models and opted for a novel system in our lab: hippocampal organotypic slice cultures (hOTCs). This technique combines many of the benefits of long-term culture with the preservation of much of the normal connectivity found in acute brain slices. It is a valuable tool that represents a complex multicellular *ex vivo* environment and enables investigators to carry out studies where *in vivo* experiments are impractical, but where it is desirable to preserve the neuronal connectivity found in a living organism. Hence, this system enables investigators to gain a better assessment of an experimental strategy before beginning time-consuming *in vivo* experiments.

Several methods can be used to prepare slice cultures[234,235]. In most cases, they are prepared from young or neonatal rodent brains and may be cultured for weeks or even months, as long as they have the appropriate sterility, oxygen (O_2), culturing media, and temperature control[234]. Simple culture dishes will sustain slice cultures for a few days while placing slices either on semi-permeable membranes at the surface of the culture medium or stuck to a glass coverslip in a roller tube[234]. These methods offer controlled environments for preserving the integrity of the slices and enable to investigate neural development, synaptic plasticity, and other dynamic processes within a well-controlled experimental setup. These cultures preserve the three-dimensional architecture and local environment of brain cells, including neurons and astrocytes, as well as neuronal connectivity and the complex glial-neuronal interactions. Indeed, this system is chosen primarily because it is believed to preserve the connectivity of the tri-synaptic hippocampal circuit[236].

The neuronal network is known to be heavily influenced by environmental experiences[131], and this would reasonably suggest that the development of hippocampal neurons maintained in slice culture might be radically different from the development of the same cell type inside the living animal. However, cells in hOTCs develop and mature largely similarly to their *in vivo* counterparts, as there are surprisingly few differences between CA1 pyramidal cells developed in hOTCs and pyramidal cells that had developed normally in the living animal[237]. Even in measures where organotypic and acute CA1 neurons differed, their change over time in slice cultures was found to be proportionally similar to the change occurring *in vivo*[237]. These findings suggest that hOTCs serve as a remarkably faithful representation of the *in vivo* environment for CA1 pyramidal cell development.

3.3.1 Epileptiform Slices

The hOTCs system is therefore an outstanding option for assessing neurogenesis; however, our interests rely on a further step: we need not just regular hOTCs but epileptiform ones that allow us the characterization of aberrant neurogenesis and its posterior prevention by the use of different drugs. Actually, hOTCs are considered an excellent model to study neuroprotection[238] and are used as a starting point for drug discovery[239], which makes them very appealing for epilepsy research due to the noncompliance with AEDs being one of the causes for developing SE[240]. In response to SE, the frontline treatment typically involves administering benzodiazepines like lorazepam and midazolam, which work by enhancing inhibitory transmission in the brain through the promotion of GABA function[241]. However, despite their initial effectiveness, the efficacy of benzodiazepines is often incomplete and tends to diminish over time during seizures. This decrease in effectiveness is attributed to internalization or desensitization of the $GABA_A$ receptor ($GABA_AR$), which is the target of benzodiazepines[242]. $GABA_AR$ activation plays a crucial role in inhibiting targets that express them, making them essential for various brain functions, including cognition and emotion.

Within the CNS, two predominant subclasses of $GABA_ARs$ are notable, often coexisting within the same cell type. γ2-containing receptors are typically situated at synapses, contributing to phasic inhibition elicited by the synaptic release of GABA. In contrast, δ-containing receptors are found in more specific neuronal populations, mediating tonic currents in response to ambient GABA and a slow component of inhibitory postsynaptic currents (IPSCs)[243,244] The distinctive features of both $GABA_AR$ subclasses make them attractive targets for therapeutic interventions in diverse scenarios, highlighting their potential in modulating neural activity for therapeutic purposes. Despite the use of these and other medications, a significant proportion of patients may still fail to respond, leading to a condition known

as refractory epilepsy or even worsening further, progressing to super-refractory epilepsy[245]. Managing SE can be challenging, particularly when patients do not respond well to frontline or second-line treatments.

Hence, ongoing research is crucial for better understanding the underlying mechanisms of SE and developing more effective therapeutic strategies to improve outcomes for patients facing this critical condition. For this reason, *ex vivo* models have emerged as a promising technique, as they allow a detailed and well-controlled research of the mechanisms of epileptogenesis, while still preserving the network phenotypic features of epilepsy. Particularly, they can mimic the development of spontaneous seizures[246], as they can develop interictal and seizure-like bursts[247,248], perhaps due to the sprouting of new synaptic connections following the deafferentation inherent in the slicing process[249]. Certainly, hOTCs have proven to be a valuable experimental model for studying epilepsy-related field potential activity[250,251], observing the development of epileptiform activity that closely resembles the characteristics of *in vivo* epilepsy. Notably, this model exhibits sensitivity to anticonvulsants and shows an increase in seizure incidence over time. The detailed characterization of spontaneous interictal and ictal-like events within this system has positioned it as an invaluable tool for investigating the intricate mechanisms underlying epileptogenesis.

Additionally, a direct model of symptomatic seizures can be obtained in this kind of culture thanks to a variety of drugs and other agents that increase activity in these *in vitro* conditions. The earliest report of the use of slice cultures in epilepsy research comes from the early 1970's, when the *in vitro* hippocampal slice preparation was secured as a reliable tool for analyzing the cellular and pharmacological mechanisms underlying epileptiform synchronization, as paroxysmal activity was shown to be induced by bicuculline, strychnine or repetitive stimulation in hOTCs[252,253]. During the last decades, we have witnessed the introduction of different *in vitro* preparations such as extended brain slices, the whole isolated hippocampus, as well as the isolated whole-brain, models that have demonstrated to be able to reproduce *in vitro* epileptiform events resembling the electrographic interictal and ictal activities occurring in the electroencephalography (EEG) of epileptic patients. As it has been largely performed in acute slices, epileptiform activity has been induced in non-epileptic hOTCs by $GABA_AR$ antagonist, glutamatergic agonists, or K^+ channel blockers[254–256], and also as a result of blocking neuronal activity for several days, presumably due to homeostatic changes in receptors following the silencing of the neuronal population[257].

In our studies in particular, the $GABA_AR$ antagonist picrotoxin (PTX) has been employed as an epileptogenic agent for the hOTCs. In terms of structure, PTX differs significantly from GABA, which is a simple and small amino acid[258]. Instead, PTX is a polycyclic compound with no nitrogen atom. Regarding its mechanism of action, it prevents the operation of $GABA_AR$, a member of the cys-loop, ligand-gated ion channel superfamily responsible for mediating the inhibitory effects of GABA.

The GABA mediated activation of this receptor typically leads to the ion flow through the chloride channel into the neuron, resulting in hyperpolarization and inhibition of neuronal activity. Unlike the competitive GABAR antagonist bicuculline, PTX is clearly a noncompetitive antagonist, acting not at the GABA recognition site but binding to a different site within the ion channel. An antagonist, by definition, is a substance that binds to a receptor without activating it (Figure I5.1). Instead of promoting a response as an agonist that mimics the action of the body's natural signaling molecules, an antagonist blocks or dampens the receptor's activity. Unlike competitive antagonists, which compete with agonists for the same binding site on the receptor, non-competitive antagonists work by binding to a site on a receptor that is distinct from the agonist-binding site (Figure I5.2). This interaction leads to the inhibition of the receptor's channel, in the case of the $GABA_AR$ blocking the passage of chloride ions through the ion channel in the cell membrane. Therefore, the PTX-induced blocking of the GABA-activated chloride ionophore prevents the inhibitory effects of GABA, leading to an excitatory influence on the neuron. This disruption of the normal inhibitory balance in the brain can result in hyperexcitability and can manifest as convulsions or seizures, further underscoring the critical role of GABAergic inhibition in maintaining the delicate balance of neuronal activity in the CNS.

1. Agonists and Antagonists

Agonist – a molecule that binds to a receptor causing activation
Antagonist - a molecule that occupies a receptor but does not activate it and attenuates the action of an agonist

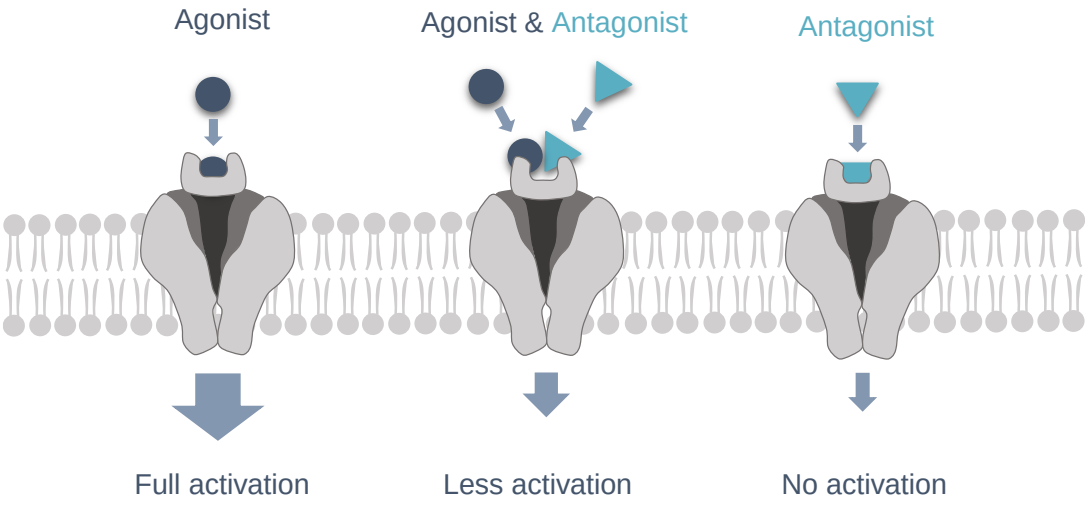

2. Types of antagonists

Natural ligand – a hormone, neurotransmitter
Antagonist - a molecule that occupies a receptor in the ligand site or in other site and does not activate it

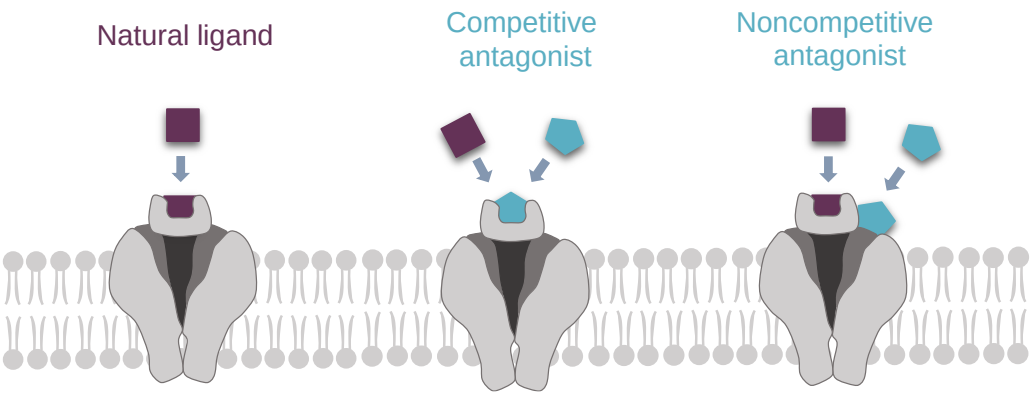

Figure I5. Agonist and Antagonist of Ligand Binding to Receptors. (1) Illustration of the mechanism of action of agonists that generate full activation of the receptor, agonist and antagonist at the same time generating less activation and the antagonist, which inhibits the activation of the receptor. **(2)** Diagram of the function of competitive antagonists occupying the receptor at the ligand site and the noncompetitive, that binds at a different site than the natural ligand.

3.4 GABAergic Neurons in Epilepsy

Within the adult CNS, GABA is the primary inhibitory neurotransmitter, however, during fetal development, it acts as an excitatory neurotransmitter[222,259,260]. GABA is thought to be the first neurotransmitter active within the developing brain, and plays a role in the proliferation of NPCs[261,262]. GABAergic interneurons are a specific type of GABAergic cell that plays a critical role in the regulation of neural activity in the brain. These cells provide inhibitory input to other neurons in the brain and are essential for maintaining the balance between excitatory and inhibitory neurotransmitters[263]. In epilepsy, alterations in the function and number of GABAergic interneurons have been observed in both animal models and in human patients[220,264–266], and these changes may contribute to the development and maintenance of epileptic seizures[267,268].

The vast literature on epilepsy and interneurons covers a wide range of phenomena observed in epileptic patients, from the complex mechanisms driving epileptogenesis and the related structural alterations, to the significance of high-frequency oscillations in maintaining ictal discharges. Seizures are the visible result of abnormal synchronized neural activity in the brain, which is believed to be caused by an imbalance in excitation and inhibition, involving a wide array of GABAergic interneurons, with a particular focus on their malfunction[257]. Typically, inhibitory interneurons play a crucial role in countering excessive excitation within the brain, but this regulatory system occasionally fails, leading to unrestrained excitatory activity[269]. During seizures, the disruption of the balance between excitatory and inhibitory neurotransmission causes a cascade of hyperactive neuron firing, in which GABAergic interneurons that usually help maintain stability, can be affected, contributing to the breakdown of inhibitory control[147]. This loss of restraint allows the spread of excitation throughout the brain, giving rise to seizures[220]. This concept is reinforced by findings where experimental reduction of inhibition, achieved by blocking GABAergic neurotransmission, triggers epileptiform activity in both *in vitro* and animal models[270].

The involvement of the GABAergic system in generating interictal spikes is supported by compelling evidence from various sources. Firstly, studies using *in vitro* models have demonstrated that solely blocking ionotropic glutamate receptors fails to suppress interictal spikes. However, when a combination of glutamate and $GABA_A$ receptor antagonists is used, interictal spikes are effectively suppressed[271,272]. Secondly, investigations into the temporal relationship between neuronal activity and interictal episodes in humans have revealed intriguing patterns. Activity in putative interneurons has been observed to precede interictal discharges, while pyramidal neuron activity coincides with their onset[273]. These findings emphasize the critical role of the GABAergic system in modulating interictal spike generation and provide valuable insights into the underlying mechanisms of epilepsy.

While the evidence supporting a failure of GABAergic inhibition is compelling, it is essential to consider the diversity of interneurons when interpreting these findings. Within the cortex, more than 20 distinct interneuron subtypes have been identified, exhibiting a broad range of electrophysiological properties, morphologies, genetic markers, innervation patterns, and GABAergic signaling profiles[274]. To better understand these complexities, molecular markers such as somatostatin (SOM), vasointestinal neuropeptides (VIP) or calcium-binding protein parvalbumin (PV) have been broadly employed. In particular, PV^+ interneurons are one of the most well-known subtypes of GABAergic interneurons. They are considered critical components of the inhibitory circuitry in the brain, being particularly vulnerable to epilepsy-associated insults such as hypoxia, ischemia, or seizures[275]. These molecular markers help distinguish between interneuron subtypes primarily responsible for somatic inhibition, dendritic inhibition, and disinhibition, respectively[274].

3.4.1 The GABAergic Stage of Newborn Neurons

In the GABAergic system, also newborn GCs have been observed to express GABA. Although hippocampal GCs are predominantly glutamatergic neurons[276], it has been established that they not only release glutamate, but also express markers of the GABAergic phenotype and release GABA during development[277–281]. This intriguing observation has been confirmed in both juvenile animals[280] and the epileptic DG in adult subjects[279]. Such coexistence of two distinct, fast-acting ionotropic neurotransmitters with opposing post-synaptic effects within GCs suggests a duality in their function. It advocates that GCs might possess the ability to switch neurotransmitter modality during the postnatal developmental stages and under pathological conditions[281]. However, studying GCs presents a challenge due to their delayed and heterogeneous maturation process. A substantial portion of GCs, more than 80%, undergoes differentiation during the initial weeks after birth[282], and neurogenesis persists within the SGZ of the DG throughout an individual's lifetime[47]. The hippocampal DG serves as a relay of cortical signals directed to the hippocampus. Here, GCs are its primary neurons, which extend their intricate axonal extensions via the mossy fiber (MF) pathway to establish excitatory glutamatergic synapses onto the pyramidal cells and local inhibitory interneurons within the CA3[283]. When neural activity is triggered, especially during the early postnatal weeks, it is likely to engage MFs originating from a remarkably varied array of GCs, each at different stages of differentiation[284].

The GCs serve as essential mediators of synaptic communication, relaying signals from the entorhinal cortex to both the hilus and Ammon's horn through their output MF axons. This process is highly dependent on the specific target of the neural pathway, resulting in a fascinating phenomenon of compartmentalization. Interestingly, the plasticity of this dual neurotransmitter release is not

uniform across the neural landscape. Instead, it demonstrates a finely tuned variability that is specific to the target destination of the signals. Adding to the complexity of this interplay is the concept of counterbalanced compensatory plasticity. This phenomenon is particularly striking as it involves the concurrent modulation of two distinct neurotransmitters released by separate terminals within the same neural pathway, and the balance ensures that any changes or fluctuations in the release of one neurotransmitter are counteracted by adjustments in the other[222]. This regulatory mechanism finely tunes neural communication, maintaining equilibrium within neural networks.

The intriguing synthesis of GABA by recently born GCs occurs within a restricted time window between the 2nd and the 4th week of the postmitotic phase, contributing to the evolving landscape of GC differentiation[259]. However, in the third week of life, the ability to trigger simple GABAergic responses in pyramidal cells using MF activation changes, and the markers for GABAergic activity in GCs and the corresponding GABAergic responses start to diminish. During the period of expression of these markers, they serve as indicators of the GABAergic nature of GCs that actively participate in the GABAergic signaling pathway, contributing to the complex balance of neurotransmission within the brain. In this context, the expression of GAD67, an enzyme crucial for GABA synthesis, emerges as an intriguing marker for the later stages of GC development, contributing to the complex neural network of the hippocampus. Furthermore, these young GCs integrate themselves synaptically within the hippocampal network, thereby becoming functional components of the neuronal circuitry. This aspect not only adds depth to our understanding of GC development but also underscores the remarkable plasticity and adaptability of the nervous system during its formative stages, opening up exciting avenues for exploring the dynamic and adaptive nature of GCs in response to different developmental stages and pathological challenges.

3.5 ATP and Purinergic 2X Receptors (P2XR)

3.5.1 ATP in the Brain

The adenosine triphosphate or adenosine-5'-triphosphate, commonly known as ATP, plays a key role in regulating hyperexcitability and epileptogenesis[285]. ATP is a crucial nucleotide that serves as a neurotransmitter and modulator within the CNS. Over the past three decades, numerous studies have recognized ATP's significance in cellular communication[286–288], and in the course of evolution, ATP likely emerged as the first extracellular signaling molecule due to its widespread availability. As a result, almost every known cell or single-cell organism possesses some degree of ATP sensitivity[289]. In the CNS, ATP acts as a ubiquitous modulator of cellular functions, exhibiting various essential roles such as exerting a crucial influence on cell proliferation, particularly in astroglial cells, as it promotes the generation of reactive astrocytes[290]. Furthermore, ATP plays a crucial role in controlling and regulating various pathological reactions of glial cells, including reactive gliosis and microglial motility and activation[291]. Still, ATP released during brain injury exhibits a dual nature, with both neuroprotective and pathophysiological effects. Certain responses to ATP provide neuroprotection, as the activation of respective receptors by released ATP can modify transmitter release leading to various functional responses, including necrosis, apoptosis, and also regeneration processes. However, under specific circumstances, ATP can also contribute to the damaging processes triggered during pathology[292]. The strong interaction between ATP and glutamatergic systems suggests that ATP-evoked release of glutamate might contribute to the deleterious consequences of high ATP concentrations[293].

This occurs during various pathological conditions and CNS insults apart from epileptogenic seizures, such as trauma, ischemic stroke, cellular stress, neuroinflammation, and neurodegenerative disorders, in which there is an abnormal release of ATP to the extracellular region[294]. In the case of epilepsy, the balance of the purines (ATP/adenosine) is imperative to determine neuronal excitability. However, ATP release during seizures is so complex that it is yet to be studied, in contrast to the potential role of adenosine as an anticonvulsant that was determined much earlier than the function of ATP in the epileptogenic process[295–298]. Despite the difficulties, there is now evidence linking extracellular ATP (eATP) to increased hyperexcitability during seizures, and it has been revealed not only in epilepsy mouse models but also in human brain tissue slices *ex vivo*[297,299–301]. In brief, during epileptogenesis, eATP concentrations increase while it functions as a ligand to purinergic receptors[285]. The intracellular cytosolic ATP concentration remains at a relatively high level, typically ranging between 5 and 10 mM. In contrast, the extracellular space contains a significantly lower concentration

in the nanomolar (nM) range, and abrupt changes may turn ATP into an excitotoxin, making it potentially harmful. By acting as a diffusible danger signal, it initiates a cascade of events that can ultimately lead to neuronal and tissue damage[302], triggering at the same time responses to damage and initiating repair processes[191]. This excess of eATP induces reactive astrogliosis, with morphogenic and mitogenic changes in astrocytes possibly triggered by synergistic interactions between purines, pyrimidines, and growth factors[290], which also induces the release of inflammatory cytokines, such as interleukins IL-1β, IL-6, or TNF-α, by microglia, further contributing to cellular damage[292].

3.5.2 Purinergic Receptors

Therefore, this made us hypothesize that acting on neuroinflammation by reducing the excess of ATP through the inhibition of purinergic receptors could have neuroprotector effects. The dysregulation of eATP levels and its interactions with glutamatergic systems and purinergic receptors can lead to detrimental consequences, and this excessive ATP release has been observed to be mediated by the ATP-activated purinergic receptors[303]. These receptors play vital roles in the CNS, actively participating in cellular neuroinflammatory responses that regulate the functions of neurons, microglial cells, and astrocytes. There are two main types of purinergic receptors: P2s are the ones responding to ATP, while P1s refer to adenosine-binding receptors. The first ones are divided into two groups based on their sequence homology, pharmacology, and mechanism of action: the ionotropic (P2XR) and metabotropic (P2YR) receptors, present and effective on both neurons and glial cells[304] (Fig. I5).

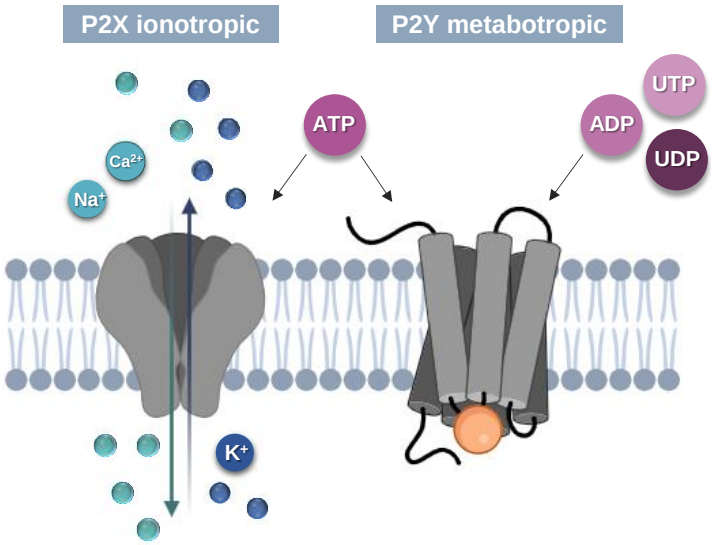

Figure I5. Purinergic signaling. The interaction between ATP and P2X receptors triggers a significant conformational shift, leading to the unblocking of the channel's pore. This alteration facilitates the influx of Ca^{2+} and/or Na^{+} ions while enabling the efflux of K^{+} ions from the cell[305]. In contrast, the binding of ATP, ADP, UTP, or UDP to P2Y receptors initiates distinctive G protein signaling cascades. The specific G protein associated with each receptor (in orange) dictates the nature of the signaling pathway activated[306]. (Adapted from Björkgren and Lishko, 2016).

The ionotropic receptors are all activated by their main endogenous agonist, ATP, and are expressed in all cell types, where they play critical roles in a wide array of physiological and pathophysiological processes. They comprise a family of seven fast-acting subreceptors, namely P2X1 to P2X7. These receptors are nonselective cation-gated channels that display heightened Ca^{2+} permeability upon activation by eATP. Numerous studies have suggested alterations in the expression of P2XR under conditions related to neuroinflammation, nerve transmission, and pain sensation, and their activation has also been linked to various pathological disorders of the CNS including neurodegeneration. Indeed, excessive stimulation of P2XR can also indirectly activate macrophages, microglia, or astrocytes[292], and in situations such as brain injury, the rapid release and diffusion of eATP or uridine triphosphate (UTP) from damaged cells trigger microglial activation[307]. Consequently, this leads to significant changes in the expression of several purinergic receptors in the brain.

Among the various subtypes of P2XR, P2X7R has gained particular attention as a promising therapeutic target for brain disorders, prompting numerous research studies in this area. Although remaining controversy has been observed regarding the cell type specificity of the P2X7R subtype[308,309], under normal physiological conditions its presence has been confirmed to be restricted to endothelial cells, microglia, oligodendrocytes, NPCs, and neuronal presynaptic termini[310–312]. Actually, P2X7Rs have been found to regulate multiple aspects of the neurogenic process (Fig I6), with their most notable function being the induction of cell death through pore formation[297,303]. However, the cellular debris resulting from this process can be cleared by NPCs and neuroblasts via P2X7-mediated phagocytosis, along with the involvement of resident microglia, which may also utilize P2X7 for phagocytic activities[309]. Additionally, the receptor appears to have potential roles in the regulation of cell proliferation, differentiation, and axonal extension during hippocampal neurogenesis[308,309,313]. The intricate interactions of P2X7Rs within the hippocampal neurogenic niche highlight their importance in shaping the dynamics of neurogenesis.

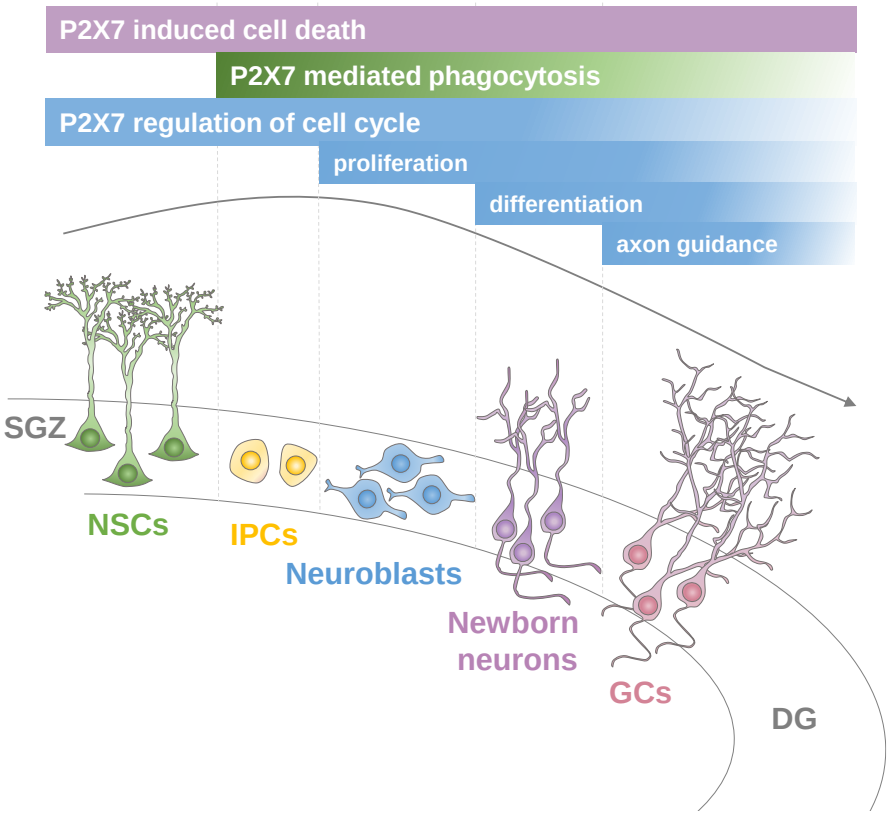

Figure I6. P2X7 receptors play a significant role in influencing the hippocampal neurogenic niche. The process begins with type 1 NSCs undergoing asymmetric division in the subgranular zone (SGZ), where P2X7Rs induce cell death and influence the regulation of the cell cycle, in which these NSCs then differentiate into proliferative type 2 cells, also known as intermediate progenitor cells. These receptors also help in the next stages of proliferation and differentiation that involves type 3 neuroblasts migrating to the granule cell (GCs) zone. Finally, they act in the axon guidance as immature neurons extend axons, known as mossy fibers, to the CA3 region before integrating into existing synaptic transmission pathways. (Adapted from Leeson *et al.* 2019).

Regarding its expression in hyperexcitability, P2X7R is consistently upregulated post-SE at both the transcriptional and expressional level in mouse models[228,311], as well as in clinical evidence from TLE patients' tissue[314,315]. Among the P2XR family, P2X7R has attracted most attention as a potential drug target in epilepsy because of its unique structural and functional characteristics. Its low affinity to ATP makes it a particularly attractive therapeutic target for the use of antagonists, which have shown a potential reduction in epileptogenic features and neurodegeneration in several studies[297,314,316]. Except for P2X7R, which requires high ATP concentrations (hundreds of μM) for activation due to its aforementioned low affinity, other P2XR subtypes are typically activated at ATP concentrations ranging from high nM to low μM levels[317]. The upregulation of P2X3, P2X4, and P2X7 receptors has been observed in CNS disorders, suggesting that their antagonists hold potential therapeutic options for treating CNS diseases, including neurodegenerative conditions and brain injuries[318,319]. In the CNS, P2XR contribute to the modulation of neurotransmission, neuron-glia communication, and apoptosis, while they have been shown to have significant effects on immune responses and the inflammatory process[320]. In the case of epilepsy, high ATP concentrations are known to be generated, and therefore, we hypothesize that a P2XR inhibitor would reduce this during epileptogenesis, restoring neurogenesis.

3.6 Inflammation in the CNS

Being the neuroinflammatory response our main target, it is relevant to dive into the complex world of inflammation in the CNS to have a clear idea of its magnitude in neuropathological disorders. Certainly, inflammation has emerged as a key common event during brain disease, with increasing implications in the development of neurological and neurodegenerative disorders over the years. In response to stress, injury, or infection, inflammation occurs as a complex defense mechanism, serving to clear dead and damaged cells and restore the affected area to a normal state[321]. In the brain, the presence of the blood-brain barrier (BBB) selectively limit the entry and exit of certain molecules and cells, as a protection against insult[322]. Under normal conditions, only macrophages and dendritic cells can enter the CNS[323]. Still, after brain injury, the release of disease-associated proteins, environmental toxins, and uncontrolled cell death initiates an inflammatory process involving resident microglia, astrocytes, and in many cases, infiltrating peripheral macrophages and lymphocytes. These cells respond to inflammation by releasing a wide range of anti-inflammatory and pro-inflammatory molecules, including cytokines such as TNF-α, IL-1β, IL-6, chemokines, neurotransmitters (e.g., glutamate, ATP), and ROS like NO[321,322].

The severity and duration of inflammation, ranging from mild and acute to chronic, lead to varying responses in the brain. While inflammation serves as a protective response against insults, uncontrolled expression of cytokines in the DG can inhibit neurogenesis[322]. Inflammation-induced reduction of hippocampal neurogenesis has been observed in several models of neuro-pathologies such as in spinal cord injury and acquired or genetic epilepsy[208,324,325]. Despite some controversies and discrepancies arising from the use of different experimental models, a majority of *in vitro* experiments consistently demonstrate that pro-inflammatory cytokines suppress NPC proliferation[326]. Furthermore, it has been observed that elevated cytokine levels can induce apoptosis in newborn neurons[327] and also trigger ROS-derived OS, an initial marker of neuro-glial inflammatory response, causing direct damage to developing neurons.

3.6.1 Reactive Oxygen Species (ROS) and Oxidative Stress (OS)

In the process of acting on neuroinflammation, the possibility of directly targeting ROS in order to reduce OS came out as a vigorous objective. But first, what are these oxygen species made of and why do we call them reactive? Briefly, ROS encompass O_2-derived free radicals, including the superoxide anion ($O_2^{\bullet-}$) and hydroxyl radical (•OH), as well as non-radical molecules like hydrogen

peroxide (H_2O_2)[328]. These ROS are produced as by-products of metabolism in various subcellular locations, such as mitochondria, endoplasmic reticulum, peroxisomes, plasma membrane, and cytosol[329–331]. Exposure to pathogens, harmful chemicals, heat, ultraviolet (UV) radiation, and heavy metals can damage mitochondria and trigger cycles of ROS production, resulting in increased cellular ROS levels[332]. Due to their high reactivity, at high concentrations, they can inflict damage to deoxyribonucleic acid (DNA), proteins, and lipids, and disrupt the plasma membrane, ultimately leading to cell death[328,333]. Oxidative damage is associated with various pathological conditions, including major neurodegenerative diseases like AD and PD, muscular dystrophy, chronic inflammation, tissue injury, diabetes mellitus, and cancer[334,335]. The reciprocal stimulation of OS and inflammation significantly contributes to the chronic nature of these illnesses. To protect against the deleterious effects of oxidative damage, healthy cells are equipped with dedicated protective mechanisms, such as antioxidant synthesis. Antioxidants can be either enzymatic, like superoxide dismutase (SOD), catalase, and glutathione peroxidases, or non-enzymatic biochemicals, such as flavonoids, ascorbic acid, tocopherol, and others[328,336]. These antioxidants help to maintain the cellular ROS concentration within an appropriate physiological range.

Under normal physiological conditions, O_2-utilizing organisms maintain a delicate balance between the production of ROS and their removal through antioxidant defense systems in cells and their microenvironment. Indeed, reactive O_2 and nitrogen species play a crucial role in microglial-driven inflammation[337]. While ROS can be damaging to macromolecules due to their high reactivity, their production as by-products during normal metabolic processes is a necessary compromise in the search for efficient energy production[338]. Moreover, controlled low levels of ROS play a crucial role in regulating redox-sensitive proteins involved in essential biochemical reactions, such as growth factor-induced cell proliferation, differentiation, and survival[339]. However, when conditions lead to excessive production of ROS or a weakened antioxidant defense system, OS occurs, resulting in disruptions to cellular homeostasis. Acute exposure to OS, such as during infections, inflammation, radiation exposure, or exposure to redox-generating chemicals, can lead to apoptotic cell death or, in severe cases, necrotic cell death[200]. Upon removal of the OS-inducing agents, cellular homeostasis may be restored, nonetheless, in certain situations, elevated levels of OS can persist chronically[334].

Depending on the balance of redox states, the altered redox homeostasis can have diverse effects on various cellular functions and influence cell fate decisions. One critical biological process affected by OS is adult neurogenesis, risking its vital role in maintaining neuronal plasticity and sustaining neurocognitive functions. Thus, the neurogenic microenvironment is exceptionally sensitive to OS and other forms of reactive species. Among them, NO stands out as the most extensively studied and understood, as the NPCs in the SVZ are situated near cells that produce NO[340]. This spatial proximity is critical for NO signaling due to its highly reactive nature and short lifespan, lasting only a few seconds. Research has demonstrated that NO is linked to decreased neurogenesis, as evidenced by the

reduced proliferation of NPCs isolated from the SVZ[341]. This finding underscores the significance of understanding the interplay between reactive species and neurogenesis in the context of microglial-driven inflammation. Research in this area is pivotal for identifying ways to protect and support the neurogenic niche and preserve the vital process of adult neurogenesis in the face of OS and related challenges.

3.6.2 Cerium Oxide Nanoparticles (CeO_2NPs)

Therefore, several studies have been conducted for the search of inert biological molecules able to reduce OS during these pathological processes. For that, our spotlight was put on the cerium, an intriguing rare earth metal situated in the lanthanide series of the periodic table that when combined with O_2 to form nanoparticles (NPs), cerium oxide (CeO_2) adopts a fluorite crystalline structure, providing it with remarkable antioxidant properties[342]. Cerium oxide nanoparticles (CeO_2NPs) exhibit remarkable electron buffering capacity in redox environments owing to their facile transition between Ce^{3+} and Ce^{4+} states[343], accompanied by O_2 capture or release (Fig I7). Consequently, these NPs function as effective electron sponges, mitigating the detrimental effects of ROS. Hence, there is growing interest in CeO_2NPs within the size range of 3–50 nm, owing to their active involvement in biochemical redox reactions, where they serve as sites for effective free radical scavenging and inflammation reduction[344,345]. Notably, these NPs have demonstrated the ability to provide cellular protection by effectively mitigating oxidative and nitrosative stress in living organisms. As a result, they present a promising alternative approach with potential therapeutic opportunities for managing physiopathological processes that lead to chronic inflammation[346].

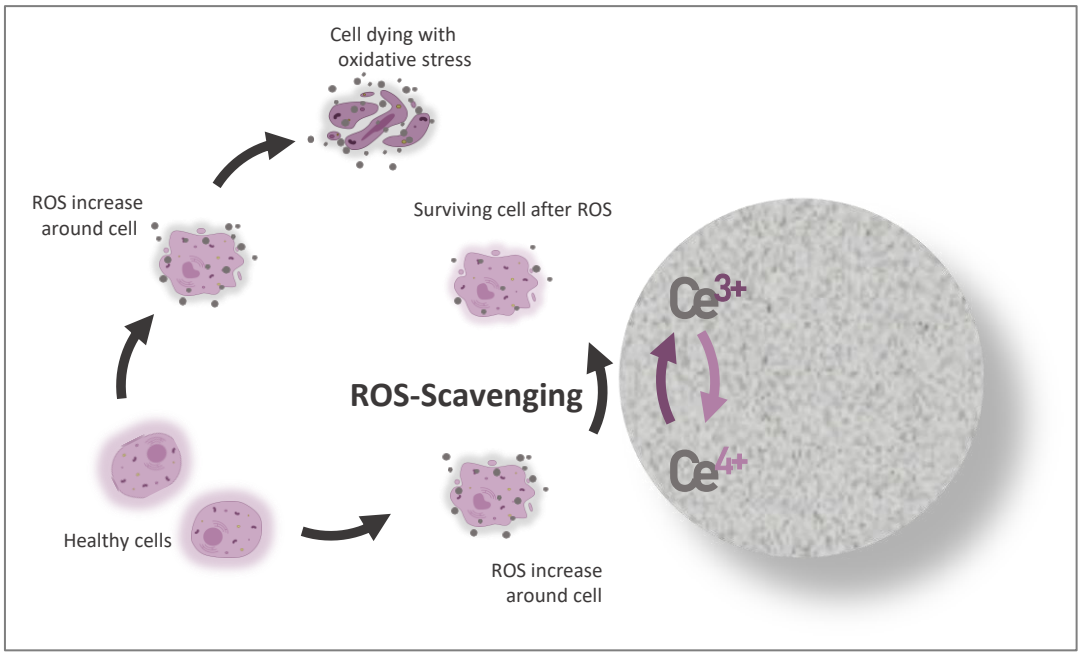

Figure I7. Schematic illustration of cerium oxide nanoparticles (CeO_2NPs) possessing antioxidant properties towards ROS around cells. When healthy cells are attacked by ROS, OS kills them. Instead, thanks to the scavenging properties of CeO_2NPs, cells can survive after ROS attack.

The therapeutic potential of CeO_2NPs is primarily derived from their ability to effectively reduce levels of ROS and, consequently, various inflammatory mediators, including inducible nitric oxide synthase, nuclear factor κβ, tumor necrosis factor-α, and interleukins[345,347,348]. Moreover, it has been revealed that CeO_2NPs possess multi-enzyme mimetic properties, acting as potent SOD, most pronounced when cerium is in its oxidized state (Ce^{4+}), and catalase and peroxidase mimetics, most evident when cerium is reduced (Ce^{3+}), broadening their applicability in various medical domains[344]. The natural SOD is responsible for catalyzing the disproportionation of the $O_2^{\bullet-}$, generating O_2 and H_2O_2. This catalytic process relies on the electron exchange between the oxidized state (Mn^{+1}) and the reduced state (Mn) of the metal center[349] (1).

$$M^{(n+1)+}\text{-SOD} + O_2^{\bullet-} \longrightarrow Mn^{+}\text{-SOD} + O_2 \qquad (1)$$

$$Mn^{+}\text{-SOD} + O_2^{\bullet-} + 2H^{+} \longrightarrow M^{(n+1)+}\text{-SOD} + H_2O_2$$

In the case of nanoscale CeO_2, the SOD-mimicking activity is directly influenced by the Ce^{3+}/Ce^{4+} ratio present on the NP surface. A higher Ce^{3+}/Ce^{4+} ratio corresponds to an enhanced SOD-mimicking activity, effectively promoting the conversion of $O_2^{\bullet-}$. Conversely, as the Ce^{3+}/Ce^{4+} ratio decreases, the SOD-mimicking activity is inhibited and transforms into catalase/peroxidase-mimicking activity[350]. This transition in activity highlights the significance of the surface Ce^{3+}/Ce^{4+} ratio in modulating the biomimetic behavior of nanoscale CeO_2 and its potential applications in diverse catalytic processes.

The overall activity of CeO_2NPs is significantly dependent on the ratio of Ce^{3+}/Ce^{4+}, which can provide insight into its pro-oxidation and antioxidant activity[351].

Regarding the peroxidase-mimicking properties of CeO_2NPs, it is known that the catalytic activity is closely linked to the specific surface area and surface O_2 content[352]. The presence of surface defects, primarily O_2 vacancies, plays a vital role in regulating the supply of O_2 to the reaction site. Notably, increasing the concentration of Ce^{3+} on the surface of CeO_2NPs enhances its ability to mimic the activity of peroxidase (2).

$$Ce^{3+} + H_2O_2 + H^+ \longrightarrow Ce^{4+} + OH^\bullet + H_2O \quad (2)$$

$$OH^\bullet + H_2O_2 \longrightarrow HO_2^\bullet + H_2O$$

$$Ce^{4+} + HO_2^\bullet \longrightarrow O_2 + Ce^{3+} + H^+$$

Finally, in various studies, CeO_2NPs have emerged as a fascinating mimic of catalase. This enzyme plays a vital role in neutralizing the potentially harmful oxidant, H_2O_2, as it effectively catalyzes the decomposition of H_2O_2 into harmless water and O_2. This remarkable property allows it to shield cells from OS caused by ROS. CeO_2 in its Ce^{4+} state exhibits catalase-like activity, converting H_2O_2 into O_2 and H^+, which results in a change in valence state to Ce^{3+} along with alterations in O_2 vacancies (3).

$$2Ce^{3+} + H_2O_2 + 2H^+ \longrightarrow 2H_2O + 2Ce^{4+} \quad (3)$$

$$Ce^{4+} + H_2O_2 \longrightarrow Ce^{3+} + H^+ + HOO^\bullet$$

$$Ce^{4+} + HOO^\bullet \longrightarrow Ce^{3+} + O_2 + H^+$$

$$2Ce^{4+} + H_2O_2 \longrightarrow 2Ce^{3+} + O_2 + 2H^+$$

Further research has demonstrated that CeO_2NPs mimic the activity of both SOD and catalase, attributing this behavior to its reversible switching capability between Ce^{3+} and Ce^{4+} (Fig 7) and the high mobility of surface O_2[353].

While nanoceria has long been utilized in industrial applications such as O_2 sensors and automotive catalytic converters, its potential in mitigating OS in various biological model systems has only recently been explored. Certainly, in the field of cardiology, intravenously administered CeO_2NPs have shown promise in a transgenic murine model of cardiomyopathy, effectively reducing myocardial OS, endoplasmic reticulum stress, and suppressing the inflammatory process, thereby offering protection against the progression of cardiac dysfunction[354]. In oncology, CeO_2NPs have demonstrated antioxidant properties that successfully protect cells from radiation-induced damage[355]. Similarly, in the case of neurodegenerative diseases, studies have highlighted the beneficial effects of CeO_2NPs,

where they exhibit the just explained SOD mimetic activity[342] (1), catalase mimetic activity[351] (3), and/or NO scavenging abilities[347], whose role in neurogenesis was addressed in the previous section (3.6.1). Furthermore, CeO_2NPs exhibit a potential for targeted and localized delivery[356], providing additional avenues for their utilization in various medical applications. Overall, the diverse range of therapeutic properties displayed by CeO_2NPs positions them as promising candidates for addressing numerous medical challenges across different fields.

Given that free radicals play a prominent role in the pathology of many neurological diseases, we explored the use of nanoceria as a potential therapeutic agent for epilepsy, aiming to provide a clearer link between OS and epileptogenesis. In a state of OS, ROS trigger a cascade of neurological changes leading to the generation of spontaneous recurrent seizures[357,358]. Mitochondrial dysfunction has been identified as one potential cause of epileptic seizures[357,359], being considered a major source of ROS generation, and thus, elevated OS. The major source of ATP in neurons is provided by mitochondrial oxidative phosphorylation, and since it participates in Ca^{+2} homeostasis and ROS production, its deterioration may dramatically affect both neuronal hyperexcitability and synaptic transmission, making it strongly relevant for seizure generation[360]. There is evidence demonstrating a contribution of ATP excess to the triggering of excessive inflammation and gliosis, such as ROS, which are also a target of great interest in terms of preventing epilepsy-derived neurodegeneration. Here, we take advantage of the ROS-scavenging properties of CeO_2NPs, since they have been observed to have the capacity to increase or decrease ROS, which directly correlates with the onset or remission of inflammation[361]. Consequently, nanoceria has been shown to safely down-regulate OS by scavenging the excess of ROS in diseases such as retinal degeneration, neurological disorders (including AD, PD and Amyotrophic Lateral Sclerosis), ischemia, cardiopathies, diabetes, gastrointestinal inflammation, liver diseases and cancer, as well as in regenerative medicine and tissue engineering[362]. In the case of epilepsy, high ROS concentrations are known to be generated[363–365], and therefore, we hypothesize that CeO_2NPs would reduce this during epileptogenesis, preserving neurogenesis.

In this study, we will focus on understanding and mitigating abnormal neurogenesis in epileptogenesis by employing an *ex vivo* model of hyperexcitable hOTCs to study the effects on newborn neurons. We will assess neurogenesis and cell survival in an epileptic-like environment, as well as specific features on newborn neurons such as the morphology of their dendritic arborization and dendritic spine growth. Inhibiting newborn neuron activity, we will link neurogenesis with neuronal firing patterns and circuit synchronization. We will also target neuroinflammation during epileptogenesis by blocking purinergic receptors and by reducing ROS to test the hypothesis of recovering aberrant neurogenesis and the emergence of epileptiform activity. This study highlights the suitability of the hOTCs model for long-term studies and reveals the specific influence of aberrant neurogenesis on neural activity during epileptogenesis.

4. HYPOTHESES AND OBJECTIVES

HYPOTHESES AND OBJECTIVES

HYPOTHESIS 1: Epileptogenic hOTCs are a suitable model for evaluating aberrant neurogenesis.

Aim 1: To validate PTX-induced epileptogenic model in hOTCs as a suitable platform for assessing aberrant neurogenesis.

Objective 1.1. To evaluate the preservation of DG structure and sustained neurogenesis in hOTCs. For this purpose, we will use hOTCs in control conditions. We will evaluate the structure of the DG as well as the persistence of neurogenesis by multichannel immunofluorescence and confocal microscopy-based quantitative imaging of the slices. Neurogenesis will be assessed in different culture media and different supplementations will be tested for the optimization of the protocol.

Objective 1.2. To examine the impact of PTX-induced epileptogenesis on cell survival and aberrant neurogenesis. For this purpose, we will use hOTCs in control and epileptogenic conditions once that the protocol is optimized to maintain neurogenesis. We will analyze the amount of neurogenesis and cell death by means of confocal microscopy-based quantitative image analysis after multichannel immunofluorescence staining. The morphological complexity of newborn neurons, as well as dendritic spine features will be evaluated following RV injection.

Objective 1.3. To quantify the loss of inhibitory neurons in epileptogenic hOTCs and specifically assess the reduction in the number of GABAergic newborn neurons. For this purpose, we will use hOTCs in control and epileptiform conditions. We will measure GABA and PV expressing cell numbers by means of confocal microscopy-based quantitative image analysis. The number of GABAergic newborn neurons will be evaluated following RV injection and co-staining with GABA.

HYPOTHESIS 2: Aberrant neurogenesis contributes to the epileptogenic imprinting induced by PTX in hOTCs.

Aim 2: To determine of the implication of aberrant neurogenesis in the brain circuitry during epileptogenesis by inhibiting newborn neuron activity.

Objective 2.1. To measure changes in neural circuitry activity after silencing of newborn neuron activity in healthy and epileptogenic hOTCs. For this purpose, we will: a) inject RVDREADDs to silence newborn neurons and b) inject AAV.Syn.GCamp6f to analyze single neuron firing, pairwise firing correlations and circuit synchronizations by calcium imaging.

Objective 2.2. To investigate the effect of newborn neuron activity silencing on activity patterns in healthy and epileptogenic hOTCs. For this purpose, we will: a) inject RVDREADDs in epileptiform and healthy hOTCs; and b) use multi-electrode array-field recordings to analyze changes in hippocampal activity patterns.

HYPOTHESIS 3: ATP contributes to the induction of aberrant neurogenesis in epileptogenic hOTCs.

Aim 3: To evaluate the effect of ATP on the induction of aberrant neurogenesis in hOTCs.

Objective 3.1. To determine the impact of excessive extracellular ATP on cell survival and aberrant neurogenesis. For this purpose, we will add vehicle or ATP to hOTCs. We will analyze neurogenesis and cell death by means of confocal microscopy-based quantitative image analysis. The morphological complexity of newborn neurons, as well as dendritic spine features will be evaluated following RV-injection.

HYPOTHESIS 4: The inhibition of ATP- P2XR signaling can preserve normal oxidative stress, neurogenesis, interneurons and neuronal network activity in PTX-induced epileptogenic hOTCs.

Aim 4: To test the effect of P2XR inhibition using TNP-ATP on oxidative stress, aberrant neurogenesis, interneurons and neuronal network activity in PTX-induced epileptogenic hOTCs.

Objective 4.1. To measure the reduction of epilepsy-related OS after TNP-ATP antagonist-induced P2XR inhibition. For this purpose, we will add P2XR inhibitor TNP-ATP (or vehicle) to control and PTX-induced epileptogenic hOTCs. We will evaluate ROS in hOTCs by means of dichlorofluorescein (DCF) intensity.

Objective 4.2. To investigate the effect of inhibiting P2XR **on cell survival and aberrant neurogenesis on PTX-induced epileptogenic hOTCs.** For this purpose, we will add P2XR inhibitor TNP-ATP (or vehicle) to control and PTX-induced epileptogenic hOTCs. We will analyze the amount of neurogenesis and cell death by means of confocal microscopy-based quantitative image analysis after multichannel immunofluorescence staining. The morphological complexity of newborn neurons, as well as dendritic spine features will be evaluated following RV injection.

Objective 4.3. To quantify the recovery of GABAergic cell numbers when P2XR are inhibited in epileptogenic conditions. For this purpose, we will use hOTCs in control, epileptiform and P2XR-inhibition conditions. We will measure GABA expressing cell numbers by means of confocal microscopy-based quantitative image analysis.

Objective 4.4. To examine changes in morphological complexity of newborn neurons and their dendritic arbor development over time by 2-photon microscopy in epileptogenic conditions and after P2XR inhibition. For this purpose, we will add P2XR inhibitor TNP-ATP (or vehicle) to control and PTX-induced epileptogenic hOTCs. We will analyze the dendritic arbor growth in time-lapse recordings through 2-photon microscopy, following RV-injection.

Objective 4.5. To assess the effect of blocking P2XR with TNP-ATP on overall neural firing in the DG of epileptogenic hOTCs and specifically of newborn neurons. For this purpose, we will add TNP-ATP (or vehicle) to control or PTX-induced epileptogenic hOTCs. We will a) inject AAV.Syn.GCamp6f to analyze single neuron firing, pairwise firing correlations and circuit synchronizations by calcium imaging.; b) inject RVGCamp to analyze newborn neuron activity by calcium imaging.

HYPOTHESIS 5: ATP triggers the generation of ROS, which in turn contribute to aberrant neurogenesis in hOTCs, and its inhibition could preserve neurogenesis.

Aim 5: To evaluate the effect of inhibiting ROS on ATP-induced aberrant neurogenesis in hOTCs.

Objective 5.1. To test the effect of inhibiting ROS with CeO_2NPs on cell survival and aberrant neurogenesis on ATP-treated hOTCs. For this purpose, we will add ROS-inhibitor CeO_2NPs (or vehicle) to control and ATP-treated hOTCs. We will analyze the amount of neurogenesis and cell death by means of confocal microscopy-based quantitative image analysis after multichannel immunofluorescence staining. The morphological complexity of newborn neurons, as well as dendritic spine features will be evaluated following RV injection.

HYPOTHESIS 6: ROS are generated in excess in PTX-induced epileptogenic hOTCs which in turn would contribute to aberrant neurogenesis. ROS inhibition would preserve neurogenesis and interneurons.

Aim 6: To evaluate the effect of inhibiting ROS on PTX-induced epileptogenic aberrant neurogenesis in hOTCs.

Objective 6.1. To test ROS generation in PTX-induced epileptogenic hOTCs and its reduction with CeO_2NPs. For this purpose, we will evaluate ROS in hOTCs by means of DCF intensity in control and PTX-induced epileptogenic hOTCs after adding CeO_2NPs (or vehicle).

Objective 6.2. To examine the effects of ROS reduction by CeO_2NPs on cell survival and aberrant neurogenesis on PTX-induced epileptogenic hOTCs. For this purpose, we will add ROS-inhibitor CeO_2NPs (or vehicle) to control and PTX-induced epileptogenic hOTCs. We will analyze the amount of neurogenesis and cell death by means of confocal microscopy-based quantitative image analysis after multichannel immunofluorescence staining. The morphological complexity of newborn neurons, as well as dendritic spine features will be evaluated following RV injection.

Objective 6.3. To measure the recovery of GABAergic cell numbers in the epileptogenic state through CeO_2NP-induced ROS decrease. For this purpose, we will use hOTCs in control, epileptiform and ROS-inhibition conditions. We will measure GABA expressing cell numbers by means of confocal microscopy-based quantitative image analysis.

HYPOTHESIS 7: Inhibitory (GABA) and excitatory (glutamate) balance contribute to the decrease of the GABAergic population.

Aim 6: Investigation of the impairment of GABAergic interneurons during epileptogenesis in presence or absence of TTX, a blocker of neurotransmitter release.

Objective 7.2. To assess the impact of blocking GABAergic signaling on interneuron survival. For this purpose, we will use hOTCs in control, epileptiform and TTX-mediated silencing of neuronal firing conditions. We will measure PV expressing cell numbers by means of confocal microscopy-based quantitative image analysis.

Objective 7.3. To examine the dependence of GABAergic newborn neuron survival on the balance between glutamatergic and GABAergic input. For this purpose, we will use hOTCs in control, epileptiform and TTX-mediated silencing of neuronal firing conditions. We will measure GABA expressing cells and specifically newborn neurons by means of confocal microscopy-based quantitative image analysis.

5. EXPERIMENTAL PROCEDURES

EXPERIMENTAL PROCEDURES

5.1 Animals

All the animals were housed with *ad libitum* food and water access, in 12:12h light cycle. The University of the Basque Country EHU/UPV Ethics Committees (Leioa, Spain) and Diputación foral de Bizkaia approved all procedures under protocol M20/2015/236. All procedures followed the European directive 2010/63/UE and NIH guidelines. Nestin-GFP transgenic mice were generated in the laboratory of Dr. Grigori Enikolopov at Cold Spring Harbor Laboratory (Cold Spring Harbor, NY, USA)[366]. The strain was kindly provided by Dr. Enikolopov and was crossbred with C57BL/6 mice for at least 10 generations. In Nestin-GFP mice, green fluorescent protein (GFP) is expressed under the regulatory elements of the intermediate filament Nestin, expressed in neural stem and progenitor cells. The experiments for hOTCs optimization were performed in either Nestin-GFP or C57BL/6 mice. For the rest of the studies, C57BL/6 mice were used.

5.2 Hippocampal Organotypic Culture Slices (hOTCs)

Slice cultures preparation was previously described[58,367]. In brief, hOTCs were prepared from 5 to 7-day-old post-natal pups from C57BL/6 (wild type, WT) or Nestin-GFP transgenic mice[368,369]. As cutting solution, modified artificial cerebrospinal fluid (mACSF) was used containing 195 mM sucrose, 2.5 mM KCl, 1.25 mM NaH_2PO_4, 28 mM $NaHCO_3$, 7 mM D-glucose, 7 mM $MgCl_2$, 1 M HEPES, 1 mM Na-Ascorbate and 3 mM Na-pyruvate in autoclaved MiliQ H_2O, which was carbogenated (5% CO_2 in 95% Oxygen) for 10 min before adding 2 M $CaCl_2$ [369]. After decapitation of the pups, the extracted brain was gently removed and kept in a cold dissection medium (pH 7.2) containing 96% HBSS, 2% HEPES, 1% penicillin-streptomycin, 2.5 M glucose, and 0.5 M NaOH. Both hippocampi were carefully extracted with the entorhinal cortex so that entorhino-hippocampal slices were obtained. Right before vibratome slicing of the hippocampi, they were placed in 4% agar so that the vertical position was maintained, and previously warmed low melting point 2% agar was also poured to avoid them from moving. Slices of 250 μm thickness were made using the *Precisionary* vibratome (VZ-300-OZ) containing iced mACSF with carbogen bubbling. The speed setting used for the vibratome was 3-4 and 5-7 for oscillation. After the slicing, slices were moved to a dish with dissection medium so that the ones with intact DG and CA regions could be selected under a magnifier. They were then transferred to air-fluid interface-style Millicell 0.4 μm pore size culture inserts (Millipore, 30 mm PICM0RG50 or 12 mm PICM01250) each containing from 1 to 8 slices,

depending on the experiment. These membranes were placed in 6 or 24 well plates (Thermo Fisher Scientific) with 1 ml or 240 µl of fresh and sterile culture medium which consisted of 50% Minimum Essential Medium supplemented with 2% B27, 25% heat-inactivated horse serum (HIHS), 2% Glutamax, 0.5% penicillin/streptomycin, 0.5% D-glucose (2.5 M), 0.8% sucrose (2.5 M), 0.5% $NaHCO_3$ and 18% HBSS[369]. Slices were maintained as interface cultures in an atmosphere of 5% CO_2 in ambient air at 37 °C and 90% relative humidity (Fig. E1). The medium was changed on day 1 and subsequently 3 times per week for 3-4 weeks. After 6 days, B27 was withdrawn from the medium[370,371]. During the stay at Prof. Jenny Hsieh's laboratory, the vibratome used was Leica VT100S, which settings were speed 3 and oscillation 3. The rest of the procedure was identical.

Membrane inserts can be recycled if they have not been used during the process of fixing the slices with PFA. To do so, they are submerged in 70% ethanol for 10-minute shaking. Then, they are rinsed 3 times and placed in a zipped bag with autoclaved MiliQ H_2O water for subsequent 10-minute sonication process. Finally, we have to let them dry out on a plate under UV light for at least 30 minutes and stored in a sterile plate sealed with parafilm.

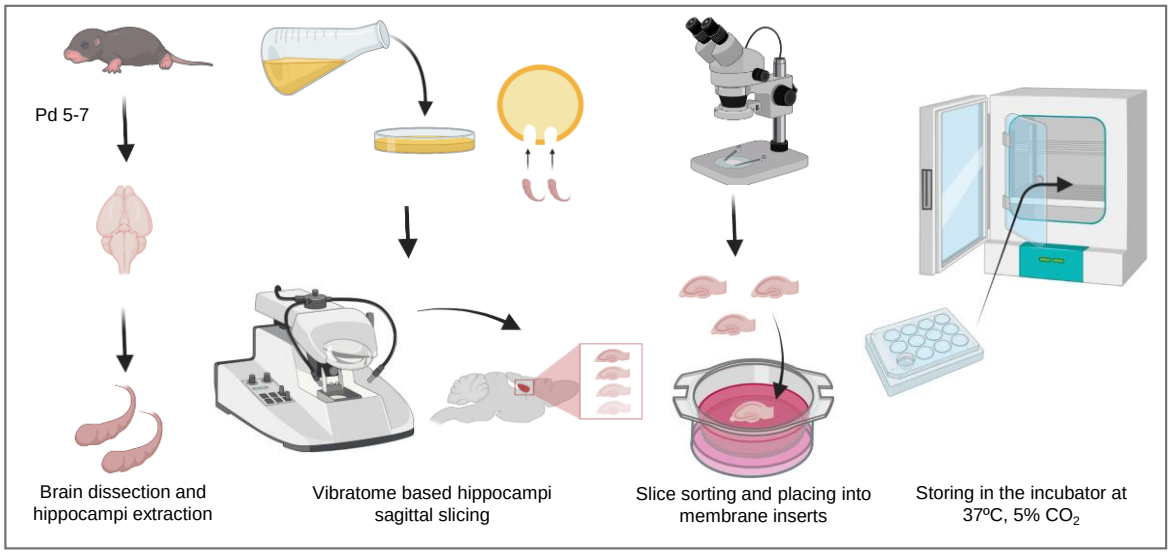

Figure E1. Hippocampal organotypic culture slice (hOTCs) preparation process. The brain is dissected and the hippocampi are extracted from 5 to 7-day-old post-natal pups. 4% agar is used as a holder for the hippocampi so that they are vertically placed, and 250 µm sagittal slices are cut in the vibratome. The best slices are sorted out and placed into previously warmed 0.4 µm pore membrane inserts with medium in a well plate. The well plates are stored in the incubator at 37ºC, 5% CO_2 (*Illustrations from Biorender*).

5.2.1 Drug Administration

For the administration of every drug in hOTCs media, we removed the horse serum from the composition mentioned above and supplemented it with B27, which ensured the stability of the administered reagents. Control slices were in all the cases placed in the same fresh serum-free culture medium with the corresponding amount of autoclaved MiliQ H_2O.

For excitotoxicity induction, hOTCs were treated with $GABA_A$ receptor antagonist picrotoxin (PTX; 100 μM) at day *in vitro* (DIV) 7 or DIV 14 for 3 days. It is important to emphasize that this prolonged exposure lasting 3 days to GABAergic synaptic blockers was required to create a sufficiently extended window of time suitable for epileptogenic processes. Actually, it was preliminarily verified in relation to single neuron and global circuits' dynamics that leads to an impact on the dynamical states of the slices[372].

After the epileptogenic induction, CeO_2NPs were used as antioxidants with a powerful catalytic activity that work as scavengers of ROS. In this case, 1μg/ml CeO_2NPs were added (in collaboration with Dr. Victor Puntes) at DIV 14 for 10 days, starting at the same time as PTX but maintaining the treatment until fixation. The increase of ROS in epileptiform conditions is observed to be related to eATP increase. To test the effects of ATP increase in epileptogenesis, hOTCs were treated with media containing 200 μM ATP at DIV 14 for 3 days. In order to revert the excess of ATP in epileptic conditions, 50 μM TNP-ATP antagonist (Triethylamonium salt, Tocris) was added to the media at DIV 14 for 3 or 10 days, starting at the same time as PTX and removing it at the same time or maintaining the treatment until fixation.

Moreover, GABAergic neurons have also been observed to be affected in epilepsy at this stage of neurogenesis. We tested the GABAergic vs glutamatergic input in our hOTCs model by the addition of tetrodotoxin (TTX, 10 μM) at DIV 14 for 3 days, which blocks voltage-dependent sodium channels and thus action potential firing in neurons, in order to know if newborn neurons need GABAergic input to be GABAergic. For GABA addition to cultures, serum-free media containing 0.5 μM GABA was used at DIV 14 for 3 days.

5.3 Retroviral procedures

All the viruses used in the current work were commercially acquired, except for the retroviral vectors (RV) used during the international stay at the laboratory of Dr. Jenny Hsieh at the University of Texas at San Antonio. During this visit, both the RVGCamp6f (GCamp6f meaning genetically encoded calcium indicator) and the mCherry hm4Di inhibitory RVDREADDs (Designer Receptors Exclusively Activated by Designer Drugs) were packaged. To accomplish this, lipofectamine transfection (Lipofectamine 2000, Invitrogen) of 293T cells was performed, with 7.5 μg of viral vector, and helper plasmids 90 μg CAG-GFP (#3001), 60 μg pCl (#3116) and 30 μg CMV-VSVG (#1102). Forty-eight hours after transfection, the virus-containing media was collected and replaced for 3 days. Media was purified (ViraTrap, Biomiga, V1172-01) and concentrated via ultracentrifugation. The purified virus was estimated around $4.5x10^8$ i.u. ml^{-1}. RetrohM4Di constructs were obtained from A. Schinder (Leloir Institute, Buenos Aires, Argentina) and the retro-CAG-GCaMP6f from S. Ge. They were cloned as explained in Lybrand *et al.* 2021[204].

5.3.1 Viral Microinjection

For assessing neuronal growth, a RV (100nL) LeGO SFFV-RV-mCherry for red or –Venus for green was used. When using wild type (WT) or $Nestin^-$ mice, RV-Venus (GFP) was injected, but when they were $Nestin^+$ mice, RV-mCherry (red fluorescent protein, RFP) was used. The EVOS FL Cell Imaging microscope was used to look at the labeled cells while in culture (Fig E2A), and after fixing the slices with PFA 4% at DIV 23, they were stained for DCX and DsRed2 or GFP (for enhancing RV-mCherry/Venus respectively) for subsequent confocal microscopy imaging (Fig E2B).

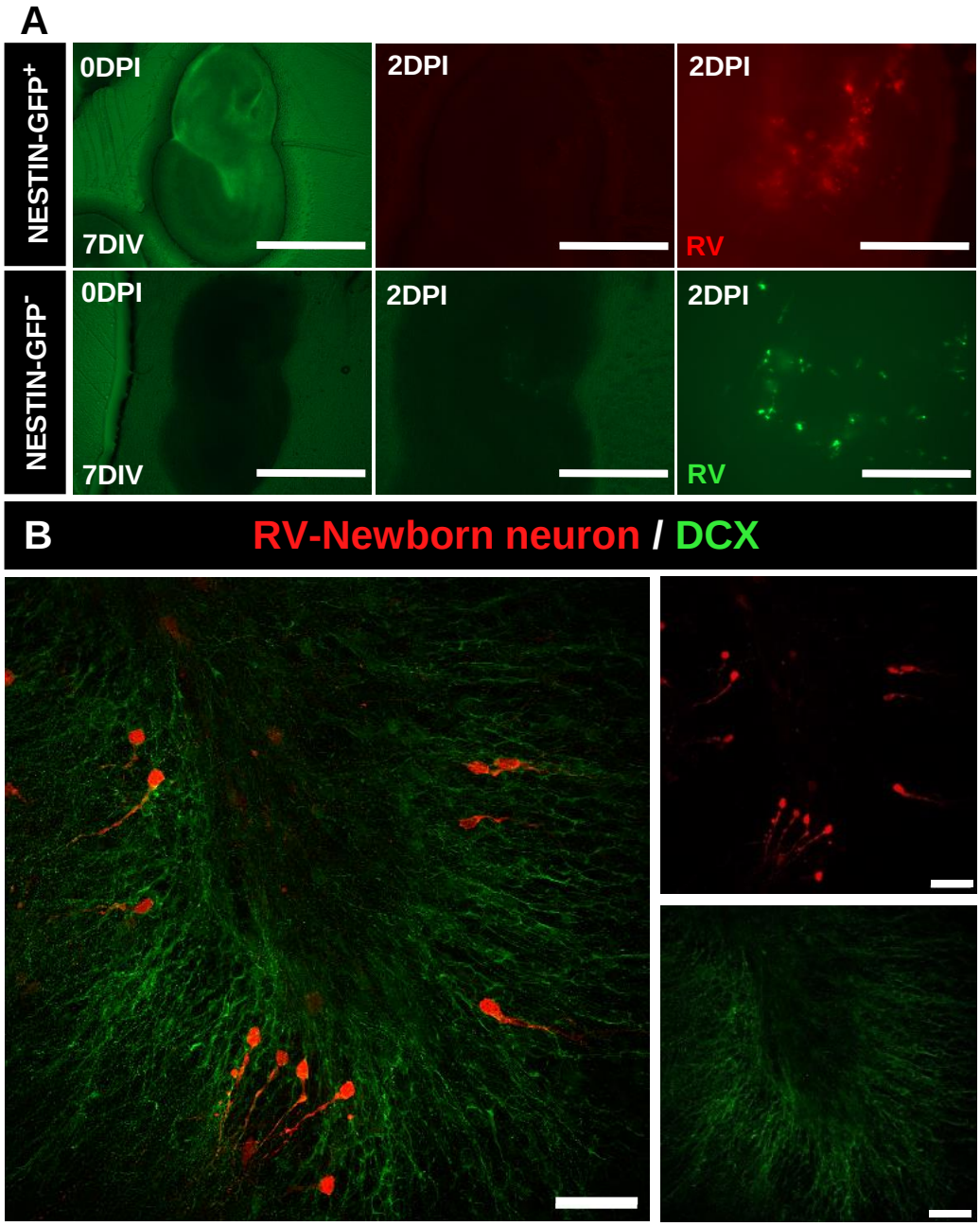

Figure E2. Optimization of viral injections in the DG of healthy and epileptiform hOTCs. (A) Representative fluorescence microscopy images, with DIV7-9 hOTCs from Nestin+ mice RV-mCherry (DsRed2) labeled or Nestin- mice RV-Venus (GFP) labeled, in both cases, 2 days post-injection. Images were taken at 2x, 4x, and 10x magnifications with scale bars being 2000, 1000, and 400 µm respectively. **(B)** Representative confocal microscopy images, after DsRed2 staining RV-mCherry labeled newborn neurons in red and DCX (neurogenesis marker) staining in green. The scale bar is 50µm in all the photographs. hOTCs were PTX-treated (100µM) for 3 days. They were fixed at DIV23, 16 days post-RV injection, and 7 days post-treatment.

Slices were microinjected in the DG after 5-7 days in culture. A magnifier was used to identify the DG by the characteristic horseshoe arrangement of the nuclei of GCs. Microinjection pipettes (glass microcapillaries, 3.5'' Drummond 3-000-203-G/X) were pulled using a micropipette puller (PC-10, Narishige, settings: step 1, heat 75). During the stay at Prof. Jenny Hsieh's laboratory, the micropipette puller used was the P-1000 (Sutter Instrument), for which the settings were the following: heat 483, pull 60, velocity 60, time 90, pressure 350, ramp 473.

Injections were performed in a laminar flow hood equipped with a magnifier to ensure aseptic conditions. The pipette tip was cut with a pair of fine scissors under visual guidance and loaded using an aspirator tube assembly for calibrated microcapillary pipettes with a syringe. Once loaded, a pressure pulse was applied with the syringe so that the load was expelled from the tip, appearing as a small droplet at the tip of the needle. The injection was confirmed by color detection at the injection site, as the viral vectors were always mixed with Fast Green dye (Sigma). The volume injected in the slices was estimated by counting the number of shots (5 shots/slice, 20 nL/shot, 0.1 µL/slice). The final volume was injected into the DG at 2-3 injection sites depending on the slice thickness at the site of needle insertion. It is important to pay attention to tissue architecture under magnifier guidance during the injection procedure to avoid injection of a large volume at a single site, which will cause rupture of the tissue and release of the virus to the surface of the hOTCs (Fig. E3). The session lasted approximately two minutes for each membrane insert holding four slices. The final volume injected in each slice was about 0.1 µL of either RV-Venus, RV-mCherry, AAV.Syn.GCamp6f, RV-GCamp6f, RV-DREADDs hm4Di mCherry, AAV1.Dlx.GCamp6f, or AAV9.Dlx.GCamp6f. The media was changed 24 hours after the injection.

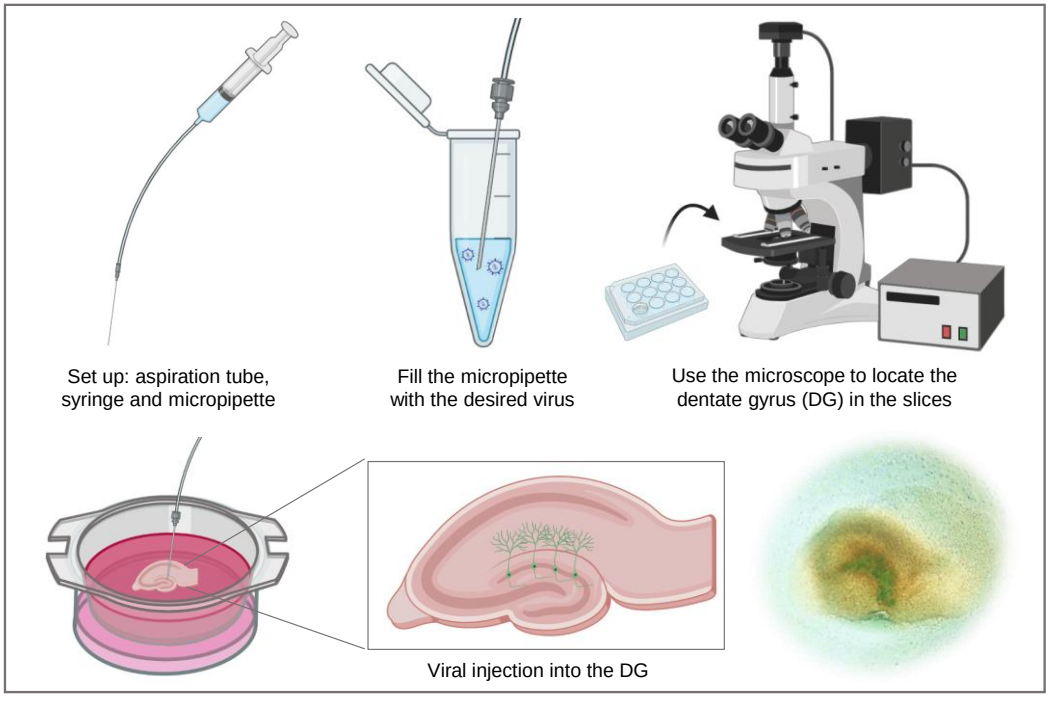

Figure E3. Step by step illustration of the viral injection into the DG of hOTCs. The aspiration tube is connected to the syringe, and the micropipette attached to the tube. The micropipette is filled with the desired virus by carefully pulling the syringe. A microscope is used for the localization of the DG in the slice, and the virus is manually injected with the micropipette releasing the virus with the syringe. Once the virus is delivered, in a couple of days colored cells will be observed under a fluorescence microscope (*Illustrations from Biorender*).

5.4 Immunohistochemistry

The hOTCs were fixed using 4% paraformaldehyde (PFA) in phosphate buffered saline (PBS) that contains 2.7 mM KCl, 12,9 mM $Na_2HPO_4 \bullet 2H_2O$, 137 mM NaCl, 1.76 mM KH_2PO_4, pH-adjusted to 7.4. The fixing of the slices was done by directly adding 4% PFA to the inserts (only below) for 15 minutes and then gently washing twice with PBS both above and below the inserts for 3 minutes per wash. Once the fixing was performed, the slices were carefully removed from the inserts using a fine brush. The slices were then placed in 24-well plates to be processed for immunohistochemistry essentially as described before[22,373].

Briefly, after fixation, slices were incubated with blocking and permeabilization solution containing 3% bovine serum albumin (BSA) and 0.15% Triton-X100 in PBS for 3-4h at room temperature (RT). Primary antibodies were prepared in the same buffer and incubated with slices overnight at 4 °C with gentle shaking. The slices were washed two times in a PBS washing buffer (0.15% Triton-X100 in PBS) for 10 minutes per wash with gentle shaking. After the final wash, slices were incubated with the appropriate fluorochrome-conjugated secondary antibodies and 4′,6-diamidino-2- phenylindole (DAPI) (Sigma, 5 mg/mL, 1:500) diluted in the same buffer for 3-4h at RT with gentle agitation and shielded from light. The slices were washed two times as explained before and mounted on glass slides using DAKO fluorescence mounting medium (Agilent-DAKO, S3023). The edges of the coverslips were sealed with nail polish. The staining of the slices can be done either by a) directly adding reagents to the free-floating slices or b) after fixing, excising the slices from the inserts with their culture membrane below using forceps and tiny scissors, and then incubating them with antibodies.

5.4.1 Antibodies

ANTIBODY	COMPANY	DILUTION
Primary antibody		
Chicken anti-GFP	Aves Laboratories	1:1000
Goat anti-DCX	Santa Cruz Biotechnology	1:1000
Goat anti-GFAP	Dako	1:1000
Guinea pig anti-DCX	Sigma	1:500
Mouse anti-H2AX	Abcam	1:300 or 1:500
Mouse anti-H2AX	Biolegend	1:250 or 1:500
Mouse anti-GFAP	Abcam	1:1000
Mouse anti-PV	Sigma	1:5000
Rabbit anti-Dsred2	Takara	1:1000
Rabbit anti-GABA	GeneTex	1:1000
Rabbit anti-Ki67	Abcam	1:1000
Rabbit anti-NeuN	Abcam	1:1000
Rabbit anti-Neurod1	Sigma	1:500
Rabbit anti-Prox1	Abcam	1:1000

Rabbit anti-RFP	Invitrogen	1:1000
Rabbit anti-S100β	Dako	1:750
Rabbit anti-VGAT	Synaptic Systems	1:500
Rat anti-GFAP	Sigma	1:500
Secondary antibody		
Alexa Fluor 488 donkey anti-chicken	Invitrogen	1:500
FITC 488 Donkey anti-chicken	Abcam	1:500
Alexa Fluor 488 Donkey anti-goat	Invitrogen	1:500
Alexa Fluor 568 Donkey anti-goat	Invitrogen	1:500
Alexa Fluor 568 Goat anti-mouse	Invitrogen	1:500
Alexa Fluor 568 Donkey anti-rabbit	Invitrogen	1:500
CY3 568 Donkey anti-rabbit	Abcam	1:500
Alexa Fluor 647 Donkey anti-mouse	Invitrogen	1:500
CY5 657 Donkey anti-guinea pig	Abcam	1:500
CY5 657 Donkey anti-rat	Abcam	1:500
Alexa Fluor 680 Donkey anti-goat	Invitrogen	1:500
DAPI	Sigma	1:1000

Table 1. Primary and secondary antibodies used in hOTCs in the current work.

5.5 Image Acquisition and Analysis

Fluorescence immunostaining images were obtained using either a Leica SP8 laser scanning confocal microscope or a Leica Stellaris 5 confocal microscope (Leica, Wetzlar, Germany) using a 40X oil-immersion objective except for the morphological complexity and dendritic spine assays in which a 63X oil-immersion objective was used with a zoom of 5X and a z-step interval of 0.75 μm. The signal from each fluorochrome was collected sequentially. Brightness, contrast, and background were adjusted equally for the entire image using the ImageJ software. Brightness and contrast were adjusted by the "auto" option of the software. All images were imported in TIFF format.

For cell death, neurogenesis, GABA, and PV quantifications, 12.6 μm-thick z-stacks located at random positions in the DG were collected per hippocampal slice. For the morphological complexity and dendritic spine assessments, the thickness of the z-stack depended on the thickness of the neuron/dendrite imaged.

5.5.1 Quantitative Analysis of Cell Populations

For the quantification of the cell populations in hOTCs, the hippocampi were sagittally sliced and the slices with the early and late DG were sorted out being the ones in the middle the only ones selected. The 250 μm slices were collected and cultured for 3 weeks, reducing their thickness up to 50 μm by the time of the imaging. Each experiment consisted of 8-4 slices per condition. The area of DG in each z-stack was established by using the ImageJ segmented line tool.

Apoptosis assessment: Apoptosis was quantified as previously described[208]. In brief, apoptotic cells were defined as cells with abnormal nuclear morphology (pyknotic, condensed/karryorhectic, fragmented). The number of apoptotic cells was quantified in the GCL+SGZ in 2-3 12.6 μm thick z-stacks per hippocampal slice (this thickness was established as the average total thickness of the DG in the slices). The DNA damage marker H2AX was also used as a cell viability assessment, in which the $H2AX^+$ cells were identified as damaged.

Neurogenesis, GABA and PV quantification: Quantitative analysis of cell populations was performed by design-based (assumption-free, unbiased) stereology using a modified optical fractionator-sampling scheme as previously described [22,373]. Briefly explained, DCX^+ (newborn neuron marker), $GABA^+$ (GABAergic cell marker) and PV^+ (interneuron marker) cells were counted in each dissector excluding those in the uppermost focal plane and those in contact with the left and bottom margins. Between 2-3 dissectors were analyzed per slice. For GABAergic newborn neuron

quantification, RV-labeled $GABA^+$ cells were identified; as well as for DCX^+ newborn neurons in which RV-labeled cells co-localizing with DCX were quantified.

Plexus intensity of GABA: We also calculated the overall density of GABA staining within the DG region of the brain. To allow comparisons, only images taken under the same conditions and with the same properties were used for analyzing the area occupied by a fluorescent signal. Individual images were imported to ImageJ and specific ROIs including only the GCL+SGZ areas were created. We used the threshold values to quantify the area occupied by GABA for each of the images. The results are presented as the intensity in the area fraction (/mm3).

Region of interest (ROI) based co-localization analysis for vesicular GABA transporter (VGAT) quantification. We used different macros in ImageJ for this analysis, as follows:

1. ROI Generation:

- For dendrites: AutoROIGenerator_v4 macro
    - Difference of Gaussians: minimum sigma 0, maximum sigma 20.
    - Particle properties: minimum particle size 0.25µm, maximum particle size 1x1022µm, selection softer size 0.
- For axons: ROICreator_SSJV_5.1 macro
- For VGAT:
    - 2DROI_FMaxiStack_generator6.3 macro
        - Subtract background: minimum sigma 1, maximum sigma 5
        - Parameters: find maxima prominence, minimum size 0.032µm.
        - Threshold: auto threshold, Huang method.
        - Fit ROIs to optimization.
    - Fuse_ZROIsv1 macro

2. Co-localization analysis:

- ROIs_Percoloc_Analizer_V2 macro

5.5.2 Cell Morphology Analysis

For assessing aberrant neurogenesis and measuring morphological changes in newborn neurons, we randomly selected between 100-150 RV-labeled cells from each experimental condition. The quantification was performed on maximum intensity projection generated from z-stack images. The morphological changes were measured using a plugin for 3D-Sholl analysis kindly provided by Dr. Jorge Valero Gómez-Lobo. The Sholl analysis is an open-source plugin for Image J, which performs

the Sholl technique directly on 2D or 3D images of fluorescence-labeled cells. In this case, 3D reconstructions from confocal stack images were obtained for the morphological analysis of newborn neurons. Single newborn neurons were analyzed using the 3D Sholl analysis plugin (http://fiji.sc/Sholl_Analysis) as previously described[374].

5.5.3 Dendritic Spine Analysis

To analyze abnormalities in hyperexcited newborn neuron dendritic spines, close-up images were obtained with the confocal microscope by using a 63X objective. For each experimental group, 4 animals were used, selecting 10 neurons per animal and 3 dendrites per neuron, with dendrites positioned at distances between 40-100µm from the soma. A zoom factor of 5X and a z-step of 0.3 µm were employed. Images were subsequently deconvoluted using Huygens Professional software. The deconvolution is a mathematical operation used in image restoration to recover an image that is degraded by blurring due to diffraction-limited imaging and noise. When the images are deconvolved, the spread light due to blurring and noise is put back in its original location, producing a better representation of the dendrite that makes it clearer to our eyes. Here, the refractory index of the mounting medium was established for our DAKO mounting medium being 1.32.

To measure the size of the head of dendritic spines, we started using the full width at half maximum (FWHM) method. However, this was such a challenging approach that we selected 1 dendrite per neuron, from 10 neurons per animal and 4 animals per group, obtaining 40 dendrites in each condition. This involved creating a line crossing the head of the spine and plotting the resulting values of the line. Then, the Gaussian values of the curve were obtained using the formula:

$$y = a + (b - a) * \exp\left(\frac{-(x - c)^2}{2d^2}\right)$$

As the Gaussian function is:

$$f(x) = a * e - \frac{(x - b)^2}{2c^2}$$

Where b=μ and c=σ (standard deviation, SD); $c^2 = \sigma^2$

From this formula, the standard deviation of each line made in each spine head is taken, and another line is made in perpendicular to the first one so that σx and σy values are obtained for spine head width and length.

There is a relation between the standard deviation and the FWHM expression:

As the normal distribution is:

$$f(x) = \frac{1}{\sigma\sqrt{2\pi}} \exp\left[-\frac{(x - x_0)^2}{2\sigma^2}\right]$$

Then, FWHM = $2\sqrt{2ln2}\sigma \approx 2.355\sigma$

The next method we used was the SpineJ plugin for ImageJ, which was developed for spine morphology analysis[375]. Except for the dendritic spines in the optimization of the model that were analyzed by the FWHM approach, the rest of the dendritic spine analysis in the current work was performed by the application of this plugin. Dendritic segments of approximately 15-30 µm were selected. Coefficient 3 was applied and the segmentation was generated in which reconnections between spines and dendrites were made. The analysis was binarized and the neck end was defined on each spine head base. The data obtained from this analysis was the following for each condition: head minor and major axis, head perimeter, and head area (µm).

5.6 Oxidative Stress Assay

To evaluate ROS levels in hOTCs, slices were exposed to vehicle, PTX, and CeO_2NPs or TNP-ATP antagonist, depending on the respective experimental paradigm. Briefly, they were loaded with 30 μM CM-H2DCFDA (2',7'–dichlorofluorescein acetate; Invitrogen, Barcelona Spain) according to the recommendations of the manufacturer to assess OS. Measurements were performed while hOTCs were placed in 30 mm Millipore inserts, so 6-well plates were used. For the incubation with the probe, 900 μL -S medium was used under the insert, and 5 μL added on top of each slice for 30 min at 37 ºC shielded from light.

After washing with a warmed dissection medium, fluorescence was measured using the plate reader CLARIOstar Plus (BMG Labtech, Ortenberg, Germany). An insert with no slices on it was used as blank. Three sets of similar experiments were conducted for each agent tested, and background levels were subtracted. Only the data of the regions with hOTCs were selected for the analysis. To check for CeO_2NPs oxidizing the probe, the same assay was performed without hOTCs, in which H_2O_2 was used as a positive control.

5.7 Two-Photon Imaging

In the context of the 2-photon imaging procedure, we followed the same method as detailed in Section 1.2 of the Methods. However, we placed additional membranes (Omnipore 0.1um PTFE Membrane filters, 25mm) on the inserts, which would help facilitate the imaging process by allowing a more effective manipulation of the slice. During the imaging process, we perfused the chamber with ACSF (see Methods 1.2). After imaging, slices were carefully returned to the original inserts and placed back into the incubator until the next imaging time-point.

In our study, we sought to develop an effective imaging protocol for longitudinal observations of newborn neurons. Our objective was to ensure the survival of these neurons throughout multiple imaging time-points, a challenging task that required systematic experimentation and optimization. Initially, we encountered difficulties in sustaining the viability of newborn neurons for repeated imaging sessions. Despite the successful imaging at the first time-point, subsequent imaging sessions led to a decline in neuron survival.

5.7.1 Time-lapse Imaging

GFP expressing cells were imaged on the 2-photon microscope at 960 nm wavelength. The microscope and software was commercially acquired from Femtonics (2D-Galvo microscope), including a Spectraphysics MaiTai femtosecond laser with tunable wavelength. We first used the low magnification 4X objective in bright-field mode to localize the slices on the membrane and the DG in each slice. Once the DG was recognized, we used epifluorescence mode to look for the RV-Venus labeled green cells of interest (Fig E3A, cells of interest in white circle). Then, the submergible 20X objective was used to carefully approach the slice with the bright-field mode until we again localized the DG (Fig. E3B) and turned to the LED lamp again to look for the cell of interest (Fig. E3C). Finally, we set the 2p mode for the imaging, in which the imaging conditions were the following: laser at 3%, UG+UR at 75%, LUT_GFP high in 326 and low in 159, LUT_RFP high in 199 and low in 78, z-step 1.25, z-stack average 8 sample/pixel and 0.4 pixel values. HCImageLive software was used for the visualization of the imaging in IR lamp and LED lamp modes.

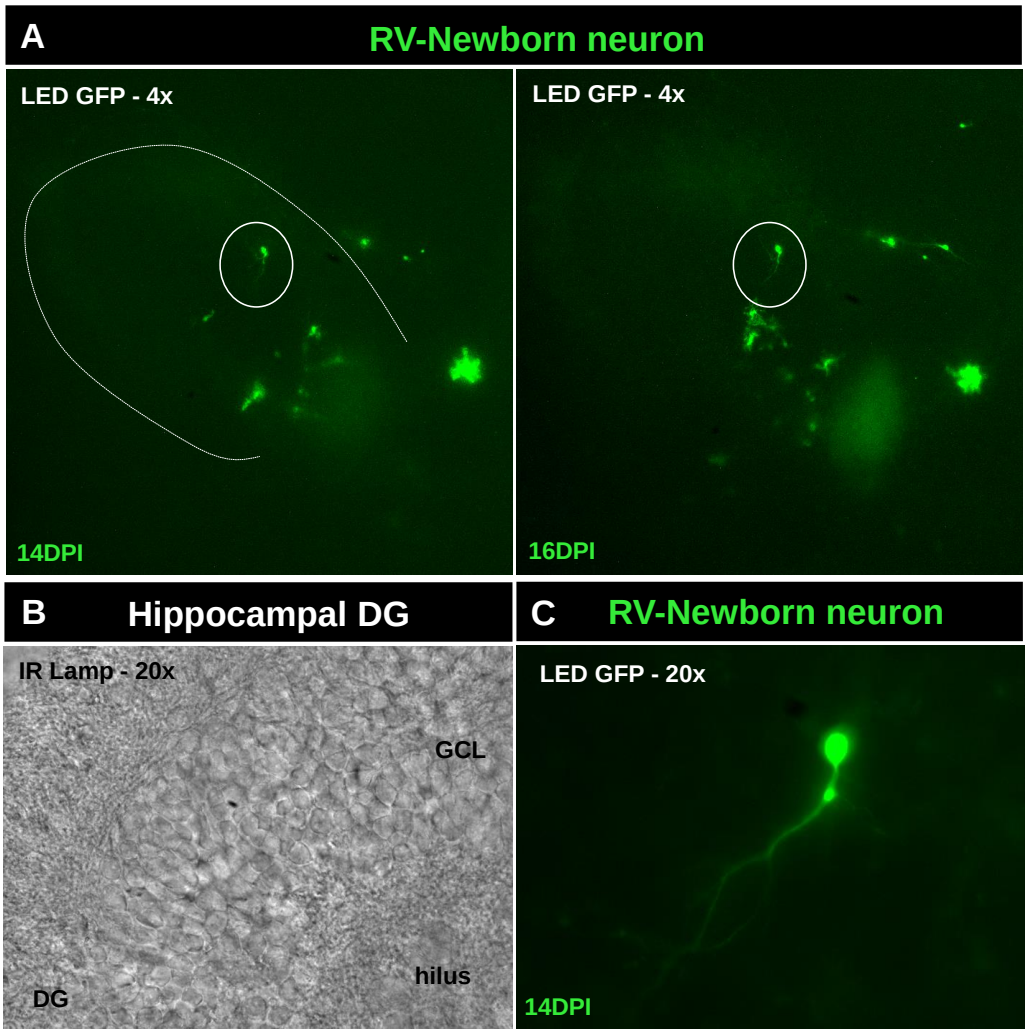

Figure E3. Newborn neuron visualization in hOTCs for subsequent time-lapse imaging. (A) Representative epifluorescence microscopy images (LED GFP, 4x objective), showing non-treated RV-Venus injected newborn neurons (white circle) in the GCL of the hippocampal DG (white dashed line) in hOTCs at two time-points: DIV 20 and 14 days post injection (DPI), and DIV 22 and 16 DPI. (B) Bright field transmission image (IR lamp, 20X objective) of the hippocampal DG in hOTCs where the GCL and hilus are observed. (C) Representative epifluorescence microscopy image (LED GFP, 20x objective), showing a non-treated RV-Venus labeled newborn neuron in hOTCs at 14DPI.

5.7.2 Line Scan Calcium Imaging

When we performed the calcium assay for the first time in the P2X7R inhibition framework, we imaged the slices in the 2-photon microscope. The slices were injected with the calcium indicator AAV1.SYN.Gcamp6f.WPRE.SV40[376]. For that, the 2p mode was chosen and with the "Line and scan area" tool the measurement length was set to 300000 ms (5 minutes). In the "Raster scan" tool, we used 12 samples/pixel and a pixel size of 920µm/pixel. Then we draw a pattern first for the background and then for every cell soma that we observed. In the pattern settings, the acquisition speed was 10 Hz.

5.8 Calcium Imaging

For the calcium imaging in Results sections 6.1.4 and 6.3.5, the slices were injected following the procedure explained above (see Methods 5.3.1) one week after the slicing. These recordings were performed at the laboratory of Dr. Jenny Hsieh at the University of Texas at San Antonio, using a 20X magnification objective on an inverted fluorescence microscope (Zeiss Axio Observer.Z1 Apotome.2) for living cell imaging, equipped with an AxioCam MRc camera, a chamber for CO2 and temperature control for keeping the same conditions as in a cell incubator. During the imaging, the 6-well plate of each condition was transferred to the microscope, containing 3-4 slices from the same animal donor so that the slice with the best viral labeling was chosen for the recording. For the first set of calcium imaging experiments, a RV-GCamp6f was injected into the DG at DIV 7. After imaging the slices for 20 minutes, we used FIJI for the analysis of the recordings. Briefly, we established the ROI in the soma of each green cell and measured the intensity in time, obtaining as a result the calcium reported intensity for each cell. In the second place, calcium imaging experiments were performed for a RV-mCherry with an inhibitory (hm4Di) DREADDs, injected in the DG at DIV 7 as well. In this scenario, the activity of cells dividing at the time of injection could be effectively blocked upon the introduction of clozapine-N-oxide (CNO). Concurrently, an AAV1.SYN.Gcamp6f.WPRE.SV40[376] vector was also administered into the DG to serve as the genetically encoded calcium indicator for assessing neural activity. Slices were imaged for 25 minutes in every condition, with the initial 5 minutes for the basal activity during the addition of CNO or vehicle to the media. In both cases, all slices were consecutively imaged without following any predefined sequence for the order of slice imaging. The plates were never opened, ensuring the maintenance of consistent culturing conditions for the slices to prevent any disturbances.

5.8.1 Calcium Imaging Analysis

Calcium imaging analysis was performed as previously described[372], in collaboration with Dr. Paolo Bonifazi. First, neuronal cell body segmentation was performed[377]. Briefly, the maximum of each pixel across all calcium images acquired for a given slice was used to reconstruct the image template and to segment neuronal cells' contours through the custom-made software HIPPO. For each frame, the average value of the pixels within a cell contour was calculated, and for each cell, a calcium time series was then constructed across all frames. Time series were first high-pass filtered above 0.05 Hz to remove slow fluctuations and baseline changes, and next, the traces were deconvolved using the MATLAB function "deconvolveCa" with default options[378]. The onsets of the calcium events were extracted from the deconvolved calcium signal with start and endpoints set by the respective threshold of 0.05 and 0.04 $\Delta F/F$. The automatic detection of calcium spikes was later visually inspected for each

cell. When the event detection was considered faulty, the starting and ending thresholds of a given calcium trace were adjusted manually always keeping respectively a 1 to 0.8 ratio. A binary time series representing the calcium activity in each frame was first reconstructed in each cell, where the ones marked the onset of calcium spikes. Given a cell, the interval between two consecutive onsets was used as the instantaneous firing rate (IF). In order to calculate the firing correlation in each neuronal pair, the binary time series were smoothed with a gaussian moving average using the MATLAB "smoothdata" function with a window length of 4 points, and the correlation C_{ij} was calculated as

$$C_{ij} = \frac{1}{\|x\| * \|y\|} * \sum_{t=1}^{T} x_t * y_t$$

where x_t and y_t represent the time series of the neuronal pair (i,j), T the total number of frames (typically 4800 for a 20-minute recording), and the symbol ‖ ‖ represents the norm of a vector (i.e. the time series in the of x_t and y_t). In the case of global synchronizations, the binary time series were smoothed with a gaussian moving average using the MATLAB "smoothdata" function with a window length of 20, to link dynamics merging over larger time windows compared to neuronal pairs' dynamics. As global synchronization index at time t ($GSI(t)$) we used the sum of the overall network activity obtained from the smoothed time series ($s(t)$) according to:

$$GSI(t) = \sum_{i=1}^{N} s_i(t)$$

where N is the total number of imaged neurons and s_i is the smoothed time series of neuron i. Network synchronizations (NSs) were identified by GSI exceeding a threshold of chance level with $p<0.05$, as calculated from a thousand reshuffled network dynamics where single neuron time series were randomized while keeping the same inter-event distribution in each neuron.

Each NS was assigned the time frame of the peak of the corresponding GSI. All the cells recruited in a time window of seven frames around the GSI peak were considered participating in the NS. The size of the NS was calculated as the percentage of cells participating in a given NS out of the total number N of imaged neurons in the circuit. The frequencies of NS in a given circuit were calculated as the inverse of the intervals (in seconds) between consecutive NSs. The similarity between two NSs was calculated as one minus the cosine between the binary vectors representing the cells participating in the synchronizations according to:

$$S_{AB} = \frac{1}{\|A\| * \|B\|} * \sum_{i=1}^{N} A_i * B_i$$

were A and B represents the vectors of the two NSs and an element A_i (B_i) is equal to one if the neuron i is participating in the network synchronization A (B).

5.9 Multi-Electrode Array (MEA) Assay

For the Multiwell-MEA (Multichannel systems) assay, the procedure involved removing the membrane insert with hOTCs from the incubator. Subsequently, the tissue around the insert was carefully trimmed using a scalpel or fine scissors. The cultured tissue was carefully lifted by the membrane using forceps and placed upside down onto the electrode field of a dry MEA, ensuring that the tissue faces the electrodes. A drop of the same media in which the slices were cultured was then slowly added, avoiding the surface adhesion from lifting the slice off. The MEA was then transferred to the amplifier to initiate the recording process. Following recording, the MEA was wiped clean with 70 % ethanol. The MEA comprises a 24-well plate, with each well containing 12 electrodes designated to record the activity of the tissue in contact with them. The experimental recording was set for a duration of 10 minutes. In the Multichannels systems setup, the recording was selected for neuronal cells, capturing a simple recording. In the spike detector settings, both rising and falling edges were selected, and the threshold values were set based on the baseline duration of each segment (1000 ms), with a standard deviation of 5.0 (rising edge) and -5.0 (falling edge). The dead time was established at 3000 µs, and for the cut-outs, the pre-trigger was set at 1000 µs, and the post-trigger at 2000 µs. Regarding the spike processing, the burst detector was set with a minimum interval between bursts of 100 ms, a minimum burst duration of 50 ms, and a minimum spike count within a burst of 4. The network burst detector required at least 4 simultaneous channels with a maximum spike rate. The sampling rate was 1000 Hz, with a high-pass filter of 1 Hz and a low-pass filter of 3500 Hz. For the result selection, dose-response and spike counts were obtained.

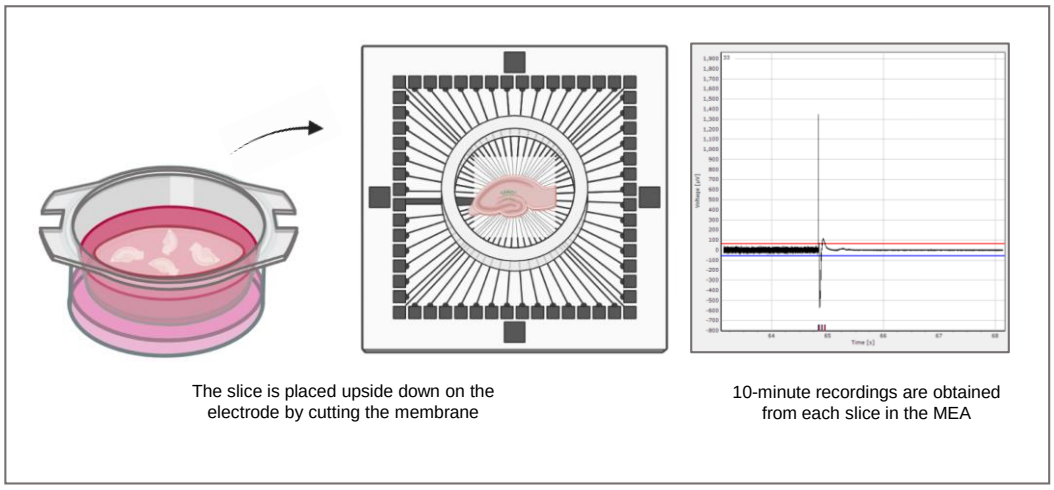

Figure 4. Slice placing on the MEA for activity recordings of hOTCs. The membrane surrounding the hOTCs are cut and the slices are carefully placed upside down on the electrodes in the MEA set up. 10-minute recordings are performed per slice (*Illustrations from Biorender*).

5.9.1 Spectral Analysis

The data was preprocessed by applying a bandpass filter between 12 and 600 Hz, and a notch filter at 60 Hz to eliminate line noise. Additionally, channels with abnormal power spectra were removed. The original signals, each lasting 10 minutes, were segmented into epochs (sliding windows) of 5 seconds, resulting in a data matrix of channels x data for each slice. Power analysis was conducted for the Beta [13–30] Hz, Low Gamma [30–45] Hz, High Gamma [45–100] Hz, High-Frequency Oscillation Slow Ripples (HFO sl) [100–250] Hz, and High-Frequency Oscillation Fast Ripples (HFO fr) [250–600] Hz bands. This analysis was performed for each channel and epoch. Subsequently, a mean value was calculated across channels, followed by another mean value across epochs, resulting in a single value for each slice. This analysis was obtained in collaboration with Diego M. Mateos.

5.10 Statistical Analysis

IBM SPSS Statistics and GraphPad Prism (Version 9 for Windows) were used for statistical analysis. Normality tests were conducted for parametric or non-parametric test correct choice. For the analysis of pairs of groups, a Student´s t-test was performed, resorting to U-Mann Whitney test when data were non parametric. For the analysis of more than two conditions 1- way-ANOVA test was performed. When more than two groups were present, one-way analysis of variance (ANOVA) test of all groups was performed to determine the overall effect of each factor, resorting to Kruskal-Wallis test when data were no parametric. Two-way ANOVA was performed to detect interaction between factors. In all cases, pairwise multiple comparisons (Holm-Sidak test) were used as a post hoc test to determine the significance between groups in each factor. For the Sholl analysis, two-way repeated measures ANOVA followed by Bonferroni posthoc test was performed. Only $p<0.05$ was reported to be statistically significant. Results were presented as mean ± standard error mean (SEM). The number of independent experiments is shown in the respective section.

MATLAB was used for the statistical analysis of the following variables quantifying networks' dynamics: single neuron firing rate, neuronal pair correlation, network synchronizations (size and frequency), and synchronizations' similarity. Specifically, given a variable, all the data obtained from different slices belonging to a given experimental group (CNT1, PTX1, CNT2, PTX2) were pooled. The statistical difference between groups was assessed using the Kruskall-Wallis's test for non-parametric group comparisons with corresponding p-values for each pair of groups. Corresponding plots represent for each group medians, 25-75% percentile limits, smallest-highest values, and outliers.

6. RESULTS

RESULTS

6.1 Implementation of the Epileptogenic hOTCs Model

6.1.1 Generation and Optimization of hOTCs

The model used as a baseline was performed as previously described[58,367], prepared from 5 to 7-day-old post-natal WT mice pups. Typically, up to 30 hippocampal slices with intact DG structure were obtained, and they were cultured in groups between 1-8 per insert, depending on the experiment and subsequent analysis (Fig. 1A). The health of every slice was checked by immunostaining 3 weeks after culture for biomarkers of glia, proliferation and neurogenesis plus the DNA marker DAPI to confirm that the structure and shape of the DG was maintained (Fig. 1B, white line). Although the overall health and structure were maintained after optimizing the dissection and initial culture, no neurogenesis was observed (Fig. 1B) in spite of the presence of other biomarkers of proliferation (Ki67) and astroglia/NSCs (GFAP) (Fig. 1C, F).

The literature pointed at horse serum being a key aspect for the culture of hOTCs[248,379]. Therefore, both serum-free (-S) and serum-based (+S) conditions were applied for the identification of the most suitable one for sustaining neurogenesis. The difference between these conditions was not just the horse serum addition to the culture media, but also the use of the B27 supplement, which depended on the presence of serum. In the -S case, this supplement was added during the whole experimental procedure to compensate for the lack of serum and its components. Whereas in the +S, it was added during the first week, as an inescapable step for the initial stages if of the development in culture, but was then removed after one week in culture as it was not necessary anymore. When neurogenesis was checked in both conditions (-S and +S), no statistical differences were observed in the hippocampal DG (Fig. 1D, E), suggesting that both were valid for newborn neuron assessment. We however chose the +S version as a tendency to more neurogenesis was detected (Fig. 1E).

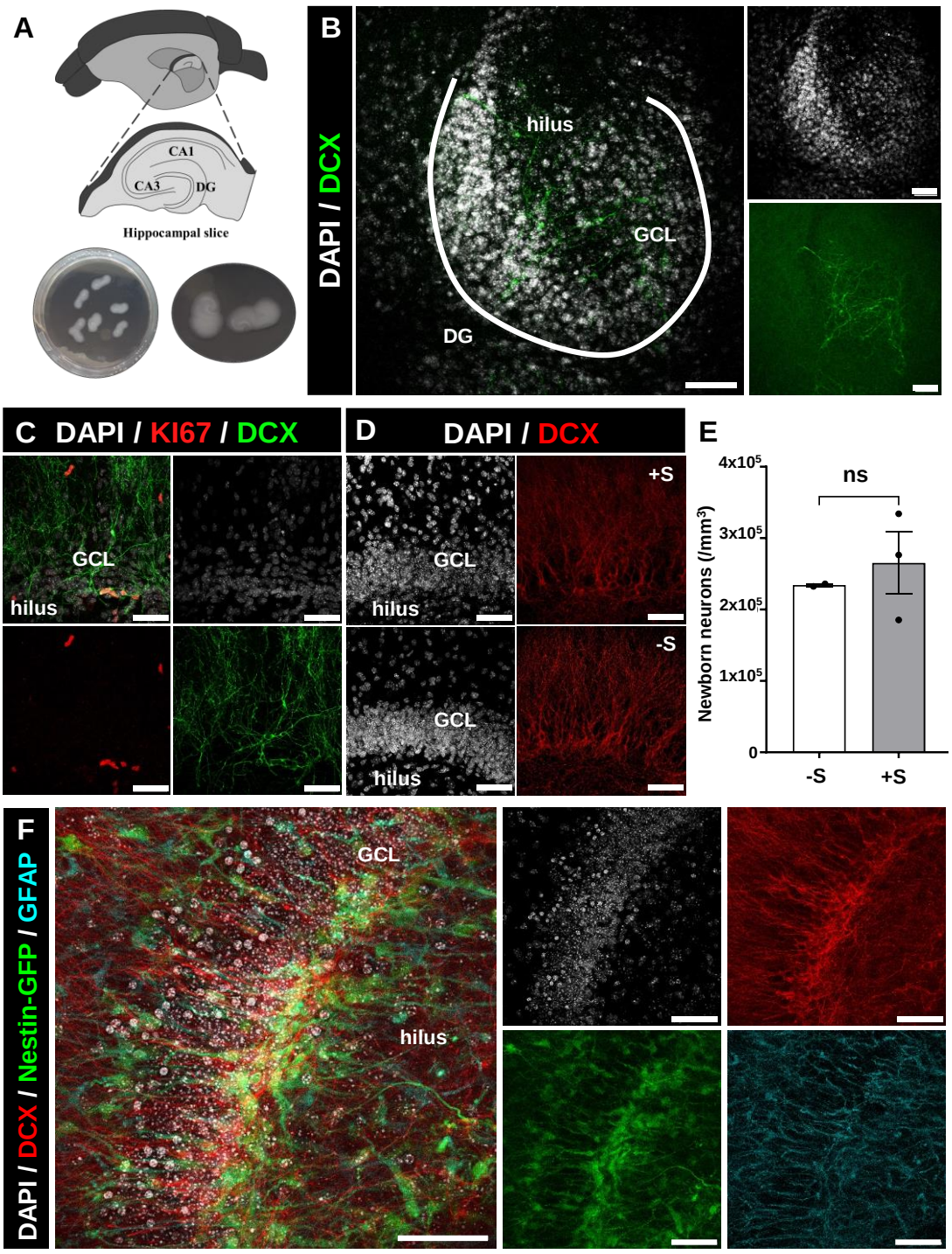

Figure 1. Optimization of hOTCs. (A) On top, a schematic representation of the mouse hippocampus showing a hippocampal slice in which the DG, the CA1, and CA3 are highlighted. The bottom images show some hOTCs cultured in membrane. **(B)** Representative confocal microscopy images, after staining for DAPI in grey and DCX in green, where the SGZ+GCL in the DG of hOTCs is pointed out in white. **(C)** Representative confocal microscopy images after staining for DAPI in grey, DCX in green, and KI67 (proliferation assessment) in red, showing the SGZ+GCL in the DG of hOTCs at DIV. 26-28 **(D)** Representative confocal microscopy images after staining for DAPI in grey and DCX in red, showing the SGZ+GCL in the hippocampus of hOTCs grown with serum-based (+S) or serum-free (-S) medium at DIV. 13-19 **(E)** Newborn neurons (/mm^3) were quantified by identifying DCX$^+$ cells in the hippocampus (SGZ+GCL) of hOTCs grown in SF and SB medium where no differences were observed. n = 3 per group. **(F)** Representative confocal microscopy images, after staining for DAPI in grey, DCX in red, GFP for Nestin$^+$ stem cells in green, and GFAP (astrocytic/stem cell marker) for neurologic damage in far red, showing the SGZ+GCL in the hippocampus of hOTCs at DIV 19. The scale bar is 50 µm in all the photographs. Data are expressed as mean ± SEM and analyzed by an unpaired t-test. ns= non-significant.

6.1.2 Epileptogenesis Impairs Neurogenesis

The present hOTCs model was established for the assessment of aberrant neurogenesis during epileptogenesis. It was accomplished by manipulating the endogenous level of neuronal hyperexcitation through chemical induction by transiently (3-day) exposing the slices to the epileptogenic agent picrotoxin (PTX, 100µM), that blocks inhibitory GABAergic transmission. This compound has been well-documented as an hyperexcitation inducer in hOTCs, making it an already characterized model displaying epileptiform activity[254,380,381]. Moreover, this PTX-based model has been recently used in a key publication[372], in which in a detailed manner it is demonstrated that the addition of PTX to the culture medium for 3 days provokes several effects: an overall increase of the firing frequency of neurons and overall increase in the number of neurons firing; and also a higher frequency of synchronized firing by groups of neurons. Notably, these effects keep taking place in a spontaneous manner after the withdrawal of PTX and until the end of the life of the hOTCs. Although these results demonstrate how epileptogenesis take place in hOTCs, the differences with humans and animal *in vivo* models should always be considered. Nevertheless, this model constitutes a useful *in vitro* approach with many advantages for the study of MTLE. Here, the effects on neurogenesis were tested at one and two weeks *in vitro* (WIV), in two paradigms. In both of them, there were two groups: a control condition (CNT group), where cultured slices were not exposed the $GABA_A$ receptor inhibitor PTX, so it was considered as a physiological state of the tissue; and a PTX group, in which PTX was continuously present for three consecutive days. In the first paradigm, PTX was added to the hOTCs from DIV 7-9 (Fig. 2A) and in the second from DIV 14-16 (Fig. 2B). The slices were fixed at the end of the 3rd WIV for subsequent immunostaining of DCX (Fig. 2C, D) and confocal microscopy-based analysis. In both time-points, a decrease by half was shown in the number of newborn neurons (DCX^+ cells) of the GCL+SGZ in the DG PTX-treated (epileptogenic) hOTCs (Fig. 2E, F).

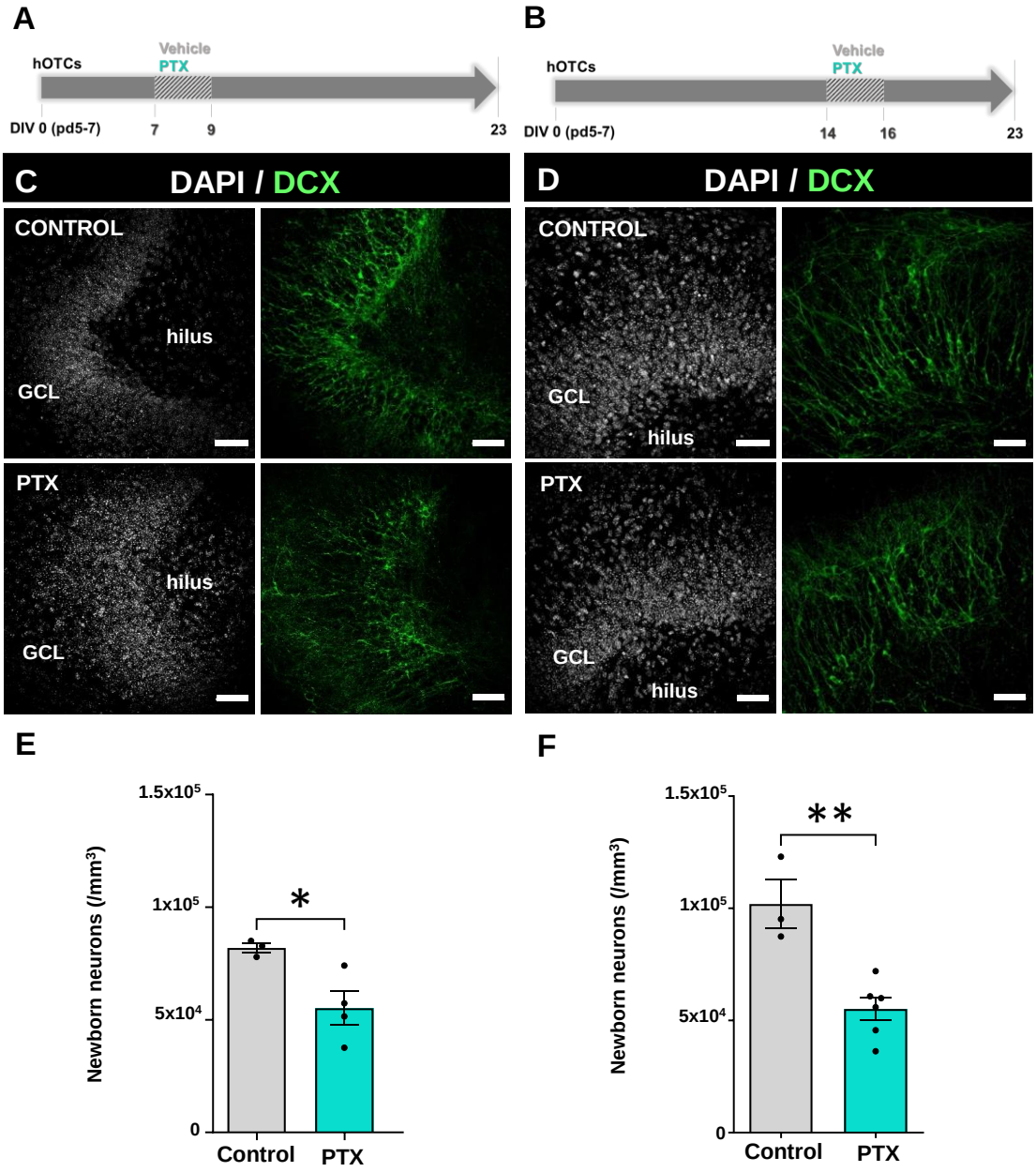

Figure 2. Neurogenesis is impaired in the DG of PTX-treated hOTCs at 1 and 3 weeks *in vitro*. (A, B) Scheme of the experimental procedure. The hOTCs are extracted at pd5-7 (DIV 0) and cultured. From DIV 7 to DIV 9 **(A)** or DIV 14 to DIV 16 **(B)** they are exposed to $GABA_A$ receptor inhibitor PTX (100µM), and immunostainings and imaging are performed 7 days after (DIV 23). **(C, D)** Representative confocal microscopy images were taken showing the SGZ+GCL in the mouse hippocampal hOTCs. **(E, F)** Newborn neurons significantly decreased in both 1 and 2 weeks *in vitro* PTX-treated slices. They were quantified (/mm^3) by identifying DCX stained cells. n=3-6 per group. The scale bar is 50 µm in all the photographs. Data are expressed as mean ± SEM and analyzed by an unpaired t-test. * $P < 0.05$, ** $P < 0.01$.

6.1.3 Epileptogenesis Induces Aberrant Neurogenesis

Given that the detrimental effect in neurogenesis due to an epileptogenic environment was consistent in both frameworks, they were both subjected to aberrant neurogenesis evaluation by focusing on different newborn neuron features. Toward this end, GFP-carrying RV was injected in the DG to transfect dividing cells. As most of the proliferation in the DG is accounted for the neuronal progenitors of the neurogenic cascade, newborn neurons would result labeled due to the persistent expression of GFP. Co-localization with the specific marker of newborn neurons DCX was assessed to verify the validity of the RV labeling, yielding a 94.26% of co-localizing cells in the control group and 91.38% in the PTX group (Fig. 3A, B).

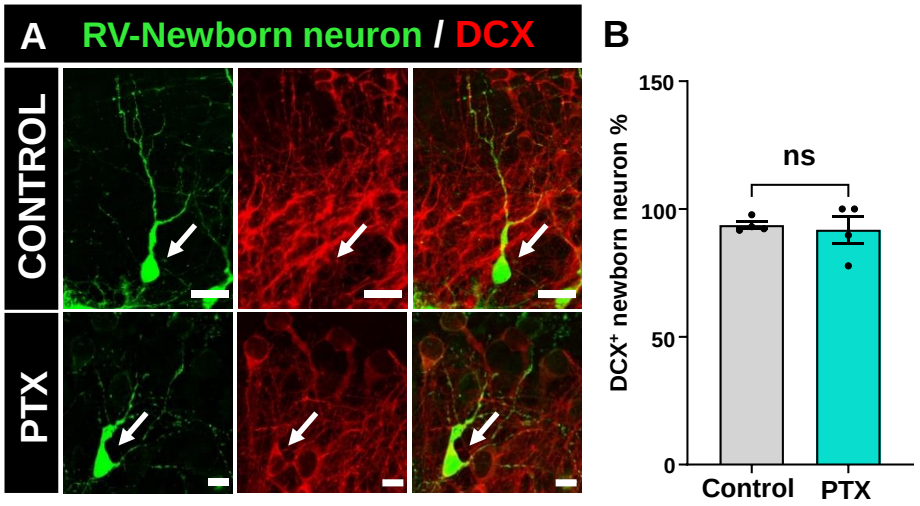

Figure 3. RV-labeled newborn neuron state confirmation in control and epileptiform hOTCs. (A) Representative confocal microscopy images, after GFP staining of 16 days old RV-Venus labeled newborn neurons in green and DCX in red (white arrows showing co-localizing newborn neurons), both 7 days post-PTX/vehicle. The scale bar is 20 µm for the top images and 10 µm for the bottom ones. **(B)** Quantification of RV-labeled DCX^+ newborn neurons. n = 4 per group. hOTCs were PTX-treated (100µM) for 3 days. They were fixed at DIV 23, 16 days post-RV injection, and 7 days post-treatment. Data are expressed as mean ± SEM and analyzed by an unpaired t-test. ns= non-significant.

In order to assess whether pathological hyperexcitation was associated with modifications in the morphology of newly generated neurons, RV injections were conducted either after 1 WIV (adding PTX for 3 days at the 2nd WIV) or after 2 WIV (adding PTX for 3 days at the 1st WIV). This allowed to test the effect of hyperexcitability on newborn neurons generated either before or after the addition of PTX (Fig. 4A, B). At DIV 23, RV-labeled newborn neuron dendritic arborization was evaluated by quantifying the number of intersections through 3D-Sholl analysis, as a measure of morphological complexity, whose alteration represents a hallmark of aberrant neurogenesis described in MTLE models[199].

Indeed, when the RV injection was administered one week prior to the addition of PTX, the RV-labeled newborn neurons, that were thus already in the process of differentiation when epileptogenesis was induced, exhibited a clearly altered morphology. This altered morphology was characterized by significantly reduced complexity between 70 µm and 180µm radius from soma, indicating the middle and final part of the dendritic arbor length (Fig. 4C, E). Here, as PTX was added one week after de viral injection, it acted only on their maturation/process of neuronal differentiation, eliminating confounding factors. These findings suggest that, similar to what is found in adult mouse models of MTLE, newborn neurons undergo abnormal morphological changes during epileptogenesis. Conversely, when it was the RV injection that was conducted one week after PTX addition, the neuroblasts generated and growing in an already epileptogenic environment presented a morphology similar to the control group (Fig. 4D, F).

This outcome was not entirely unexpected, as inducing hyperexcitability before neurons are even born can impact all stages of their development, from mitosis to the initial stages of maturation. It is possible that, through compensatory mechanisms, neurons adapt to the pathological environment, ultimately not exhibiting aberrant features in their dendritic structure. Also, the overall time allowed for differentiation is shorter in this paradigm (neurons being 7 days vs 16 of age at the moment of the analysis), which suggests that alterations might have not had enough time to be significant. For this reason, the most suitable framework for the objectives involved performing first the RV injection and then applying PTX, which is the protocol used for the rest of the experimental work.

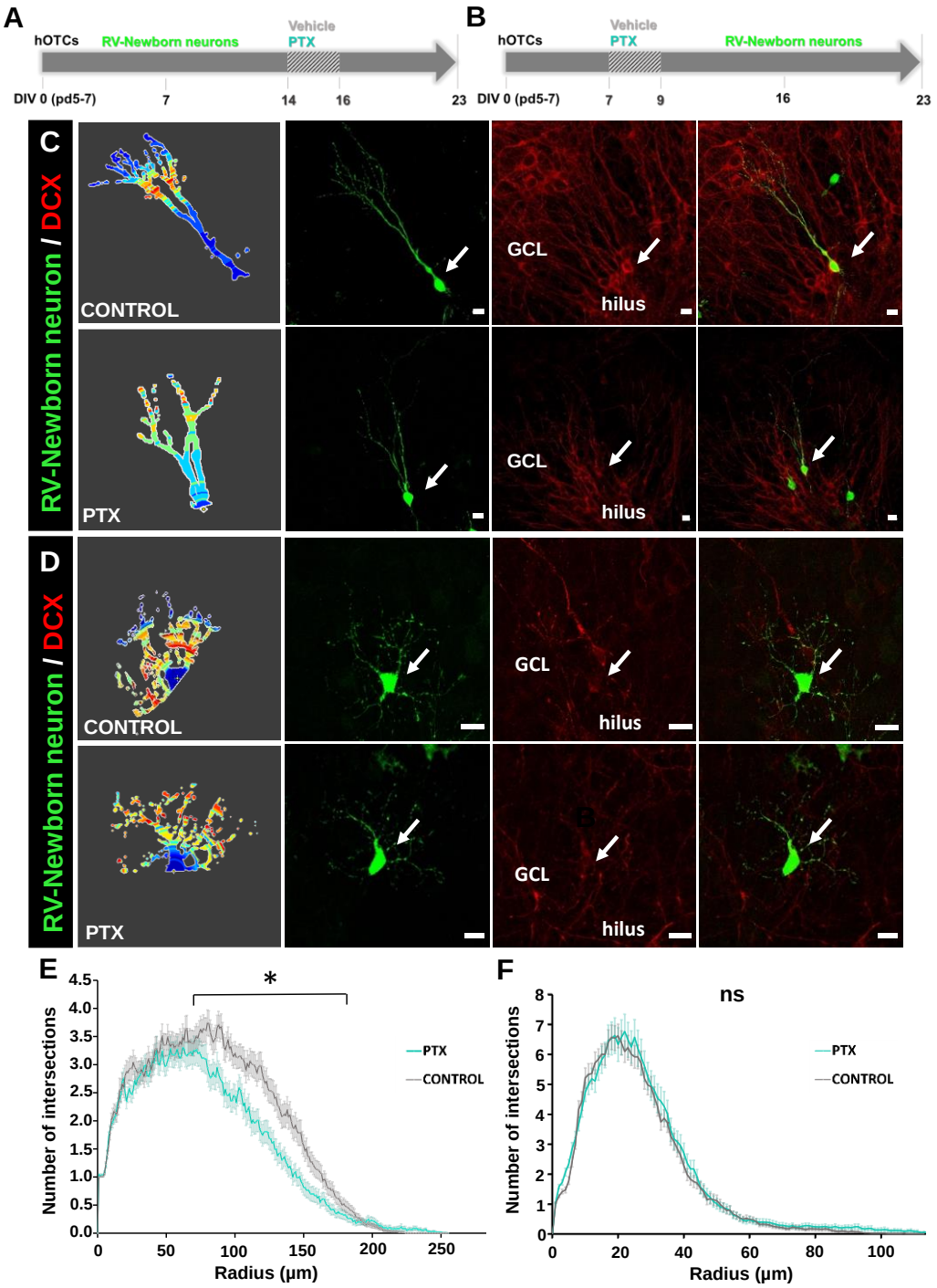

Figure 4. Morphological evaluation of newborn neurons in PTX-treated and non-treated hOTCs. (A, B) Scheme of the experimental procedure. The hippocampi are extracted, sliced, and cultured at pd5-7 (DIV 0). After 1 or 2 WIV, hOTCs are rather exposed to a $GABA_A$ receptor inhibitor (picrotoxin, PTX 100µM) for 3 days or RV-injected. Immunostainings are performed 1 week later, at DIV 23. **(C, D)** Representative confocal microscopy images, showing PTX-treated and non-treated neurons born before **(C)** or after **(D)** hyperexcitability was induced. Z-stack projections were analyzed and color-coded according to their 3D-Sholl profile, in which warmer hues indicate a higher number of intersections (as shown in the 3-D reconstruction of neurons). **(E, F)** Quantification of the number of intersections between circles of increasing (1 µm) radius, where PTX-treated newborn neurons were significantly less complex when treated during development (CNT, n=103 cells; PTX, n=98 cells) **(E)**, but no differences were observed when they were born in an epileptogenic environment (CNT, n=81 cells; PTX, n=76 cells) **(F)**. n = 6. The scale bar is 50µm in all the photographs. hOTCs were fixed at DIV 23, 16 days post-RV injection, and 7 days post-PTX/vehicle. Data are expressed as mean ± SEM and analyzed by ANOVA repeated measures and Bonferroni post-hoc correction. * $P < 0.05$, ns= non-significant.

6.1.4 Epileptogenesis Induces Cell Death and Damages GABAergic Interneurons

For further confirmation of the effects of PTX, and as an extra readout of the health of hOTCs, the number of dead cells was assessed by identification of pyknosis (DNA condensation) or karyorrhexis (nuclear fragmentation) after staining for the marker of DNA (and therefore cell nuclei) DAPI. As predicted, after PTX exposure there is a progressive increase in the number of apoptotic cells over time in culture, showing a 3-fold difference compared to control (Fig. 2A, B).

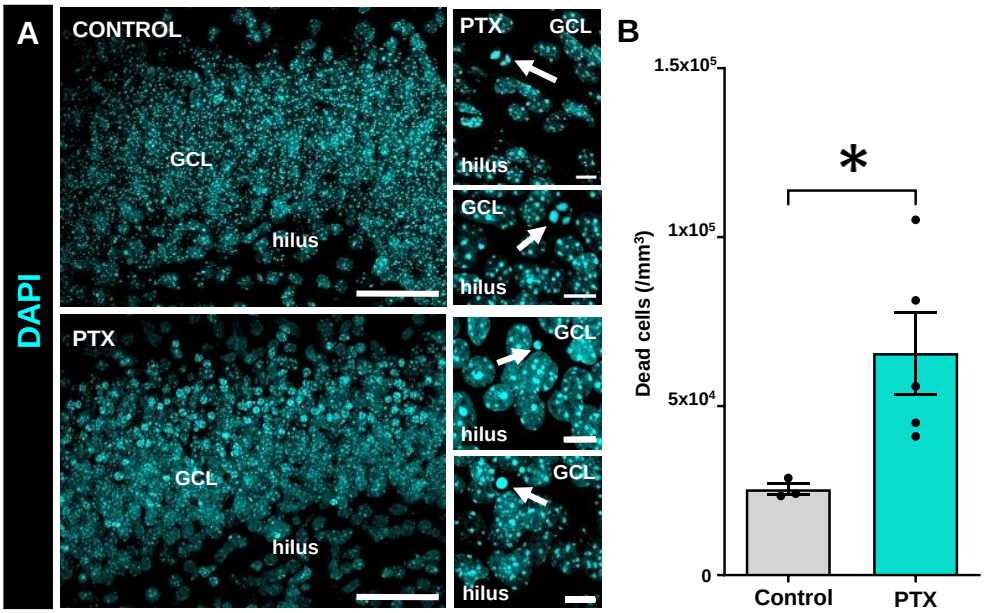

Figure 5. Cell survival is impaired in the DG of PTX-treated hOTCs. (A) Representative confocal microscopy images after DAPI nuclear staining in control and 3-day PTX-treated hOTCs at DIV 23. **(B)** Cell death was quantified by identifying nuclei presenting pyknosis (DNA condensation) and/or karyorrhexis (nuclear fragmentation), both detected by condensed staining of DAPI. Examples of pyknotic/karyorrhexic nuclei are also shown at higher magnification. An increase in dead cells was observed in the PTX-treated hOTCs group. n=3-6 per group. The scale bar is 50 μm in the lower magnification photographs and 10 μm in the higher magnification ones. Data are expressed as mean ± SEM and analyzed by an unpaired t-test. * $P < 0.05$.

As other indicators of interest for the posterior analysis of manipulations aimed at preventing the damage associated with pathological neuronal hyperexcitation, changes in the density of the GABAergic neuronal population was investigated both using immunostaining for GABA and for PV subpopulation for PTX- and non-treated hOTCs. It was not a surprise to observe a decrease in both of them, concluding that in this model, there is a significant reduction by half of $GABA^+$ and PV^+ cells (Fig. 6A-D). These results that are supported by experiments both *in vitro* and in animal models in the literature, in which these interneuron population is also reduced in an epileptogenic environment [220,264–266,382–384].

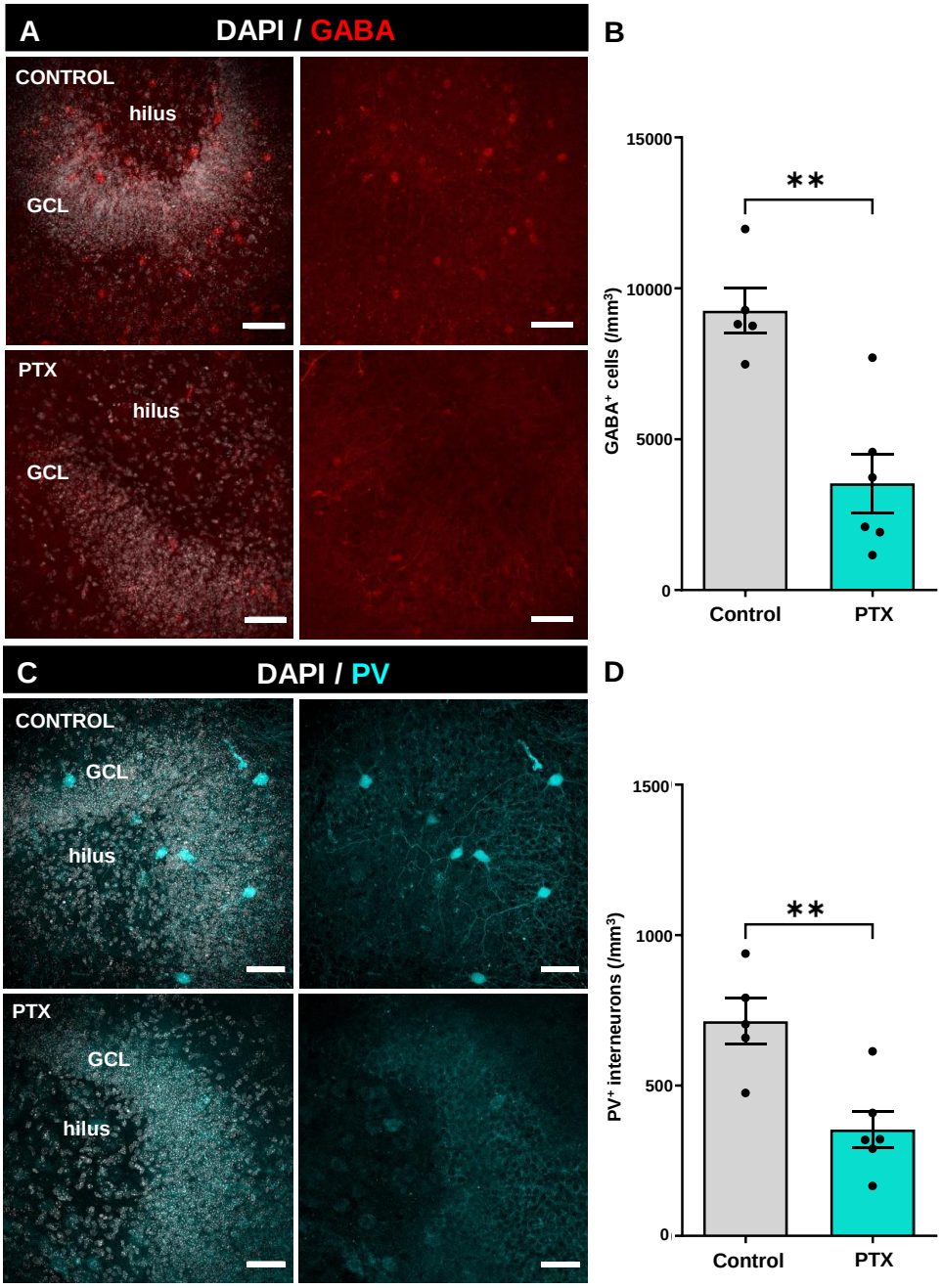

Figure 6. GABAergic interneurons are impaired in the DG of epileptogenic hOTCs. (A, C) Representative confocal microscopy images of PTX- and non-treated hOTCs from mouse hippocampus, after staining for DAPI and GABA (GABAergic cell marker in red) or PV (interneuron marker in cyan) showing the SGZ+GCL. **(B, D)** Interneurons were quantified by identifying $GABA^+$ cells (red) and PV^+ cells (cyan), showing a significant decrease in epileptogenic hOTCs. n=4-6 per group. The scale bar is 50 µm in all the photographs. hOTCs were PTX-treated (100µM) for 3 days. They were fixed at DIV 23 and 7 days post-treatment. Data are expressed as mean ± SEM and analyzed by an unpaired t-student test. ** $P < 0.01$.

6.1.5 Epileptogenesis Reduces GABAergic Newborn Neurons in the DG

Further, because both the population of newborn neurons and of GABAergic cells are decreased in PTX-treated hOTCs, RV labeling and co-staining with GABA were also performed to address the effect of PTX on GABAergic newborn neurons. Certainly, it is already stablished that newborn neurons undergo a GABAergic period: recently born GCs synthesize GABA during a restricted time window of their differentiation, and it is between the 2nd and 4th week when these post-mitotic cells express GABAergic markers and are synaptically integrated into the hippocampal network[259]. In the experimental framework, 16-day-old newborn neurons are studied, meaning that they were evaluated during their GABAergic period. However, it is not known what happens during this GABAergic period in epilepsy.

In some cases of epilepsy, there is a reduction in the number of GABAergic neurons in general or a dysfunction in their ability to release GABA, leading to an imbalance between excitatory and inhibitory neurotransmitters, which can result in an increased neuronal excitability and a higher likelihood of seizures[385]. However, with a specific focus on GABAergic newborn neurons and in light of the disruption observed in GABAergic interneurons, the subset of these cells that were immature and GABAergic were identified in the present hOTCs model. To address this, a simple test was first made by DCX staining to confirm the presence of DCX-GABA^{+} newborn neurons that had not been labeled with the virus and were also in an immature and GABAergic state (Fig. 7A). Subsequently, when looking for RV-Venus labeled immature neurons that co-localized with GABA^{+} cells (Fig. 7B, C), a reduction by half in the percentage of GABAergic newborn neuron cells that develop under hyperexcitable conditions was stablished, despite no alteration was observed in GABA intensity in the general plexus (Fig. 7B-E).

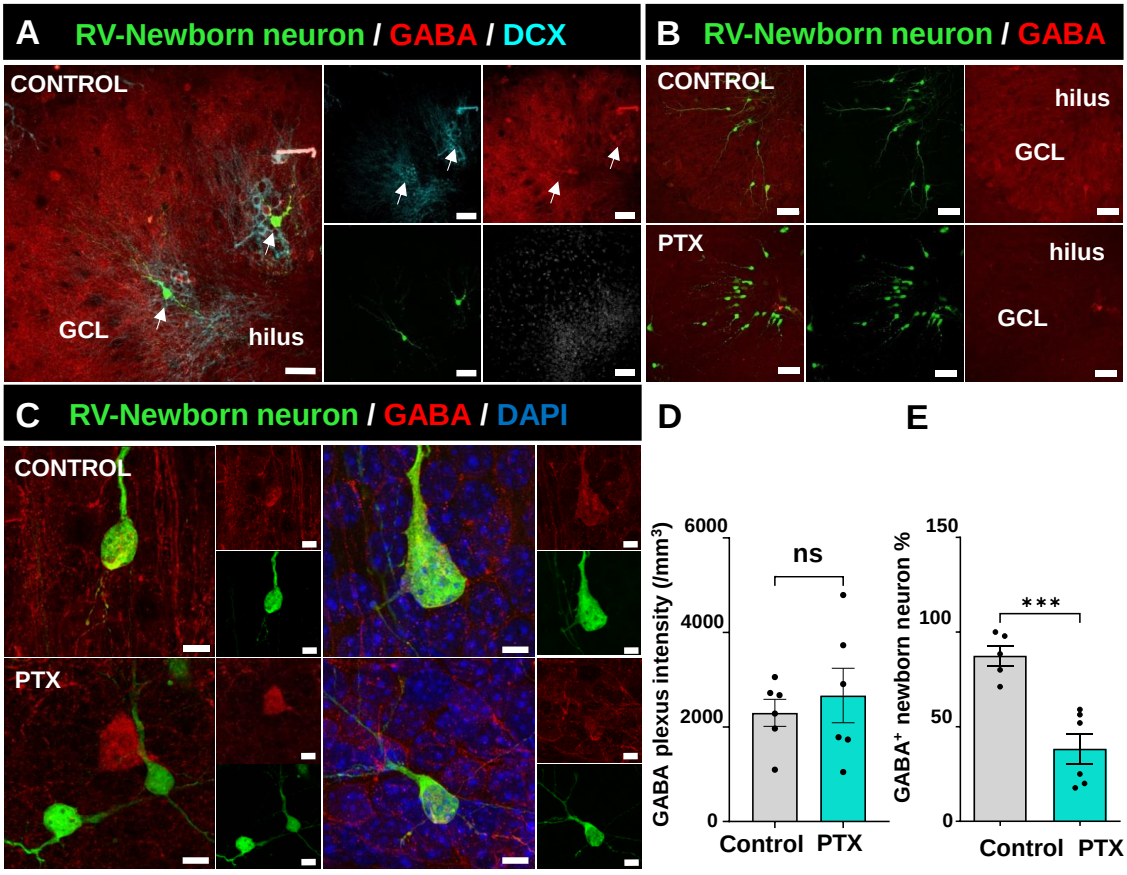

Figure 7. GABAergic newborn neurons are impaired in the DG of epileptogenic hOTCs. (A) Representative confocal microscopy images of non-treated hOTCs from mouse hippocampus, after staining for DAPI in blue, GABA in red, GFP in green, and DCX in cyan showing the SGZ+GCL in which arrows indicate GABA-DCX co-localizing cells. **(B)** Representative confocal microscopy images of RV-Venus marked newborn neurons and GABAergic cells in the DG of PTX- and non-treated hOTCs from mouse hippocampus, showing the SGZ+GCL. **(C)** Representative confocal microscopy close-up images of a RV-Venus marked newborn neurons co-localizing or not with GABA cell marker in the SGZ+GCL of PTX- and non-treated hOTCs. **(D)** GABA plexus mean intensity was measured in the DG (SGZ+GCL), showing no statistically significant difference between conditions. n=6 per group. **(E)** Quantification of GABAergic newborn neurons in the hippocampus (SGZ+GCL), showing a statistically significant decrease in PTX-treated hOTCs. GABAergic newborn neurons were quantified by identifying $GABA^+$ and RV-Venus-labeled cells co-localizing. n=5-6 per group. The scale bar is 50 µm in all the photographs except for the close-up images being 5 µm. hOTCs were PTX-treated (100µM) for 3 days. They were fixed at DIV 23, 16 days post-RV injection, and 7 days post-treatment. Data are expressed as mean ± SEM and analyzed by unpaired t-student test. ns=non-significant, *** $P < 0.001$.

6.1.6 Epileptogenesis Induces Aberrant Neurogenesis

Although altered dendritic arborization is a common readout for aberrant neurogenesis assessment, the RV-labeling allows a more detailed study of the morphology of these cells by investigating the dendritic spines, as they have been reported to be strongly altered in animal and clinical studies[386–388] and which are more likely to be a better readout for functional anomalies. In fact, the development of dendritic spines is one of the most important features of newborn neurons as they are in the maturation process. This essential property can be affected in epilepsy and suffer from functional consequences at the synaptic level.

Therefore, going further into detail at the subcellular level, the presence of abnormalities in newborn neuron dendritic spines were analyzed (Fig. 8A, C). The quantification of dendritic spines decreased by half in the epileptogenic hOTCs, (Fig. 8B). At the same time, the analysis involved the FWHM technique to measure spine geometries (for details, see Methods 5.5.3), in which an increase in the size of the spine heads was observed, being 28% longer and 13% wider compared to the control spines (Fig. 8D, E).

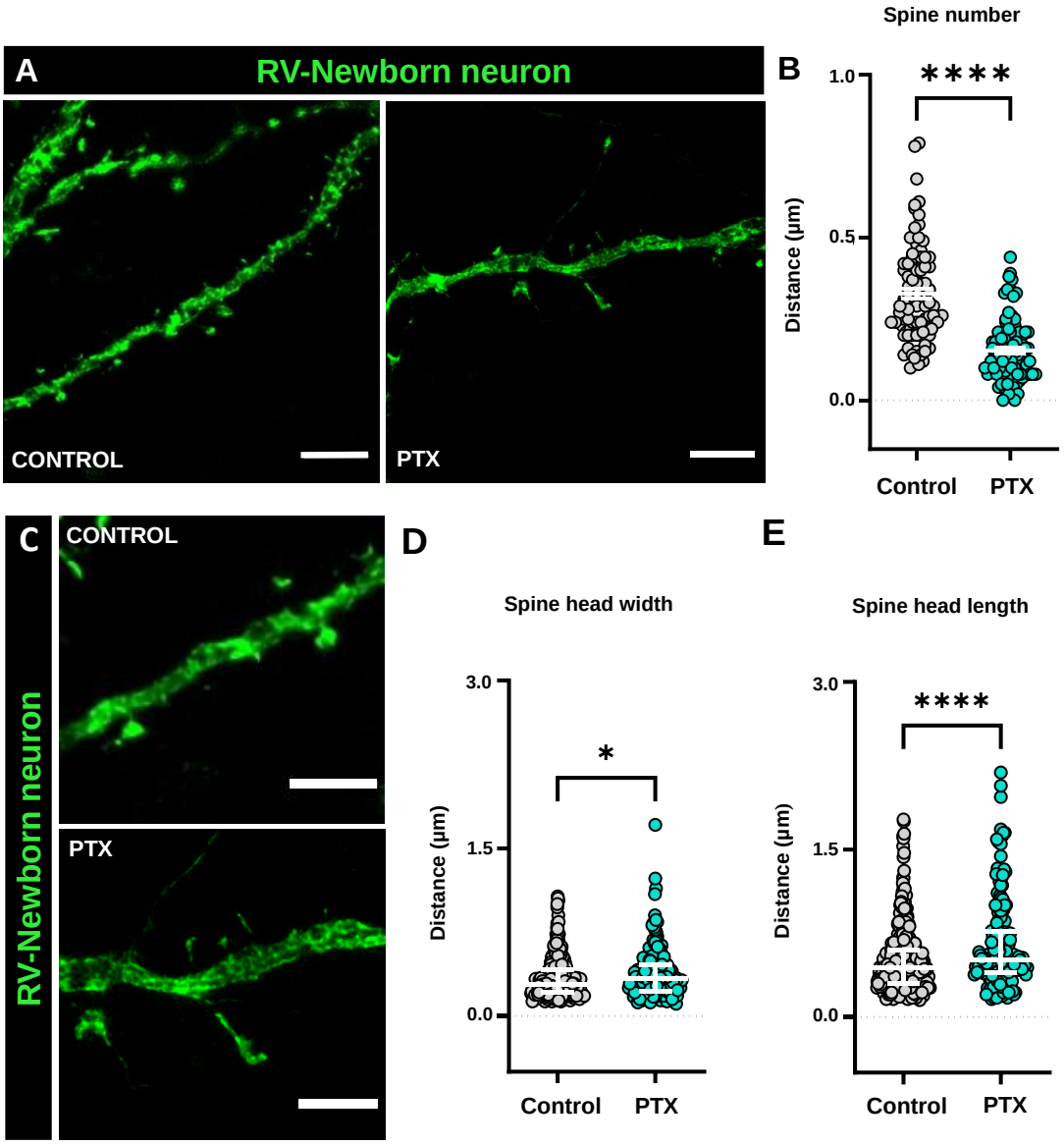

Figure 8. Newborn neuron dendritic spines are impaired in the DG of PTX-induced epileptogenic hOTCs. (A, C) Representative confocal microscopy images showing dendritic spines from segments of PTX- and non-treated RV-Venus labeled and GFP$^+$ dendrites. Z-series images of 30-100 µm from soma were captured (63X oil objective, zoom factor 5X). Images were deconvoluted by using the Huygens program to enhance their quality. **(B)** Quantification of spine number, which is significantly reduced in the PTX-treated group. **(D, E)** Quantification of FWHM. Both the spine head width and length are significantly increased in the PTX-treated group. n=4 animals per group, n=4 slices per animal, n=4 neurons per slice, 32 dendritic segments of 30µm per neuron. A total of 960µm of dendrite was analyzed. The scale bar is 50 µm in the lower magnification photographs and 5 µm in the higher magnification ones. hOTCs were PTX-treated (100µM) for 3 days. They were fixed at DIV 23, 16 days post-RV injection, and 7 days post-treatment. Data are expressed as mean ± SEM and analyzed by non-parametric Mann-Whitney test. * $P < 0.05$, **** $P < 0.0001$.

6.1.7 Neuronal Firing and Network Synchronization during Newborn Neuron Inhibition in Epileptogenesis

In the *in vivo* studies, neurogenesis has been reported to be increased or decreased depending on the model or time point of analysis. However, the few functional studies suggest that aberrant neurogenesis, although not directly able to generate seizures, can contribute to epileptogenesis, especially in early time points[203,204]. In this context, it was hypothesized that the pathological alterations of both dendritic arbor and spines could be directly related to an abnormal neural firing within this area. Therefore, the most effective approach for studying this effect involved the suppression of newborn neuron activity while concurrently monitoring the electrical activity of the neural network. For achieving this objective, and thanks to the collaborative work in the laboratory of Dr. Jenny Hsieh at the University of Texas at San Antonio, a RV carrying DREADDs was used for the hOTCs transfection to express the inhibitory DREADD receptor hm4Di. The DREADDs are modified G-protein-coupled receptors that are unresponsive to endogenous ligands, and can only be activated by CNO, which is biologically inert. The hm4Di as an inhibitory DREADD acts in presynaptic inhibition and silencing of, in this case, the newborn neurons transfected by the RV.

At the same time, the adenoviral vector AAV1.SYN.Gcamp6f.WPRE.SV40 was injected into the system in order to monitor neuronal activity through calcium imaging. This adeno-associated viral vector carries the expression of a fluorescent calcium indicator. The intensity of the signal depends directly on the amount of calcium bound to it, reflecting thus the amount of intracellular calcium and therefore neuronal activity. Following viral injection, in which both the RVDREADDs hm4Di and the AAV.Syn.GCamp6 were used at the same time, hOTCs were 1 week in culture until the PTX-treatment was initiated as previously described (for methods refer to Methods 5.2.1). The experimental framework was as follows: a) CNT1 and PTX1 groups: vehicle or PTX-treated hOTCs with both viral injections but no CNO addition (as a control for newborn neuron activity blockage); b) CNT2 and PTX2 groups: vehicle or PTX-treated hOTCs with both viral injections and CNO addition to block newborn neuron activity; c) CNT and PTX groups: vehicle or PTX-treated hOTCs with just adenoviral vector injection as a control for RVDREADDs labeling effects (Fig. 9A). The slices obtained from each of the animals used were separated to cover the different experimental conditions and imaged on the same DIV for 20 minutes (see Methods 5.8).

After pooling instantaneous firing rates (IFs) across all neurons from all slices within the same group and day of recording, non-parametric group comparison (Kruskal-Wallis test) revealed a significant difference between CNT and PTX groups, showing a much higher firing frequency at single neuron levels in epileptogenic slices (PTX1 group, Fig. 9B). Thus, these higher levels of single-neuron firing in the circuits exposed to epileptogenic conditions confirmed the induction of a hyper-excitable

epileptiform state in the present hOTCs model, similar to the observations in the key paper mentioned before[372]. Additionally, when the newborn neurons were inactive during epileptogenesis (PTX2 group, Fig. 9B), the firing frequency stayed at physiological levels, meaning that the acute inhibition of newborn neuron activity preserved the level of single-neuron firing to baseline control conditions, which suggests a direct relationship between aberrant neurogenesis and abnormal neural activity.

Since ictal and inter-ictal epileptic dynamics are characterized by pathological synchronous events across neurons and brain circuits, the coordinated firing across cells in the circuits was analyzed next, first focusing on the firing at the level of neuronal pairs (Fig. 9C). Physiologically, the communication between neuronal pairs leads to correlated neuronal pair activity. However, synchronous epileptic dynamics could emerge from pair-wise level scaling up to circuits. Therefore, the hypothesis involved higher pair-wise correlation in the spontaneous firing of epileptic circuits, calculating the correlation between the smoothed time series of neuronal firing (for further details see Methods 5.8.1). Here, non-parametric group comparison on pooled statistic of firing's correlations across all neuronal pairs and slices showed significant differences between the PTX1 group (PTX-treated slices) and the rest, while the physiological levels of pair-wise synchronized dynamics were preserved after inhibiting newborn neuron activity during epileptogenesis (PTX2 group, Fig. 9C).

Synchronization is a key feature of epileptic activity, but also a physiological feature of spontaneous circuit dynamics. Therefore, the subsequent step involved quantifying the synchronizations within networks (Fig. 9D Frequency (Hz)). Synchronized events could also be detected by chance simply as a consequence of the background neuronal activity. To address this, synchronizations were considered with just a number of recruited cells above chance level. The chance level was estimated through reshuffled random firing, keeping the same firing frequency for individual neurons (see Methods 5.8.1). As aforementioned, previous research has indicated that a prolonged exposure (3 days) to GABAergic synaptic blockers creates an extended epileptogenic time window, leading to an impact on networks' synchronizations[372].

When the frequency of circuit synchronizations in slices treated with PTX were examined (PTX1 group, Fig.9D Frequency (Hz)), a significant increase was observed in the frequency of circuit synchronizations compared to the corresponding control conditions, which were also preserved after inhibiting newborn neuron activity (PTX2 group, Fig. 9D Frequency (Hz)). Next, synchronizations were measured as a percentage of recruited cells from the total imaged neural population (Fig. 9D Size (%)). The pooled statistics of circuit synchronizations revealed significant distinctions between the PTX-treated group (PTX1 group, Fig.9D Size (%)) and all other groups in terms size of circuit synchronization ($p<0.05$), size referring to the number of cells involved in a synchronized event within neural circuits. As in the previous measurements, they also preserved control levels after inhibiting newborn neuron activity during epileptogenesis (PTX2 group, Fig. 9D Size (%)).

Summarizing the results, synchronized ensemble dynamics in the epileptic group were more frequent and recruited a larger number of neurons, which recovered the control condition after newborn neuron activity inhibition.

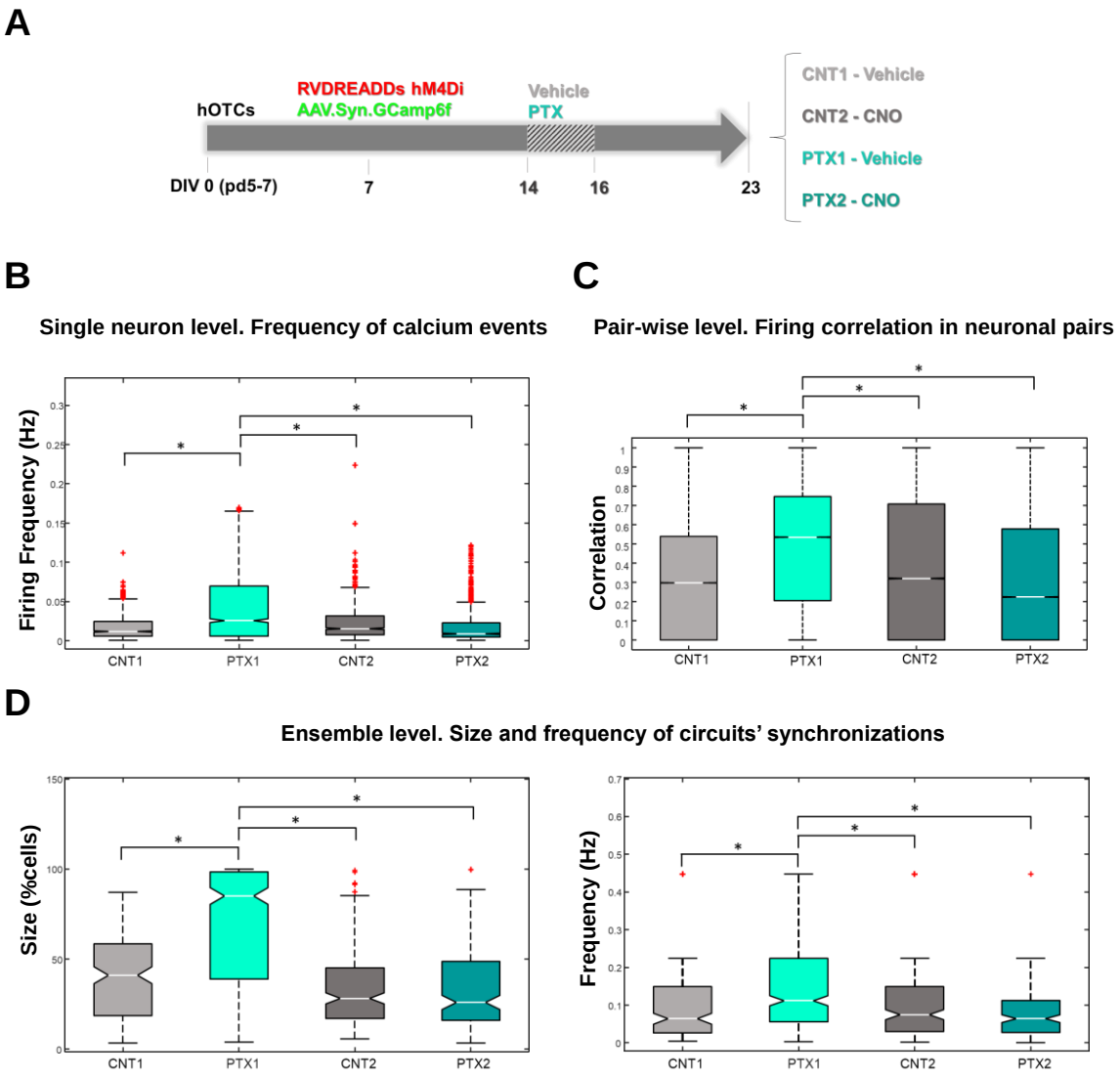

Figure 9. Single neuron firing, pair-wise firing correlation, and circuit synchronizations increase during PTX-induced epileptogenesis and are recovered after inhibiting newborn neuron activity. (A) Scheme of the experimental procedure. The hOTCs are extracted at pd5-7 (DIV 0) and cultured. After 1WIV, the DG is retrovirally- (RVDREADDs hm4Di) and adenovirally- (AAV.Syn.GCamp6f) injected, and 1 week after that, slices are exposed to a $GABA_A$ receptor inhibitor (picrotoxin, PTX 100µM) for 3 days. Recordings are performed 1 week later, at DIV 23, where clozapine-N-oxide (CNO, for DREADDs activation) or vehicle (as a control) are added. Results from the following 4 conditions are shown: CNT1 (non-treated), CNT2 (non-treated and RVDREADDs-induced newborn neuron inactivation), PTX1 (PTX-induced epileptogenic), and PTX2 (PTX-induced epileptogenic and RVDREADDs-induced newborn neuron inactivation). **(B)** For each cell the average inverse of the intervals between consecutive calcium spikes are considered as firing rate. Pooled values at CNT1, CNT2, PTX1, PTX2 across all slices are showing median (horizontal line) 25-75 percentile limits, bottom-top range values and outliers (marked by red asterisks). **(C)** Pooled values at CNT1, CNT2, PTX1, PTX2 across all slices of the firing correlation are showing median (horizontal line) 25-75 percentile limits, bottom-top range values and outliers (marked by red asterisks). **(D)** Pooled values of synchronizations' sizes and frequencies at CNT1, CNT2, PTX1, PTX2 across all slices are showing median (horizontal line) 25-75 percentile limits, bottom-top range values and outliers (marked by red asterisks). Data are expressed as mean ± SEM and analyzed by Kruskal-Wallis ANOVA test with Dunn post-hoc correction. * $P < 0.05$.

6.1.8 Neural Spike Counts during Newborn Neuron Inhibition in Epileptogenesis by MEA-based Recordings

The investigation was extended by conducting MEA-based recordings on similar experimental groups. To achieve this, the slices were placed in the MEA setup, where 12 electrodes monitored the hippocampal activity within the tissue (Fig. 10A). Notably, control groups exhibited minimal differences. Specifically, expected to be similar since the only distinction was the injection of RVDREADDs without CNO activation, displayed comparable oscillation frequencies. Thus, the viral injection itself seemed to have no effect. In the CNT2 group, where newborn neuron activity was suppressed, possible alterations in the neural activity were considered. However, despite their inactivation, results indicated a similar tendency to the other controls, suggesting that newborn neuron activity may not be crucial, at least in high frequencies, in this hOTCs model.

When looking at the epileptogenic groups, the results were quite interesting, involving alterations in the different oscillation patterns. In terms of beta oscillations [13-30] Hz, an increase in power spectrum density was observed in epileptogenic conditions (PTX and PTX1 groups) compared to the rest (Fig. 10B). The expected similarities between PTX and PTX1, given the only difference being the viral injection, were also evident. The substantial difference between these epileptogenic groups and the control ones implies a notable impact of hyperexcitation on neural activity.

Notably, in the PTX2 group, where newborn neurons were inactivated during epileptogenesis, control conditions were preserved (Fig. 10B). Examining higher oscillation frequencies, such as low and high gamma [30-50] and [50-100] Hz, respectively (Fig. 10C, D), and even higher frequencies as HFO slow ripples [100-250] Hz and fast ripples [250-600] Hz (Fig. 10E, F), revealed a consistent effect: the inhibition of newborn neuron activity during epileptogenesis (PTX2 group) showed no discernible alterations compared to control groups.

This remarkable observation suggests inactivating aberrant newborn neurons during epileptogenesis preserves the physiological state of high frequencies in the hippocampal DG, providing evidence linking alterations in newborn neurons to neural network activity effects. It is crucial to note that these are preliminary results without statistical analysis, but the robust trend strongly indicates promising outcomes for subsequent studies.

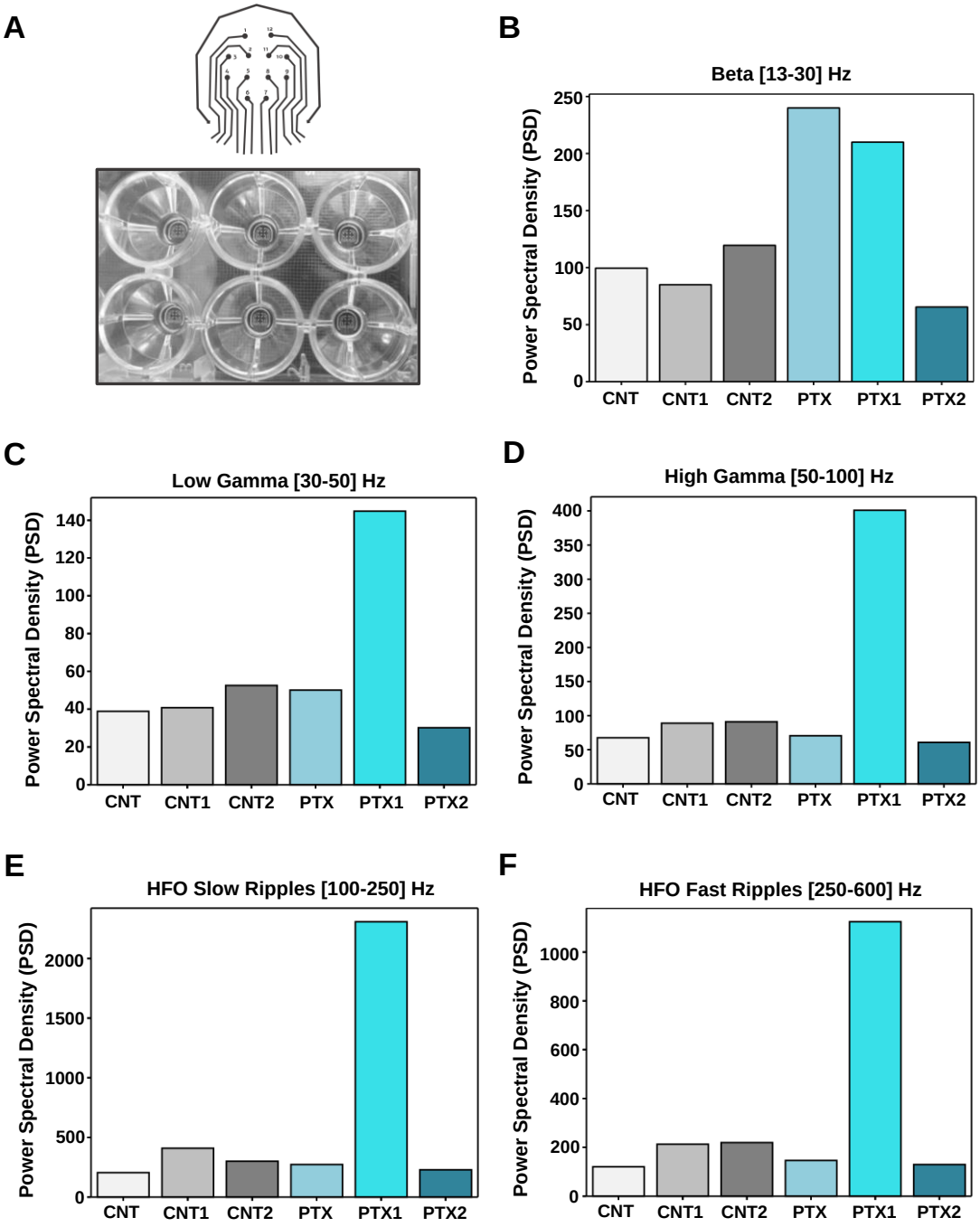

Figure 10. Newborn neuron activity inactivation preserves high oscillation frequencies in epileptogenic hOTCs. **(A)** Illustration showing the twelve electrodes of the MEA setup (on top) and a six-well plate MEA setup with the twelve electrodes in the bottom of each well (on the bottom). **(B-F)** The power spectral density (PSD) was studied for individual recordings in the six conditions: CNT (non-treated, no RVDREADDs), CNT1 (non-treated and RVDREADDs without CNO activation), CNT2 (non-treated and RVDREADDs with CNO-induced newborn neuron inactivation), PTX (PTX-induced epileptogenesis, no RVDREADDs), PTX1 (PTX-induced epileptogenesis and RVDREADDs without CNO activation), and PTX2 (PTX-induced epileptogenesis and RVDREADDs-induced newborn neuron inactivation). **(B)** Beta oscillation frequency [13-30] Hz, **(C)** low gamma oscillation frequency [30-50] Hz, **(D)** high gamma oscillation frequency [50-100] Hz, **(E)** high oscillation frequency (HFO) slow ripples [100-250] Hz and **(F)** HFO fast ripples [250-600] Hz increase in epileptogenic hOTCs (PTX1 group) and are preserved after newborn neuron inactivation (PTX2 group). hOTCs were PTX-treated (100µM) for 3 days. They were analyzed at DIV 23 and 7 days post-treatment. Data was expressed by mean values. Results were visualized in a bar chart, where the height of each bar was obtained by taking the median across all values of the sliding windows belonging to each state.

In summary, the results obtained in the implementation of the epileptogenic hOTCs model reveal that under healthy conditions, newborn neurons exhibit well-developed dendritic arborization, along with favorable density and shape of dendritic spines (Fig. 11.1). However, following PTX-induced epileptogenesis, the neurogenesis is reduced and increased pathological cell death is observed (Fig. 11.3). In this context, newborn neurons display aberrant features such as smaller dendritic arbors and fewer dendritic spines, but bigger spine heads (Fig. 11.2). Additionally, they have been linked to a hyperexcited neural network, as their lack of activity could be associated to the preservation of normal activity in terms of single neuron firing, pairwise correlations, circuit synchronizations, and even high frequency oscillations.

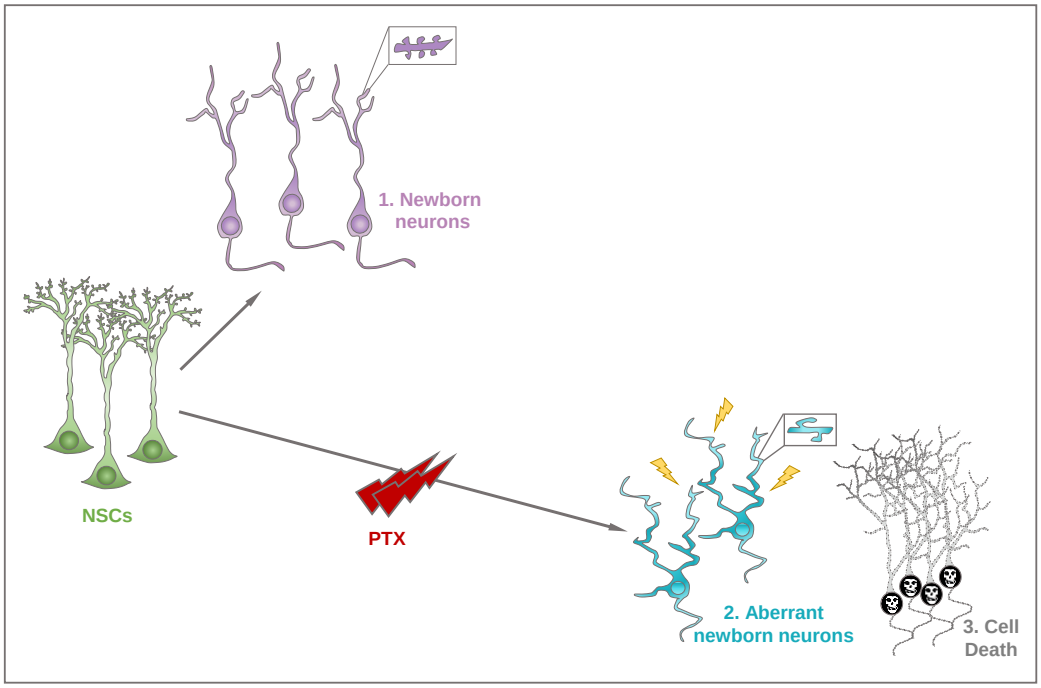

Figure 11. The differential fate of multipotent adult hippocampal NSCs in health and disease in a hOTCs model. In normal conditions, the hippocampal NSCs of the DG, after activating, divide and differentiate into immature neurons (newborn neurons, **(1)**), which present a developed dendritic arbor and already show dendritic spines. In situations of pathological neuronal hyperexcitation such as epilepsy, NSCs can generate aberrant newborn neurons **(2)**, characterized by reduced neurogenesis, abnormal dendritic arborization, dendritic spine density and shape, and also increased cell death **(3)**. These newborn neurons are also related to an increased hyperexcitability in the neural network.

6.2 ATP Addition to hOTCs

6.2.1 ATP Impairs Neurogenesis

In epilepsy, it has been already addressed that ATP release increases[297,299–301], and due to the inflammatory response related to that increment, in the present work it was hypothesized that it may contribute to aberrant neurogenesis. There, the addition of excessive eATP to hOTCs was speculated to have the same damaging effect as in PTX-induced epileptogenic conditions in terms of cell survival and newborn neuron development. To test this, two groups were stablished: a control condition (CNT group), where cultured slices were not exposed to excessive eATP, so it was considered as a physiological state of the tissue; and an ATP group, where cultured slices underwent an additional extracellular presence of eATP (200 μM) during 3 days (from DIV 14 to DIV 16, Fig. 12A). Here, neurogenesis was characterized in both groups by quantifying DCX^+ cells in the GCL+SGZ, where a statistically significant decrease by half was found in the ATP-treated compared to the non-treated hOTCs (Fig. 12B, C). In contrast, the number of dead cells showed a significant increase by 2-fold (Fig. 12D, E), confirming the hypothesis of the excessive eATP having the same deficient effect as the epileptogenic agent PTX in culture in terms of cell survival.

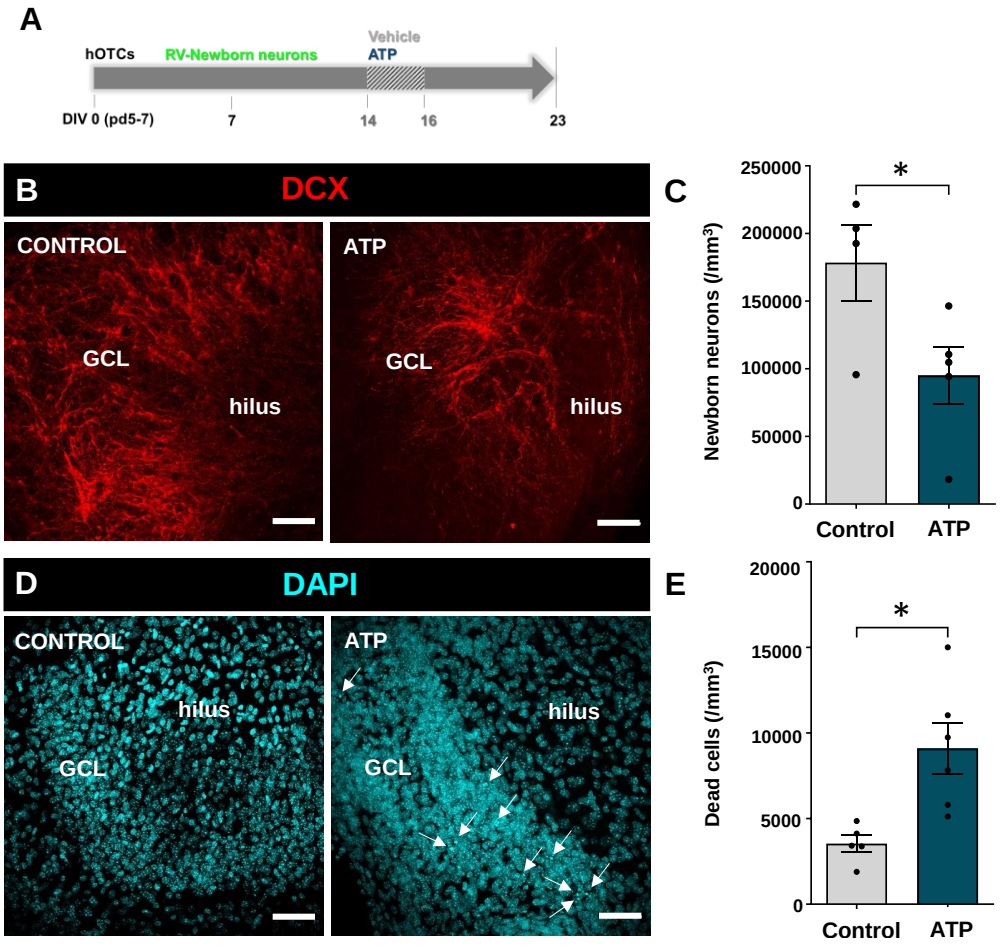

Figure 12. Newborn neurons and cell death are impaired in the DG after eATP excess in hOTCs. (A) Scheme of the experimental procedure. The hOTCs are extracted at pd5-7 (DIV 0) and cultured. After 1WIV, the DG is RV-injected (Venus, GFP^+), and 1 week after that, slices are exposed to ATP (200µM) for 3 days. Immunostainings are performed 1 week later, at DIV 23. **(B)** Representative confocal microscopy images were taken after staining for DCX, showing the SGZ+GCL in the mouse hippocampal hOTCs. **(C)** Newborn neurons (/mm^3) were quantified by identifying DCX^+ cells. **(D)** Representative confocal microscopy images were taken after staining for DAPI, showing the SGZ+GCL in the mouse hippocampal hOTCs. **(E)** Cell death (/mm^3) was quantified by identifying nuclei presenting pyknosis (DNA condensation) and/or karyorrhexis (nuclear fragmentation), both detected by condensed staining of DAPI. n = 4 per group. The scale bar is 50 µm in all the photographs. hOTCs were fixed at DIV 23, 16 days post-RV injection and 7 days post-treatment. Data are expressed as mean ± SEM and analyzed by non-parametric Mann-Whitney test. * $P < 0.05$.

6.2.2 ATP Induces Aberrant Neurogenesis

Regarding the hypothesis of excessive eATP having a harmful effect on newborn neuron development, exploring its impact on their morphology was a very relevant aspect. To assess newborn neuron complexity, the 3D-Sholl analysis was again used, as it is a very useful technique to examine the number of intersections within cell structures, and that in the case of newborn neurons, suitably detects dendritic arborization complexities such as dendrite bifurcations on their total length. After such a detailed analysis of newborn neuron morphology, a strong alteration was observed as the complexity of the dendritic arbor dramatically decreased between the radius 50µm and 180µm in excess of eATP-treated hOTCs compared to control (Fig. 13A, B), suggesting a potential link between ATP upregulation and the aberrant neurogenesis that occurs during epileptogenesis.

Consequently, after these observations in the morphology of newborn neurons in excessive eATP conditions, the presence of abnormalities in their dendritic spines was analyzed. This quantification was for the first time in the project's data analysis performed using the SpineJ plugin in ImageJ. With this technique for measuring spines, it was possible to obtain a more detailed characterization of the dendritic spines with not just the density and the width and length of the spine heads but also their perimeter and area. Most importantly, all these features analyzed were almost automatically obtained after a confocal-based imaging of the dendritic spines, reducing the time spent in their quantification and study. After this analysis, the investigation with SpineJ in newborn neuron dendritic spines from excessive eATP-treated hOTCs indicated a 30% decrease in spine number, along with an increase in spine head size, measuring 54% longer in major axis (µm) and 58% wider in minor axis (µm), with a 48% larger perimeter (µm) and a 63% greater area (μm^2) compared to control conditions (Fig. 13C-I).

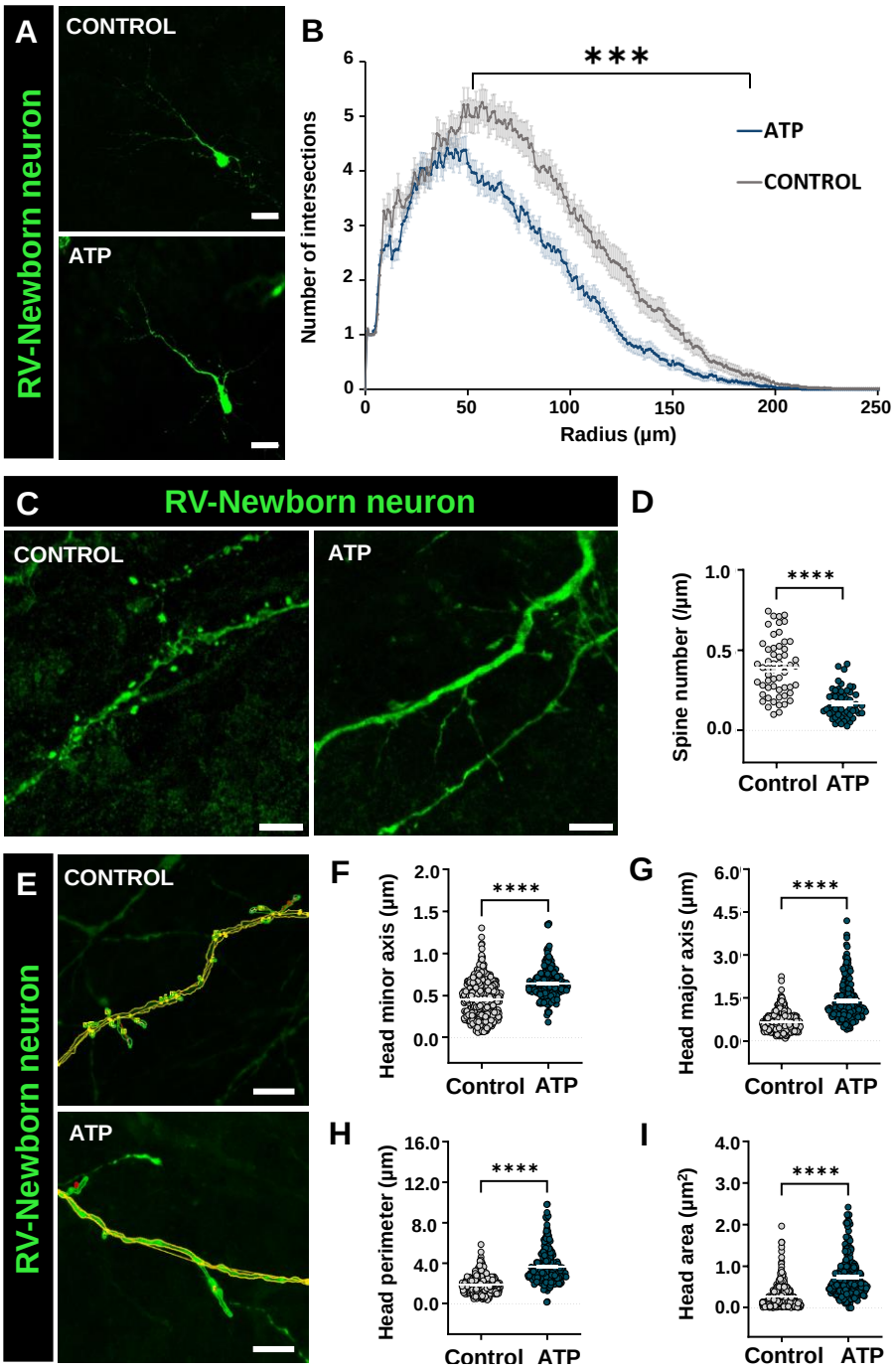

Figure 13. Newborn neuron morphology and dendritic spines are impaired in the DG after eATP excess in hOTCs. (A) Representative confocal microscopy images, showing ATP-treated and non-treated developing neurons. **(B)** Z-stack projections were analyzed and color-coded according to their 3D-Sholl profile. Quantification of the number of intersections between circles of increasing (1µm) radius showed a statistically significant reduction in their morphological complexity in the ATP-treated group. The scale bar is 50 µm in all the photographs. Data are expressed as mean ± SEM and analyzed by ANOVA repeated measures test with Bonferroni post-hoc correction. **(C, E)** Representative confocal microscopy images, with and without SpineJ processing (in yellow), showing dendritic spines from segments of ATP-treated and non-treated RV-Venus injected and GFP-stained dendrites. **(D)** Quantification of spine number (/µm), which is significantly reduced in the ATP-treated group. Data are expressed as mean ± SEM and analyzed by an unpaired t-student test. **(F-I)** Quantification of spine head minor axis (µm), major axis (µm), parameter (µm), and area (µm^2) respectively. n=4 animals per group, n=4 slices per animal, n=4 neurons per slice, 32 dendritic segments of 30µm per neuron. A total of 960µm of dendrite was analyzed. The scale bar is 5 µm in all the photographs. hOTCs were ATP-treated (200µM) for 3 days. They were fixed at DIV 23, 16 days post-RV injection, and 7 days post-treatment. Data are expressed as mean ± SEM and analyzed by non-parametric Mann-Whitney test. *** $P < 0.001$, **** $P < 0.0001$.

Hence, in the case of excessive eATP, parallel results to those in PTX-induced hyperexcitability conditions were observed in terms of aberrant neurogenesis. In direct comparison to newborn neurons under healthy conditions, where their dendritic arbors and spines exhibit a physiological appearance (Fig. 14.1), an elevated ATP concentration similarly resulted in reduced neurogenesis and cell death increase (Fig. 14.3). Once again, newborn neurons showed abnormal dendritic arbors with their dendritic spines also impaired, characterized by a reduced number and longer and wider spine heads (Fig. 14.2).

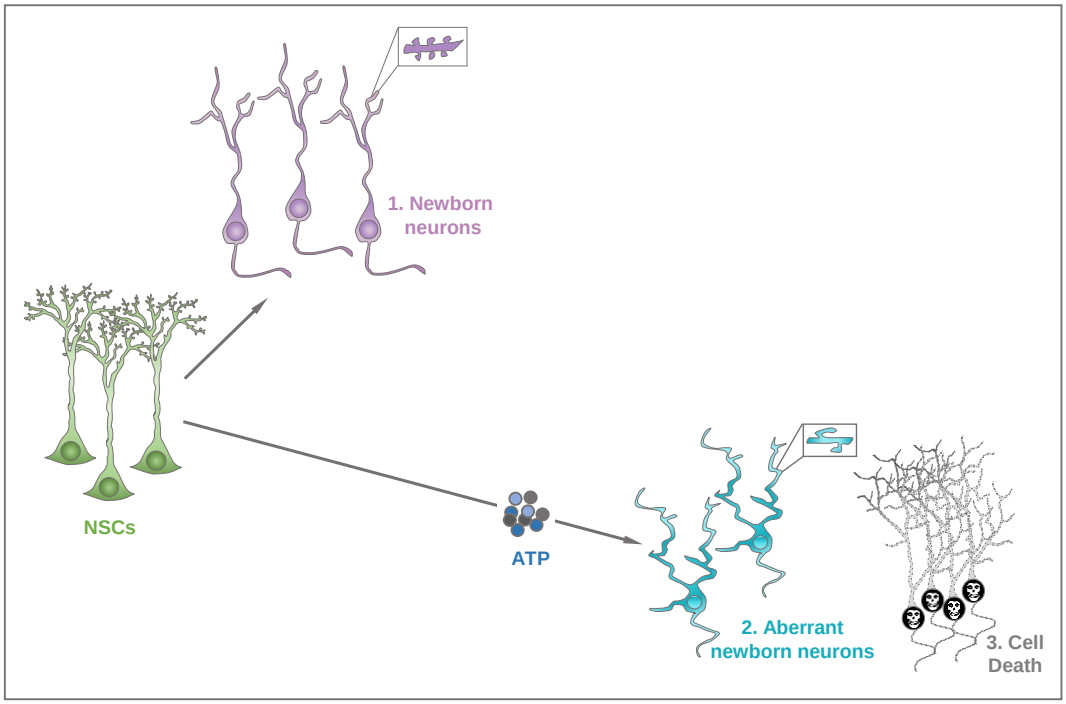

Figure 14. The differential fate of multipotent adult hippocampal NSCs in health and after increased eATP concentrations in a hOTCs model. In normal conditions, the hippocampal NSCs of the DG, after activating, divide and differentiate into immature neurons (newborn neurons, **(1)**), which present a developed dendritic arbor and already show dendritic spines. In eATP excess, the newborn neurons generated present aberrant features **(2)**, characterized by reduced neurogenesis, abnormal dendritic arborization, dendritic spine density and shape, and also increased cell death **(3)**.

6.3 P2XR Inhibition in hOTCs

6.3.1 P2XR Inhibition Preserves Neurogenesis during Epileptogenesis

The verification of excessive eATP causing detrimental effects in the present epileptogenic hOTCs model was key for the next hypothesis, in which purinergic receptors were blocked for neurogenesis preservation. Thus, a selective antagonist of purinergic 2X receptors (P2XR) was used, the called trinitrophenyl-adenosine-triphosphate (TNP-ATP), in the following experimental groups: a) the control condition (CNT group): the cultured slices were never exposed to hyperexcitability induction nor P2XR inhibition; b) epileptogenic condition (PTX group): the cultured slices underwent suppression of GABAergic transmission in extracellular presence of PTX (100µM) from DIV 14 to DIV 16 (3 days); c) the control under inhibited- P2XR condition (TNP group): the cultured slices were exposed to TNP-ATP (50µM) from DIV 14 to DIV 16 (3 days, TNP3d group) or DIV 22 (7 days, TNP7d group); and d) the epileptogenic and inhibited- P2XR condition (PTX+TNP group): the cultured slices underwent suppression of GABAergic transmission as in the PTX group (100µM, 3 days), with simultaneous extracellular application of P2XR-antagonist TNP-ATP (50µM, 3 days PTX+TNP3d group, or 7 days PTX+TNP7d group) (Fig. 16A, B). The slices obtained from each of the animals used were separated to cover the four different experimental conditions and imaged on the same DIV (see Methods 5.2.1).

First, the optimal treatment duration for the addition of TNP-ATP antagonist was assessed by comparing the well-being of the slices after 3 days of treatment with that after 7 days of treatment. The objective was to elucidate whether a 3-day P2XR inhibition period would be enough to achieve the hypothesized recovering effect, or if, on the opposite, a full week of treatment would be damaging instead of beneficial. For that, the staining procedure for a newly acquired antibody in our laboratory was first optimized: H2AX, designed to detect DNA damage. Fixed slices from KA-induced epileptic adult mouse brains were utilized, and the same antibody was tested in two different brands at varying concentrations (Biolegend 1:250 and 1:500; Abcam 1:300 and 1:500) to establish the most effective staining protocol. The findings indicated that the Biolegend antibody worked well both at 1:250 and at 1:500 dilution, whereas the Abcam antibody required a 1:300 dilution to show satisfactory staining results as at 1:500 no labeling was observed (Fig. 15A, B). Therefore, the antibody chosen for the subsequent immunostaining in the rest of the experiments was the one from Biolegend at a dilution of 1:500, as it is the one in which the antibody works perfectly by using a higher dilution, meaning that we waste less obtaining the same results.

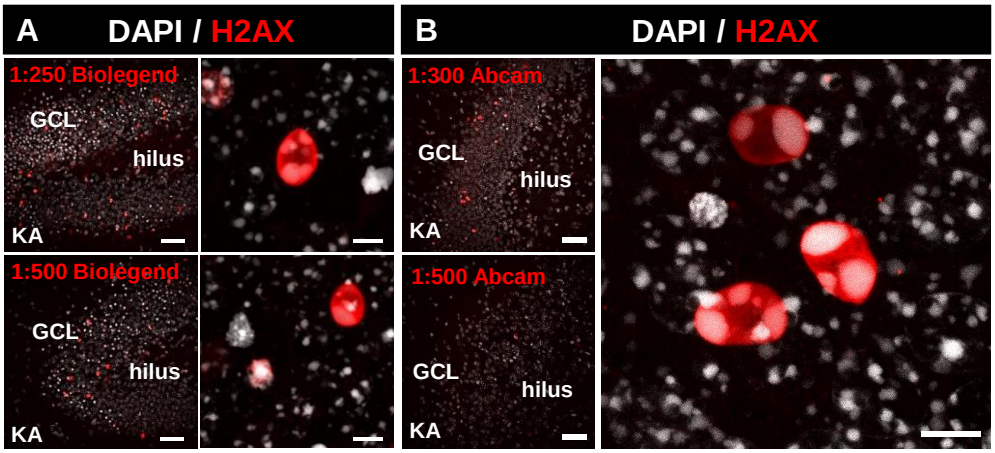

Figure 15. Optimization of DNA damage marker H2AX in KA-induced epileptic adult mouse brain slices. Ipsilateral slices were obtained from WT mice that were stereotactically injected with KA (20mM) at 3 months old and perfused at 3 days post-injection. **(A)** Representative confocal microscopy images showing the SGZ+GCL in the hippocampus of KA-induced epileptic adult mouse brain after staining for DAPI (a marker of cell nuclei) and H2AX from Biolegend in different concentrations (1:250 and 1:500). Examples of HA2X stained nuclei are also shown at higher magnification. **(B)** Representative confocal microscopy images showing the SGZ+GCL in the hippocampus of KA-induced epileptic adult mouse brain after staining for DAPI and H2AX from Abcam in different concentrations (1:300 and 1:500, in which no staining was observed). An example of 1:300 HA2X stained nuclei is also shown at higher magnification. The scale bar is 50 μm in lower magnification and 5 μm in higher magnification photographs.

Once the H2AX antibody was functional and the concentrations for the experiments in tissue established (Biolegend in 1:500 dilution), it was used in hOTCs to assess the P2XR inhibitor's effect. First, a quantification was conducted after both H2AX and DAPI staining in slices of all the conditions mentioned before (CNT, PTX, TNP3d, TNP7d, PTX+TNP3d, PTX+TNP7d), in which co-localizing DNA damage staining and pyknotic/karyorrhexic nuclei were identified at both 3 and 7 days post-treatment. As a result, when the antagonist was continuously added for 7 days, both in control (TNP7d group) and epileptogenic conditions (PTX+TNP7d group), an increment by half was observed in damaged cell population. This outcome discarded the P2XR inhibitor treatment period of 7 days for the next of the experimental work due to the toxicity it presented. In contrast, the slices recovered their physiological state in terms of survival when TNP was added to epileptogenic slices for just 3 days (PTX+TNP3d group), indicating reduced cell death (Fig. 16C) and thus showing neuroprotection. However, when the P2XR was blocked for 3 days in non-epileptogenic and thus, non-excessive eATP conditions (TNP3d group), an even higher increase in cell death was observed (65%), indicating a higher toxicity rate of this treatment in healthy slices. Anyway, it is yet a great tool for the study of aberrant neurogenesis in epileptogenic conditions due to the neuroprotection shown after PTX-induced epileptogenesis in the hOTCs, being reason enough for its utilization in the model for aberrant neurogenesis assessment.

Therefore, once the 7-day TNP treatment was discarded and the 3-day P2XR inhibition through TNP treatment was selected for the experimental framework stablished, the TNP3d group was termed TNP group and PTX+TNP3d became just PTX-TNP group for the rest of the experimental work in order to simplify the reading (Fig. 16D). Then, the cell death was one more time analyzed with the already characterized H2AX antibody (1:500 Biolegend), in which similar results were obtained: cell death conditions improved when P2XR was inhibited in PTX-induced epileptogenic hOTCs (Fig. 16D, E).

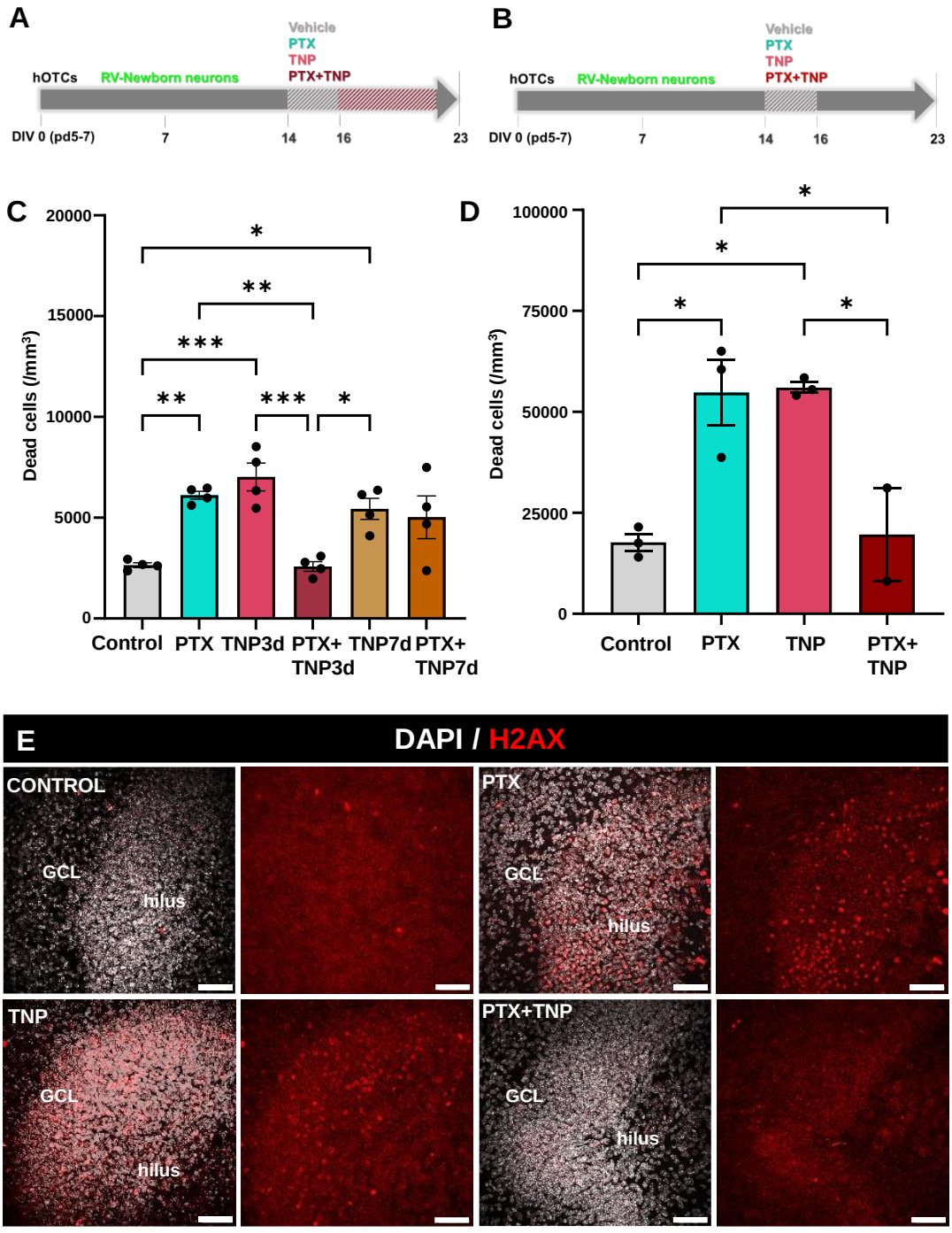

Figure 16. Cell death assessment after P2XR inhibition during different time-points in epileptogenic hOTCs. (A, B) Scheme of the experimental procedure. The hOTCs are extracted at pd5-7 (DIV 0) and cultured. At DIV 7, slices are injected for the expression of RV-Venus (GFP^+). From DIV 14 to DIV 16 or DIV 22 they are exposed to $GABA_A$ receptor inhibitor PTX (100µM) and/or P2XR antagonist TNP-ATP (50µM), and immunostainings and imaging are performed 7 days after (DIV 23). **(C)** Quantification of dead cells (/mm^3) after DAPI staining in the hippocampus, observing a deterioration in 1-week treatment but a recovery in 3-day treated hOTCs. Cell death was quantified by identifying nuclei presenting pyknosis (DNA condensation) and/or karyorrhexis (nuclear fragmentation), detected by condensed staining of DAPI. n=4 per group. Data are expressed as mean ± SEM and analyzed by 2-way ANOVA with repeated measures test and Holm Šídák post-hoc correction. **(D)** Quantification of dead cells (/mm^3) in the hippocampus, observing a recovery in 3-day treated hOTCs in terms of DNA damage (H2AX staining). n=3 per group. **(E)** Representative confocal microscopy images after staining for H2AX showing the SGZ+GCL in the hippocampal PTX-, TNP-, PTX+TNP-, and non-treated hOTCs. The scale bar is 50 µm in all the photographs. Data are expressed as mean ± SEM and 1-way ANOVA test with Bonferroni correction. * $P < 0.05$, ** $P < 0.01$, *** $P < 0.001$.

The neuroprotective effects of inhibiting P2XR in epileptogenic hOTCs was then further investigated in relation to ROS production. For that, the assessment was made with three different aims: (**a**) to study the increase in ROS production observed in previous reports that show epileptiform conditions leading to an increase in ROS production[363–365]; (**b**) to confirm the hypothesis relating the inhibition of P2XR in epileptogenic conditions to a decrease in ROS generation; and (**c**) to evaluate the toxicity induced by the P2XR inhibitor in healthy conditions in terms of oxidative stress due to the results previously obtained in cell survival. To test so, the CM-DCFDA (2',7'-Dichlorofluorescein, DCF) probe was used, which undergoes oxidation by ROS generating a fluorescent product. In such a manner, the rate of increase in the fluorescent signal indicated the rate of ROS generation, meaning that a higher signal represents more oxidative stress in the slice.

Following a 30-minute incubation with the DCF probe (30µM), under the previously mentioned four different conditions (CNT, PTX, TNP, and PTX+TNP groups), a 2-fold increase was detected in the epileptogenic state (PTX group) compared to control (Fig. 17A, B). These results supported the previously mentioned observations in literature of ROS production increasing during epileptogenesis (**a**). But is the P2XR inhibition enough for preserving the physiological state of oxidative stress? When looking at the inhibition of P2XR in epileptogenic slices (PTX+TNP group), a reduction by half was detected in the ROS reported signal when compared to untreated epileptiform slices (Fig. 17A, B), indicative of a reduction of oxidative stress and the preservation of the physiological state in the slice, confirming the mentioned hypothesis (**b**). In contrast, the inhibition of P2XR in control slices (TNP group) showed a significant increase of the 43% in DCF intensity (Fig. 17A, B), suggesting an increase in ROS generation (**c**). This increase in oxidative stress could be closely related to the increase in apoptotic cells observed before (Fig. 16D, E), due to the stress that might be induced by the addition of TNP-ATP antagonist. Indeed, the blockage of P2XR in lack of excessive eATP during a physiological state may generate an inflammatory response and thus, an increase in the production of ROS, leading to cell death. However, the mechanisms underlying these effects are not yet well understood, and may depend on the specific experimental conditions.

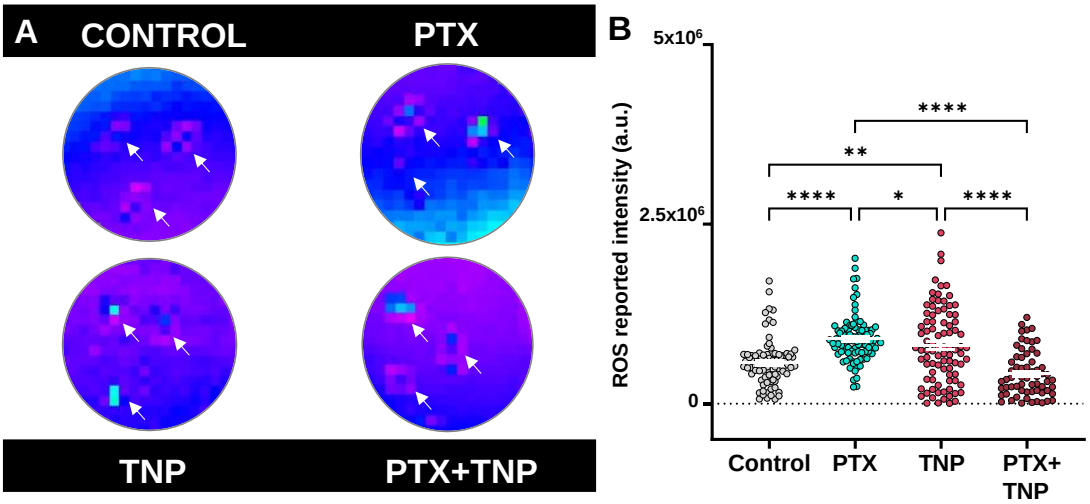

Figure 17. OS assessment in epileptogenic hOTCs where control levels are recovered after P2XR inhibition. DCF probes were used for ROS assessment in hOTCs. **(A)** Representative images from CLARIOStar Plus Plate Reader of the insert membranes with PTX-, TNP-, PTX+TNP- and non-treated mouse hippocampal hOTCs in them, analyzed and color-coded according to their fluorescence intensity profile, in which warmer hues indicate higher OS. **(B)** Quantification of ROS reported fluorescence intensity (a.u.) in PTX-, TNP -, PTX+TNP- and non-treated mouse hippocampal hOTCs showing a significant preservation of control conditions in PTX+TNP-treated hOTCs. n=3 per group, containing 4 slices in each. The intensity was measured at DIV 18 and 1 day post-treatment. PTX and TNP were added for 3 days. Data are expressed as mean ± SEM and analyzed by Kruskal-Wallis ANOVA test with Dunn post-hoc correction. * $P < 0.05$, ** $P < 0.01$, **** $P < 0.0001$.

In the same line, the characterization of neurogenesis and cell survival was performed following the exact framework in the four conditions. The evaluation of neurogenesis through the quantification of DCX^+ cells (/mm³) in the GCL+SGZ showed a statistically significant recovery by half in PTX+TNP-treated slices compared to the PTX group (Fig. 18A, B), meaning that when epileptogenic slices were treated with the P2XR inhibitor, neurogenesis preserved control levels. Moreover, the number of dead cells decreased to control levels in the PTX+TNP group (Fig. 18C, D), indicating a neuroprotective behavior of the purinergic receptor blockage during epileptogenesis. And what about P2XR-inhibited control slices (TNP group)? As previous experiments have demonstrated, this treatment in healthy slices provokes an increased DNA damage in the hOTCs (as shown by H2AX staining, Fig. 16D, E). Therefore, when evaluating cell death by pyknotic/karyorrhectic nuclei identification, it was not a surprise to obtain the same results: a statistically significant increase by 55% of dead cell population (Fig. 18C, D). In this particular case, the damage was not applied for the newborn neuron population density, as the control state was maintained in terms of DCX^+ cell quantification (Fig. 18A, B). These results suggest that in the time point studied, the cells that are dying by apoptosis in an increased manner following P2XR inhibition in control (TNP group) are not newborn neurons but other type of cells, due to the maintenance of the physiological state regarding neurogenesis and the concurrent increase in cell death in this condition.

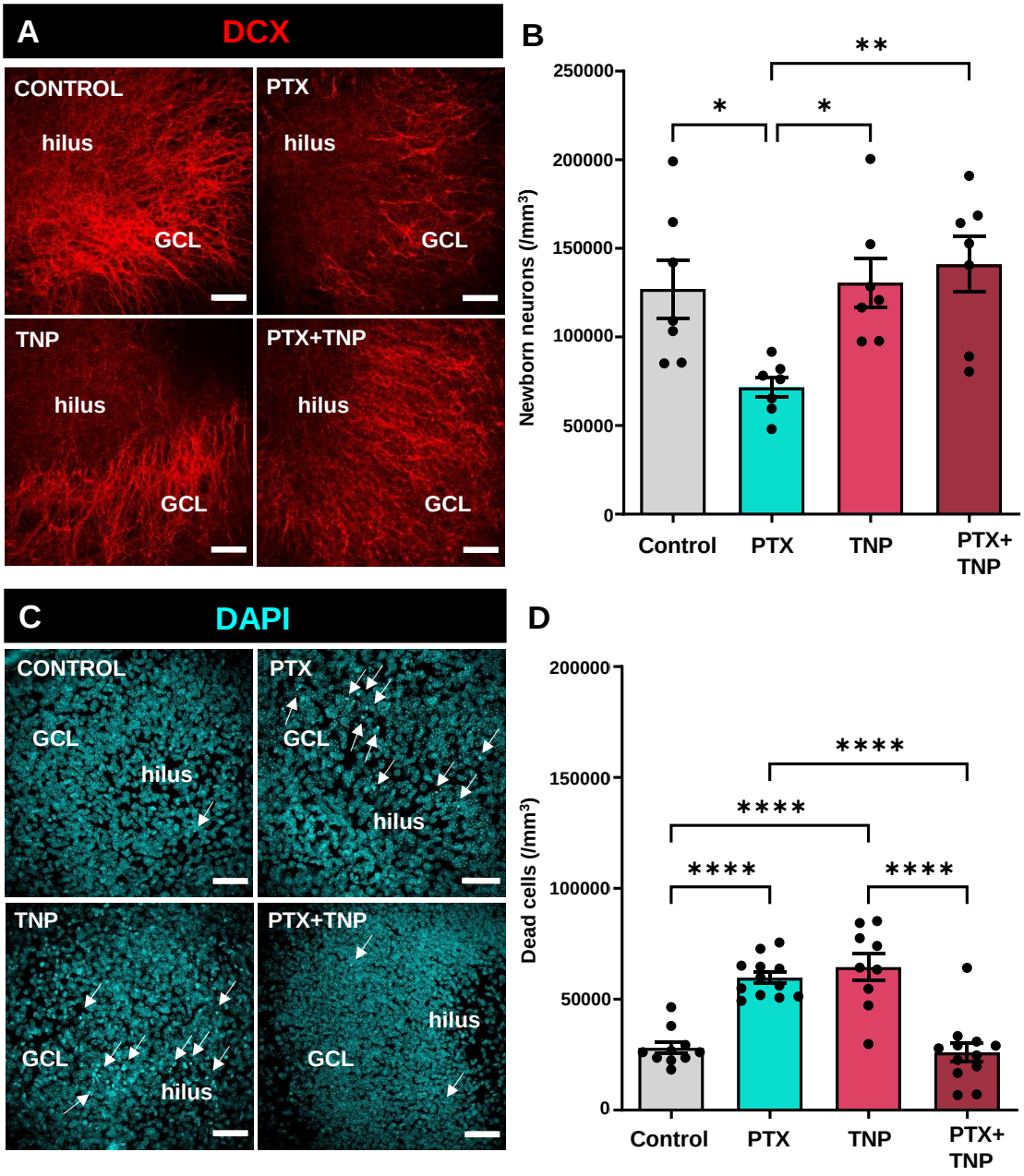

Figure 18. Neurogenesis and cell survival preserve control levels in the DG after P2XR inhibition in epileptogenic hOTCs. (A) Representative confocal microscopy images were taken after staining for DCX, showing the SGZ+GCL in the mouse hippocampal hOTCs. **(B)** Newborn neurons (/mm^3) were quantified by identifying DCX$^+$ cells. n=7 per group. **(C)** Representative confocal microscopy images were taken after staining for DAPI, showing the SGZ+GCL in the mouse hippocampal hOTCs. **(D)** Cell death (/mm^3) was quantified by identifying nuclei presenting pyknosis (DNA condensation) and/or karyorrhexis (nuclear fragmentation), both detected by condensed staining of DAPI. n = 9-12 per group. The scale bar is 50 µm in all the photographs. hOTCs were treated with P2XR antagonist TNP-ATP (50µM) and/or PTX (100µM) from DIV14 to DIV16 and fixed 7 days afterwards (DIV 23). Data are expressed as mean ± SEM and analyzed by Kruskal-Wallis ANOVA test with Dunn post-hoc correction. * $P < 0.05$, ** $P < 0.01$, **** $P < 0.0001$.

6.3.2 P2XR Inhibition Preserves Physiological GABAergic Cell Number in Epileptogenesis

To further confirm the neuroprotective effects of inhibiting P2XR, evaluating GABAergic cell population resulted a feasible readout. Moreover, it was an interesting approach for evaluating the general well-being of the slice, this time by focusing on the primary inhibitory neurotransmitter in the brain, GABA. The number of GABAergic cells was assessed following P2XR inhibition by employing a marker for GABA in the four conditions (CNT, PTX, TNP and PTX+TNP group). Here, it was hypothesized that the number of GABAergic cells would preserve physiological levels in epileptogenesis after TNP-ATP antagonist addition to cultures, which aligned with the observations following quantification: the GABAergic cell population preserved control conditions after purinergic receptor inhibition was applied in epileptogenic slices (PTX+TNP group, Fig. 19A, B), keeping with the neuroprotective properties observed before. However, the toxicity in terms of TNP addition to healthy slices (TNP group) continued to be evident in the case of GABAergic interneurons, as there was also an evident 72% decrease in the density of these cells, comparable to the one observed in the epileptogenic slices (Fig. 19A, B).

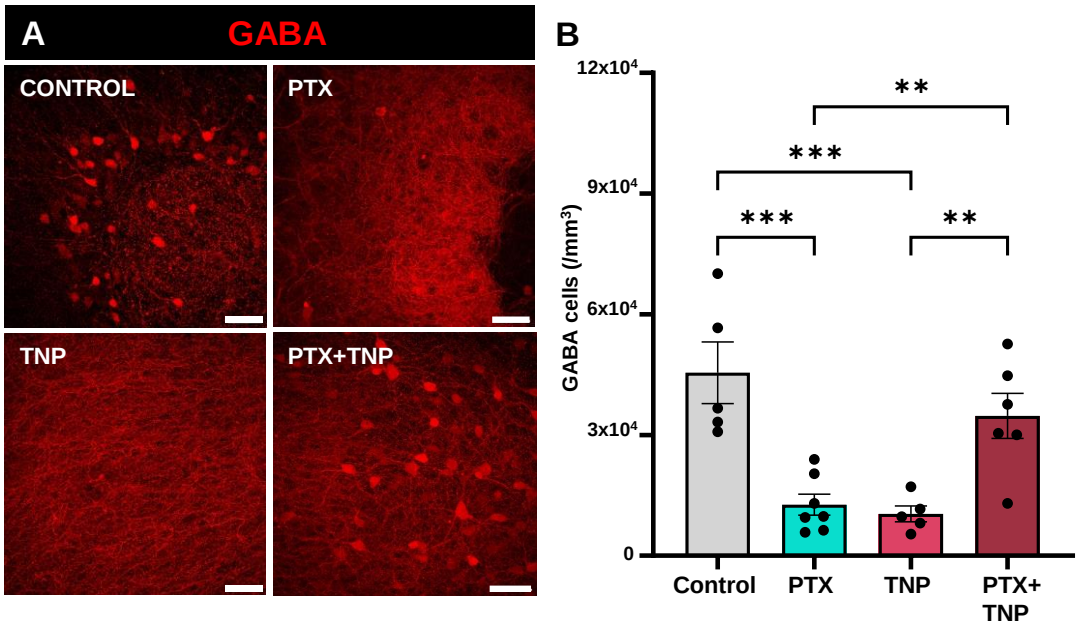

Figure 19. GABAergic cell number preserves control levels in the DG after P2XR inhibition in epileptogenic hOTCs. (A) Representative confocal microscopy images of PTX-, TNP-, PTX+TNP-treated and non-treated hOTCs from mouse hippocampus, after staining for GABA (GABAergic interneuron marker) showing the SGZ+GCL. **(B)** GABAergic interneurons were quantified by identifying $GABA^+$ cells, showing a significant recovery in P2XR-inhibited epileptogenic hOTCs (PTX+TNP group). n=4-7 per group. The scale bar is 50 µm in all the photographs. hOTCs were PTX- (100µM) and/or TNP-ATP- (50µM) treated for 3 days. They were fixed at DIV 23 and 7 days post-treatment. Data are expressed as mean ± SEM and analyzed by 2-way ANOVA with repeated measures test and Holm Šídák post-hoc correction. ** $P < 0.01$, *** $P < 0.001$.

6.3.3 P2XR Inhibition Prevents Aberrant Neurogenesis

With what has been shown so far, it could be affirmed that blocking P2XR by an antagonist emerges as an effective strategy for preserving the overall health of the slice during epileptogenesis. However, its effects in terms of aberrant neurogenesis remained to be elucidated. Considering that newborn neurons are particularly vulnerable to the effects of epileptogenesis, it was of outmost interest to investigate whether it was possible to preserve their functionality following P2XR inhibition. Morphological evaluation, employing the 3D-Sholl analysis as in previous experiments, revealed a significant recovery in the complexity of dendritic arbors of newborn neurons within the radius of 50µm to 170µm in the PTX+TNP group compared to hyperexcited newborn neurons (Fig. 20A, B). This recovery extended to dendritic spine density and features, as analyzed using the SpineJ automatic tool, demonstrating the preservation of control levels in various parameter, including spine number (/µm) and spine head perimeter (µm), minor and major axis of head diameter (µm), and head area (μm^2) (Fig. 20C-I). Consequently, with the results showing the preservation of the physiological state in both the morphological complexity and the dendritic spine growth of newborn neurons, it could be concluded that P2XR inhibition effectively prevents aberrant neurogenesis in this model of epileptogenic hOTCs.

Conversely, the dramatic effect of the P2XR inhibition in control conditions (TNP group) was also applied on the complexity of the dendritic arbor in newborn neurons, which was consistent throughout all the measures that evaluate cell survival, except for neurogenesis. Despite not diminishing the number of newborn neurons, it reduced the complexity of their dendritic arborization, even more than the PTX (Fig. 20A, B). As a result, the next question would involve dendritic spines, which not necessarily need to result in the same kind of patterns. Indeed, spines were also affected across all the parameters evaluated, exhibiting 28.1% fewer spines (/µm) that were larger in size (µm) compared to the control group (13% higher minor and 16.17% higher major axis of head diameter), along with a 14.63% increase in spine head perimeter (µm) and a 30.6% larger area (μm^2) (Fig. 20C-I). Interestingly, although the impact followed the trend seen in the PTX-treated slices (fewer but larger spines), the effect was comparatively less significant, indicated by a smaller percentage of change. Therefore, in alignment with prior assessments of cell survival and newborn neuron development, P2XR inhibition in healthy newborn neurons negatively influences their development.

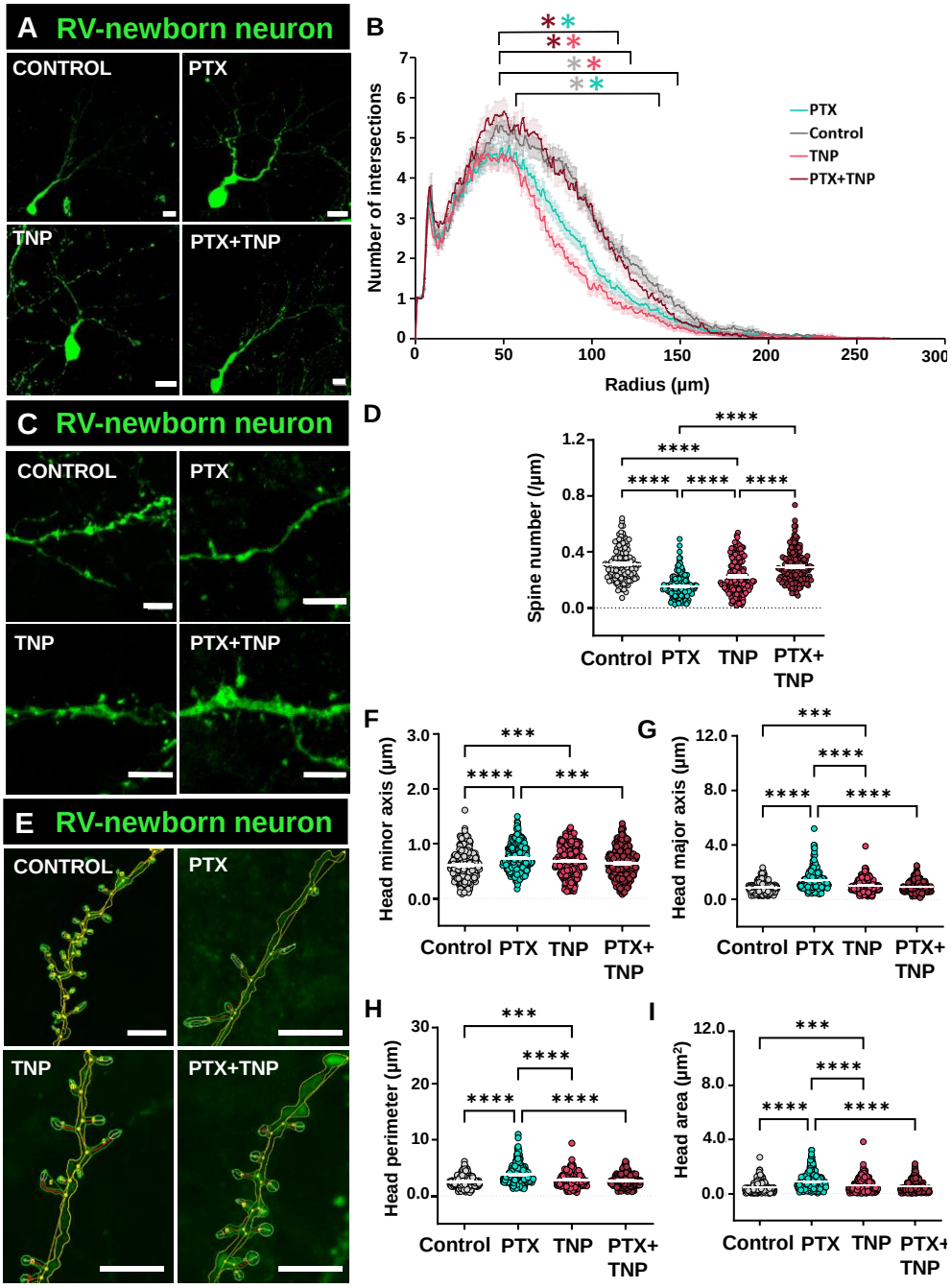

Figure 20. Newborn neuron morphology and dendritic spines are preserved after P2XR inhibition in epileptogenic hOTCs. (A) Representative confocal microscopy images, showing PTX-, TNP-, PTX+TNP-treated and non-treated RV-Venus injected and GFP-stained dendrites. **(B)** Z-stack projections were analyzed and color-coded according to their 3D-Sholl profile. Quantification of the number of intersections between circles of increasing (1µm) radius showed a statistically significant preservation of the physiological state of the morphological complexity of the PTX+TNP-treated group. The scale bar is 50 µm in all the photographs. Data are expressed as mean ± SEM and analyzed by ANOVA repeated measures test with Bonferroni post-hoc correction. **(C,E)** Representative confocal microscopy images, with and without SpineJ processing (in yellow), showing dendritic spines from segments of PTX-, TNP-, PTX+TNP-treated and non-treated RV-Venus injected and GFP-stained dendrites. **(D)** Quantification of spine number (/µm), which is significantly reduced in the PTX-treated group and the control conditions are preserved in PTX+TNP-treated group. **(F-I)** Quantification of spine head minor axis (µm), major axis (µm), parameter (µm), and area (µm^2) respectively. n=8 animals per group, n=4 slices per animal, n=4 neurons per slice, 32 dendritic segments of 30µm per neuron. A total of 960µm of dendrite was analyzed. The scale bar is 5 µm in all the photographs. hOTCs were PTX- (100µM) and/or TNP- (50µM) treated for 3 days. They were fixed at DIV 23, 16 days post-RV injection, and 7 days post-treatment. Data are expressed as mean ± SEM and analyzed by Kruskal-Wallis ANOVA test with Dunn post-hoc correction. ** $P < 0.01$, *** $P < 0.001$, **** $P < 0.0001$.

6.3.4 Time-lapse Imaging of Newborn Neurons after P2XR Inhibition

In order to monitor the functional response of neurons, the live imaging conditions at the 2-photon microscope were optimized. One week after the RV injection, slices were treated as in previous experiments with vehicle, PTX and/or P2XR inhibitor (referring to CNT, PTX, TNP and PTX+TNP groups). Later, 2-photon imaging of newborn neurons was performed in the DG of hOTCs at 8, 15, 22, and 29 days post-injection (DPI) (which corresponds to waiting a full week between taking each image) (Fig. 21A).

Initially, the imaging method was configured to precisely locate the same cell (refer to Methods 5.7.1 section for details). Consequently, the initial experiments were performed on control slices, which began by introducing short intervals between image captures (every 2 days). Here, high-quality images were obtained highlighting the expansion of dendritic arborization and the formation of dendritic spines in the cells (Fig. 21B). Once the time-lapse imaging was established under healthy conditions, the epileptogenic model was introduced into the imaging process. This enabled to compare cell sizes at up to three distinct time points (15, 22, 29 DPI; Fig. 21C), with 1-week intervals, allowing to capture images of cells that were nearly 1 month old in some instances. Finally, the actual experiment started by introducing the treatment: P2XR inhibition by TNP-ATP addition. In this phase, images of groups of cells were captured rather than isolating individual cells for imaging (Fig. 21D). This strategic decision was key in avoiding photobleaching that could occur in the remaining neurons while one cell was being imaged, and it minimized the exposure time outside the incubator. Additionally, this approach proved valuable in increasing the number of cells imaged, thereby enhancing the reliability of the results by reducing variability.

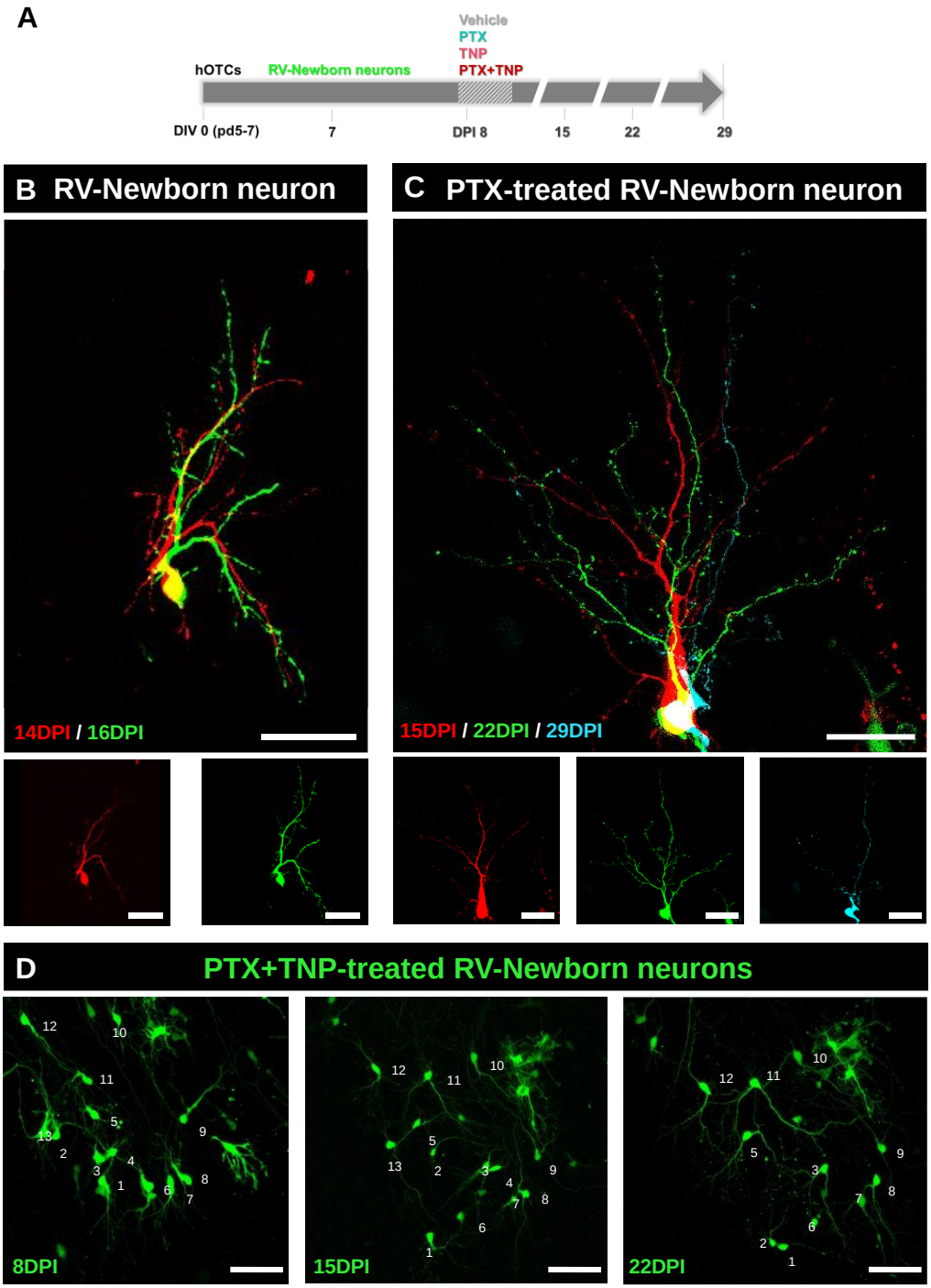

Figure 21. Optimization of newborn neuron time-lapse monitoring by 2-photon microscopy in health, hyperexcitability, and/or P2XR inhibition in hOTCs. (A) Scheme of the experimental procedure. The hOTCs are extracted at pd5-7 (DIV 0) and cultured. At DIV 7, slices are injected for the expression of RV-Venus (GFP^+). From DIV 14 to DIV 16 they are exposed to $GABA_A$ receptor inhibitor PTX (100µM) and/or P2XR antagonist TNP-ATP (50µM), and 2-photon images are performed at 8 days post-injection (DPI), 15DPI, 22DPI and 29DPI (numbers refer to the same neuron at the different time-points). **(B)** Merged 2-photon microscopy images showing the development of a non-treated RV-Venus injected newborn neuron at 20DIV and 14 days post-injection (DPI) (LUT red), and two days later at DIV 22 and 16DPI (LUT green). The scale bar is 30µm in all the photographs. **(C)** Overlapped 2-photon microscopy images of a RV-Venus injected epileptogenic newborn neuron during 3 consecutive weeks: DIV 20, 15 DPI, 6 days post-PTX (DPPTX) (LUT red); DIV 27, 22 DPI, 13 DPPTX (LUT green) and DIV 34, 29 DPI, 20 DPPTX (LUT cyan). Scale bar 100µm. **(D)** Representative 2-photon microscopy images of PTX-, TNP-, PTX+TNP-treated and non-treated RV-Venus labeled twelve newborn neurons during 3 consecutive weeks: DIV 14, 8 DPI, 1 day in PTX+TNP; DIV 21, 15 DPI, 6 DPPTX+TNP, and DIV 28, 22 DPI, 13 DPPTX+TNP. The scale bar is 100µm in all the photographs.

Following this framework and with the images obtained, the morphological changes were analyzed through the previously used 3D-Sholl analysis of the dendritic arborization on the virally labeled newborn neurons. It was performed in every cell during the time course established for 3 weeks in a row: 8, 15 and 22 DPI; 29 DPI was discarded from the analysis as the images at this time point were obtained just in few cells. The morphological evaluation at different time points was key for elucidating whether the complexity of newborn neurons in epileptogenesis was aberrant from the first steps of the neuronal development (during the first week, 8 DPI) or it worsened with time (during the second and third weeks 15-22 DPI). Additionally, the time-lapse imaging of the same neurons each week enabled to observe their specific growth at different time points, taking into account the behavior of the very same cell during its growth and thus, giving more detailed and reliable results.

The assessment of the morphology in healthy newborn neurons (CNT group) led to significant dendritic arbor growth during their development from the first (8DPI) to the third week (22DPI) of imaging (Fig. 22A). Although from 8 to 15 DPI there is no significant increase in their dendritic arbor complexity, within 130 and 300 µm of distance from the soma it is possible to observe a more complex arborization when compared to the third week (8 and 15 DPI compared to 22 DPI) (Fig. 22A, B). Contrary, it was particularly interesting to note that the newborn neurons in epileptogenic conditions showed no significant growth (PTX group, Fig. 22C), suggesting they stopped growing after 1 WIV and thus, kept the same rate of complexity for the next two weeks of developmental stages. However, after closer examination by radius, differences became apparent between both 8-15 DPI with 22DPI, with variations primarily within the first 25 µm and beyond 175 µm distance from the soma (Fig. 22D).

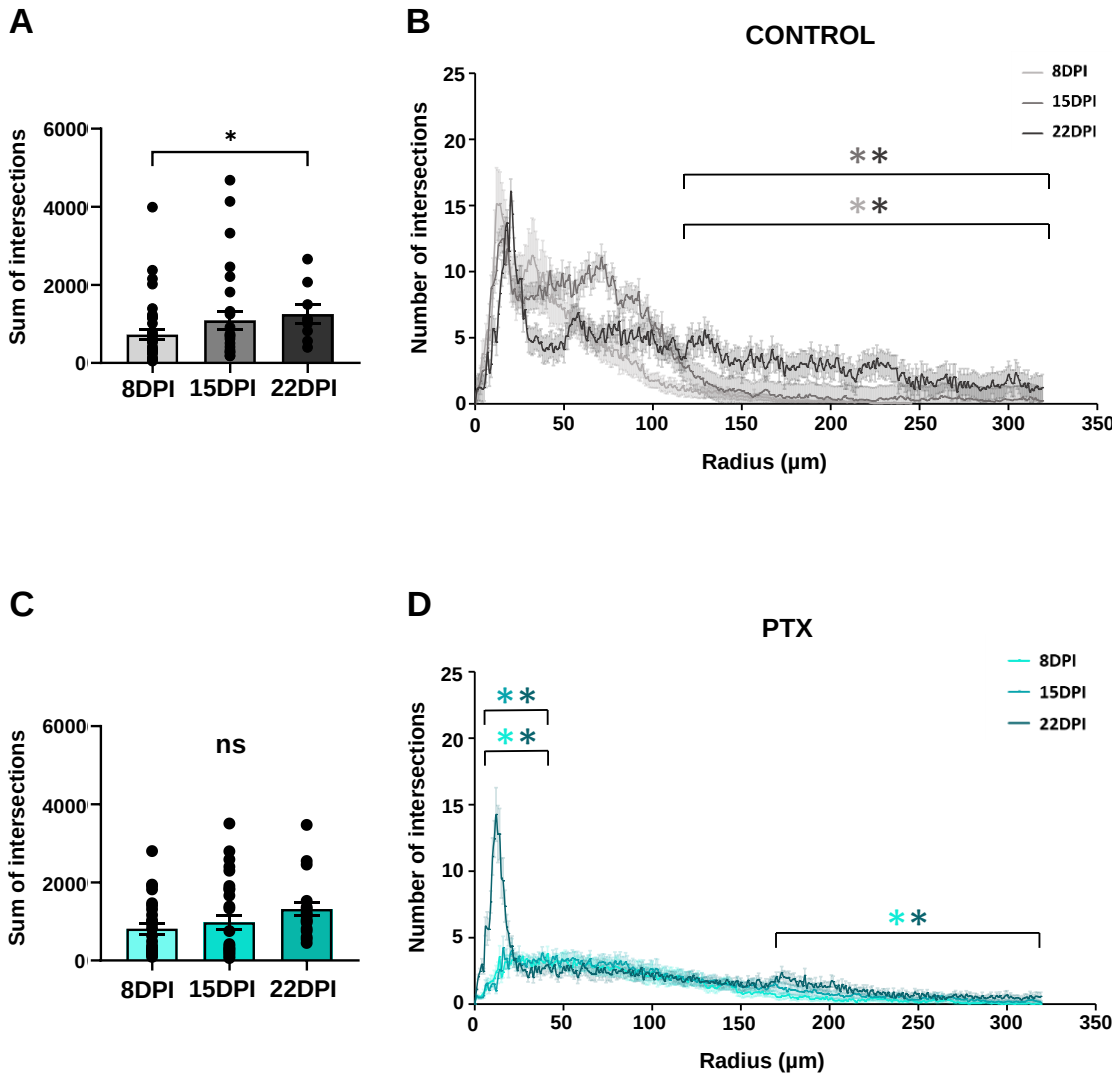

8 DPI: 1 day in PTX; 15 DPI: 6 DPPTX; 22 DPI: 13 DPPTX

Figure 22. Unlike in health conditions, newborn neurons do not significantly grow during epileptogenesis. Z-stack projections were analyzed and color-coded according to their 3D-Sholl profile, in which the number of intersections between circles of increasing (1µm) radius was quantified for the control and PTX groups at 3 different time points (8 DPI, 1 day in PTX; 15 DPI, 6 DPPTX; and 22 DPI, 13 DPPTX). **(A)** The comparison between the total number of intersections at different time points in control conditions showed statistically significant growth of the dendritic arborization between 8 and 22DPI. **(B)** The changes in morphological complexity in health primarily occur at 130-300 µm distance from the soma. **(C)** There were no statistical differences in the total number of intersections between any of the time points in PTX conditions, suggesting a lack of growth. **(D)** The changes in morphological complexity during epileptogenesis occur just at 22DPI, primarily in the first 25 µm and after the 175 µm distance from the soma. Data are expressed as mean ± SEM and analyzed by Kruskal-Wallis ANOVA test with Dunn post-hoc correction (A, C) and by ANOVA repeated measures test with Bonferroni post-hoc correction (B, D). ns= non-significant, * $P < 0.05$, ** $P < 0.01$.

Once the morphological complexity was evaluated by time points comparing newborn neurons of the same groups (CNT/PTX vs 8 DPI/15 DPI/22DPI), the next comparison focused on the total number of intersections between groups (CNT 8 DPI/15 DPI/22DPI vs PTX 8 DPI/15 DPI/22DPI), starting at 8 DPI. Given that PTX-induced epileptogenesis was applied for just 1 day at this stage, it was rational not to expect significant changes yet among groups (Fig. 23A, B). The brief exposure to PTX might not have allowed sufficient time for neurons to manifest noticeable differences in the epileptogenic group, making any potential impact not yet observable.

In contrast, when newborn neurons were analyzed one week later, after 6 days of exposure to PTX (15 DPI and 6 days post PTX, or DPPTX, Fig. 23C, D), a markedly less complex dendritic arbor was evident. This observation indicated that the effect on dendritic growth becomes apparent after 6 days of PTX exposure, highlighting that a single day in PTX is insufficient for observable changes in dendritic arbor development. However, the specific timeframe for when these changes become evident remains uncertain, as examination between the 2nd and 5th DPPTX was not conducted. Consequently, it cannot be claimed that a full 6 days post PTX exposure is required to observe significant changes in dendritic development.

Furthermore, the significant reduction in newborn neuron morphological complexity at 15 DPI and 6 DPPTX aligns with earlier studies during the optimization of the hOTCs model in this project (Fig. 4C). Having established that newborn neuron development is impaired one week after the completion of a 3-day PTX treatment, the focus now shifts to the impact observed two weeks after the treatment cessation. Comparing CNT and PTX at 22 DPI and 13 DPPTX revealed a continued decrease in newborn neuron morphological complexity (Fig. 23E, F), suggesting that aberrant neurogenesis persists even after PTX removal from the media.

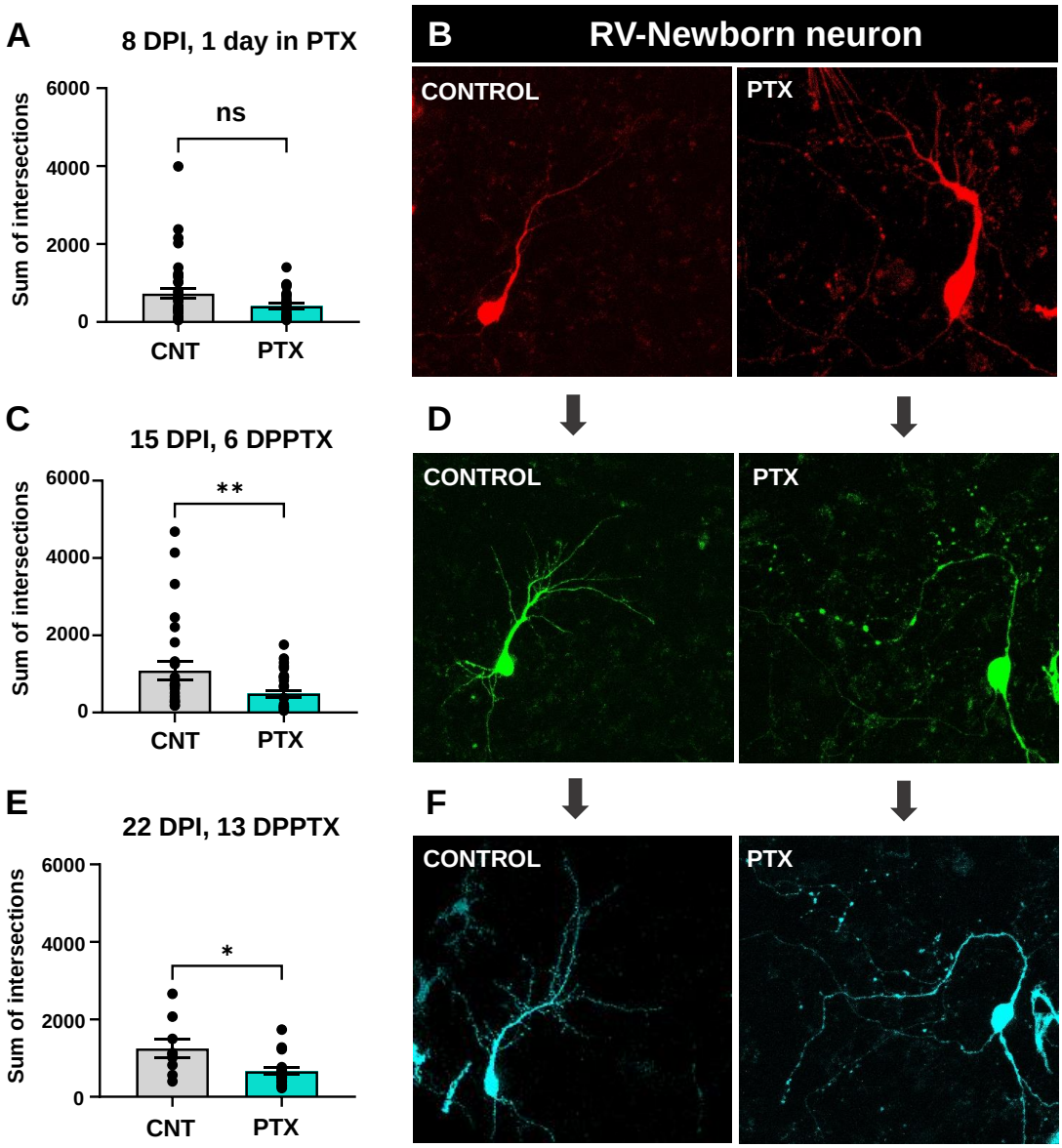

Figure 23. The total number of intersections decreases in epileptogenic conditions after 1 week of PTX exposure. **(A, D, F)** Representative 2-photon microscopy images showing the development of a PTX- and non-treated RV-Venus injected newborn neuron at DIV 15, 8 days post-injection (DPI) and 1 day in PTX (LUT red) **(A)**; 1 week later at DIV 22, 15 DPI and 6 days post-PTX (DPPTX) (LUT green) **(D)**; and another week later at DIV 29, 22 DPI and 13DPPTX (LUT cian). The scale bar is 30µm in all the photographs. Z-stack projections were analyzed and color-coded according to their 3D-Sholl profile, in which the total number of intersections between circles of increasing (1µm) radius was quantified for the control and PTX groups at the three different time points. **(A)** The total number of intersections at acute PTX exposure (8 DPI, 1 day in PTX) showed no significant differences compared to control. **(C, E)** There is a significant decrease in the dendritic arborization of newborn neurons at 15 DPI, 6 DPPTX and 22 DPI, 13 DPPTX compared to control. Data are expressed as mean ± SEM and analyzed by non-parametric Mann-Whitney test. ns= non-significant, * $P < 0.05$, ** $P < 0.01$.

After the evaluation of the dendritic growth over time in epileptogenic conditions, the TNP-ATP antagonist was examined to determine whether the aberrant complexity of newborn neurons during epileptogenesis could be recovered after inhibiting P2XR during the first two weeks of development (8 and 15 DPI). These observations revealed a significant increase in the dendritic growth within the 60-130 µm range of dendritic length in the CNT group (Fig. 24A), while no growth was observed in the PTX group, aligning with previous reports.

In the TNP group, where P2XR are inhibited in control conditions and alterations have been already noted in prior studies, minimal growth was observed between 8 and 15 DPI (Fig. 24C), showing a very similar behavior as in the PTX group. This suggests that when P2XR are blocked in a healthy state, dendritic growth is also stopped, maintaining a consistent level of complexity 1 WIV later.

Finally, in epileptogenic slices with inhibited P2XR (PTX+TNP group), growth during the 2nd WIV was preserved, mainly around the first 80 µm (Fig. 24D). Turning attention to the total number of intersections, each condition was again compared at 8 and 15 DPI. Here, a significant difference was observed exclusively in epileptogenic slices subjected to P2XR inhibition (Fig. 24E-H), marking a meaningful discovery as there was no growth even in the case of the control conditions.

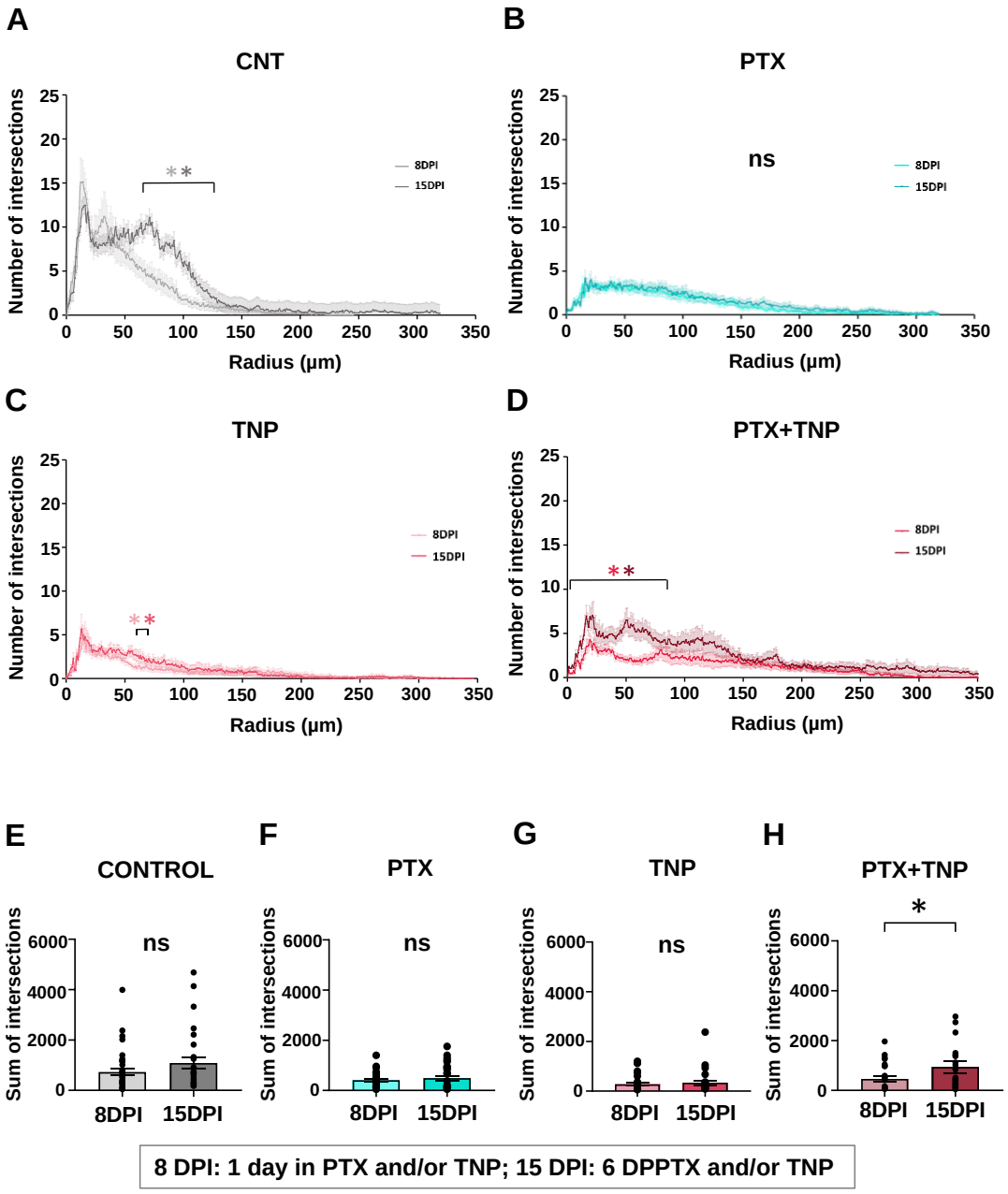

Figure 24. The dendritic arbor growth in newborn neurons is recovered after P2XR inhibition in epileptogenic hOTCs. Z-stack projections were analyzed and color-coded according to their 3D-Sholl profile, in which the total number of intersections between circles of increasing (1µm) radius was quantified for the PTX-, TNP-, PTX+TNP-treated and non-treated newborn neurons at two different time points (8 DPI, 1 day in PTX and/or TNP; and 15 DPI, 6 DPPTX and/or TNP). **(A)** The quantification of the number of intersections at the different time points in control conditions showed statistically significant growth of the dendritic arborization in the range of 60-130 µm. **(B)** There was no dendritic arbor growth in epileptogenic conditions between 8 and 15 DPI. **(C)** There was almost no dendritic arbor growth in P2XR-inhibited slices (TNP group). **(D)** The dendritic arborization was again different after P2XR inhibition in epileptogenic hOTCs in the first 80 µm (PTX+TNP group). Data are expressed as mean ± SEM and analyzed by ANOVA repeated measures test with Bonferroni post-hoc correction. **(E-H)** The total number of intersections at the different time points showed no significant differences except for the PTX+TNP group, in which a significant growth was observed. Data are expressed as mean ± SEM and analyzed by non-parametric Mann-Whitney test. ns= non-significant, * $P < 0.05$, ** $P < 0.01$.

Ultimately, the objective was to compare the complexity of the newborn neurons under the different conditions, aiming to understand how dendritic growth varied over time based on the treatment. Notably, the differences in total number of intersection numbers at 8 DPI were only evident between the control and TNP-treated groups (Fig. 25A). This implies that 1 day of exposure to the P2XR inhibitor is enough for influencing newborn neuron development, unlike PTX, which at this stage, shows no significant differences compared to the CNT group. Upon a more detailed analysis, when comparing intersections by radius, both PTX and TNP-treated slices exhibited variations within the initial 100 µm (Fig. 25B) in contrast to control. Interestingly, under epileptogenic conditions with inhibited P2XR (PTX+TNP group), the observed differences start diminishing, and the reduction in morphological complexity becomes not noticeable, particularly within 40-70 µm of the dendritic length.

After a one-week recovery period following the 3-day PTX treatment, at 15 DPI, 6 DPPTX and/or TNP, despite epileptogenic slices with P2XR blocked (PTX+TNP group) did not show a significant recovery in morphological complexity compared to PTX-treated neurons, the decrease in complexity observed at 8 DPI compared to control disappeared (Fig. 25C, D). Indeed, the relevant difference arises when compared to P2XR inhibition in a healthy state (TNP group). As demonstrated in previous experiments (Fig. 20B), the dendritic arbor is even less complex than the PTX group. Therefore, the differences in complexity when treated with TNP become more pronounced, primarily observed between 90 and 250 µm within the range of dendritic length (Fig. 25D, C).

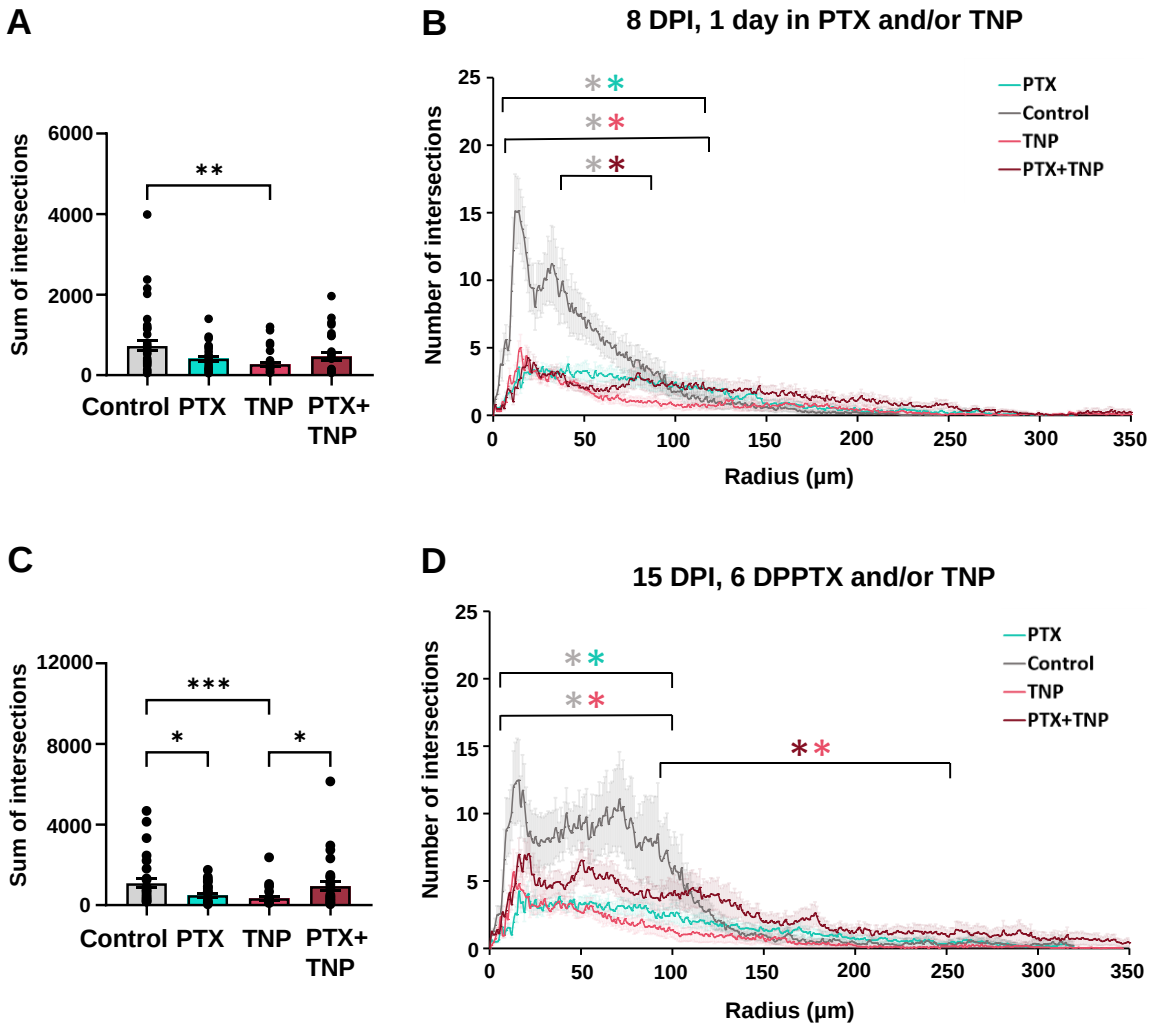

Figure 25. The dendritic arbor growth in newborn neurons is recovered after P2XR inhibition in epileptogenic hOTCs 6 days after PTX-induced epileptogenesis. Z-stack projections were analyzed and color-coded according to their 3D-Sholl profile, in which the total number of intersections between circles of increasing (1µm) radius was quantified for the PTX-, TNP-, PTX+TNP-treated and non-treated newborn neurons at two different time points (8 DPI, 1 day in PTX and/or TNP; and 15 DPI, 6 DPPTX and/or TNP). **(A)** The total number of intersections at 8 DPI, 1 day in PTX and/or TNP after the Kruskal-Wallis ANOVA test, showed no significant differences except from the control and TNP group. **(B)** Regarding the morphological complexity, significant differences were observed in PTX and TNP groups compared to CNT around the first 100 µm, although the differences were smaller in the PTX+TNP group (40-70 µm). This was analyzed by ANOVA repeated measures test with Bonferroni post-hoc correction. **(C, D)** The total number of intersections and morphological complexity of the newborn neurons at 15 DPI, 6 DPPTX and/or TNP showed a significant recovery of the dendritic arbor growth after P2XR inhibition during epileptogenesis (PTX+TNP group) compared to TNP group. Data are expressed as mean ± SEM and analyzed by Kruskal-Wallis ANOVA test with Dunn's correction (C) or by ANOVA repeated measures test with Bonferroni post-hoc correction (D).* $P < 0.05$, ** $P < 0.01$, *** $P < 0.001$.

6.3.5 P2XR Inhibition Preserves Neuronal Firing

In light of the results obtained in aberrant neurogenesis after P2XR inhibition in epileptogenic conditions, it became crucial to evaluate the potential impact of these abnormal features on neural activity; and if such impact existed, to study the hypothetical recovery facilitated by the P2XR inhibitor. To achieve this, the experiment required to longitudinally monitor the activity of neural circuits, for what AAV1.SYN.Gcamp6f.WPRE.SV40 (see Methods 5.3.1; Fig. 26A) was specifically chosen. This adenoviral vector, under the Syn promoter, specifically labeled neurons, and through the green fluorescent GCaMP6f (a genetically encoded calcium indicator), exhibited calcium activity.

The viral injection, performed at DIV 7 (Fig. 26A), allowed for calcium imaging in neurons of the GCL region (Fig. 26B) at DIV 19, 23 and 26, corresponding to 3, 7 and 10 days following the application of PTX and/or TNP (Fig. 26A). Here, spontaneous circuit dynamics were simultaneously monitored in dozens of neurons over a 20-minute period while maintaining the culturing conditions intact. Following semi-automated cell contour segmentation and detection of calcium spikes, the onsets of calcium events were extracted from each neuronal trace to reconstruct the dynamics of single neuron firing properties (Fig. 26C, D). Consequently, an average of 30 neurons per slice were imaged across all experimental conditions at 3, 7, and 10 days after PTX and/or TNP exposure. The comparison of single neuron firing frequency between groups was done both on the values of IFs pooled across all slices and neurons (obtaining one global distribution per group; Fig. 26E-G). After pooling IFs across all neurons from all slices within the same group and day of recording, the parametric one-way ANOVA comparison test revealed a significant difference at 3, 7, and 10 days post-PTX and/or TNP between the epileptogenic condition (PTX group) and all other groups (Fig. 26E-G). This implies that treating epileptogenic hOTCs with P2XR inhibitor not only prevents aberrant neurogenesis as verified in previous sections, but is also a valid tool for recovering the normal neural activity of the hippocampal slice.

Remarkably, the control slices treated with the P2XR inhibitor (TNP group) maintained the physiological neural activity at every time point (3, 7 and 10 days post PTX and/or TNP treatment). This suggests that the impact this treatment generates on healthy slices regarding aberrant morphology and dendritic spine features is not enough to affect the activity of the neural circuits. This is a crucial observation, indicating that even if blocking P2XR induces some disturbances to newborn neurons in a health state, the doses and duration of the treatment do not significantly impact the neural network.

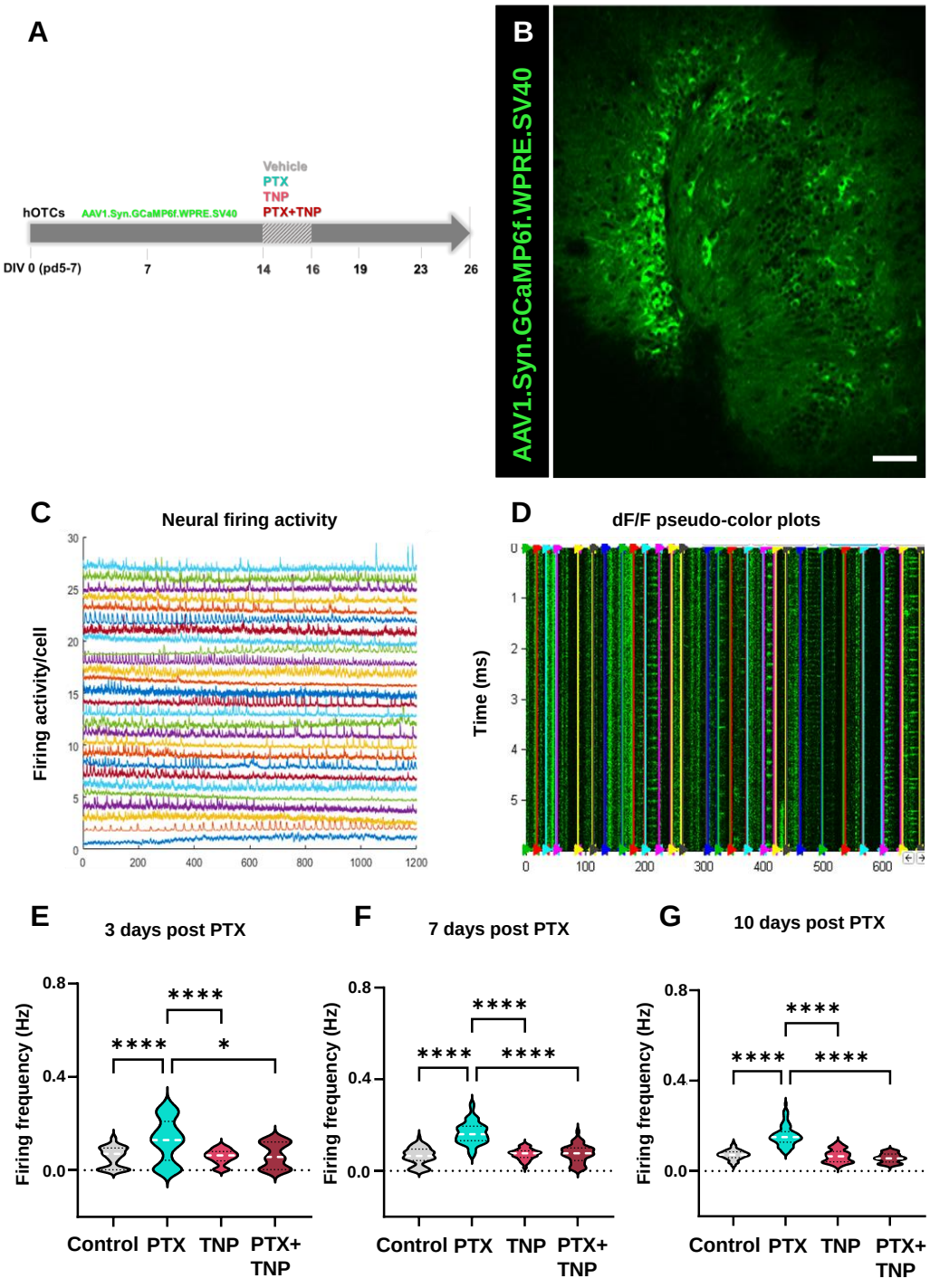

Figure 26. Neural firing recovery in the DG after P2XR inhibition in epileptogenic hOTCs. For each cell, the average inverse of the intervals between consecutive calcium spikes is considered as firing rate. **(A)** Scheme of the experimental procedure. The hOTCs are extracted at pd5-7 (DIV 0) and cultured. At DIV 7, slices are injected with the adenoviral vector AAV1.Syn.GCamp6f.WPRE.SV40 for the expression of GCamp6f. From DIV 14 to DIV 16 they are exposed to $GABA_A$ receptor inhibitor PTX (100µM) and/or P2XR antagonist TNP-ATP (50µM), and imaging is performed 3, 7, and 10 days after (DIV 19, 23, 26). **(B)** Representative fluorescence microscopy image of the hippocampal DG of GCamp6f in hOTCs. In bright green, injected cells during calcium release. The scale bar is 50 µm. **(C, D)** An example of the firing activity and pseudo color plots of 27 calcium-releasing cells (control group, 7 days post-PTX). **(E-G)** From left to right, results from slices respectively at 3, 7, and 10 days post-PTX are shown. Neural firing frequency was recovered at every time-point after P2XR inhibition in epileptogenic hOTCs. n=4 per group. Data are expressed as mean ± SEM and analyzed by Kruskal-Wallis ANOVA test with Dunn post-hoc correction. * $P < 0.05$, **** $P < 0.0001$.

6.3.6 P2XR Inhibition Preserves Newborn Neuron Firing

Having successfully preserved the functional activity of the neural circuit through P2XR inhibition, the subsequent aim focused on the impact of epileptogenesis on the activity of newborn neurons, and whether inhibiting P2XR could facilitate their recovery. To address these questions, a GCaMP6f was again employed, this time through RV injection, which would selectively label dividing cells allowing for the evaluation of newborn neuron activity. The viral injection was administered at DIV 7, and one week later, hOTCs underwent PTX and/or TNP treatment. Subsequently, calcium imaging was conducted in the DG (Fig. 27B) at DIV 23, corresponding to 7 days post-treatment (Fig. 27A).

The neural dynamics were simultaneously monitored for 20 minutes in all the cells labeled (approximately 10-12 cells per slice), while culturing conditions were again fully preserved. Due to the limited number of newborn neurons labeled per slice, the experimental procedure required a considerable number of animals (n=12). Following manual cell contour detection of calcium spikes in ImageJ, the onsets of calcium events were extracted from the mean intensity over time. After pooling data from the same group, a significant increase of calcium release in newborn neurons was observed in PTX-induced hyperexcited hOTCs (Fig. 27C), indicating a hyperexcited state of newborn neurons during epileptogenesis. Interestingly, when epileptogenic hOTCs were treated with the P2XR inhibitor (PTX+TNP group), the activity of newborn neurons reverted to a physiological state. This implied that the treatment not only preserved physiological neural network activity, as observed in the preceding section (Fig. 26E-G), but also recovered the specific activity of newborn neurons (Fig. 27C).

Additionally, in control slices treated with the P2XR inhibitor (TNP group), a decrease in the activity was significant compared to the rest of the conditions, including the control. Hence, the TNP treatment in a healthy state was not inert; rather, it actively diminished the activity of newborn neurons below physiological levels (Fig. 27C).

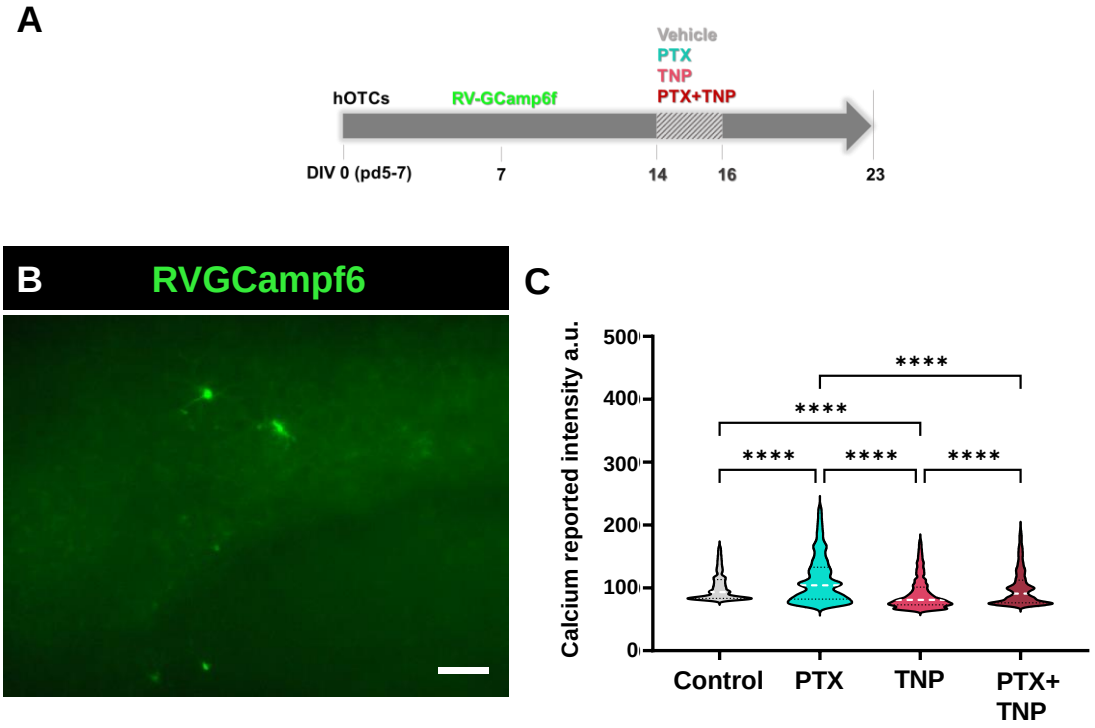

Figure 27. Newborn neuron firing recovery in the DG after P2XR inhibition in epileptogenic hOTCs. (A) Scheme of the experimental procedure. The hOTCs are extracted at pd5-7 (DIV 0) and cultured. At DIV 7, slices are injected with the RV-GCamp6f for the expression of GCamp6f in newborn neurons. From DIV 14 to DIV 16 they are exposed to $GABA_A$ receptor inhibitor PTX (100µM) and/or P2XR antagonist TNP-ATP (50µM), and imaging is performed 7 days after (DIV 23). **(B)** Representative fluorescence microscopy image of the hippocampal DG of RV-GCamp6f labeled newborn neurons in hOTCs. In bright green, RV-labeled cells during calcium release. The scale bar is 50 µm. **(C)** Calcium release results (mean intensity, a.u.) showing a significant increase after PTX-induced hyperexcitability. Newborn neurons recover the control calcium release after P2XR inhibition in epileptogenic hOTCs. n=12 animals per group, n=1 slices per animal was recorded, n=10-12 newborn neurons per slice. Data are expressed as mean ± SEM and analyzed by Kruskal-Wallis ANOVA test with Dunn post-hoc correction. **** $P < 0.0001$.

In conclusion, considering ATP as one of the mediators of aberrant neurogenesis, the introduction of a P2XR inhibitor, such as the TNP-ATP antagonist, effectively reverses the aberrant features observed in newborn neurons back to those characteristic of control conditions. As depicted in Figure 28, under healthy conditions, newborn neurons present physiological features (Fig. 28.1). However, in epileptogenic conditions, both morphology and neural activity are adversely affected (Fig. 28.2, 3). Conversely, the inhibition of P2XR plays a crucial role in preserving the situation in a healthy state, where all studied features return to a physiological state upon the application of the treatment (Fig. 28.4).

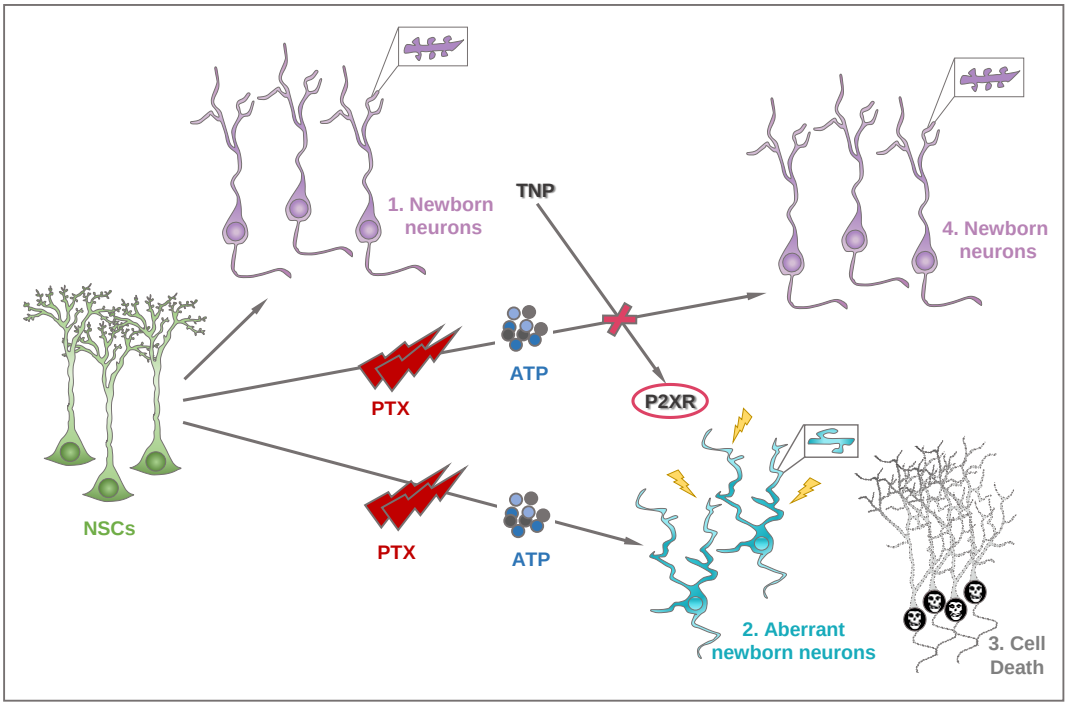

Figure 28. The differential fate of multipotent adult hippocampal NSCs in health, disease and after treatment with a P2XR inhibitor in a hOTCs model. In normal conditions, the hippocampal NSCs of the DG, after activating, divide and differentiate into immature neurons (newborn neurons, **(1)**), which present a developed dendritic arbor and already show dendritic spines. However, when epileptogenesis occurs, there is much more cell death **(3)** and newborn neurons become aberrant: there is less density, they are less complex and their dendritic spines grow abnormally **(2)**. When purinergic 2X receptors (P2XR) are inhibited by the TNP-ATP antagonist, these aberrant features are restored to normality **(4)**.

6.4 ROS Inhibition in hOTCs

6.4.1 ROS Inhibition after ATP Exposure Preserves Neurogenesis and Cell Survival

After thoroughly assessing aberrant neurogenesis and neural activity during P2XR inhibition, another focus within the ATP signaling pathway was identified: ROS generation. It was hypothesized that, if directly blocking P2XR had such an impact on epileptogenic hOTCs and aberrant neurogenesis, it might be feasible to revert these abnormalities downstream these receptors by directly acting on ROS. In this context, cerium oxide nanoparticles (CeO_2NPs) were chosen to be applied as a treatment, known for their excellent catalytic activity and their potential as antioxidants towards almost all noxious intracellular ROS, acting as ROS-scavengers[362].

Prior to studying the impact of ROS inhibition during epileptogenesis, its effects were assessed in elevated eATP conditions. This investigation was crucial to understand its behavior in the presence of excessive eATP, as during epileptogenesis, the increase in eATP in the ATP signaling pathway triggers an inflammatory response leading to ROS generation. Thus, by initially assessing whether ROS inhibition improves aberrant neurogenesis induced by elevated eATP, it lays a logical foundation for investigating the reduction of aberrant neurogenesis also during epileptogenesis. Therefore, the next hypothesis involved reducing ROS potentially reverting the abnormalities associated with excessive eATP levels.

To explore this hypothesis, four experimental groups were designed: a) the control condition (CNT group): the cultured slices were never exposed to excessive eATP nor ROS inhibition; b) the ATP group: the cultured slices underwent an additional extracellular presence of ATP (200 µM) from DIV 14 to DIV 16 (3 days); c) control under inhibited-ROS condition (CeO_2 group): the cultured slices were exposed to CeO_2NPs (1µg/ml) from DIV 14 to DIV 23 (10 days); and d) elevated eATP and inhibited-ROS condition (ATP+CeO_2 group): the cultured slices underwent additional extracellular presence of ATP (200 µM, 3 days) with simultaneous extracellular application of the ROS-scavenger CeO_2NPs (1µg/ml, 10 days) (Fig. 29A). The slices obtained from each of the animals used were separated to cover the four different experimental conditions, and imaged on the same DIV (see Methods 5.2.1).

As in previous experiments, the evaluation started by staining hOTCs with both the neuroblast marker DCX and the marker of cell nuclei DAPI. Subsequently, DCX^+ cells were quantified within the GCL+SGZ across the four conditions (CNT, ATP, CeO_2, and ATP+CeO_2) for neurogenesis assessment. Notably, newborn neuron population increased by more than 2-fold following the administration of CeO_2NPs in conditions of excessive eATP (ATP+CeO_2 group, Fig. 29B, C). This suggests a neuroprotective behaviour of CeO_2NPs in scavenging ROS during elevated eATP, leading to enhanced survival of newborn neurons. Furthermore, upon identifying pyknotic/karyorrhectic cells through DAPI-stained nuclei, a corresponding decrease in cell death was observed after the application of CeO_2NPs in conditions of increased eATP (ATP+CeO_2 group, Fig. 29D, E). This indicates that the reduction of ROS potentially improves cell survival in the DG of the slice.

Interestingly, the effect of CeO_2NPs under control conditions (CeO_2 group) remained inert in both the evaluation of newborn neuron population and cell survival, where physiological conditions were maintained. When comparing the effects of this treatment with the previously used P2XR inhibitor TNP, which exhibited detrimental effects on aspects such as cell survival, CeO_2NPs result an advantage.

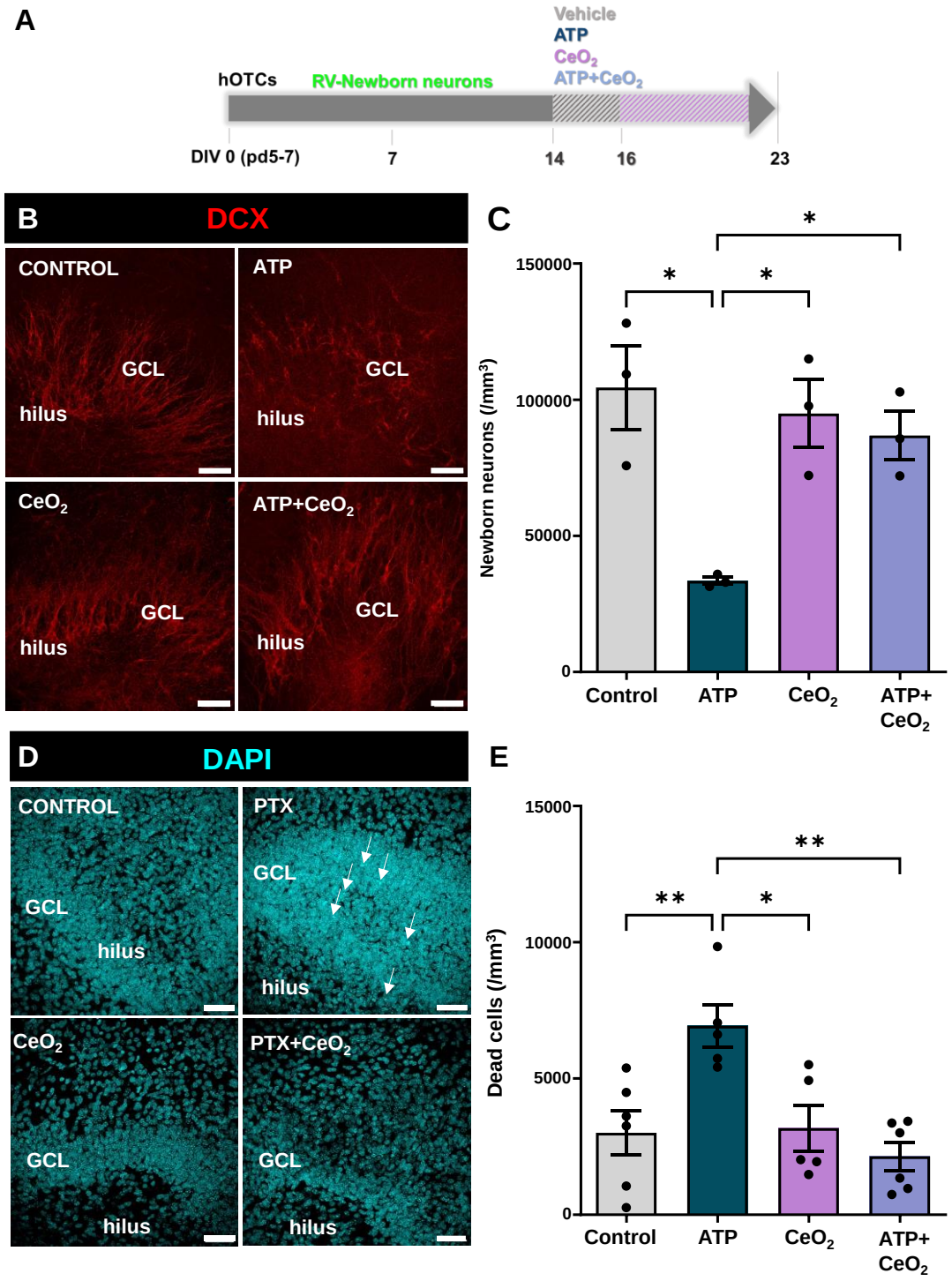

Figure 29. Newborn neurons and cell death preserve control levels after ROS-inhibition in hOTCs with eATP excess. (A) Scheme of the experimental procedure. The hOTCs are extracted at pd5-7 (DIV 0) and cultured. After 1 WIV, the DG is RV-injected (Venus, GFP^+), and 1 week after that, slices are exposed to ATP (200µM) and/or ROS-scavenger CeO_2NPs (1µg/mL) for 3 or 10 days. Immunostainings are performed 1 week later, at DIV 23. **(B)** Representative confocal microscopy images were taken after staining of the neurogenesis marker DCX, showing the SGZ+GCL in the mouse hippocampal hOTCs. **(C)** Newborn neurons (/mm^3) were quantified by identifying DCX^+ cells. **(D)** Representative confocal microscopy images were taken after staining for DAPI, showing the SGZ+GCL in the mouse hippocampal hOTCs. **(E)** Cell death (/mm^3) was quantified by identifying nuclei presenting pyknosis (DNA condensation) and/or karyorrhexis (nuclear fragmentation), both detected by condensed staining of DAPI. n = 4 per group. The scale bar is 50 µm in all the photographs. hOTCs were fixed at 16 days post-RV injection and 7 days post-treatment. Data are expressed as mean ± SEM and analyzed by 2-way ANOVA with repeated measures test and Holm Šídák post-hoc correction. * $P < 0.05$, ** $P < 0.01$.

6.4.2 ROS Inhibition after ATP Exposure Prevents Aberrant Neurogenesis

Based on these findings concerning the neuroprotective role of inhibiting ROS in conditions of eATP, the investigation expanded to assess aberrant neurogenesis, focusing specifically on newborn neurons. In this context, the dendritic arborization of newborn neurons was evaluated, aiming to determine whether reducing ROS could have a favorable impact on aberrant neurogenesis. Utilizing 3D-Sholl analysis to evaluate the number of intersections, it was determined that inhibiting ROS in the presence of eATP excess (ATP+CeO_2 group, Fig. 30A, B) did not result in a significant recovery of the complexity of newborn neurons' dendritic arbor. However, despite the lack of a notable increase in complexity compared to the CNT group, there was a tendency towards a less complex dendritic arbor.

Remarkably, a very interesting aspect laid on the effect of CeO_2NPs in control conditions (CeO_2 group), which exhibited even greater complexity than the CNT group within the dendritic length between radius 140 and 230 µm (Fig. 30B). This was a noteworthy observation because the increased size of these dendritic arborizations highlighted significant differences with both the ATP group (between radius 100 and 230 µm) and, more importantly, with conditions of elevated eATP following ROS inhibition (ATP+CeO_2 group, Fig. 30B). In comparison to nanoparticles under control conditions, the dendritic arbor in the ATP+CeO_2 group appeared less complex between 125 and 220 µm within the dendritic length (Fig. 30B), suggesting that the hypothesis of ROS inhibition during eATP excess preventing aberrant neurogenesis was not accomplished in terms of dendritic arborization complexity.

Hence, it was meaningful to stablish the effect of ROS inhibition during eATP excess on dendritic spine growth, recognizing the potential for distinct outcomes. Given that the regulatory pathways for dendritic arbor development and spine growth might diverge, there was a possibility that while physiological complexity might not be fully preserved, dendritic spines could exhibit recovery. Remarkably, the physiological spine number (/µm) was effectively preserved after ROS-inhibition in conditions of enhanced eATP (ATP+CeO_2 group, Fig. 30C, D). However, when looking at the dendritic spine head features (Fig. 30E), the minor axis (µm) showed an increase of the 11.5% (Fig. 30F). If it is compared to the increase that ATP alone causes (42.4%), it can be concluded that the nanoparticle addition reduces this abnormal increase in a 30.9%. In the case of the major axis (µm), an increase of the 16% was observed compared to control (Fig. 30G), when in the case of ATP alone there is a 110.97% of increase, meaning a reduction of the 94.97% due to nanoparticle addition. On the other hand, the spine head perimeter (µm) presented an increase of the 12.59% (Fig. 30H), and in the ATP-treated hOTCs a 93.87% of increase was observed, which means that nanoparticles reduced the abnormal spine head growth in an 81.27%. Finally, in the head area (μm^2) a 21.62% of increase was obtained (Fig. 30I), when the ATP group had a 168.5% of increase, that thanks to the CeO_2NPs it decreased in a 146.89%. This outcome supported the suspect of different pathways regulating dendritic

arborization and spines during newborn neuron development, and suggested CeO_2NPs as a potential candidate for preserving normal neurogenesis.

In the study of the dendritic spines in newborn neurons, control nanoparticles (CeO_2 group) exhibited an inert behavior in terms of spine density all along the dendritic arbor (Fig. 30 C, D). However, they generated a slight increase in terms of dendritic spine heads, in which the head minor axis (µm) was an 11.3% larger, the major axis a 10.13%, the head perimeter an 8.73%, and the head area a 14.19%.

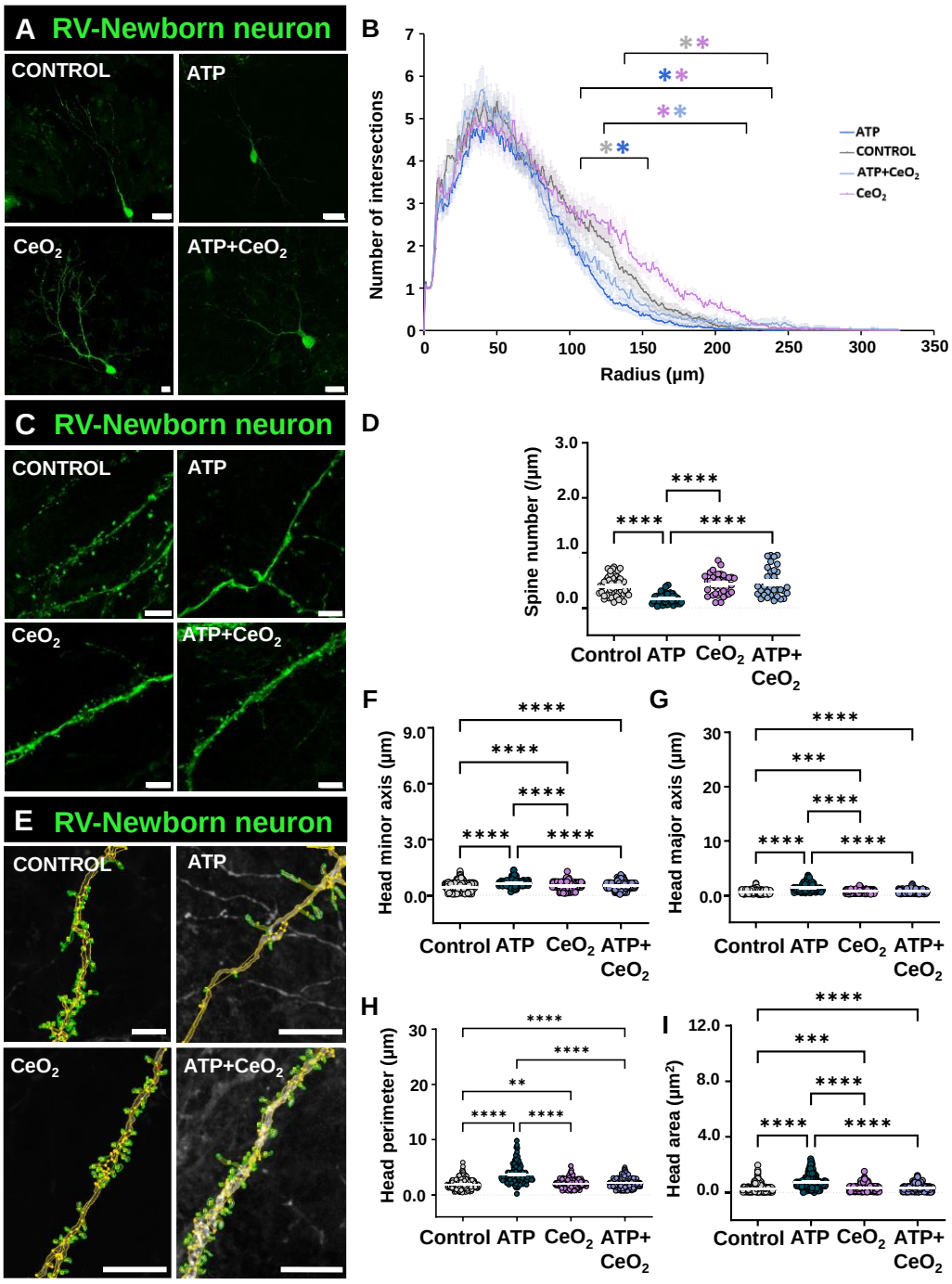

Figure 30 Newborn neuron morphology is impaired but dendritic spines are preserved in hOTCs with eATP excess. (A) Representative confocal microscopy images, showing ATP-, CeO_2-, ATP+ CeO_2-treated and non-treated RV-Venus labeled and GFP-stained dendrites. **(B)** Z-stack projections were analyzed and color-coded according to their 3D-Sholl profile. Quantification of the number of intersections between circles of increasing (1µm) radius showed a statistically significant preservation of the physiological morphological complexity of the ATP+ CeO_2-treated group. Data are expressed as mean ± SEM and analyzed by ANOVA repeated measures test with Bonferroni post-hoc correction. The scale bar is 50µm in all the photographs. **(C, E)** Representative confocal microscopy images, with and without SpineJ processing (in yellow), showing dendritic spines from segments of ATP-, CeO_2-, ATP+ CeO_2-treated and non-treated RV-Venus labeled and GFP-stained dendrites. **(D)** Quantification of spine number (/µm), which is significantly reduced in the PTX-treated group, and the control conditions are preserved in the ATP+CeO_2-treated group. **(F-I)** Quantification of spine head minor axis (µm), major axis (µm), parameter (µm), and area (μm^2) respectively. n=4 animals per group, n=4 slices per animal, n=4 neurons per slice, 32 dendritic segments of 30µm per neuron. A total of 960µm of dendrite was analyzed. The scale bar is 5µm in all the photographs. hOTCs were ATP- (200µM) and/or CeO_2NPs- (1µg/mL) treated for 3 or 10 days respectively. They were fixed at DIV 23, 16 days post-RV injection, and 7 days post-treatment. Data are expressed as mean ± SEM and analyzed by 2-way ANOVA with repeated measures test and Holm Šídák post-hoc correction. ** $P < 0.01$, **** $P < 0.0001$.

6.4.3 ROS Inhibition during Epileptogenesis Preserves Neurogenesis and Cell Survival

Following the findings of the preceding section, in which the efficacy of CeO_2NPs in preventing aberrant neurogenesis related to eATP excess was proved, the next step was to verify whether these ROS scavengers could exert a similar beneficial effect in the context of epileptogenesis. For that, four four experimental groups were again designed: a) the control condition (CNT group): the cultured slices were never exposed to hyperexcitability induction by PTX nor ROS inhibition; b) epileptogenic condition (PTX group): the cultured slices underwent suppression of GABAergic transmission in the extracellular presence of PTX (100 µM) from DIV 14 to DIV 16 (3 days); c) control under inhibited-ROS condition (CeO_2 group): the cultured slices were exposed to CeO_2NPs (1µg/ml) from DIV 14 to DIV 23 (10 days); and d) epileptogenic and inhibited-ROS condition (PTX+CeO_2 group): the cultured slices underwent suppression of GABAergic transmission as in the PTX group (100 µM, 3 days) with the simultaneous extracellular application of ROS-scavenger CeO_2NPs (1µg/ml, 10 days) (Fig. 32A). The slices obtained from each of the animals used separated to cover the four different experimental conditions, and imaged on the same DIV (see Methods 5.2.1).

Initially, despite previous examination when the P2XR inhibitor was used (Fig. 17A, B), the evident increase in ROS during epileptogenesis was reaffirmed through a DCF assay conducted to test CeO_2NPs effects in these terms. In this evaluation, a rapid and transient 2-fold increase in the DCF signal of PTX-treated hOTCs was detected compared to untreated slices (Fig. 31A, B), aligning with previous observations during TNP treatment.

Upon examining the impact of the ROS scavenger in conjunction with the epileptogenic agent (PTX+CeO_2 group), the signal was reduced by half, effectivelly preserving the control scenario (Fig. 31C). This highlights the antioxidant properties of these nanoparticles and their affirmed role in ROS scavenging, as they successfully reduced the excessive ROS to physiological levels.

Unexpectedly, in the control group under inhibited-ROS production (CeO_2 group), an increase in DCF intensity was obtained (Fig. 31C). Despite this unpredicted result contradicted the anticipated ROS-scavenging properties of nanoceria, it is worth noting that, in some cases, antioxidant properties offer challenges in accurately measuring ROS[362,389,390]. Consequently, it was possible that nanoceria induced the increase in DCF intensity by oxidizing the probe, even in the absence of ROS. To test the hypothesis that the increase in DCF intensity in this experiment was due to nanoceria oxidizing the probe rather than an actual elevation of ROS, a control test was performed without cells.

In this test, the intensity of the probe alone (CNT group) was compared with the probe combined with CeO_2NPs (CeO_2 group), in which a significant 25% increase in DCF intensity was observed (Fig. 31D). Comparatively, when examining the intensity of DCF in CeO_2NPs without the probe, it was approximately one-third below the control levels, suggesting that nanoceria does not exhibit autofluorescence. As a positive control, H_2O_2 was introduced at different concentrations (10 μM and 100 μM), which, by oxidizing DCF, led to a 20% increase in intensity compared to the control. As predicted, when CeO_2NPs were added to both concentrations of H_2O_2, a 20% recovery was obtained (Fig. 31D). Taken together, these data demonstrate that PTX-induced hyperexcitability triggers ROS in this epileptogenic hOTCs model, which can be effectively mitigated by CeO_2NPs.

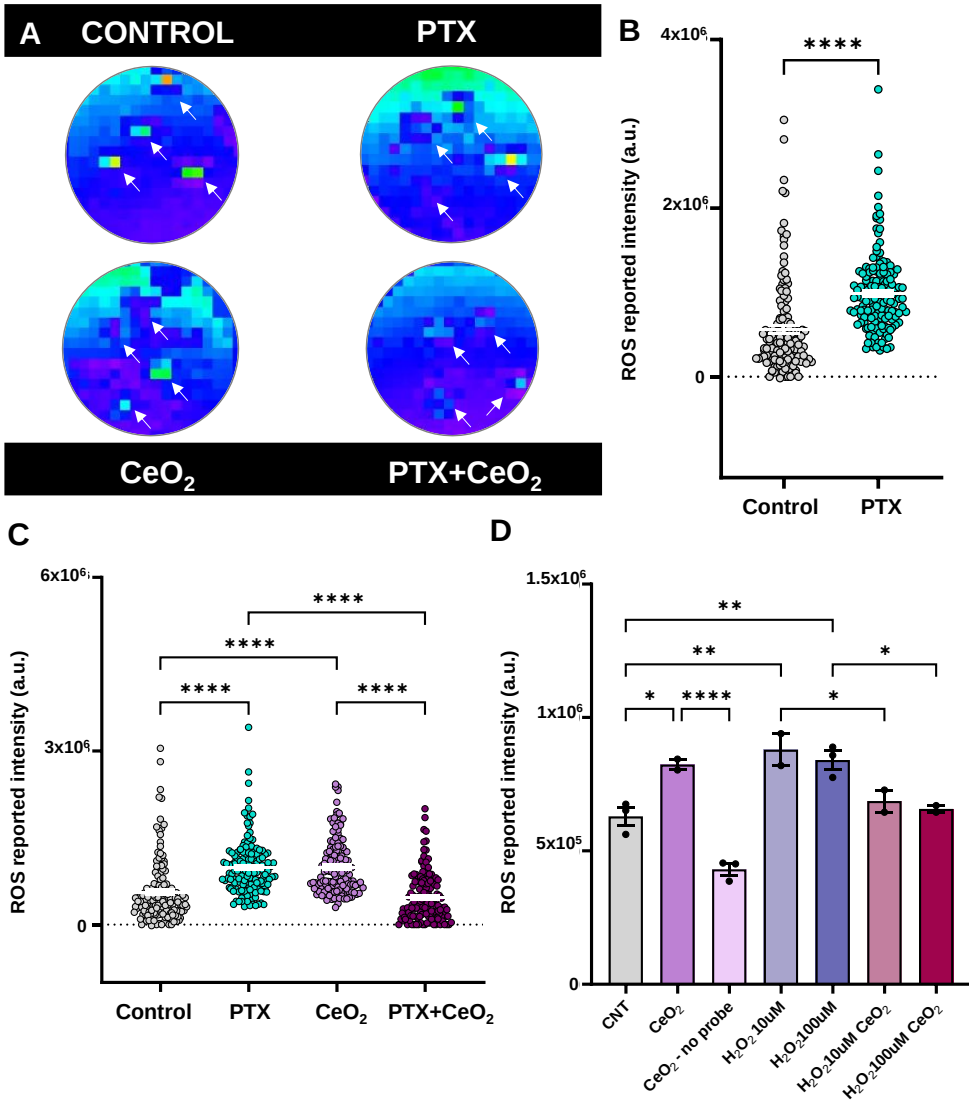

Figure 31. OS assessment in epileptogenic hOTCs where control levels are recovered after ROS-scavenger addition. DCF probes were used for ROS assessment in hOTCs. **(A)** Representative images from CLARIOStar Plus Plate Reader of the insert membranes with PTX-, CeO_2, PTX+CeO_2- and non-treated mouse hippocampal hOTCs in them, analyzed and color-coded according to their fluorescence intensity profile, in which warmer hues indicate higher OS. **(B, C)** Quantification of ROS reported fluorescence intensity (a.u.) in PTX-, CeO_2-, PTX+CeO_2- and non-treated mouse hippocampal hOTCs showing a significant increase in PTX-induced epileptogenic conditions (analyzed by non-parametric Mann-Whitney test) and preserving of control conditions in PTX+ CeO_2-treated hOTCs (analyzed by Kruskal-Wallis ANOVA test with Dunn post-hoc correction). n=3 per group, containing 4 slices in each. Intensity was measured at DIV 18 and 1 day post-treatment. PTX (100µM) and CeO_2NPs (1µg/mL) were added for 3 days. **(D)** Quantification of fluorescence intensity (a.u.) without hOTCs, showing CeO_2NPs significantly oxidizing the probe compared to CNT (probe alone). CeO_2NPs without probe showed no autofluorescence. H_2O_2 was used as a positive control in two different concentrations (10 and 100µM) with and without CeO_2NPs, showing a significant decrease when CeO_2NPs was added analyzed by 2-way ANOVA with repeated measures test and Holm Šídák post-hoc correction. Data are expressed as mean ± SEM. * $P < 0.05$, ** $P < 0.01$, **** $P < 0.0001$.

The preceding test was key for the subsequent use of nanoceria for preventing aberrant neurogenesis in the epileptogenic hOTCs model. The verification of these nanoparticles effectively reducing ROS supported the hypothesis that this reduction is a crucial factor in preventing aberrant neurogenesis.

Following the established efficacy of nanoceria in reducing ROS, the well-being of the slices was assessed under the chosen treatment (CeO_2NPs) across four conditions (CNT, PTX, CeO_2, and PTX+ CeO_2). The initial evaluation involved neurogenesis assessment after DCX staining of the hOTCs. Upon identifying DCX^+ cells in the DG of the epileptogenic slices after ROS inhibition (PTX+CeO_2 group Fig. 32B, C), a significant recovery of 70% was observed. This physiological level preservation indicated a return to the neurogenic physiological state, suggesting neuroprotection. In parallel, apoptotic cells were quantified through DAPI staining, revealing that cell survival was also reinstated after the application of CeO_2NPs in the context of PTX-induced epileptogenesis (PTX+CeO_2 group, Fig. 32D, E), leading to enhanced survival of hippocampal cells. Interestingly, under control conditions (CeO_2 group), the effect of CeO_2NPs remained inert in both the evaluation of newborn neuron population and cell survival, maintaining physiological conditions.

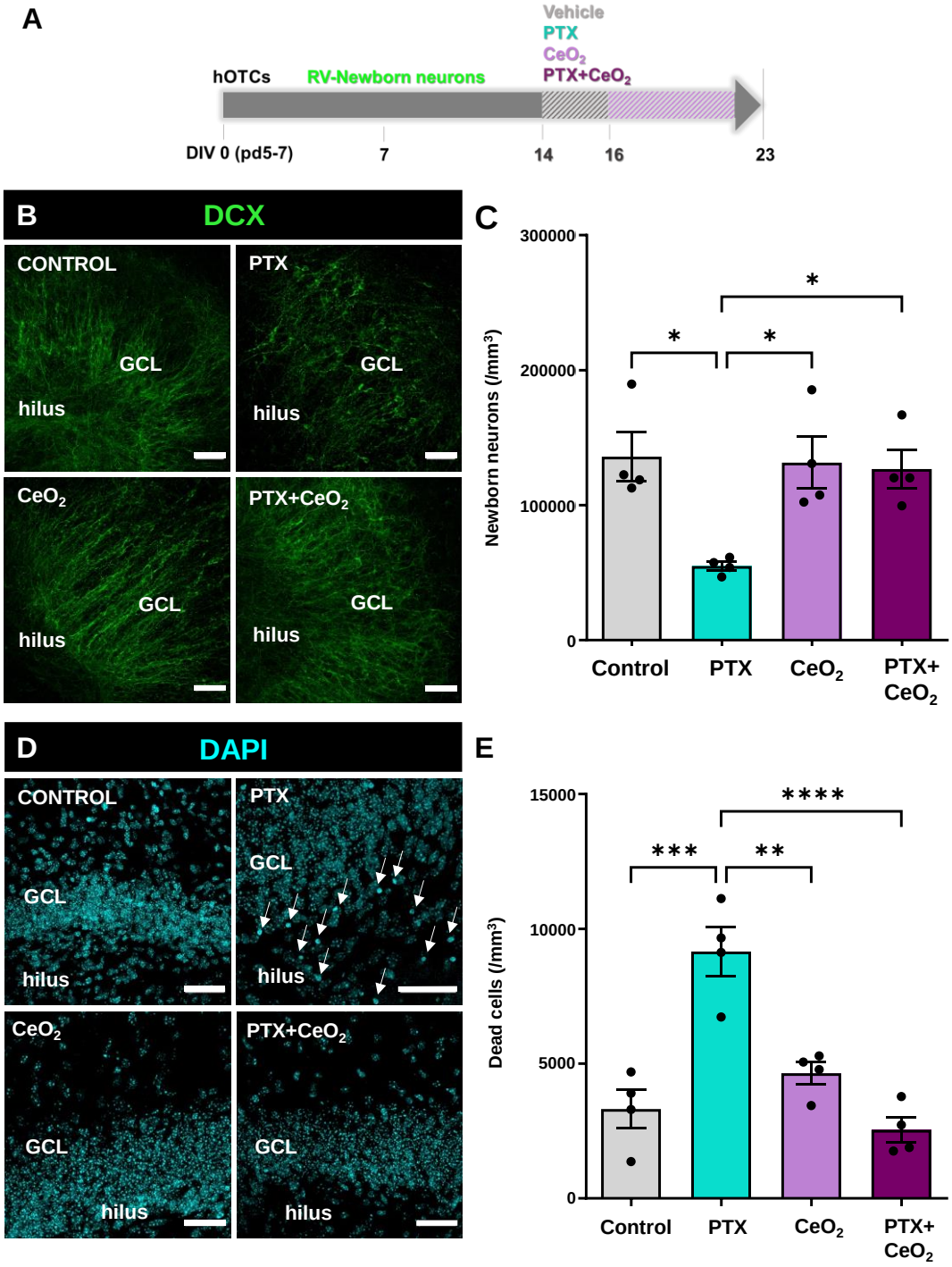

Figure 32. Newborn neurons and cell death preserve control levels in the DG after ROS inhibition in epileptogenic hOTCs. (A) Scheme of the experimental procedure. The hOTCs are extracted at pd5-7 (DIV 0) and cultured. At DIV 7, slices are injected for the expression of RV-Venus (GFP^+). From DIV 14 to DIV 23 they are exposed to $GABA_A$ receptor inhibitor PTX (100µM) and/or ROS-scavenger CeO_2NPs (1µg/mL), and immunostainings and imaging are performed 7 days after (DIV 23). **(B)** Representative confocal microscopy images were taken after staining of the neurogenesis marker DCX, showing the SGZ+GCL in the mouse hippocampal hOTCs. **(C)** Newborn neurons (/mm^3) were quantified by identifying DCX^+ cells. **(D)** Representative confocal microscopy images were taken after staining for DAPI, showing the SGZ+GCL in the mouse hippocampal hOTCs. **(E)** Cell death (/mm^3) was quantified by identifying nuclei presenting pyknosis (DNA condensation) and/or karyorrhexis (nuclear fragmentation), both detected by condensed staining of DAPI. n=4 per group. The scale bar is 50 µm in all the photographs. Data are expressed as mean ± SEM and analyzed by 2-way ANOVA with repeated measures test and Holm Šídák post-hoc correction. * $P < 0.05$, ** $P < 0.01$, *** $P < 0.001$, **** $P < 0.0001$.

6.4.4 ROS Inhibition Preserves GABAergic Cell Number in Epileptogenesis

To further validate the neuroprotective effects associated with inhibiting ROS, and as an additional measure to assess the well-being of the slices, the GABAergic cell population was examined next in the context of CeO_2NPs under epileptogenic conditions. Substantial evidence suggests that ROS has the potential to impair GABAergic neurons by disrupting GABAergic signaling and influencing the function of GABA receptors, resulting in compromised release and uptake of the GABA neurotransmitter[391,392]. Moreover, ROS can damage mitochondria, which can lead to energy depletion and ROS increase in GABAergic neurons[330,357,359]. Thus, the following hypothesis was committed: ROS inhibition is beneficial for GABAergic cells in epileptogenic hOTCs.

In conducting this evaluation, $GABA^+$ cells ($/mm^3$) were identified following ROS inhibition after staining hOTCs with GABA across the four conditions (CNT, PTX, CeO_2, and PTX+CeO_2). The GABAergic cell population preserved control conditions after ROS inhibition in epileptogenic slices (PTX+CeO_2 group, Fig. 33A, B), aligning with the abovementioned neuroprotective properties. In terms of CeO_2NPs addition in control conditions (CeO_2 group), their inert behavior persisted for GABAergic interneurons (Fig. 33B).

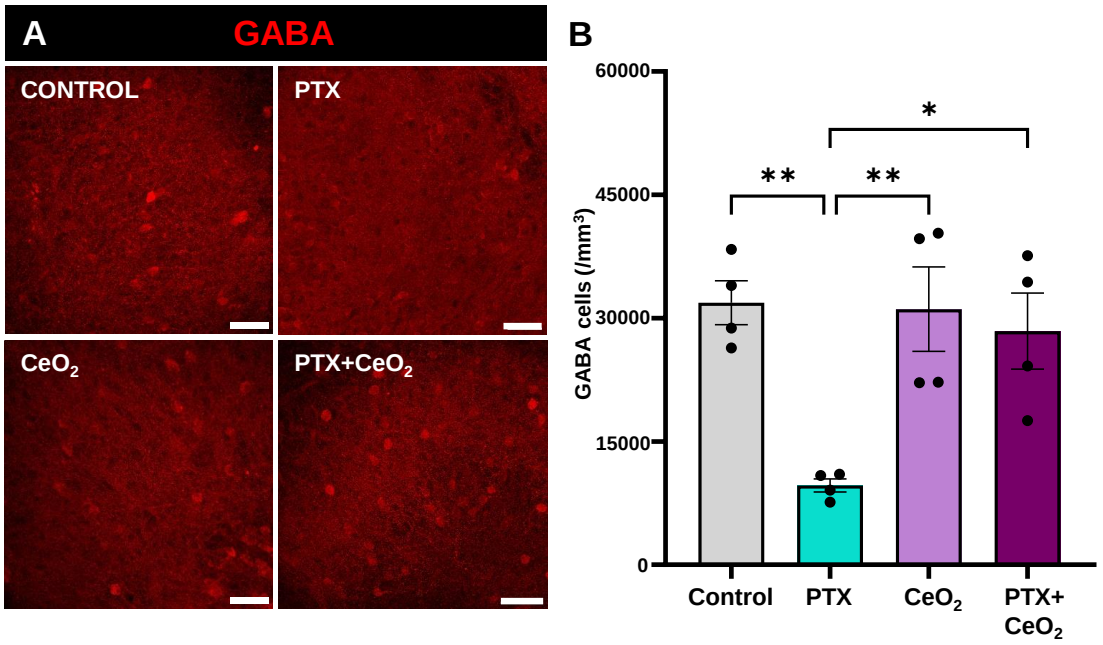

Figure 33. GABAergic cell number preserved control levels in the DG after ROS inhibition in epileptogenic hOTCs. (A) Representative confocal microscopy images of PTX-, CeO_2-, PTX+CeO_2-treated and non-treated hOTCs from mouse hippocampus, after staining for GABA (GABAergic interneuron marker) showing the SGZ+GCL. **(B)** GABAergic interneurons were quantified by identifying $GABA^+$ cells, showing a significant recovery in ROS-inhibited epileptogenic hOTCs (PTX+CeO_2 group). n=4 per group. The scale bar is 50 μm in all the photographs. hOTCs were PTX- (100μM) and/or CeO_2NPs- (1μg/mL) treated for 3 or 10 days respectively. They were fixed at DIV 23 and 7 days post-treatment. Data are expressed as mean ± SEM and analyzed by 2-way ANOVA with repeated measures test and Holm Šídák post-hoc correction. * $P < 0.05$, ** $P < 0.01$.

6.4.5 ROS Inhibition during Epileptogenesis Preserves Dendritic Spines but not Dendritic Arborization

Building on the insights gained regarding the neuroprotective impact of ROS inhibition during epileptogenesis, the study extended its focus to evaluate aberrant neurogenesis, specifically focusing on the development of newborn neurons. Following the same steps as in previous sections, the dendritic arbor complexity of the RV-labeled newborn neurons was assessed by 3D-Sholl analysis as previously described. In this context, the results showed a significant decrease between the radius 70 and 150 µm in the complexity of hyperexcited newborn neurons after nanoceria treatment (PTX+CeO_2 group, Fig. 34A, B). These nanoparticles in control conditions (CeO_2 group) had no effect in terms of complexity compared to control, keeping with their inert behavior (Fig. 34B). Indeed, their similarities with the CNT group resulted in differences compared to PTX between 145 and 165 µm and also, as of the decrease produced after nanoparticle treatment during epileptogenesis, an difference is also observed compared to the PTX+CeO_2 group, particularly within 90 and 150 µm (Fig. 34B).

These results in mind, it was significant to establish the impact of ROS inhibition during epileptogenesis on dendritic spine growth, acknowledging the potential for varied results as previously observed in eATP excess conditions. Therefore, basing on the results obtained in the prior investigation involving nanoparticles and ATP excess, the premise was that, considering the potential divergence in regulatory pathways for dendritic arbor development and spine growth, it was plausible that while full preservation of physiological complexity might not occur, there could be a potential recovery in dendritic spines. In fact, in this context, the physiological dendritic spine features were preserved in every parameter studied: the spine number (/µm), the spine head perimeter (µm), the minor and major axis (µm), and the head area (µm^2) (Fig. 34C-I). This result reinforced the suspicion that distinct pathways govern dendritic arborization and spines during the development of newborn neurons, pointing again to CeO_2NPs as a promising candidate for preventing aberrant neurogenesis.

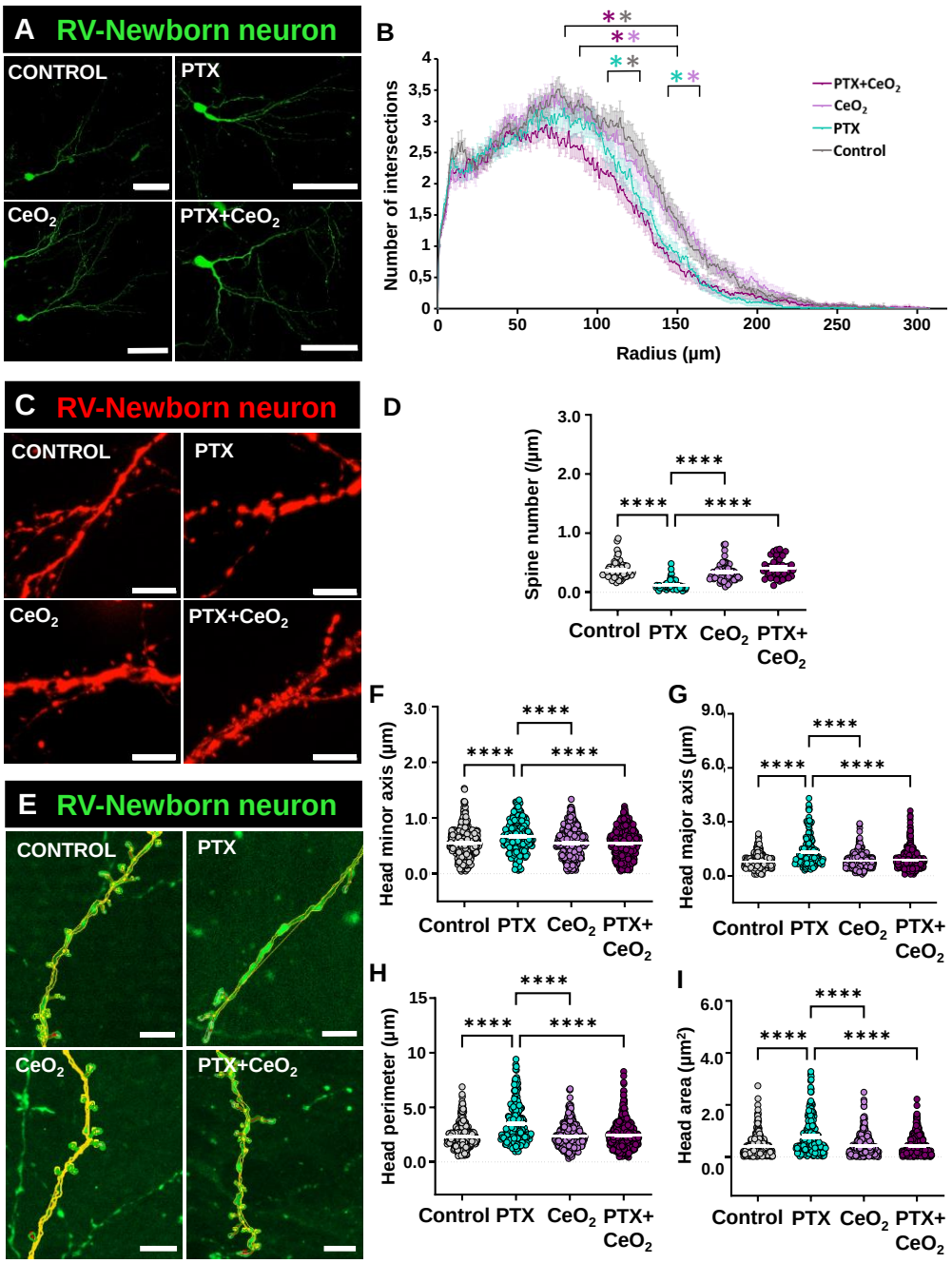

Figure 34. Newborn neuron morphology is impaired but dendritic spines are preserved in the DG after ROS inhibition in epileptogenic hOTCs. (A) Representative confocal microscopy images, showing PTX-, CeO_2-, PTX+CeO_2-treated and non-treated RV-Venus labeled and GFP-stained dendrites. **(B)** Z-stack projections were analyzed and color-coded according to their 3D-Sholl profile. Quantification of the number of intersections between circles of increasing (1µm) radius showed a statistically significant impairment in the morphological complexity of the PTX+CeO_2-treated group. Data are expressed as mean ± SEM and analyzed by ANOVA repeated measures test with Bonferroni post-hoc correction. The scale bar is 50 µm in all the photographs. **(C, E)** Representative confocal microscopy images, with and without SpineJ processing (in yellow), showing dendritic spines from segments of PTX-, CeO_2-, PTX+CeO_2-treated and non-treated RV-mCherry/Venus labeled and DsRed2/GFP-stained dendrites. **(D)** Quantification of spine number (/µm), which is significantly reduced in the PTX-treated group, and the control conditions are preserved in PTX+CeO_2-treated group. **(F-I)** Quantification of spine head minor axis (µm), major axis (µm), parameter (µm), and area (µm^2) respectively. n=4 animals per group, n=4 slices per animal, n=4 neurons per slice, 32 dendritic segments of 30µm per neuron. A total of 960µm of dendrite was analyzed. The scale bar is 5 µm in all the photographs. hOTCs were PTX- (100µM) and/or CeO_2NPs- (1µg/mL) treated for 3 or 10 days respectively. They were fixed at DIV 23, 16 days post-RV injection, and 7 days post-treatment. Data are expressed as mean ± SEM and analyzed by Kruskal-Wallis ANOVA test with Dunn post-hoc correction. ** $P < 0.01$, **** $P < 0.0001$.

To summarize all the observed in terms of ROS inhibition, it is recommendable to have a look at Figure 35. Here, the NSCs are observed to have differential fates depending on the experimental condition. In healthy conditions, the newborn neurons show a complex dendritic arbor and normally developed dendritic spines (Fig. 35.1). However, epileptogenesis disrupts their regular growth impairing their morphology, dendritic spines, and neural activity (Fig. 35.2, 3). The inhibition of ROS by CeO_2NPs can recover partially their health state, because although newborn neuron dendritic arbor does not reach the complexity observed in physiological conditions, normal dendritic spines and neural activity are preserved (Fig. 35.4).

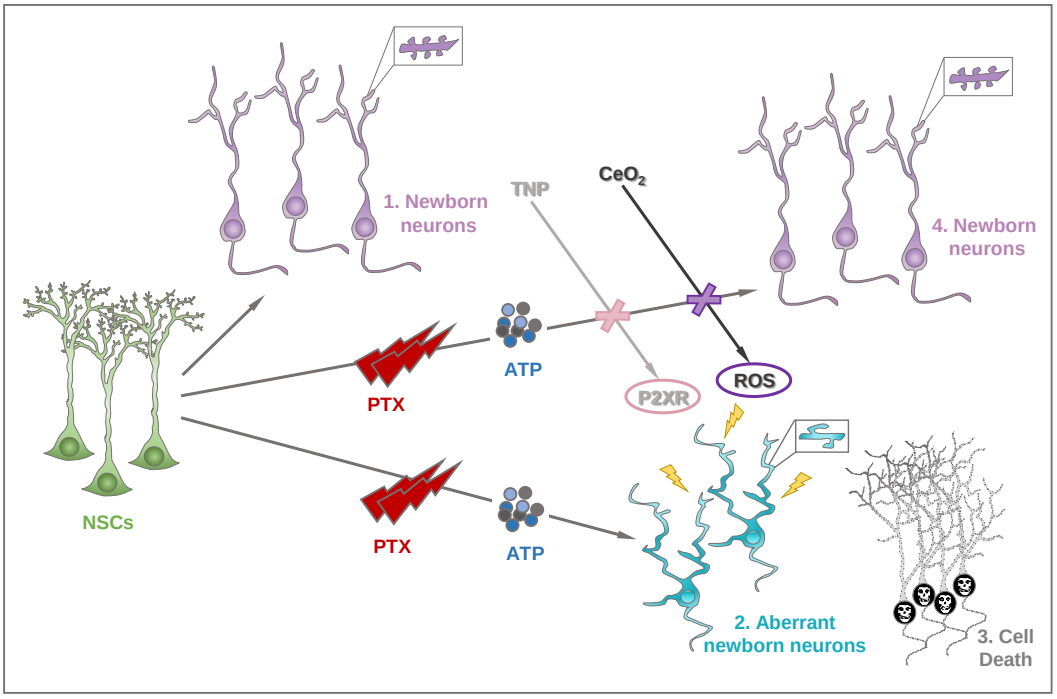

Figure 35. The differential fate of multipotent adult hippocampal NSCs in health, disease and after treatment with a ROS-scavenger in a hOTCs model. In health, the hippocampal NSCs of the DG, after activating, divide and differentiate into immature neurons **(1)**, which present a developed dendritic arbor and already show dendritic spines. However, when epileptogenesis occurs, there is much more cell death **(3)** and newborn neurons become aberrant: there is less density, they are less complex and their dendritic spines grow abnormally **(2)**. When CeO_2NPs that act as ROS-scavengers are added as a treatment, these aberrant features are restored to normality as in the case of the purinergic 2X receptor inhibitor (P2XR) TNP-ATP antagonist, except for the morphological complexity that is not reverted **(4)**.

6.5 GABAergic Cells in hOTCs

Throughout the progression of this study, GABAergic interneuron quantification has served as a readout for evaluating the overall health of the slice. Additionally, it functioned as a tool for assessing the effect of the two different treatments applied in the commitment of the main aim of this whole project: preventing epilepsy-related aberrant neurogenesis. In both the inhibition of P2XR through the TNP-ATP antagonist and in the scavenging of ROS by CeO_2NPs during epileptogenesis, the GABAergic interneuron population was successfully rescued.

Furthermore, the assessment of newborn neurons involved co-localization with GABA staining, highlighting the GABAergic period of some of the studied neuroblasts. This particular experiment provided clues of the state of the newborn neurons, which, in the present work, were analyzed at 2 weeks old, precisely when these neurons exhibit a GABAergic state. Therefore, taking advantage of this GABAergic period, different approaches were performed to help optimize the model.

6.5.1 Vesicular GABA Transporter Expression in Newborn Neurons is not Altered during Epileptogenesis

The initial observation addressed the fact that GABAergic neurons are responsible for producing and releasing GABA. These neurons are widely distributed throughout the brain and have been found to play an important role in the development and progression of epilepsy[220,263]. A key question arises: how does GABA transmission occur in GABAergic newborn neurons? The vesicular GABA transporter (VGAT) plays a relevant role in the release of GABA-containing vesicles, and is considered essential for GABAergic neurotransmission. Therefore, to investigate whether newborn neurons in a GABAergic state release GABA and whether this release is affected during PTX-induced epileptogenesis, the activity of this transporter was examined using a VGAT antibody in both control and epileptogenic conditions.

By quantifying the puncta surrounding the dendrites and axons of newborn neurons, VGAT vesicles were identified in these newborn neurons both in control and PTX groups, confirming the release of GABA in both scenarios. Notably, under epileptogenic conditions, no discernible differences were observed compared to control (Fig. 36A-C), suggesting that GABA release remains unaltered during epileptogenesis.

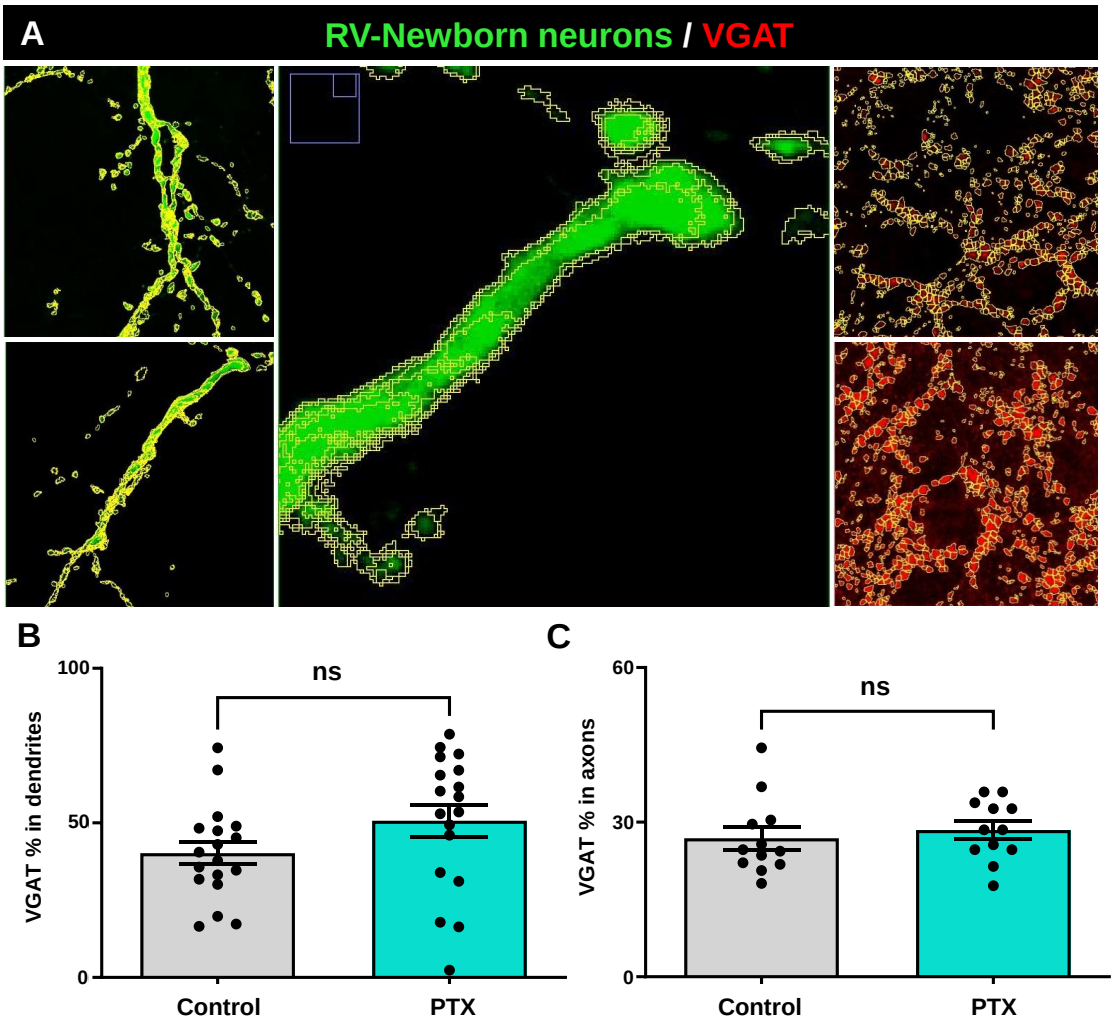

Figure 36. Vesicular GABA transporter (VGAT) assessment in newborn neuron dendrites and axons of epileptogenic hOTCs. VGAT was quantified by the use of FIJI plugins (see Methods 5.5.1) after staining of a VGAT marker. **(A)** Representative confocal microscopy close-up images of dendrites and axons of RV-Venus marked newborn neurons and vesicular GABA transporter (VGAT) in non-treated hOTCs from mouse hippocampus, after staining for GFP in green and VGAT in red showing the plugin based analyzed areas in yellow. **(B, C)** Quantification of VGAT percentage in dendrites and axons with inconclusive results. n=12-18 per group. hOTCs were PTX-treated (100µM) for 3 days. They were fixed at DIV 23, 16 days post-RV injection, and 7 days post-treatment. Data are expressed as mean ± SEM and analyzed by an unpaired t-test. ns=non-significant.

6.5.2 Neural Firing Disruption Impairs Interneuron Number in the DG

The next challenge was to find out the underlying cause behind the decrease in GABAergic newborn neurons during PTX-induced epileptogenesis observed during the optimization of the model (section 6.1.5). Two different reasons were considered: (a) the newly born GABAergic newborn neurons may be more susceptible to dying under hyperexcitability conditions, or (b) the GABAergic developmental period during which these cells express GABA might be altered during epileptogenesis,

missing it during the assessments. Thus, it could be that PTX avoids the GABA input, preventing newborn neurons from becoming GABAergic.

Based on this notion, the next hypothesis was that newborn neurons require GABAergic input to become transiently GABAergic during development. To test this hypothesis, TTX was employed, a compound that selectively blocks voltage-dependent sodium channels in neurons, thereby preventing action potential firing. TTX effectively inhibits the firing of all neurons, which includes both inhibitory and excitatory ones, resulting in much less activity in the slices. Although there is still some synaptic release through the spontaneous fusion of the synaptic vesicles that release transmitters such as GABA and glutamate, it does not follow the normal action potential-related release. Consequently, synaptic signaling persists but is not as robust as under normal conditions.

As in previous experiments, four groups were designed: a) control condition (CNT group): the cultured slices were never exposed to any kind of firing inhibition; b) epileptogenic condition (PTX group): the cultured slices underwent suppression of GABAergic transmission in the extracellular presence of PTX (100 µM) from DIV 14 to DIV 16 (3 days), where GABAergic inhibition is lost on both inhibitory and excitatory neurons; c) control under TTX-induced neural firing inhibition (TTX group): the cultured slices were exposed to TTX (50 µM) from DIV 14 to DIV 16 (3 days); and d) epileptogenic and inhibited neural firing inhibition condition (PTX+TTX group): the cultured slices underwent suppression of GABAergic transmission as in the PTX group (100 µM, 3 days) with the simultaneous extracellular application of the neural firing inhibitor TTX (50 µM, 3 days), where slices underwent suppression of GABAergic transmission with simultaneous neural firing (Fig. 37A). The slices obtained from each of the animals used were separated to cover the four different experimental conditions and imaged on the same DIV (see Methods 5.2.1).

The initial objective was to investigate how silencing neural firing during epileptogenesis affects interneurons, as accumulating evidence in animal models supports the notion that GABA neuron loss can promote the epileptic state[257,393]. In fact, a preferential loss of PV^+ interneurons has been observed in the subiculum of TLE patients and animal models of TLE. This has been further tested through experiments involving the permanent inhibition of GABA release from PV-containing neurons, suggesting their critical role in epilepsy development[257]. Thus, PV-assay was considered the best validation of the experimental framework for TTX addition to cultures, as it was predicted to see a critical reduction of these GABAergic cells in neural firing disruption during epileptogenesis. As predicted, there was a significant decrease of PV^+ cells by half in the presence of TTX, both in control (TTX group) and epileptogenic conditions (PTX+TTX group, Fig. 37B-D).

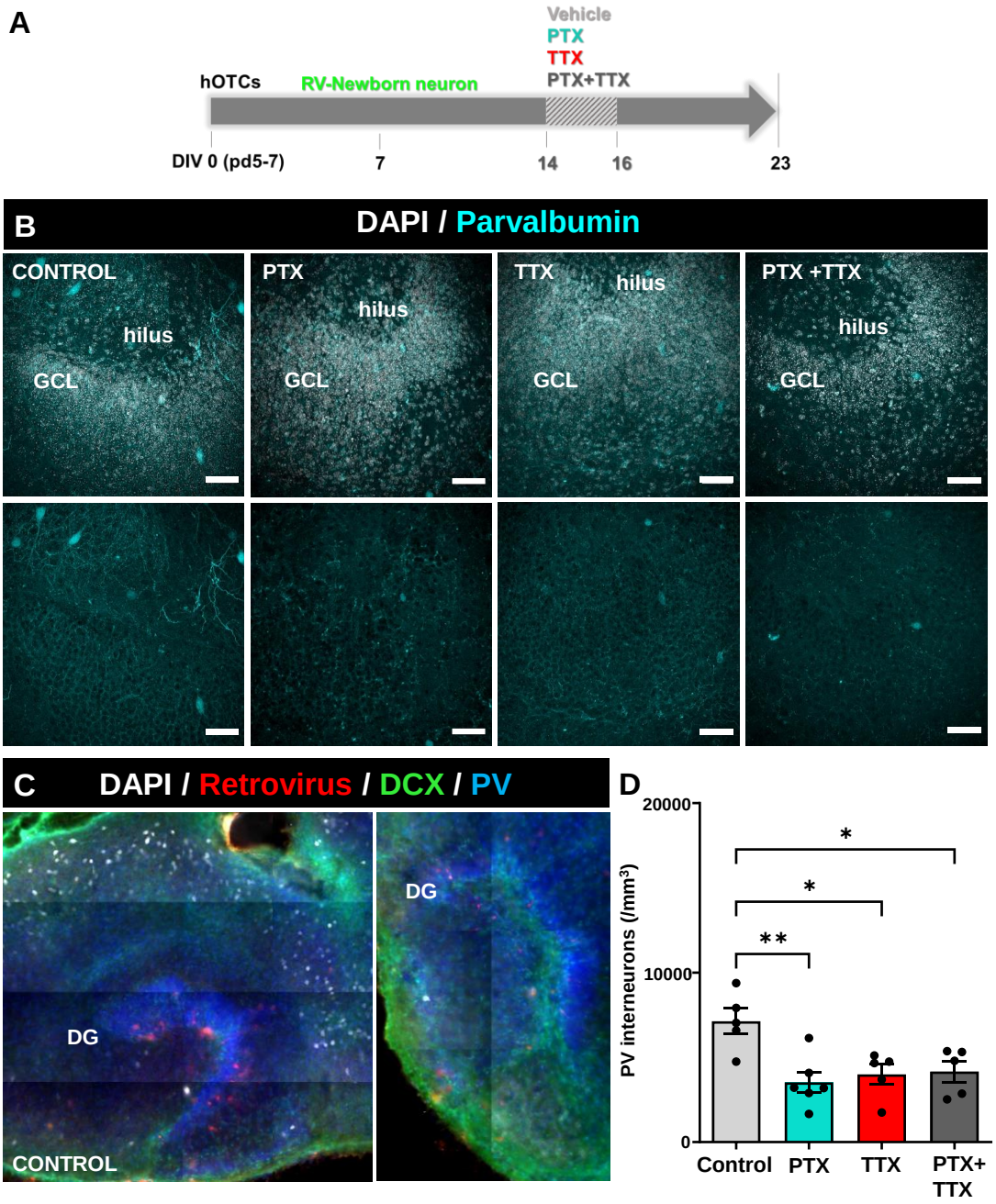

Figure 37. Interneuron numbers are reduced in the DG of epileptogenic hOTCs after silencing neuronal firing. **(A)** Scheme of the experimental procedure. The hOTCs are extracted at pd5-7 (DIV 0) and cultured. At DIV 7, slices are injected for the expression of RV-Venus (GFP^+). From DIV 14 to DIV 16 they are exposed to $GABA_A$ receptor inhibitor PTX (100µM) and/or neural firing disruptor TTX (50µM), and immunostainings and imaging are performed 7 days after (DIV 23). **(B)** Representative confocal microscopy images of PTX-, TTX-, PTX+TTX- and non-treated hOTCs from mouse hippocampus, after staining for DAPI in grey and PV in cyan showing the SGZ+GCL. The scale bar is 50 µm in all the photographs. **(C)** Representative fluorescence microscopy images of non-treated hOTCs from mouse hippocampus, after staining for DAPI in grey, RFP (red fluorescent protein to enhance RV-mCherry labeling) in red, DCX in green, and PV in cyan, showing the SGZ+GCL in which the DG is highlighted. Images were taken with an air objective of 10x. **(D)** Interneurons were quantified by identifying PV^+ cells (in cyan), showing a significant decrease in TTX-treated epileptogenic hOTCs. n=5 per group. hOTCs were PTX- (100µM) and/or TTX-treated (10µM) for 3 days. They were fixed at DIV 23, 16 days post-RV injection, and 7 days post-treatment. Data are expressed as mean ± SEM and analyzed by 2-way ANOVA with repeated measures test and Holm Šídák post-hoc correction. * $P < 0.05$, ** $P < 0.01$.

6.5.3 Silencing Neural Firing Increases Cell Death

When epileptogenesis is induced by PTX addition to cultures, GABAergic inhibition is lost on both inhibitory and excitatory neurons, and signaling is much stronger, even the hyperexcitatory due to the excess of glutamate. Thus, combining both PTX and TTX, there is a scenario closer to the one of TTX alone: no action potentials and little activity (while the spontaneous release of GABA may still occur, it has little effect as the $GABA_A$ receptors are blocked).

Because of that, in TTX addition the hypothesis would be to have an almost normal condition in terms of GABAergic cells, but it is not that easy as there is evidence of TTX causing cell death because of the prolonged period of activity deprivation[394–397]. This was the reason why it was decided to check the cell death after TTX addition to the media, so that it could be elucidated if there was a possible relation between the reduction of the interneuron number and the suppression of the network activity. As predicted, a 2-fold increase in the number of dead cells was observed both in control (TTX group) and in epileptogenic conditions (PTX+TTX group) when the neural firing was suppressed (Fig. 38A, B).

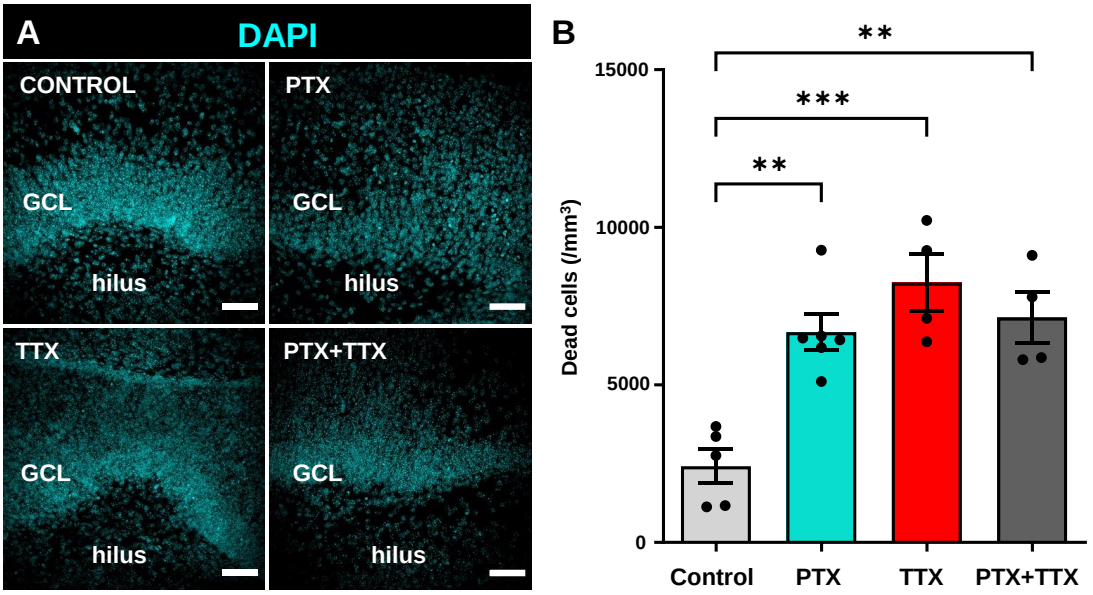

Figure 38. Cell death assessment after TTX-induced neural firing disruption in epileptogenic hOTCs. (A) Representative confocal microscopy images after staining for DAPI showing the SGZ+GCL in the hippocampal PTX-, TTX-, PTX+TTX-, and non-treated hOTCs. **(B)** Cell death was quantified by identifying nuclei presenting pyknosis (DNA condensation) and/or karyorrhexis (nuclear fragmentation), both detected by condensed staining of DAPI, in which a dead cell (/mm^3) increase was observed both in TTX and PTX+TTX groups. n=4-6 per group. Data are expressed as mean ± SEM and analyzed by 2-way ANOVA with repeated measures test and Holm Šídák post-hoc correction. ** $P < 0.01$, *** $P < 0.001$.

6.5.4 Newborn Neurons do Not Depend on GABAergic Input to be transiently GABAergic

To further verify the effect of disrupting neural firing in GABAergic interneurons, the quantification of the $GABA^+$ cell population was performed in the presence of TTX. Surprisingly, the results differed from previous expectations: blocking general neural firing was detrimental on $GABA^+$ cells in control conditions (TTX group), but during epileptogenesis, it did not significantly affect these cells (PTX+TTX group, Fig. 39A, C).

For examining the GABAergic newborn neuron population in the context of TTX inhibition of neural firing, GABA+ cells co-localizing with RV-labeled newborn neurons were identified. Here TTX addition did not show a significantly damaging effect (TTX group, Fig. 39B, D), even if the tendency was higher than in the PTX group. On the contrary, the addition of TTX to epileptogenic conditions (PTX+TTX group) showed a significant recovery of the GABAergic newborn neuron population (Fig. 39D). This finding contradicts the initial hypothesis, indicating that GABAergic neurons do not depend on GABAergic input.

Accordingly, it appears that blocking $GABA_A$ receptors is not the primary reason for the reduced GABA expression in newborn neurons. Instead, the hyperexcitatory activity that occurs seems to disrupt this blocking mechanism, promoting hyperexcitation. In fact, it has been largely tested that the pathological changes observed in PTX-induced epileptogenic conditions can be prevented by the simultaneous application of the convulsant (PTX) together with TTX, suggesting that the pathological features might result from the epileptiform activity itself rather than the direct toxic effect of the convulsant[254].

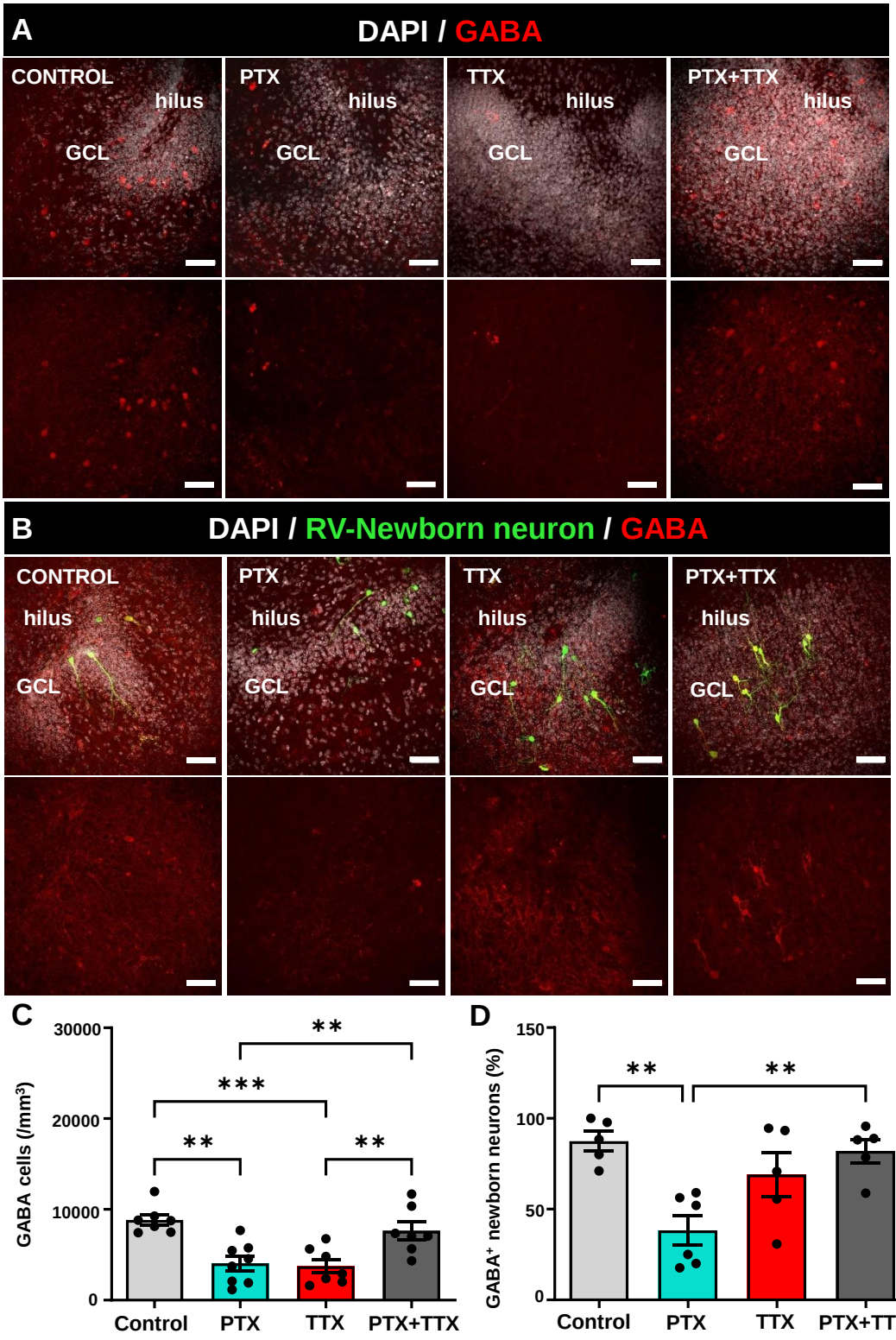

Figure 39. GABAergic newborn neuron numbers are recovered after neural firing disruption in epileptogenic hOTCs. (A, B) Representative confocal microscopy images of PTX-, TTX-, PTX+TTX- and non-treated hOTCs from mouse hippocampus, after staining for DAPI in grey, GABA in red, and GFP in green showing the SGZ+GCL. **(C, D)** GABAergic cells were quantified by identifying $GABA^+$ cells, from which the ones co-localizing with RV-Venus labeled cells were classified as GABAergic newborn neurons, showing a statistically significant recovery in PTX+TTX-treated hOTCs. n=5-6 per group. The scale bar is 50 μm in all the photographs. hOTCs were PTX- (100μM) and/or TTX-treated (10μM) for 3 days. They were fixed at DIV 23, 16 days post-RV injection, and 7 days post-treatment. Data are expressed as mean ± SEM and analyzed by 2-way ANOVA with repeated measures test and Holm Šídák post-hoc correction. ** $P < 0.01$, *** $P < 0.001$.

6.5.5 GABA Addition Reduces GABAergic Cells during Epileptogenesis

Consequently, the previous results raised the following question: Does the transient GABAergic period of newborn neurons depend on neuronal activity? And thus, does the GABAergic newborn neurons need a GABA input to enter the GABAergic transient period? For that, extracellular GABA was added to the cultures in the next experimental framework: a) control condition (**CNT group**): the cultured slices were never exposed to extracellular GABA addition; b) epileptogenic condition (**PTX group**): the cultured slices underwent suppression of GABAergic transmission in the extracellular presence of PTX (100 µM) from DIV 14 to DIV 16 (3 days), where GABAergic inhibition is lost on both inhibitory and excitatory neurons; c) control under GABA additional input (**GABA group**): the cultured slices were exposed to GABA (0.5 µM) from DIV 14 to DIV 16 (3 days); and d) epileptogenic and GABA additional input (**PTX+GABA group**): the cultured slices underwent suppression of GABAergic transmission as in the PTX group (100 µM, 3 days) with the simultaneous application of extracellular GABA input GABA (0.5 µM, 3 days), where slices underwent suppression of GABAergic transmission with simultaneous GABA input (Fig. 40A). The slices obtained from each of the animals used were separated to cover the four different experimental conditions, and imaged on the same DIV (see Methods 5.2.1).

Here, inconclusive results were obtained regarding the GABAergic newborn neuron population in GABA input conditions both in control (GABA group) and epileptogenic scenarios (PTX+GABA group, Fig. 40B, D), and further research has to be performed.

However, in terms of GABAergic cell population in the DG of epileptogenic hOTCs, results show a decrease by half in epileptogenic conditions after GABA input (PTX+GABA group, Fig. 40C, E). This suggests that the decrease in the GABA input is not the reason why the $GABA^+$ cell population is reduced, but the actual reason cannot be claimed. Interestingly, the GABA input in control conditions (GABA group) shows similar results as in control conditions (Fig. 40E), suggesting that the GABA input in a health state does not harm GABAergic interneurons, but it does not increase the population neither, suggesting that these cells do not need an extra GABA input to express GABA.

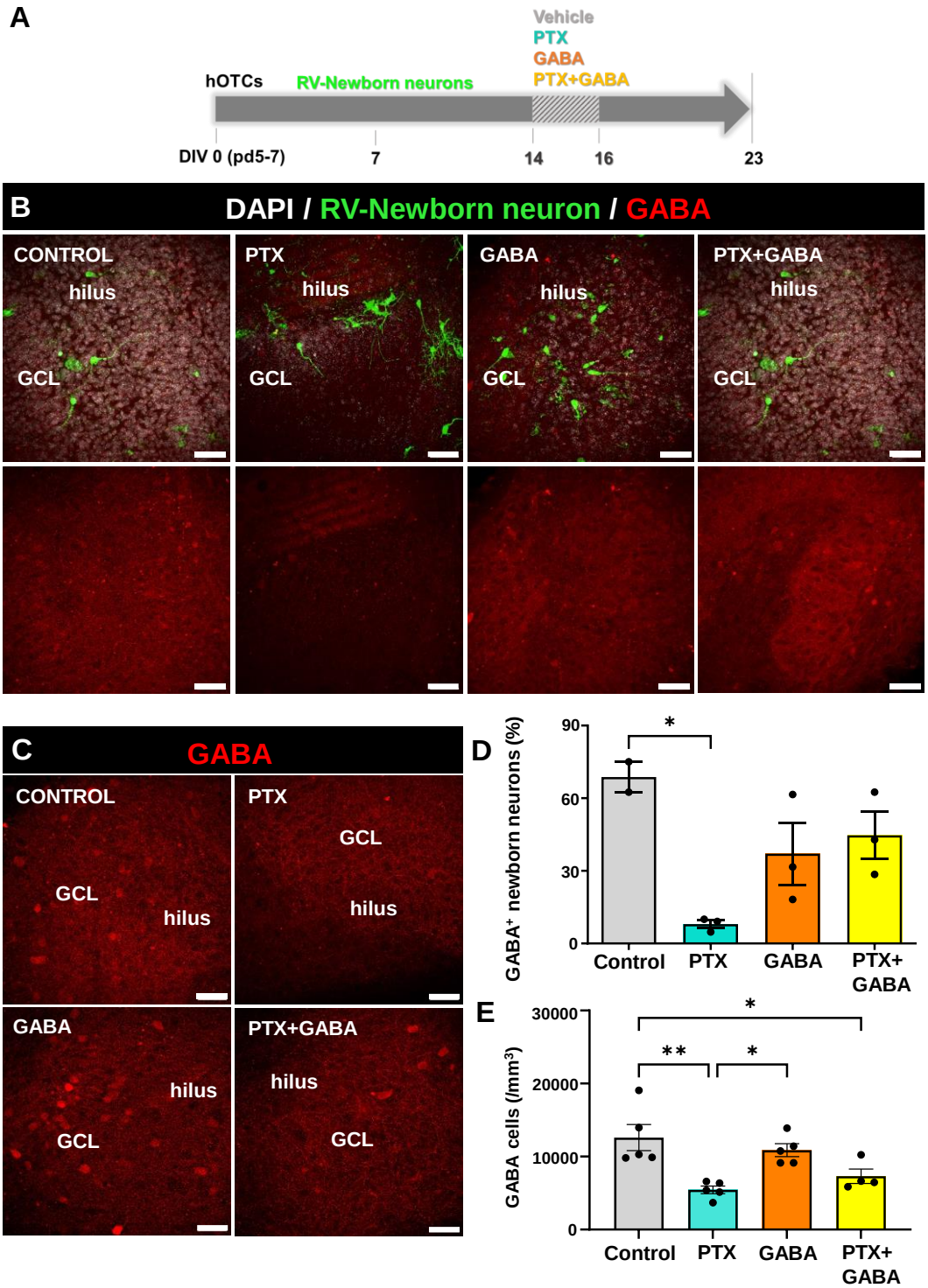

Figure 40. GABAergic newborn neurons are impaired after GABAergic input in epileptogenic hOTCs. (A) Scheme of the experimental procedure. The hOTCs are extracted at pd5-7 (DIV 0) and cultured. At DIV 7, slices are injected for the expression of RV-Venus (GFP^+). From DIV 14 to DIV 16 they are exposed to $GABA_A$ receptor inhibitor PTX (100µM) and/or inhibitory neurotransmitter GABA (0.5 µM), and immunostainings and imaging are performed 7 days after (DIV 23). **(B, C)** Representative confocal microscopy images of PTX-, GABA-, PTX+GABA- and non-treated hOTCs from mouse hippocampus, after staining for DAPI in grey, GABA in red, and GFP in green showing the SGZ+GCL. **(D, E)** GABAergic cells were quantified by identifying $GABA^+$ cells, from which the ones co-localizing with RV-Venus labeled cells were classified as GABAergic newborn neurons, showing a statistically significant decrease in GABAergic cells after TTX treatment in epileptogenic hOTCs. n=3-5 per group. The scale bar is 50 µm in all the photographs. hOTCs were fixed at DIV 23, 16 days post-RV injection and 7 days post-treatment. Data are expressed as mean ± SEM and analyzed by 2-way ANOVA with repeated measures test and Holm Šídák post-hoc correction. * $P < 0.05$, ** $P < 0.01$.

6.5.6 Newborn Neurons are Transiently GABAergic in hOTCs

As aforementioned, the transient GABA expression has been observed to occur in GABAergic newborn neurons during just the first 2 to 3 weeks of neuronal development. Then, this GABA expression is supposed to diminish. Therefore, it was interesting to elucidate whether the newborn neurons in the current model also followed this temporal pattern.

To explore this, the slices were allowed to mature until newborn neurons reached 30 DPI, equivalent to DIV 37, indicating that the newborn neurons were 1 month old. Subsequently, PTX was added for 3 days during DIV 21 and 23, one week before analysis. The assessment of GABA expression was conducted at 7 DPPTX (Fig. 41A). This preliminary experiment utilized a single animal for both the designed control and PTX groups, with three slices per imaged group. All slices underwent immunostaining with GABA and DCX antibodies, revealing the presence of $GABA^+$ cells in both cases. However, no co-localization of $GABA^+$-RV-Venus or $GABA^+$-DCX^+ newborn neurons was identified (Fig. 41B).

Further investigation is required for confirmation, but these results suggest that at four weeks of age, there may be an absence of GABAergic newborn neurons in the DG for both control and epileptogenic hOTCs, as expected based on existing evidence[259]. However, given the hypothesis of this period being altered in epileptogenic conditions, the presence of immature neurons expressing GABA could have been predicted. Unless these preliminary results are validated, it is not yet possible to reject the hypothesis of an altered GABAergic period, but it would allow claim that the period has not been advanced. Therefore, I suggest a more detailed hypothesis of this period starting earlier during epileptogenesis.

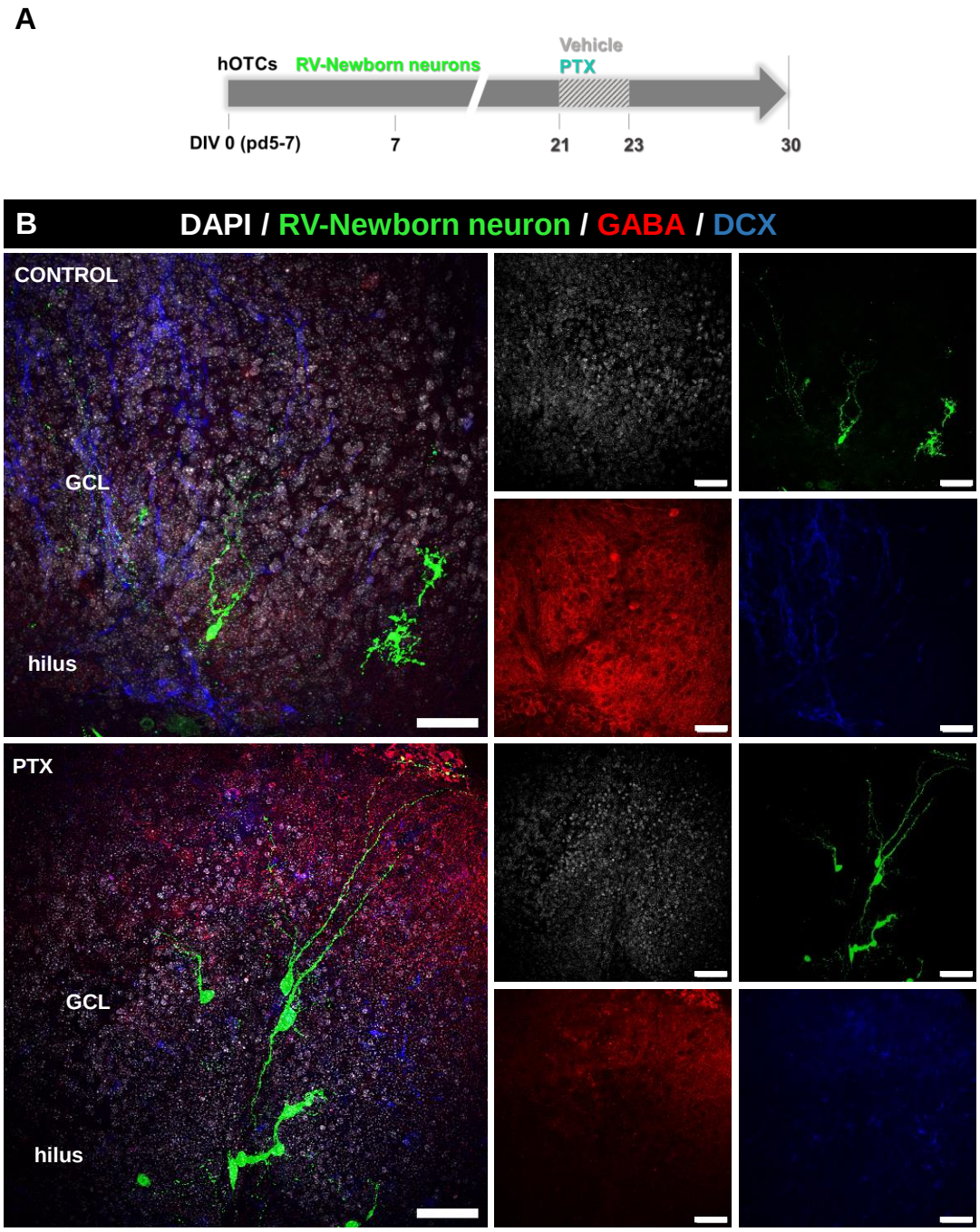

Figure 41. There are no GABAergic one-month-old newborn neurons in the DG of hOTCs. (A) Scheme of the experimental procedure. The hOTCs are extracted at pd5-7 (DIV 0) and cultured. At DIV 7, slices are injected for the expression of RV-Venus (GFP^+). From DIV 21 to DIV 23 they are exposed to $GABA_A$ receptor inhibitor PTX (100µM, 3 days), and immunostainings and imaging are performed 7 days after (DIV 30). **(B)** Representative confocal microscopy images of PTX- and non-treated hOTCs from mouse hippocampus, after staining for DAPI in grey, GABA in red, GFP in green and DCX in blue showing the SGZ+GCL. n=1 per group. The scale bar is 50 µm in all the photographs. The hOTCs were fixed at DIV 37, 30 days post-RV injection, and 7 days post-treatment.

6.6 Viral Vector Gene Delivery Optimization in hOTCs

6.6.1 Challenges in Viral Vector Selection for Investigating GABA Release in Newborn Neurons

This is the attempt to find a suitable viral vector for investigating the functional effects of GABA release in newborn neurons. Indeed, a RV-containing shRNA targeting GAD1 was aimed to use to specifically inhibit GABAergic newborn neurons[398] and assess the resulting consequences in the brain slice. However, this objective resulted challenging as no companies or laboratories that could provide with the required viral preparation were found, and the resources to produce it in the research center were lacking. Thus, the viral vector unit at the Universitat Autonoma de Barcelona (Miguel Chillon group) were contacted for an alternative solution. They suggested to use an adenoviral vector with GFP for visualization in green, incorporating two promoters (DCX, a gene specifically and transiently active in neuronal precursors and young neurons[399–401]; and proopiomelanocortin, POMC, present in newly born granule cells of the DG)[402,403] to selectively mark newborn neurons in the DG. Additionally, shRNA-targeting GAD1 would be included to silence its expression.

Once the AAV.GFP was received, it was necessary to confirm its functionality in the hOTCs model, as it was required to co-localize with DCX for the next steps of the experimental process. However, when the slices were DCX-immunostained following AAV.GFP viral injection, no co-localization occurred (Fig. 42A). Therefore, the collaboration for the viral preparation stopped. Anyhow, the curiosity about the identity of the cells labeled by this virus remained, so different stainings were performed using markers such as NeuN (neuronal nuclear protein, for post-mitotic neurons), Prox1 (prospero homeobox protein 1, for intermediate progenitor cells), S100β (S100 calcium-binding protein β, for astrocytes) and GFAP (for astrocytes and stem cells) (Fig. 42B-D). These stainings revealed co-localizing cells just for some $GFAP^+$ and $S100\beta^+$ cells, suggesting that the AAV predominantly labels astrocytes in the hippocampus.

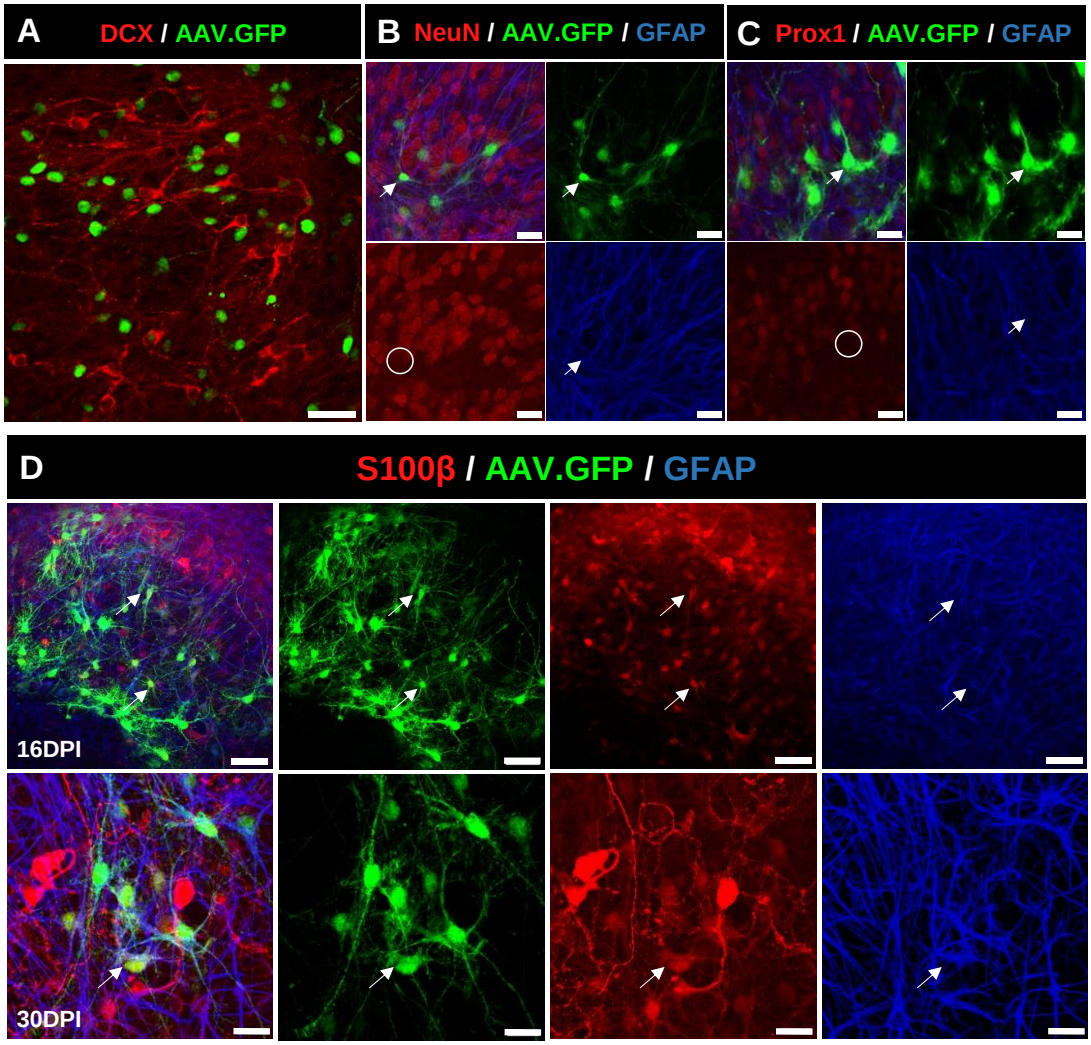

Figure 42. Optimization of adenoviral vector AAV.GFP labeling in mouse hOTCs. Representative confocal images are shown. **(A)** 7 days after AAV.GFP was injected showing labeled cells in green (GFP, for viral signal enhancing) and DCX staining in red, with no co-localization observed. **(B, C)** 14 days after viral injection showing labeled cells in green (GFP^+), NeuN and Prox1 staining in red (white circles showing non-co-localizing cells), and GFAP staining in blue with white arrows showing co-localization with GFAP. **(D)** 16 or 30 DPI showing labeled cells in green (GFP^+), S100β staining in red, and GFAP staining in blue with co-localization shown with white arrows in both GFAP and S100β. The scale bar is 50 μm in all the photographs. hOTCs were made with P5-7 mice and they were fixed at DIV 23-35.

6.6.2 Interneuron Labeling of a Calcium Indicator Containing Dlx Promoter

In the next section a GCaMP was employed, a calcium-dependent fluorescent maker, which enabled the detection of *in vivo* neuronal firing activity. The GCaMP was combined with a Dlx promoter, which is expressed in several regions of the brain, including the hippocampus. Dlx genes encode a family of homeodomain transcription factors that control multiple aspects of embryonic development including neurogenesis[385,404]. Therefore, it is a neuronal marker, which among other neuronal stages, appears in neuroblasts.

The next aim was to assess specifically the activity of the newborn neurons that are transiently GABAergic. For that, the expression of AAV.Dlx.GCamp6 was first evaluated by immunostaining the slices one week after the viral injection. Additionally, two different AAVs were tested, as by using different serotypes different types of cells can be labeled, making the AAV a very useful system for preferentially transducing specific cell types. In this case, AAV1 and AAV9 were used, as both are reported to be successfully used in brain tissue. However, AAV9 has been observed to elicit extensive hippocampal neuronal transduction[405], so it might have greater efficacy in the hOTCs.

Contrary to previous predictions, neither vector labeled DCX^+ neuroblasts (Fig. 43A), preventing the next aim from being carried out. While this virus was no longer suitable for evaluating GABAergic newborn neuron activity, the curiosity remained regarding the labeled cells being mature neurons. Thus, $NeuN^+$ cells were stained, as they were expected to co-localize with the virally labeled cells, but found none (Fig. 43B). Ultimately, a staining using the GABA antibody was performed, revealing that the majority of AAV-labeled cells indeed co-localized, confirming their status as GABAergic interneurons (Fig. 43C).

This will be a very useful tool for future objectives, as it will enable to assess the activity of GABAergic interneurons in the mouse hippocampus and determine whether their firing is impaired in epileptogenic conditions. Additionally, if such impairment exists, the possible preservation of their physiological activity can be further studied through ROS or P2XR inhibition.

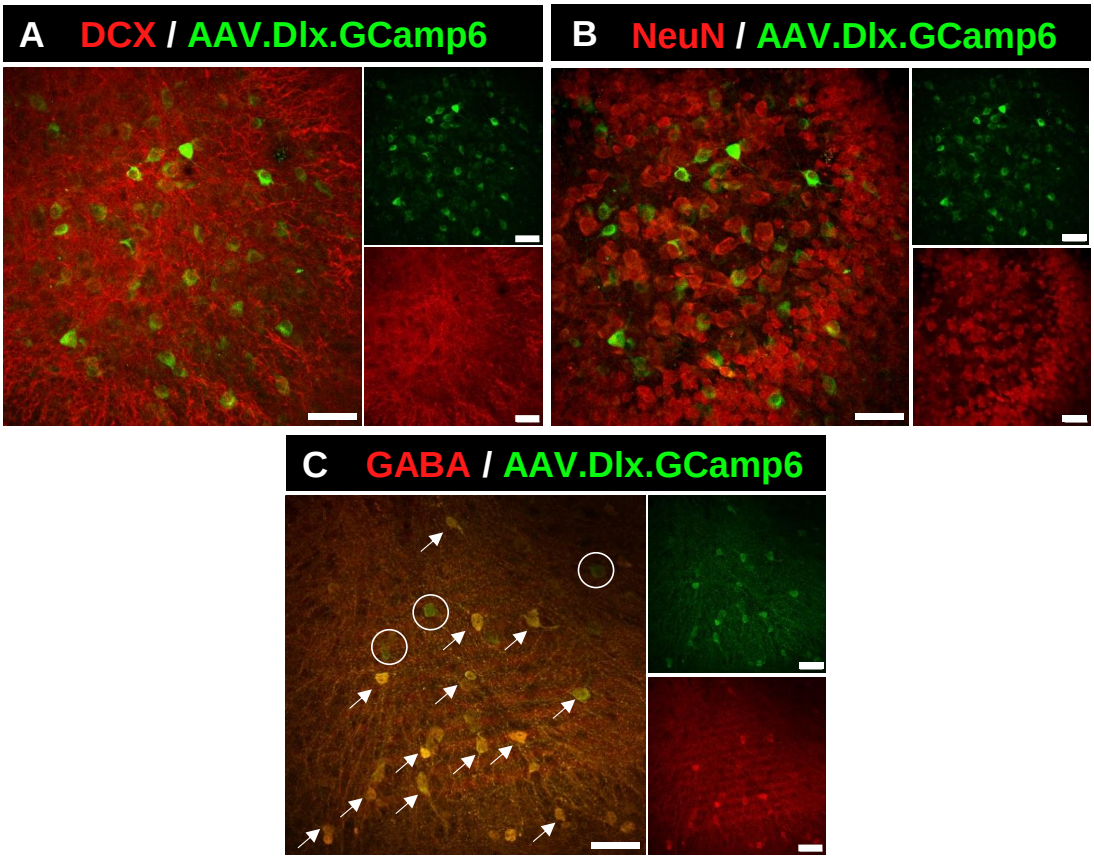

Figure 43. Optimization of AAV.Dlx.GCamp6 in mouse hOTCs. Representative confocal images are shown 7 days after AAV.Dlx.GCamp6 (GFP^+) was injected, showing virally labeled cells in green and DCX **(A)** or NeuN **(B)** staining in red, with no co-localization observed in either of them. **(C)** 20 days after viral injection, virally labeled cells are shown in green and GABA staining in red, with white arrows showing co-localization in some of the cells and white circles in non-co-localizing ones. The scale bar is 50 μm in all the photographs. hOTCs were made with P5-7 mice and they were fixed at DIV 13-23. Both AAV1 and AAV9 serotypes were used in all cases with similar results.

7. DISCUSSION

DISCUSSION

7.1 Validation of the hOTCs Epileptogenic Model for Assessing Aberrant Neurogenesis

This work compares several variables of interest in healthy organotypic slices versus those in which the development of epileptic-like activity is induced by the transient blocking of $GABA_A$ receptors. The model has been fully characterized recently as a useful model to study epileptogenesis and implement manipulations[372]. The main characteristic of this model is that seizure-like activity, defined as hypersynchronous bursts of activity or large groups of neurons, is induced by PTX. Importantly, these bursts of hypersynchronous activity keep taking place spontaneously after PTX has been removed and for the duration of the slice. This phenomenon shows that the circuit has been imprinted to become epileptogenic during the addition of PTX, in a similar fashion to what takes during epileptogenesis in *in vivo* models or humans. Associated to this epileptogenic imprinting or even as an integral part of it, neurons fire with more frequency; more neurons fire in a given period and neuroinflammation increases, contribution to originate the seizure-like phenotype. To make a clear distinction with epilepsy and the *in vivo* models, the terms seizure or epilepsy are consciously avoided when referring directly to the results and data obtained with the models of hOTCs.

An essential upgrade over the previous work, and which is at the core of this study, is to make sure that neurogenesis is maintained in hOTCs, in order to study a pathological biological process associated with epilepsy[21,406] and epileptic models[201,202,407,408], i.e. aberrant neurogenesis.

This work is driven by the hypothesis that neuroinflammation contributes to the induction of aberrant neurogenesis in epileptogenesis. Conversely, the main objective is to preserve normal neurogenesis by influencing the neuroinflammatory response. The use of hOTCs as a research tool brings several advantages, as it combines the speed of long-term culture with the preservation of all the cell types of the brain and its connectivity. This system enables to maintain a complex multicellular *ex vivo* environment that closely resembles the complex interactions found within living organisms, providing a compromise of maintaining essential aspects of neuronal connectivity. Additionally, by opting for hOTCs and its higher throughput over animal models we are able to significantly reduce the number of animals, contributing to the ethical principles of the Rs for animal experimentation, replacement, refinement and reduction.

In more detail, we herein show that slices exhibiting spontaneous epileptiform activity resembling *in vivo* MTLE also depict abnormal features found in animal models of MTLE. Similarly

to what has been previously described in literature[369,372,409], we used hOTCs as an *ex vivo* model of MTLE, which is characterized by the focal origin of seizures in the (unilateral) or very closely related structures. The model is based on transitorily exposing circuits to PTX (for 3 days) in order to achieve GABAergic synaptic transmission suppression, thus creating hyperexcitability conditions. We used a prolonged exposure of 3 days with the GABAergic synaptic blocker PTX, which has been previously described to have a clear impact on neural dynamics[372]. This disruption leads to an increase in neural excitability favored by the cytoarchitecture of the hippocampal formation, rich in recurrent circuits, triggering chronic abnormal patterns of electrical activity resembling those seen in epileptogenic conditions. This controlled manipulation allows for the study of the underlying mechanisms of epileptogenesis, focusing in our case on aberrant neurogenesis, and providing insights that may contribute to a better understanding of epilepsy and potential therapeutic interventions.

7.1.1 Neurogenesis and Survival are Impaired in Epileptogenesis

In the present study, we describe increased overall cell death and decreased neurogenesis. It is broadly accepted that repeated neuronal hyperexcitation can directly cause neuronal death, and either animal models or pathology and neuroimaging work in patients have shown that SE causes neuronal loss[189,410–412]. But, which could be the intrinsic reason why neuronal death increases during epileptogenesis? There are several factors influencing cell survival in pathology, starting with the excessive release of excitatory neurotransmitters, particularly glutamate, which can lead to overstimulation of neurons. This overstimulation can cause an influx of calcium ions into the cells, triggering various cellular processes that ultimately result in cell death[413]. It is the case of NMDA receptors in the adult DG, which play a crucial role in the survival of newly generated neurons shortly after birth[414]. Studies involving single-cell knock-out of NMDA receptors showed that glutamate, through NMDA signaling, mediates the survival and functional integration of migrating neuroblasts[415]. Concurrently, excitotoxicity holds the potential to induce mitochondrial dysfunction, compromising energy production and leading to the generation of ROS and OS, which intensifies cellular injury. These conditions may trigger inflammatory responses in the brain, characterized by the release of pro-inflammatory cytokines and the activation of microglia and astrocytes.

This neuroinflammatory environment can contribute to the disruption of neurotrophic support systems by interfering with the synthesis, release, or effectiveness of neurotrophic factors, including critical ones like BDNF. There are studies suggesting BDNF as a possible factor that when altered, can have an impact in neural death due to its role in regulating neurogenesis, influencing survival, proliferation, and integration of newly-generated neurons[416]. In the context of epilepsy, alterations in BDNF signaling have been associated with both pro- and anti-epileptic effects, and the impact on cell death is influenced by various factors. The BDNF/TrkB signaling pathway is implicated in various aspects of neurogenesis, but its role in the broader context of epileptogenesis remains unclear as a

consequence of its duality[46,417]. In the chronic phase of epilepsy, BDNF decreases alongside reduced neurogenesis[418], indicating a potential link between decreased BDNF and impaired generation of new neurons. Both BDNF and its receptor TrkB show activation in epilepsy models and patients[419], and augmenting BDNF-TrkB signaling increases seizure susceptibility, which implies that an overactivation or dysregulation of this pathway may contribute to the generation or exacerbation of seizures in epilepsy. Conversely, modulating the activity of the TrkB receptor could have a neuroprotective role, as inhibiting it offers protective effects against epileptogenesis[420], potentially mitigating the development or progression of epilepsy.

These findings pertain to overall neuronal death/survival and cannot be extrapolated directly to the survival of newborn neurons, which can be dictated by intrinsic properties and mechanisms particular to the neurogenic niche. As much as happens with newborn neurons during development, survival is promoted by establishment of synaptic contacts[421]. This mechanism is however a late checkpoint and does not account for most of the bulk of cell death of newborn neurons, which takes place early on, only a few days after neuronal precursors are born and are still undifferentiated and without synaptic contacts[58]. Herein the particular timepoint of cell death that could explain the decrease in neurogenesis has not been addressed and remains to be elucidated. Nevertheless, because of the experimental paradigm, much of the loss of neurogenesis should be taking place in earlier stages rather than later ones. Another important factor to consider is cell proliferation, which alteration can also have a strong impact on the amount of newborn neurons generated. However, we did not assess it due to the multitude of factors being addressed during the model optimization. Nevertheless, recognizing its importance, we may consider studying it using the Ki67 cell proliferation marker or even BrdU, which allows for lineage tracking and proves to be a valuable tool in such investigations.

However, the general outcome in the case of neurogenesis in each epileptic model is not consistent. Elevated levels of neurogenesis in the DG and the integration of newly generated neurons into the epileptogenic hippocampal network are hallmark features observed in the initial stages following a triggering event like SE[422]. Following acute seizures in adult animals, there is a notable increase in neurogenesis, but this elevation tends to revert to baseline or even fall below it approximately one month after the initial seizure episode in rats[407,423,424]. Parent showed for the first time, in the pioneering work on an experimental model of MTLE, that seizures trigger a sharp increase in neurogenesis[408], which has been observed on many different occasions later on[208,425–428].

Remarkably, contrasting results are observed in the assessment of adult neurogenesis in the chronic phase. Research by Hattiangady et al. (2004) utilizing DCX as a marker demonstrated a decline in neurogenesis at 5 months post-KA administration[423]. Similarly, Heinrich and colleagues reported a gradual decrease in neurogenesis, reaching below baseline levels by 4-6 weeks post-initial seizure episode[424]. Besides, the chronic phase also manifests a notable reduction in DG neurogenesis[423], as in cases such as in seizure induction by injection of KA in the amygdala or in the hippocampal DG[184,189],

where, in the long term, a decrease in neurogenesis is observed. This decline in adult neurogenesis might be attributed to the potential exhaustion of the NSC pool or alterations in the supportive neurogenic niche for NSCs[184,423,429].

Interestingly, neurogenesis in young pups has also been observed to decrease following acute SE, with only a modest recovery at 2 months after SE[430,431]. During the first week of rodent post-natal life, seizures decrease cell birth in the post-ictal period[432], which can be considered a reasonable basis for the diminishing neurogenesis in the present work with P5-7 mouse pup based epileptogenic hOTCs. This suggests a possibility of the modulation of adult neurogenesis being dependent on the developmental state of the brain at the time of the initial seizure induction.

And what about the severity of the SE? How does it impact on the survival of newborn neurons? The initial SE emerges as a key factor influencing both the degree of abnormal adult neurogenesis and the subsequent development of chronic spontaneous recurrent seizures (SRS). In a hippocampal-kindling model, the severity of SE was shown to impact the long-term outcome, with animals experiencing less severe SE states exhibiting greater survival of newborn GCs after 4 weeks compared to those with fully convulsive SE. Interestingly, the severity of SE did not significantly influence short-term neurogenesis after 1 week, which could make us think that there is just a subtle relationship between SE severity and subsequent neurogenic outcomes[210,433].

Conversely, in a pilocarpine-induced SE model, the frequency of severe seizures was found to be a determining factor in seizure-induced damage and aberrant adult neurogenesis observed 10 days after seizure induction. Fewer severe seizures were associated with enhanced neurogenesis, while more severe seizures had the opposite effect[434]. Therefore, the dynamic changes in neurogenesis observed across the course of epileptogenic progression highlight the complex interaction between neural plasticity and the epileptic state within the hippocampus. While increased neurogenesis in the DG initially contributes to the response to acute injury, its subsequent decline during the chronic phase or in a young brain emphasizes the varying nature of epilepsy-associated comorbidities and the difficulties in the correct diagnosis and treatment[435–437]. The severity and frequency are variables that might play an important role in determining the particular neurogenic outcome. It is reasonable to argue that a higher frequency or higher severity will accelerate the depletion of neurogenesis, be it by direct conversion of NSCs into React-NSCs and then reactive astrocytes or by depleting the pool of NSCs by neurogenic activation-dependent differentiation[59,94]. Indeed, the recent use of human hippocampal samples from epilepsy patients strongly support this scenario, as longer periods of disease associate with lower levels of neurogenesis and more astrogliosis[94].

7.1.2 Hyperexcitation Induces Aberrant Neurogenesis in hOTCs

Epileptic seizures have been shown to cause abnormal hippocampal neurogenesis, with altered progenitor proliferation, aberrant integration, neuronal hypertrophy, and impaired excitability[201], which may prevent the hippocampus from properly regulating excitatory activity and may prompt further seizures[406]. Thus, the inconsistency between epileptogenic models regarding the number of immature neurons is not accomplished when it comes to their dystrophic morphology, which has been persistently observed[189,208,422,425–428]. Abnormal morphology can be interpreted as a decline in their maturation when dendrites are underdeveloped and the density of dendritic spines is diminished, as is the case in models of neuroinflammation and neurodegeneration[192,193]. In the present work, regardless of the total number of neuroblasts, it is clear that their morphology and dendritic features are abnormal. The features of aberrant neurogenesis described herein are similar to previous studies[195,438–440], in which seizure activity in early life may initially induce dendrite branch retraction as a precursor of longer-term growth suppression.

Alterations in dendritic morphology and spine loss mainly in hippocampal neurons have been reported both in neuropathological investigations of epilepsy animal models and human brain tissues from patients with epilepsy[386–388]. In a recent example of an animal model of pilocarpine-induced acute seizures in mice, it was observed that regardless of the total number of new neurons, their morphology is found to be abnormal[201]. Dendrites are underdeveloped, and the density of dendritic spines is diminished, which is observed in models of neuroinflammation and neurodegeneration. In line with these results in the literature, we have also observed a decrease in the number of dendritic spines in newborn neurons, together with an anomalous enlargement and widening of these spines that have also been reported in hOTCs before[441], and that suggests a cellular mechanism of recovery for increasing synaptic contacts. These are common dendritic abnormalities also documented in the neocortical and hippocampal tissue of epilepsy patients, including changes in dendritic length, shape, and branching patterns[442]. Therefore, these findings not only align with previous research but also draw parallels between animal models and human brain tissue, emphasizing the clinical relevance of these observations.

7.1.3 Neural Circuit Activity is Preserved after Newborn Neuron Inhibition

The development of an abnormal dendritic tree has been confirmed to be a significant feature of adult hippocampal neurogenesis, because low synaptic connectivity prevents immature neurons from responding broadly to cortical activity, potentially contributing to an imbalance between excitation and inhibition[406]. The question now is whether these aberrant features in newborn neurons are related to

the hyperexcitability occurring during epileptogenesis. As a result of this hypothesis, we have observed an association between aberrant neurogenesis in the hippocampus and abnormal neural activity. These abnormalities in the number and morphology of newborn neurons can result in the recruitment of newly generated neurons into functional hippocampal networks, creating recurrent excitatory circuits[443]. Abnormal neurogenesis in the hippocampus can disrupt its ability to regulate excitatory activity, potentially leading to the recurrence of seizures. Indeed, there is a big impact of aberrant neurogenesis on the hippocampal circuitry, as abnormal neurons disrupt the normal wiring of hippocampal circuits, which can have implications for cognitive functions and seizure generation[204]. As we have seen so far, there are studies highlighting that epileptic seizures can lead to abnormal neurogenesis in the hippocampus, including altered proliferation of neural progenitors, improper integration of new neurons, neuronal hypertrophy, and impaired excitability[201,204]. Therefore, features of aberrant neurogenesis align with previous studies and may be a consequence of seizure activity early in life, which can lead to dendrite branch retraction as a precursor to long-term growth suppression.

Thus, with these experiments we could confirm the impact of aberrant neurogenesis in neural activity in our hOTCs model, which has been previously observed in animal models. However, the most interesting finding after ablating newborn neuron activity in slices was the one related to a more specific study of the hippocampal circuitry in these conditions: high oscillation frequencies in particular. Oscillation frequencies refer to rhythmic patterns of neural activity in the brain, characterized by repetitive cycles of electrical or neurochemical events[444]. In the context of epilepsy, alterations in neural oscillation frequencies are often observed[445,446]. Gamma oscillations play a crucial role in the coordination of neural activity and information processing, and in epilepsy models, alterations in these oscillations have been linked to hyperexcitability and network instability[176,177]. Also, abnormal HFOs, particularly fast ripples, are often considered potential biomarkers for epileptogenic zones, as they are observed in areas of the brain prone to generating seizures[181]. There are studies showing an increase in these oscillation patterns during epileptogenesis[177,447], which supported our observation of a strong increase in the PTX-induced epileptogenic hOTCs model. Additionally, we further discovered that the physiological frequency of these critical oscillations in the hippocampus was successfully preserved after newborn neuron activity inhibition. This novel outcome not only enhances our understanding of the consequences of aberrant neurogenesis on network activity, but also emphasizes that it is not just the overall firing frequency that is preserved; specific oscillations, like high frequency oscillations, could be directly influenced by aberrant neurogenesis.

7.2 ATP Induces Aberrant Neurogenesis

7.2.1 Excessive Extracellular ATP Impairs Neurogenesis and Cell Survival

We hypothesized that eATP could be a mediator in the developing newborn neuron conversion to aberrant, because although under normal conditions ATP is released by neurons and astrocytes as neurotransmitter/neuromodulator[304], during seizures ATP is released in much larger amounts[297,299,301] due to neuronal excitotoxicity. Also, several studies have demonstrated the presence of purinergic receptors in developing neurons[448] and ATP is known to mediate cell proliferation and reactive responses in the astrocytes[290]. Moreover, ATP also mediates neuroinflammation through reactive astro and microgliosis, therefore, the effect of ATP on newborn neurons could be indirect, direct, or a mix of both. Indeed, future investigation in the host laboratory is focused on addressing the expression of the particular P2XR in hippocampal newborn neurons.

In this project, to assess whether ATP was able to induce or at least act as a mediator in aberrant neurogenesis, we added extracellular ATP to the hOTCs media. We wanted to mimic the amount of ATP released during the insults by damaged cells, as most P2Rs are sensitive to micromolar concentrations of eATP[449]. However, P2X7 requires a very high concentration (>100 μM) of ATP for its activation and is thus, a specific detector of large increases in eATP concentration, such as those that occur on cell death[450]. Thus, the dose used in this work for the study of the effect of ATP is within the range of ATP released during pathological conditions. The excess of eATP in hOTCs media induced similar responses than the addition of PTX: an increment in cell death and a decreased neurogenesis, as well as changes in dendritic arborization and dendritic spine features. These results strongly suggest that indeed ATP could be a mediator in newborn neuron growth and survival in pathological hyperexcitation.

It was not a surprise to observe an increase in cell death after high eATP exposure. Following pathology, higher than normal amounts of ATP released from neurons undergoing excitotoxicity and necrotic cells have been observed to activate certain P2XR on the surface of both neurons and glial cells, allowing inward current and an overload of cytosolic calcium levels, triggering pro-neuroinflammatory signaling cascades plus leading to mitochondrial depolarization, OS, and cell death[451]. *In vitro*, in embryonic NPCs, it has been validated that prolonged eATP exposure results in membrane disruption and cell death via activation of the P2X7R[452]. Hence, it is reasonable to suggest that excessive eATP levels can escalate cell death; but what about their specific impact on neurogenesis? Neuronal vulnerability has been closely related to high concentrations of eATP, which at the same time depend on P2XR expression levels[453]. Indeed, activation of specifically P2X7R has been associated with neuroinflammation and can lead to neurotoxic effects, including inhibition of

neurogenesis. The direct activation of P2X7R through eATP seems to be a key signal in brain pathologies, being endowed with the unique capacity to promote and integrate neuroinflammation, reactive astrogliosis, synaptic dysfunction/loss, and increased susceptibility of neurons to damage[294].

Consequently, the relationship between excessive eATP and hippocampal neurogenesis appears to depend on factors such as the expression levels of P2XR and the activation of P2X7R associated with neuroinflammation and neurotoxicity, with evidence suggesting that elevated eATP levels can have detrimental effects on neuronal health. Neuroinflammation is a strong inhibitor of neurogenesis while hyperexcitation associates with increased neurogenesis. However, higher levels of neuronal hyperexcitation, which comprise excitotoxity and cell death, will be ineluctably accompanied by neuroinflammation. Thus, the balance between these two factors determines the neurogenic outcome[454]. In this case, ATP, in a similar fashion to PTX, impairs neurogenesis, suggesting that ATP-induced neuroinflammation overpowers the effect of neuronal hyperexcitation on neurogenesis.

7.2.2 Excessive Extracellular ATP induces alterations in The Dendritic Arbor of Newborn Neurons

As we have previously mentioned, a high eATP level not only affects cell survival in our hOTCs model but also specifically impairs newborn neuron dendritic arborization and alters dendritic spine features. Indeed, it is of fundamental importance to maintain adequate control of eATP levels in the CNS interstitium, as different aspects of the general brain health such as neuronal physiology, synaptic activity, dendrite arborization or astrocyte and microglia function have been observed to be affected[455]. But what is the mechanism related to the impairment of neural dendritic arborization in excessive eATP conditions? Certainly, it was not an unexpected outcome as it is known that there is a regulatory role associated with the eATP, which takes part in the dynamic interplay between glial cells and neurons[456]. It shows that ATP can induce the recruitment of microglial protrusions to sites of neuronal activity, particularly at synapses, contributing to the downmodulation of neuronal firing. This process is focused on the activation of microglial purinergic receptors and the subsequent production of adenosine by microglia, which acts on neuronal adenosine A1 receptors, effectively suppressing neuronal firing[456,457]. In a healthy brain, microglial processes are in constant communication with synaptic connections situated along neuronal dendrites[458]. These interactions between microglia and dendrites play a vital role in the early developmental phase, where they engage in a process called synaptic pruning. This pruning effectively removes inactive, abnormal, or surplus synapses through what is known as *en passant* phagocytosis[20], a very important activity for sculpting neuronal groups and promoting neuroplasticity[63]. Interactions between microglia and dendrites are finely tuned by neuronal activity: when neuronal firing intensifies, it leads to a higher frequency and more extensive connections between microglial processes and synapses[64]. In this broader context, microglia emerges as a central

regulator of synaptic activity, with its ability to prune excessive dendritic branches and eliminate damaged or surplus synapses through phagocytosis. Thus, in epileptogenic conditions, when neuronal firing increases, the role of microglia as a regulator of synaptic activity could activate a compensatory mechanism by pruning dendritic branches and thus, suppress the dendritic arbor growth as we have seen in our epileptogenic hOTCs model. It is crucial to mention that, the majority of synaptic pruning is associated with the refinement of neural circuits during early development, and that, the extent and significance of synaptic pruning during postnatal neurogenesis are not as pronounced as during earlier developmental stages.

Accordingly, the alterations we have observed in dendritic spine morphophysiology could also be induced by microglia-associated immune responses, as in animal models of neurodegenerative disorders, microglial cell proliferation has been already related to increased levels of proinflammatory cytokines and alterations in dendritic spine morphology and density[459]. By modulating synaptogenesis, microglia are most specifically involved in restoring neuronal connectivity in pathology. These cells release immune mediators, such as cytokines, in the brain parenchyma that are closely linked to plastic morphophysiological changes in neuronal dendritic spines, as they modulate synaptic transmission and alter the number and morphology of dendritic spines during the inflammatory process following injury[460].

In summary, we could demonstrate that elevated eATP levels in hOTCs impact not only cell survival but also hinder newborn neuron dendritic arborization and spine features, which are associated with microglial responses and their regulatory role in synaptic activity.

7.3 Neurogenesis is Preserved after P2XR Inhibition

7.3.1 Recovering Neurogenesis and Survival by Targeting P2XR

Excessive inflammation caused by high concentrations of ATP may be counterproductive to attempts to repair the acute damage, as the cytotoxic effects of these modulators impact healthy tissue and exacerbate the initial injury[461]. As a result of these high concentrations of ATP, a pore allowing macromolecule exchange is known to be opened in the activation of the P2X7R, leading to cell death[462]. Consequently, this purinergic receptor was in the first place described as the "cell death" receptor, as its activation during prolonged ATP exposure results in membrane disruption[452]. P2X7R expression was also found to be increased on neuronal progenitor cells following SE induced via systemic KA in mice[311], potentially impacting SE-induced aberrant neurogenesis. Therefore, there is evidence showing that antagonizing P2XR brings neuroprotection[463,464], and they have been proven to be safe during clinical trials[465]. Further, in a nerve crush model, pharmacological inhibitors of the P2X7R improved the morphology of regenerating nerves[466]. The use of P2XR antagonists has demonstrated a reduced number of seizures during treatment in mouse epileptic models, with a persisting effect one week after the drug-washout period, suggesting disease-modifying potential[467]. Interestingly, we have been able to confirm this effect in our model regarding aberrant neurogenesis, in which the TNP-ATP antagonist was used for inhibiting P2XR, as physiological features were observed to be preserved during epileptogenesis one week after the treatment with the TNP-ATP antagonist was removed.

It has been largely observed that targeting P2XR promotes neuroprotection in brain-related pathologies such as PD, AD, HD, and ischemic stroke[463,468–470]. Furthermore, in the specific case of the TNP-ATP P2XR antagonist, it has been also found to be neuroprotective against ischemic cell death[471], similar to what we have observed in the present hOTCs model. When it comes to neuron survival, by inhibiting P2XR we were able to preserve neurogenesis. This is a common outcome when a P2XR is blocked during brain insult, as it has been demonstrated that the number of neurons undergoing apoptotic cell death is reduced and an increase in the survival of neurons in the injured area and adjacent regions is also observed[472,473]. This reduction in neuroinflammatory responses and the consequent protection of neurons from damage also includes GABAergic interneurons. Certainly, as aforementioned, activation of P2XR can lead to increased neuronal excitability, which may have adverse effects on GABAergic interneurons' function, and also in their survival[474]. Inhibiting these receptors can help preserve the balance of neuronal excitability, supporting the proper functioning of inhibitory circuits. Overall, our findings show that in our epileptogenic hOTCs model, targeting P2XR with TNP-ATP preserved neurogenesis, reducing apoptotic cell death and enhancing neuron survival, including GABAergic interneurons.

7.3.2 P2XR Inhibition is Key in Dendritic Arbor Feature Preservation

The previous approach demonstrates that P2XR antagonists hold potential as a therapeutic strategy for mitigating neuroinflammatory responses and promoting neuronal protection, but what about the effect of P2XR inhibition in neuronal outgrowth particularly? To elucidate this, we performed a Sholl analysis of dendritic branches on newborn neurons in the DG of our hOTCs model, observing a recovery of the abnormal reduction on the dendritic branching during epileptogenesis. As previously explained, this is a hallmark of certain neurodevelopmental disorders, not only in epilepsy but also in other pathologies such as schizophrenia, in which neurons in some regions of the brain also show reduced dendritic length[475].

It has been already seen that the overactivation of the P2XR compromises the dendritic outgrowth, which might contribute to developmental and functional deficits[476]. Thus, as we hypothesized, the inhibition of P2XR counteracted the effect and preserved the physiological growth of the dendritic arbor. This outcome can be related to the involvement of these receptors in triggering neuroinflammatory responses in the brain[477], as therefore, their inhibition may help reduce the harmful effects of that neuroinflammation, which could disrupt their growth and connectivity. The role of P2XR in influencing the excitability of neurons[478,479] could also be key in the subsequent effect after blocking them, as it could help regulate the balance of neuronal activity, preventing excessive excitability that could lead to abnormal dendritic growth.

Moreover, inhibiting these receptors contributes to the stability of the synaptic connections, ensuring that they function correctly and support the growth of not only dendritic arbors but also spines[80]. Indeed, the physiological dendritic spine density and features were preserved in the present epileptogenic hOTCs model after P2XR inhibition, which supports what has been observed in animal models with a P2XR knock-out mouse model, in which the dendritic spine plasticity was also preserved together with a reduction in the dendritic spine loss[480]. It is however important to mention that, in health, the inhibition of P2XR with the TNP-ATP antagonist in our hOTCs model impairs both the dendritic arbor and the spine growth. This shows that it is just in excessive activation of these receptors that their inhibition is neuroprotective, as in health, when their expression is not massive, the inhibition of P2XR is detrimental for normal neuronal growth, suggesting that higher transient expression of these receptors is necessary for normal dendritic outgrowth during neuronal development, proliferation, and maturation.

Indeed, the TNP-ATP antagonist is not specific for a P2XR in particular, and despite in the experiments performed we successfully preserved neurogenesis, the use of a specific P2X7R inhibitor would have been noteworthy. Indeed, the use of the TNP-treatment offered promising results in terms of epileptogenesis, but in a healthy state, it was damaging in many aspects such as cell survival and

newborn neuron dendritic arborization. This could have been expected due to the fact of non-specifically inhibiting P2XR, as their functionality might be necessary for the normal development of the neurogenic processes. Thus, for future research, the use of a specific P2X7R-inhibitor could be key for avoiding this damage in physiological conditions, as this receptor is only activated in increased extracellular ATP conditions, as it occurs during epileptogenesis.

Our model has been primarily performed in a determined period of the development of newborn neurons. Indeed, most findings to date focused on targeting ATP signaling pathways are based on similar rodent models of TLE, and just a few studies are showing antiepileptic effects in mouse and rat pups subjected to hypoxia- or intra-amygdala KA-induced seizures[481–483], suggesting that anticonvulsive effects are independent of developmental stage. Therefore, we considered it important to investigate whether these mechanisms implicated in TLE and its development apply at different developmental stages. For that, we implemented a 2-photon-based time-lapse imaging protocol in which we imaged the same newborn neurons for 3 weeks. It was a very interesting point for evaluating the growing process of the newborn neurons, as the reduction in the dendritic arbor of epileptogenic newborn neurons could have been a matter of the determined period we were studying. However, with this approach, we could observe a disruption of newborn neuron development after the first week in an epileptogenic environment, which was maintained for at least a week more. When it came to P2XR inhibition, the dendritic arbor growth was preserved in its physiological developmental state as expected.

Meanwhile, GABAergic cells were also observed to be related to P2XR, the reason why we evaluated them in our framework. In fact, neuronal P2XR have been reported to influence the release of GABA and glutamate[312,484], and there is evidence suggesting that blocking P2XR increases the number of GABAergic cells, indicating a regulatory influence in their formation; which supports our findings. Moreover, this blockage could modulate neurotransmitter release and prevent synchronous network firing, reducing the number and duration of spontaneous seizures[467]. These results emphasize the relevance of exploring the developmental stage-specific effects of ATP-related mechanisms in the context of epilepsy and highlight the potential for interventions that can preserve normal neuronal development, irrespective of the stage at which they are applied.

7.3.3 Blocking P2XR leads to the Preservation of Network Activity and Firing in Newborn Neurons

At this point, we already know a lot about P2XR and their important role in neuron health. However, their impact on brain circuitry during pathology is yet to be explored in the present work. As important neurotransmitters and components of signaling pathways, purines, and their receptors

participate in the transmission of information in the peripheral and CNS, regulate the physiological activities of nerve cells, and promote the regeneration of the nervous system[485]. Thus, we successfully measured neural activity in our hOTCs model during epileptogenesis to elucidate how the network would react to P2XR inhibition, although all the previous research in aberrant neurogenesis recovery gave us clues on the results we were going to obtain. Indeed, it was easy to hypothesize the preservation of the physiological neural activity in the slices following the same arguments that P2XR, when activated, can increase neuronal excitability, leading to abnormal network activity or hyperactivity. Blocking P2XR in hOTCs helped reduce this excess of excitability, allowing the network to return to a more balanced state, but the mechanism through which this was performed is yet a matter of discussion.

As previously argued, this could be mediated by microglia, as it can regulate neural activity in the brain. Microglia can sense and respond to neuronal activation and can also produce negative feedback against excessive neuronal activity[456]. This novel microglia-mediated neuroregulatory mechanism plays an important role in protecting the brain from disease. ATP is released upon neuronal activation, microglia then sense it and drive themselves toward active neurons. There they metabolize ATP to adenosine, which then inhibits the activity and the overactivation of neurons by acting on adenosine A1 receptors expressed in the neurons. P2XR affect neuronal activity and mediate microglial and neuron-glial interactions in the pathophysiological processes involved in CNS diseases[486], while the preservation of physiological network activity by blocking P2XR suggests that these receptors are involved in regulating the excitability and connectivity of neural circuits.

Therefore, after observing that the physiological neural circuit activity was preserved when P2XR are blocked, it was of great interest to explore the impact of this inhibition on the functional activity of specifically newborn neurons during epileptogenesis. Through real-time tracking of neural dynamics, we monitored the activity of these neurons by calcium imaging. Following the imaging, we observed a significant increase in calcium release within the newborn neurons in the PTX-induced hyperexcited hOTCs compared to control conditions. This observation suggests that epileptogenic conditions led to heightened activity levels in these immature neurons. Indeed, it is already known that during epileptogenesis, neurons, including immature ones, can become hyperexcitable, leading to heightened electrical activity[487]. Moreover, epileptogenic conditions can trigger neuroplasticity, and immature neurons are particularly susceptible to these changes[488]. Therefore, they may undergo alterations in dendritic branching, synaptic connectivity, and excitability as a response to the abnormal neural activity associated with epilepsy. When targeting P2XR, newborn neuron activity preserves normality, which could be explained by their previously mentioned regulatory properties, indicating that P2XR play a role in modulating neural activity and excitability. This finding provides valuable insights into the impact of epileptogenesis on the functional activity of newborn neurons and demonstrates that P2XR inhibition, through the use of TNP-ATP, may play a beneficial role in preserving or normalizing the activity of these neurons.

All these interactions are relevant because in this study we cannot differentiate the direct mechanisms of ATP on newborn neurons versus those indirect mediated through glia. Indeed, we are in the process of confirming the expression of P2XR in newborn neurons, supporting the direct action, despite this option would not rule out the indirect action, which in itself is a whole new venue of research. Even though we could assume that cytokines released by glia could be altering newborn neurons, these effects have not been addressed mechanistically. One pathway of interest in this regard, as we will see next, is the generation of ROS.

7.4 ROS Inhibition Preserves Newborn Neuron Features

7.4.1 CeO_2NP-mediated ROS Scavenging Enhances Cell Viability and Newborn Neuron Dendritic Features in High Extracellular ATP Conditions

In excess, ROS can damage cellular components due to their high reactivity and, by reducing its levels, cells are better protected against OS. Focused on this aim, we used CeO_2NPs that, thanks to their catalytic antioxidant scavenging activity towards ROS, we hypothesized that would diminish the neurological changes related to OS. Moreover, it is necessary to point out that at homeostatic ROS levels, nanoparticles are inactive due to the several free radicals that have to be simultaneously absorbed onto their surface to be recombined into non-radical adducts, a condition that only happens for high ROS concentrations[362]. Certainly, it has been observed that the catalase-like activity safely downregulates OS by scavenging the excess of ROS in diseases[489], with better performance than other antioxidant substances in both efficacy and efficiency, as it becomes active at high ROS concentrations.

In the present work, for 10 days, we continually exposed the slices in excessive eATP conditions to CeO_2NPs, which successfully preserved both cell survival and neurogenesis in the DG. This was not a surprising outcome, as the increment in eATP is related to an excessive neuroinflammatory response in which overmuch ROS is generated[490,491]. This is often associated with conditions where cellular energy demands are elevated, such as during periods of intense physical activity or in situations of cellular stress as in the case of neurodegenerative diseases[492]. This is because the process of oxidative phosphorylation in the mitochondria, which produces ATP, also generates ROS as a natural byproduct, and when there is an excess of ATP production, it can lead to an imbalance in the electron transport chain, increasing the production of ROS[491]. In these conditions, it could be that mitochondria become overwhelmed and produce more ROS than the cell can efficiently neutralize, which can contribute to OS leading to cellular damage[357]. ROS-induced damage can, not only harm organelles but also cellular structures, thus, when ROS levels are reduced, cells are more likely to maintain the integrity of their membranes. Cell membranes can be vulnerable to radical damage because they contain polyunsaturated fatty acids, that when interact with oxygen-derived free radicals, an oxidizing agent generated by ROS, lead to the formation of highly reactive electrophilic aldehydes as part of the lipid peroxidation process[493,494]. By reducing ROS levels and neutralizing the radicals involved in lipid peroxidation, antioxidants effectively terminate the lipid peroxidation chain reaction. This prevents the continuous generation of lipid peroxides and stops the propagation of oxidative damage to cellular membranes, ensuring that the cell's structural and functional integrity is preserved[495,496].

ATP plays a critical role in providing energy for various cellular processes, including those involved in cellular repair and structural maintenance[497], thus, adequate ATP levels are essential for the energy-intensive processes required for dendritic growth, maintenance, and synaptic connectivity. When the eATP increases excessively, the processes mentioned can be impaired due to the increased OS to which newborn neurons are specifically vulnerable. Certainly, the damage that the OS can induce to the dendritic structures and spines in these cells leads to structural abnormalities, such as reduced arbor branching and complexity, or loss and deterioration of dendritic spines[498]. Because of that, the ROS scavenging properties of CeO_2NPs were thought as a very promising tool for the preservation of the morphology, and after testing them, they offered a complete preservation in terms of dendritic spines. It makes sense as with lower ROS, there is less oxidative damage to the proteins and lipids within dendritic spines, and creates a more favorable environment for dendritic spine regeneration and stabilization. However, the dendritic complexity was worsened when these nanoparticles were added to the hOTCs, suggesting a differentiated pathway in terms of the development and growth of the dendrites and spines. Indeed, ROS, including free radicals like superoxide radicals and hydroxyl radicals, can play a role in the regulation of dendritic growth and branching[499]. Under normal conditions, a certain level of OS may promote dendritic development as a response to environmental cues and synaptic activity, which in excessive OS conditions can be detrimental. By reducing ROS levels, the excessive stimulation of dendritic growth and branching may be mitigated, leading to a decrease in complexity. However, these are just possible answers to the results obtained, but the specific impact on newborn neuron dendrite arborization depends on various factors and the overall cellular context so it needs to be further studied.

7.4.2 Inhibiting ROS using CeO_2NPs during Epileptogenesis Reduces ROS and Preserves both Neurogenesis and Cell Survival

Keeping in mind the observed results with CeO_2NPs in excessive eATP conditions, we applied the same treatment in the context of epileptogenic hOTCs, expecting to ameliorate the effect of the increased ROS and preserved neural morphology. Although the increase in ROS in epileptic conditions is broadly accepted[365,500], we wanted to validate it in our hOTCs model as well as test the viability of CeO_2NPs as ROS scavengers in this system. Here we observed a ROS reduction in epileptogenic conditions after nanoceria application in the media, in line with the hypothesis aforementioned. Unexpectedly, the control CeO2NPs generated an increase in ROS levels, which challenges the initial assumption and interpretation of nanoceria as an ROS scavenger. However, it is already studied that the measurement of ROS can be challenging due to the antioxidant properties of nanoceria, as in some cases, these properties may interfere with accurate ROS measurements[362,389,390]. The hypothesis was

then presented that the increase in DCF intensity might be a result of nanoceria oxidizing the DCF probe itself, even in the absence of actual ROS. To test this hypothesis, a control test without cells was conducted, exposing the DCF probe to CeO_2NPs in the absence of cellular components. It was then observed that the increase in DCF intensity observed in the inhibited-ROS production group was indeed linked to nanoceria's interaction with the probe rather than a genuine elevation of ROS levels. This experimental design and control test was crucial for ensuring the validity and reliability of the results. Nonetheless, opting for an alternative probe could have been a more prudent decision to guarantee optimal ROS measurement, even in the presence of CeO_2NPs added to hOTCs. Currently, we lack knowledge about which specific ROS measurement method would avoid this issue, given the previously mentioned challenges associated with accurate measurements.

The use of CeO_2NPs consequently gave rise to the preservation of cell survival and a neuroprotective effect regarding neurogenesis. This was an anticipated elucidation due to the already known vulnerability of neurons to the OS, which arises from several factors, including the high metabolic rate of neurons, their abundant lipid content, and their dependence on oxygen for energy production[200]. Actually, the oxidative modifications of macromolecules in the epileptogenic environment turn on a variety of defensive mechanisms, including the activation of antioxidant enzymes (e.g., superoxide dismutase, catalase, glutathione peroxidase) and the upregulation of molecular pathways involved in cell survival and repair that compromise neural homeostasis, leading to damage and/or death[200,501].

Linked to this, increased OS has recently been observed to lead to GABAergic interneuron damage in the developing brain[502,503], supporting our hypothesis of its decrease in epileptogenic conditions and its subsequent preservation when reducing ROS with CeO_2NPs treatment. Thus, since neuronal loss appears as one of the major neurobiological abnormalities in the epileptic brain, the capability of antioxidants to attenuate epileptogenic features further supports their important role of having a recognized antiepileptic potential.

7.4.3 ROS Inhibition Preserves the Dendritic Spine Features while the Dendritic Arborization is Impaired during Epileptogenesis

However, regarding aberrant neurogenesis in terms of the morphological complexity of newborn neurons, the dendritic arborization was diminished after CeO_2NPs-induced ROS inhibition. It is well-known that the plasticity of dendritic arbors is utilized by neurons to compensate for changes in the synaptic input, which requires ROS for activity-regulated plasticity[504]. Moreover, ROS signaling has recently emerged as a necessary positive regulator for dendritic structural remodeling to occur in motor neurons in *Drosophila*[505], and its inhibition has been observed to disrupt the timing of neuronal

polarization of cultured hippocampal neurons from rat embryos[338,506]. Therefore, it may be justified that there is a reduction in the number of intersections of newborn neurons in the present epileptogenic hOTCs model when ROS is inhibited with nanoceria, although the understanding of the mechanisms for physiological regulation by ROS will be key to revealing the interplay between OS and dendritic arborization.

Regardless of the dendritic arbor depletion in newborn neurons of ROS-inhibited epileptogenic hOTCs, it was yet interesting to look further into detail by analyzing the status of dendritic spines in these conditions. It has been previously addressed how chronic unpredictable stress reveals new dendritic spine formation decrease and pre-existing spine loss increase[507], suggesting that stress deprivation may bring the control situation back, as occurred in the present model. Nevertheless, it is not only the density but also the structure of dendritic spines that are important factors in synaptic functions, dynamic changes in the shapes and sizes of dendritic spines can also affect spine stability and synaptic strength. Increased OS and neuroinflammation are some of the main causes of these changes in dendritic spine structure[498], and they have been observed to change the rate between thin and mushroom spines in neurons in the DG and CA1 in young adult mice, which suggests a potential change in synaptic activity[508]. Even though we have not assessed the type of dendritic spines, their size and structure have been thoroughly measured after ROS inhibition, showing how large dendritic spines in hyperexcited newborn neurons recovered their physiological size. The fact that the spine density decreases and average spine head volume increases suggests a homeostatic balance between spine head volume and spine density, which could imply that epileptogenesis is accompanied by an abnormality in the mechanisms that control synapse growth and maturity. Besides, the mechanisms driving the recovery of these abnormalities after CeO_2NPs-induced ROS inhibition remain to be fully explored.

7.5 Epileptogenesis Affects GABAergic Interneurons

7.5.1 GABAergic Neurons are Impaired in Hyperexcitatory Conditions

Its role in regulating a wide range of brain functions[261] through the modulation of the inhibitory-excitatory balance necessary for proper brain function, and thus, its implication in several neurological disorders when in a dysfunctional state, makes GABA a key factor in this study. Furthermore, in our epileptogenic hOTCs model, we observed a decrease in number of interneurons, both $GABA^+$ and PV^+ ones, supporting the dramatic effect that hyperexcitation induces on the previously mentioned neural network functioning. In animal models of epilepsy, PV^+ interneurons have been shown to be particularly susceptible to cell death or dysfunction[382–384], and loss of PV^+ interneurons has been observed in human patients with epilepsy[509], which is thought to contribute to the development of hyperexcitability and seizures[267,268]. However, elucidating what was going on with $GABA^+$ newborn neurons within our framework was of utmost interest due to the controversy in terms of their GABAergic/glutamatergic nature.

The GCs residing within the DG, which serve as the point of origin for the MFs, have long been characterized as primarily glutamatergic in nature[510]. Nonetheless, emerging data from various experimental methodologies in recent years have initiated a debate, calling for a redefinition of their phenotypic identity. While there is no denying their capacity to release glutamate for rapid neurotransmission, evidence has unveiled a surprising twist in their functional profile suggesting that these traditionally glutamatergic cells also exhibit the expression of GABAergic markers, opening up a previously unexplored feature in our understanding of these neurons. These markers include GABA-synthesizing enzymes and GABA transporters, which are typically associated with inhibitory neurons[259,511]. This co-expression of glutamatergic and GABAergic markers challenges the conventional classification of these cells as purely excitatory, suggesting that they may play a multifaceted role in hippocampal circuitry, potentially participating in both excitatory and inhibitory signaling pathways.

Indeed, the GABAergic phenotype of these cells appears to show age-dependent shifts in its functional effects. Early in life, during a critical period spanning approximately 1.5 to 4 weeks post-mitosis, GABA paradoxically acts as an excitatory neurotransmitter within the DG[259]. This unique phenomenon has significant implications for the development and operation of the hippocampal network. During this specific developmental window, GABAergic signaling takes on an excitatory role in young GCs within the DG. Unlike the typical inhibitory action of GABA observed in mature neurons, GABA at this stage plays a pivotal role in promoting spike initiation and enhancing neuronal excitability within the hippocampal network. This means that, in these young GCs, GABAergic

transmission leads to the generation of action potentials and supports the overall network activity, particularly during periods of moderate neural activity[512].

This reduced period is the exact time at which we studied the developmental changes of newborn neurons during epileptogenesis in hOTCs. This is the reason why we wondered if there could be an effect on the GABAergic phenotype during the development of the disease. Thus, our hypothesis was directly formulated by thinking of the GABAergic period being altered, and it was confirmed when we observed the reduction in GABAergic interneurons in the DG. Moreover, we also assessed the percentage of GABAergic newborn neurons in this area, obtaining the same results. The alteration of this period raised intriguing questions about the functional significance of the dual identity within the DG granule cells. Could these cells be involved in fine-tuning the balance between excitatory and inhibitory neurotransmission within the hippocampus? Might they play a critical role in regulating the overall network dynamics and information processing in this crucial brain region? Answering this kind of questions was not an easy approach, so we started with the hypothesis of GABAergic neurons needing GABAergic input to be GABAergic.

In this study, we aimed to investigate the impact of disrupting neural firing, specifically in GABAergic interneurons, by using TTX, in order to elucidate whether these neurons needed GABAergic input to be GABAergic. Surprisingly, the study did not yield the expected results, as blocking general neural firing was found to be detrimental for $GABA^+$ cells in control but not in the case of the slices with epileptiform activity. These unexpected results led to the rejection of the initial hypothesis that GABAergic neurons depend on GABAergic input for their functioning, suggesting that blocking $GABA_A$ receptors is not the reason for the decreased expression of GABA in newborn neurons. This outcome highlights a crucial point: the observed pathological changes in conditions resembling epilepsy (induced by PTX, a convulsant) are prevented when TTX (a sodium channel blocker) is simultaneously applied. This suggests that the pathological features associated with epilepsy may result from the epileptiform activity itself, rather than being a direct toxic effect of the convulsant. These findings have significant implications for our understanding of epileptogenesis and the role of GABAergic neurons, as they suggest that the changes in GABAergic cell function during epileptogenesis are not solely due to disruptions in GABAergic signaling but may be influenced by the overall neural activity and network dynamics associated with epilepsy.

Briefly summarizing what we have observed in this work, the PTX-induced hyperexcitability model in hOTCs proves valuable for studying aberrant neurogenesis during epileptogenesis. This model demonstrates the suitability of healthy hOTCs for long-term studies while revealing that PTX-induced epileptogenesis disrupts neurogenesis, dendritic morphology, and synaptic plasticity. Excessive eATP and OS play crucial roles in this process, and their inhibition through P2XR and ROS modulation preserves neurogenesis and neural function. Furthermore, GABAergic interneurons are significantly impaired during epileptogenesis, shedding light on their intricate role in the neural circuitry. Overall, these findings contribute to our understanding of epileptogenic mechanisms and suggest potential therapeutic avenues for epilepsy treatment.

8. CONCLUSIONS

CONCLUSIONS

1. PTX-induced Hyperexcitability in hOTCs Results in a Suitable Model for Assessing Aberrant Neurogenesis During Epileptogenesis

   I. Serum-free based cultured healthy hOTCs maintain the DG structure after ~3-4 weeks *in vitro*, as well as persisting neurogenesis in the DG.
   II. The blocking of $GABA_A$ receptors with PTX to induce epileptogenesis reduces neurogenesis and increases cell death.
   III. The identity of retrovirally-labeled newborn neurons is confirmed by DCX expression, confirming their neuroblast state.
   IV. PTX-induced epileptogenesis in hOTCs causes a decrease in the morphological complexity of the dendritic arbor of the differentiating newborn neurons.
   V. Alterations in dendritic spine density and growth are observed in epileptogenic conditions, showing a reduced number of spines but with larger heads.
   VI. Single neuron firing, pair-wise firing correlation, and circuit synchronizations increase during PTX-induced epileptogenesis, confirming the epileptogenic state of the model.

2. Inhibiting Newborn Neuron Activity during Epileptogenesis Confirms the Implication of Aberrant Neurogenesis in the Brain Circuitry

   I. Neuronal firing and network synchronization are recovered after inhibiting newborn neuron activity, suggesting the occurrence of aberrant neurogenesis a key factor in the dysfunction of the neural circuit.
   II. Newborn neuron activity inactivation shows a tendency for the preservation of high frequency oscillation patterns in epileptogenic hOTCs.

3. ATP Acts as a Mediator in the Induction of Aberrant Neurogenesis

I. Excessive extracellular ATP reduces neurogenesis and increases cell death as in epileptogenic conditions.
II. The morphological complexity of newborn neurons is also reduced when there is an excess of extracellular ATP.
III. Addition of ATP also alters dendritic spines in newborn neurons, decreasing their number and increasing their head size.

4. P2XR Inhibition Preserves Neurogenesis

I. Epilepsy-induced ROS generation is reduced after blocking P2XR with the antagonist TNP-ATP.
II. P2XR blockage with TNP-ATP during epileptogenesis recovers the control levels of neurogenesis and cell death, as well as dendritic arborization complexity and dendritic spine density and shape.
III. The time-lapse assessment of the morphological complexity of newborn neurons suggests an impairment in the growth of the dendritic arbor during the first weeks of their differentiation in epileptogenic conditions, which is recovered after P2XR inhibition.
IV. Blocking P2XR recovers the neuronal firing in the DG of epileptogenic hOTCs, as well as the activity of newborn neurons.
V. The number of GABAergic cells number is preserved in control levels when P2XR are inhibited in epileptogenic conditions.

5. ROS Inhibition Preserves Neurogenesis

I. CeO_2NPs-induced ROS inhibition during excessive extracellular ATP preserve the control level of cell death, neurogenesis and dendritic spine density and head features. Cell morphological complexity is, however, worsened.
II. ROS generation is increased in PTX-induced epileptogenic hOTCs, and can be reduced thanks to the ROS scavenging properties of CeO_2NPs.

III. ROS reduction by CeO_2NPs in epileptogenesis preserves neurogenesis and cell death levels, as well as the dendritic spine density and head features, while the dendritic arbor complexity decreases.

IV. Decrease of ROS generation by CeO_2NPs preserves the number of GABAergic cells in hOTCs.

6. GABAergic Interneurons are Impaired during Epileptogenesis

I. There is a loss of inhibitory neurons in epileptogenic hOTCs, as well as a specific reduction in the number of newborn neurons in GABAergic phase.

II. Blocking GABAergic release, thus disrupting interneuronal firing, dramatically impairs interneuron survival.

III. GABAergic newborn neuron survival does not depend on GABAergic input alone, but rather on the balance between glutamatergic and GABAergic input.

IV. Excessive extracellular GABA reduces the number of GABAergic cells.

V. Newborn neurons are transiently GABAergic in hOTCs, as it occurs in *in vivo*.

9. REFERENCES

REFERENCES

1. Altman J, Das GD. Autoradiographic and histological evidence of postnatal hippocampal neurogenesis in rats. *J Comp Neurol*. 1965;124(3):319-335. doi:10.1002/cne.901240303

2. Terreros-Roncal J, Moreno-Jiménez EP, Flor-García M, et al. Impact of neurodegenerative diseases on human adult hippocampal neurogenesis. *Science*. 2021;374(6571):1106-1113. doi:10.1126/science.abl5163

3. Boldrini M, Fulmore CA, Tartt AN, et al. Human Hippocampal Neurogenesis Persists throughout Aging. *Cell Stem Cell*. 2018;22(4):589-599.e5. doi:10.1016/j.stem.2018.03.015

4. Moreno-Jiménez EP, Terreros-Roncal J, Flor-García M, Rábano A, Llorens-Martín M. Evidences for Adult Hippocampal Neurogenesis in Humans. *J Neurosci Off J Soc Neurosci*. 2021;41(12):2541-2553. doi:10.1523/JNEUROSCI.0675-20.2020

5. Bonfanti L, Charvet CJ. Brain Plasticity in Humans and Model Systems: Advances, Challenges, and Future Directions. *Int J Mol Sci*. 2021;22(17):9358. doi:10.3390/ijms22179358

6. Sorrells SF, Paredes MF, Cebrian-Silla A, et al. Human hippocampal neurogenesis drops sharply in children to undetectable levels in adults. *Nature*. 2018;555(7696):377-381. doi:10.1038/nature25975

7. Ohira K. Regulation of Adult Neurogenesis in the Cerebral Cortex. *J Neurol Neuromedicine*. 2018;3(4). Accessed July 14, 2023. https://www.jneurology.com/articles/regulation-of-adult-neurogenesis-in-the-cerebral-cortex.html

8. Magavi SS, Leavitt BR, Macklis JD. Induction of neurogenesis in the neocortex of adult mice. *Nature*. 2000;405(6789):951-955. doi:10.1038/35016083

9. Inta D, Cameron HA, Gass P. New neurons in the adult striatum: from rodents to humans. *Trends Neurosci*. 2015;38(9):517-523. doi:10.1016/j.tins.2015.07.005

10. García-González D, Dumitru I, Zuccotti A, et al. Neurogenesis of medium spiny neurons in the nucleus accumbens continues into adulthood and is enhanced by pathological pain. *Mol Psychiatry*. 2021;26(9):4616-4632. doi:10.1038/s41380-020-0823-4

11. Zhao M, Momma S, Delfani K, et al. Evidence for neurogenesis in the adult mammalian substantia nigra. *Proc Natl Acad Sci U S A*. 2003;100(13):7925-7930. doi:10.1073/pnas.1131955100

12. Mourtzi T, Dimitrakopoulos D, Kakogiannis D, et al. Characterization of substantia nigra neurogenesis in homeostasis and dopaminergic degeneration: beneficial effects of the microneurotrophin BNN-20. *Stem Cell Res Ther*. 2021;12(1):335. doi:10.1186/s13287-021-02398-3

13. Bernier PJ, Bedard A, Vinet J, Levesque M, Parent A. Newly generated neurons in the amygdala and adjoining cortex of adult primates. *Proc Natl Acad Sci U S A*. 2002;99(17):11464-11469. doi:10.1073/pnas.172403999

14. Roeder SS, Burkardt P, Rost F, et al. Evidence for postnatal neurogenesis in the human amygdala. *Commun Biol*. 2022;5(1):1-8. doi:10.1038/s42003-022-03299-8

15. Bond AM, Ming GL, Song H. Adult Mammalian Neural Stem Cells and Neurogenesis: Five Decades Later. *Cell Stem Cell*. 2015;17(4):385-395. doi:10.1016/j.stem.2015.09.003

16. Rodríguez-Bodero A, Encinas-Pérez JM. Does the plasticity of neural stem cells and neurogenesis make them biosensors of disease and damage? *Front Neurosci*. 2022;16:977209. doi:10.3389/fnins.2022.977209

17. Avchalumov Y, Mandyam CD. Plasticity in the Hippocampus, Neurogenesis and Drugs of Abuse. *Brain Sci*. 2021;11(3):404. doi:10.3390/brainsci11030404

18. Stuchlik A. Dynamic learning and memory, synaptic plasticity and neurogenesis: an update. *Front Behav Neurosci*. 2014;8. Accessed July 18, 2023. https://www.frontiersin.org/articles/10.3389/fnbeh.2014.00106

19. Encinas JM, Sierra A. Neural stem cell deforestation as the main force driving the age-related decline in adult hippocampal neurogenesis. *Behav Brain Res*. 2012;227(2):433-439. doi:10.1016/j.bbr.2011.10.010

20. Sierra A, Encinas JM, Deudero JJP, et al. Microglia shape adult hippocampal neurogenesis through apoptosis-coupled phagocytosis. *Cell Stem Cell*. 2010;7(4):483-495. doi:10.1016/j.stem.2010.08.014

21. Bonaguidi MA, Wheeler MA, Shapiro JS, et al. In vivo clonal analysis reveals self-renewing and multipotent adult neural stem cell characteristics. *Cell*. 2011;145(7):1142-1155. doi:10.1016/j.cell.2011.05.024

22. Encinas JM, Michurina TV, Peunova N, et al. Division-Coupled Astrocytic Differentiation and Age-Related Depletion of Neural Stem Cells in the Adult Hippocampus. *Cell Stem Cell*. 2011;8(5):566-579. doi:10.1016/j.stem.2011.03.010

23. Steiner B, Kronenberg G, Jessberger S, Brandt MD, Reuter K, Kempermann G. Differential regulation of gliogenesis in the context of adult hippocampal neurogenesis in mice. *Glia*. 2004;46(1):41-52. doi:10.1002/glia.10337

24. Seri B, García-Verdugo JM, McEwen BS, Alvarez-Buylla A. Astrocytes give rise to new neurons in the adult mammalian hippocampus. *J Neurosci Off J Soc Neurosci*. 2001;21(18):7153-7160. doi:10.1523/JNEUROSCI.21-18-07153.2001

25. Encinas JM, Enikolopov G. Identifying and Quantitating Neural Stem and Progenitor Cells in the Adult Brain. In: *Methods in Cell Biology*. Vol 85. Elsevier; 2008:243-272. doi:10.1016/S0091-679X(08)85011-X

26. Kronenberg G, Reuter K, Steiner B, et al. Subpopulations of proliferating cells of the adult hippocampus respond differently to physiologic neurogenic stimuli. *J Comp Neurol*. 2003;467(4):455-463. doi:10.1002/cne.10945

27. Jessberger S, Toni N, Clemenson GD, Ray J, Gage FH. Directed differentiation of hippocampal stem/progenitor cells in the adult brain. *Nat Neurosci*. 2008;11(8):888-893. doi:10.1038/nn.2148

28. Vinci L, Ravarino A, Fanos V, et al. Immunohistochemical Markers of Neural Progenitor Cells in the Early Embryonic Human Cerebral Cortex. *Eur J Histochem EJH*. 2016;60(1):2563. doi:10.4081/ejh.2016.2563

29. Stergiopoulos A, Elkouris M, Politis PK. Prospero-related homeobox 1 (Prox1) at the crossroads of diverse pathways during adult neural fate specification. *Front Cell Neurosci*. 2015;8:454. doi:10.3389/fncel.2014.00454

30. Saito K, Koike T, Kawashima F, et al. Identification of NeuN immunopositive cells in the adult mouse subventricular zone. *J Comp Neurol*. 2018;526(12):1927-1942. doi:10.1002/cne.24463

31. Pataskar A, Jung J, Smialowski P, et al. NeuroD1 reprograms chromatin and transcription factor landscapes to induce the neuronal program. *EMBO J*. 2016;35(1):24-45. doi:10.15252/embj.201591206

32. Spampanato J, Sullivan RK, Turpin FR, Bartlett PF, Sah P. Properties of Doublecortin Expressing Neurons in the Adult Mouse Dentate Gyrus. *PLoS ONE*. 2012;7(9):e41029. doi:10.1371/journal.pone.0041029

33. Rao MS, Shetty AK. Efficacy of doublecortin as a marker to analyse the absolute number and dendritic growth of newly generated neurons in the adult dentate gyrus. *Eur J Neurosci*. 2004;19(2):234-246. doi:10.1111/j.0953-816x.2003.03123.x

34. Ayanlaja AA, Xiong Y, Gao Y, et al. Distinct Features of Doublecortin as a Marker of Neuronal Migration and Its Implications in Cancer Cell Mobility. *Front Mol Neurosci*. 2017;10. Accessed November 14, 2023. https://www.frontiersin.org/articles/10.3389/fnmol.2017.00199

35. Raponi E, Agenes F, Delphin C, et al. S100B expression defines a state in which GFAP-expressing cells lose their neural stem cell potential and acquire a more mature developmental stage. *Glia*. 2007;55(2):165-177. doi:10.1002/glia.20445

36. Cullen DK, Simon CM, LaPlaca MC. Strain rate-dependent induction of reactive astrogliosis and cell death in three-dimensional neuronal-astrocytic co-cultures. *Brain Res*. 2007;1158:103-115. doi:10.1016/j.brainres.2007.04.070

37. Ahmed AI, Shtaya AB, Zaben MJ, Owens EV, Kiecker C, Gray WP. Endogenous GFAP-Positive Neural Stem/Progenitor Cells in the Postnatal Mouse Cortex Are Activated following Traumatic Brain Injury. *J Neurotrauma*. 2012;29(5):828-842. doi:10.1089/neu.2011.1923

38. Bernal GM, Peterson DA. Phenotypic and gene expression modification with normal brain aging in GFAP-positive astrocytes and neural stem cells. *Aging Cell*. 2011;10(3):466-482. doi:10.1111/j.1474-9726.2011.00694.x

39. Kee N, Sivalingam S, Boonstra R, Wojtowicz JM. The utility of Ki-67 and BrdU as proliferative markers of adult neurogenesis. *J Neurosci Methods*. 2002;115(1):97-105. doi:10.1016/s0165-0270(02)00007-9

40. Hancock A, Priester C, Kidder E, Keith JR. Does 5-Bromo-2′-deoxyuridine (BrdU) Disrupt Cell Proliferation and Neuronal Maturation in the Adult Rat Hippocampus In Vivo? *Behav Brain Res*. 2009;199(2):218-221. doi:10.1016/j.bbr.2008.11.050

41. Kurian KM, Watson CJ, Wyllie AH. Retroviral vectors. *Mol Pathol*. 2000;53(4):173-176.

42. Gabriel R, Schmidt M, von Kalle C. Integration of retroviral vectors. *Curr Opin Immunol*. 2012;24(5):592-597. doi:10.1016/j.coi.2012.08.006

43. Coffin JM, Hughes SH, Varmus HE. Principles of Retroviral Vector Design. In: *Retroviruses*. Cold Spring Harbor Laboratory Press; 1997. Accessed November 14, 2023. https://www.ncbi.nlm.nih.gov/books/NBK19423/

44. Deng W, Saxe MD, Gallina IS, Gage FH. Adult-Born Hippocampal Dentate Granule Cells Undergoing Maturation Modulate Learning and Memory in the Brain. *J Neurosci*. 2009;29(43):13532-13542. doi:10.1523/JNEUROSCI.3362-09.2009

45. Saxe MD, Battaglia F, Wang JW, et al. Ablation of hippocampal neurogenesis impairs contextual fear conditioning and synaptic plasticity in the dentate gyrus. *Proc Natl Acad Sci U S A*. 2006;103(46):17501-17506. doi:10.1073/pnas.0607207103

46. Bergami M, Rimondini R, Santi S, Blum R, Götz M, Canossa M. Deletion of TrkB in adult progenitors alters newborn neuron integration into hippocampal circuits and increases anxiety-like behavior. *Proc Natl Acad Sci U S A*. 2008;105(40):15570-15575. doi:10.1073/pnas.0803702105

47. Kempermann G, Jessberger S, Steiner B, Kronenberg G. Milestones of neuronal development in the adult hippocampus. *Trends Neurosci*. 2004;27(8):447-452. doi:10.1016/j.tins.2004.05.013

48. Kempermann G. The neurogenic reserve hypothesis: what is adult hippocampal neurogenesis good for? *Trends Neurosci*. 2008;31(4):163-169. doi:10.1016/j.tins.2008.01.002

49. Henderson CE. Role of neurotrophic factors in neuronal development. *Curr Opin Neurobiol*. 1996;6(1):64-70. doi:10.1016/S0959-4388(96)80010-9

50. Kristiansen M, Ham J. Programmed cell death during neuronal development: the sympathetic neuron model. *Cell Death Differ*. 2014;21(7):1025-1035. doi:10.1038/cdd.2014.47

51. Zhu G, Sun C, Liu W. Effects of neurotrophin-3 on the differentiation of neural stem cells into neurons and oligodendrocytes. *Neural Regen Res*. 2012;7(19):1483-1487. doi:10.3969/j.issn.1673-5374.2012.19.006

52. Cohen-Cory S, Kidane AH, Shirkey NJ, Marshak S. Brain-Derived Neurotrophic Factor and the Development of Structural Neuronal Connectivity. *Dev Neurobiol*. 2010;70(5):271-288. doi:10.1002/dneu.20774

53. Bonafina A, Trinchero MF, Ríos AS, et al. GDNF and GFRα1 Are Required for Proper Integration of Adult-Born Hippocampal Neurons. *Cell Rep*. 2019;29(13):4308-4319.e4. doi:10.1016/j.celrep.2019.11.100

54. Ciucci F, Putignano E, Baroncelli L, Landi S, Berardi N, Maffei L. Insulin-Like Growth Factor 1 (IGF-1) Mediates the Effects of Enriched Environment (EE) on Visual Cortical Development. *PLoS ONE*. 2007;2(5):e475. doi:10.1371/journal.pone.0000475

55. Carrier M, Šimončičová E, St-Pierre MK, McKee C, Tremblay MÈ. Psychological Stress as a Risk Factor for Accelerated Cellular Aging and Cognitive Decline: The Involvement of Microglia-Neuron Crosstalk. *Front Mol Neurosci*. 2021;14. Accessed July 27, 2023. https://www.frontiersin.org/articles/10.3389/fnmol.2021.749737

56. Kettenmann H, Hanisch UK, Noda M, Verkhratsky A. Physiology of microglia. *Physiol Rev*. 2011;91(2):461-553. doi:10.1152/physrev.00011.2010

57. Tjalkens RB, Popichak KA, Kirkley KA. Inflammatory Activation of Microglia and Astrocytes in Manganese Neurotoxicity. *Adv Neurobiol*. 2017;18:159-181. doi:10.1007/978-3-319-60189-2_8

58. Abiega O, Beccari S, Diaz-Aparicio I, et al. Neuronal Hyperactivity Disturbs ATP Microgradients, Impairs Microglial Motility, and Reduces Phagocytic Receptor Expression Triggering Apoptosis/Microglial Phagocytosis Uncoupling. Barres BA, ed. *PLOS Biol*. 2016;14(5):e1002466. doi:10.1371/journal.pbio.1002466

59. Tremblay MÈ, Stevens B, Sierra A, Wake H, Bessis A, Nimmerjahn A. The role of microglia in the healthy brain. *J Neurosci Off J Soc Neurosci*. 2011;31(45):16064-16069. doi:10.1523/JNEUROSCI.4158-11.2011

60. Paolicelli RC, Bolasco G, Pagani F, et al. Synaptic pruning by microglia is necessary for normal brain development. *Science*. 2011;333(6048):1456-1458. doi:10.1126/science.1202529

61. Cunningham CL, Martínez-Cerdeño V, Noctor SC. Microglia Regulate the Number of Neural Precursor Cells in the Developing Cerebral Cortex. *J Neurosci*. 2013;33(10):4216-4233. doi:10.1523/JNEUROSCI.3441-12.2013

62. Harry GJ. Microglia During Development and Aging. *Pharmacol Ther*. 2013;139(3):313-326. doi:10.1016/j.pharmthera.2013.04.013

63. Sakai J. Core Concept: How synaptic pruning shapes neural wiring during development and, possibly, in disease. *Proc Natl Acad Sci U S A*. 2020;117(28):16096-16099. doi:10.1073/pnas.2010281117

64. Li Y, Du XF, Du JL. Resting microglia respond to and regulate neuronal activity in vivo. *Commun Integr Biol*. 2013;6(4):e24493. doi:10.4161/cib.24493

65. Nimmerjahn A, Kirchhoff F, Helmchen F. Resting microglial cells are highly dynamic surveillants of brain parenchyma in vivo. *Science*. 2005;308(5726):1314-1318. doi:10.1126/science.1110647

66. Cserép C, Schwarcz AD, Pósfai B, et al. Microglial control of neuronal development via somatic purinergic junctions. *Cell Rep*. 2022;40(12):111369. doi:10.1016/j.celrep.2022.111369

67. Chung WS, Clarke LE, Wang GX, et al. Astrocytes mediate synapse elimination through MEGF10 and MERTK pathways. *Nature*. 2013;504(7480):394-400. doi:10.1038/nature12776

68. Christopherson KS, Ullian EM, Stokes CCA, et al. Thrombospondins are astrocyte-secreted proteins that promote CNS synaptogenesis. *Cell*. 2005;120(3):421-433. doi:10.1016/j.cell.2004.12.020

69. Luo L, Guo K, Fan W, et al. Niche astrocytes promote the survival, proliferation and neuronal differentiation of co-transplanted neural stem cells following ischemic stroke in rats. *Exp Ther Med*. 2017;13(2):645-650. doi:10.3892/etm.2016.4016

70. Fulmer CG, VonDran MW, Stillman AA, Huang Y, Hempstead BL, Dreyfus CF. Astrocyte-Derived BDNF Supports Myelin Protein Synthesis after Cuprizone-Induced Demyelination. *J Neurosci*. 2014;34(24):8186-8196. doi:10.1523/JNEUROSCI.4267-13.2014

71. Chen W, He B, Tong W, Zeng J, Zheng P. Astrocytic Insulin-Like Growth Factor-1 Protects Neurons Against Excitotoxicity. *Front Cell Neurosci*. 2019;13:298. doi:10.3389/fncel.2019.00298

72. Van Wagoner NJ, Oh JW, Repovic P, Benveniste EN. Interleukin-6 (IL-6) Production by Astrocytes: Autocrine Regulation by IL-6 and the Soluble IL-6 Receptor. *J Neurosci*. 1999;19(13):5236-5244. doi:10.1523/JNEUROSCI.19-13-05236.1999

73. Kummer KK, Zeidler M, Kalpachidou T, Kress M. Role of IL-6 in the regulation of neuronal development, survival and function. *Cytokine*. 2021;144:155582. doi:10.1016/j.cyto.2021.155582

74. Chung WS, Allen NJ, Eroglu C. Astrocytes Control Synapse Formation, Function, and Elimination. *Cold Spring Harb Perspect Biol*. 2015;7(9):a020370. doi:10.1101/cshperspect.a020370

75. Meyers EA, Kessler JA. TGF-β Family Signaling in Neural and Neuronal Differentiation, Development, and Function. *Cold Spring Harb Perspect Biol*. 2017;9(8):a022244. doi:10.1101/cshperspect.a022244

76. Liu Y, Zhou LJ, Wang J, et al. TNF-α Differentially Regulates Synaptic Plasticity in the Hippocampus and Spinal Cord by Microglia-Dependent Mechanisms after Peripheral Nerve Injury. *J Neurosci Off J Soc Neurosci*. 2017;37(4):871-881. doi:10.1523/JNEUROSCI.2235-16.2016

77. Malarkey EB, Parpura V. Mechanisms of glutamate release from astrocytes. *Neurochem Int*. 2008;52(1-2):142-154. doi:10.1016/j.neuint.2007.06.005

78. Khakh BS, McCarthy KD. Astrocyte Calcium Signaling: From Observations to Functions and the Challenges Therein. *Cold Spring Harb Perspect Biol*. 2015;7(4):a020404. doi:10.1101/cshperspect.a020404

79. Cuellar-Santoyo AO, Ruiz-Rodríguez VM, Mares-Barbosa TB, et al. Revealing the contribution of astrocytes to glutamatergic neuronal transmission. *Front Cell Neurosci*. 2023;16:1037641. doi:10.3389/fncel.2022.1037641

80. Ren J, Bertrand PP. Purinergic receptors and synaptic transmission in enteric neurons. *Purinergic Signal*. 2008;4(3):255-266. doi:10.1007/s11302-007-9088-5

81. Sofroniew MV, Vinters HV. Astrocytes: biology and pathology. *Acta Neuropathol (Berl)*. 2010;119(1):7-35. doi:10.1007/s00401-009-0619-8

82. Daneman R, Prat A. The Blood–Brain Barrier. *Cold Spring Harb Perspect Biol*. 2015;7(1):a020412. doi:10.1101/cshperspect.a020412

83. MacVicar BA, Newman EA. Astrocyte Regulation of Blood Flow in the Brain. *Cold Spring Harb Perspect Biol*. 2015;7(5):a020388. doi:10.1101/cshperspect.a020388

84. Bradl M, Lassmann H. Oligodendrocytes: biology and pathology. *Acta Neuropathol (Berl)*. 2010;119(1):37-53. doi:10.1007/s00401-009-0601-5

85. Hughes EG, Stockton ME. Premyelinating Oligodendrocytes: Mechanisms Underlying Cell Survival and Integration. *Front Cell Dev Biol*. 2021;9:714169. doi:10.3389/fcell.2021.714169

86. Bechler ME, Swire M, ffrench-Constant C. Intrinsic and adaptive myelination—A sequential mechanism for smart wiring in the brain. *Dev Neurobiol*. 2018;78(2):68-79. doi:10.1002/dneu.22518

87. Das S, Basu A. Inflammation: a new candidate in modulating adult neurogenesis. *J Neurosci Res*. 2008;86(6):1199-1208. doi:10.1002/jnr.21585

88. Ekdahl CT, Claasen JH, Bonde S, Kokaia Z, Lindvall O. Inflammation is detrimental for neurogenesis in adult brain. *Proc Natl Acad Sci U S A*. 2003;100(23):13632-13637. doi:10.1073/pnas.2234031100

89. Monje ML, Toda H, Palmer TD. Inflammatory blockade restores adult hippocampal neurogenesis. *Science*. 2003;302(5651):1760-1765. doi:10.1126/science.1088417

90. Martín-Suárez S, Encinas JM. The future belongs to those who prepare for it today. *Cell Stem Cell*. 2021;28(5):783-785. doi:10.1016/j.stem.2021.04.014

91. Schouten M, Bielefeld P, Garcia-Corzo L, et al. Circadian glucocorticoid oscillations preserve a population of adult hippocampal neural stem cells in the aging brain. *Mol Psychiatry*. 2020;25(7):1382-1405. doi:10.1038/s41380-019-0440-2

92. Harris L, Rigo P, Stiehl T, et al. Coordinated changes in cellular behavior ensure the lifelong maintenance of the hippocampal stem cell population. *Cell Stem Cell*. 2021;28(5):863-876.e6. doi:10.1016/j.stem.2021.01.003

93. Bin Imtiaz MK, Jaeger BN, Bottes S, et al. Declining lamin B1 expression mediates age-dependent decreases of hippocampal stem cell activity. *Cell Stem Cell*. 2021;28(5):967-977.e8. doi:10.1016/j.stem.2021.01.015

94. Ibrayeva A, Bay M, Pu E, et al. Early stem cell aging in the mature brain. *Cell Stem Cell*. 2021;28(5):955-966.e7. doi:10.1016/j.stem.2021.03.018

95. Martín-Suárez S, Valero J, Muro-García T, Encinas JM. Phenotypical and functional heterogeneity of neural stem cells in the aged hippocampus. *Aging Cell*. 2019;18(4):e12958. doi:10.1111/acel.12958

96. Kalamakis G, Brüne D, Ravichandran S, et al. Quiescence Modulates Stem Cell Maintenance and Regenerative Capacity in the Aging Brain. *Cell*. 2019;176(6):1407-1419.e14. doi:10.1016/j.cell.2019.01.040

97. Adusumilli VS, Walker TL, Overall RW, et al. ROS Dynamics Delineate Functional States of Hippocampal Neural Stem Cells and Link to Their Activity-Dependent Exit from Quiescence. *Cell Stem Cell*. 2021;28(2):300-314.e6. doi:10.1016/j.stem.2020.10.019

98. Kohman RA, Rhodes JS. NEUROGENESIS, INFLAMMATION AND BEHAVIOR. *Brain Behav Immun*. 2013;27C:22-32. doi:10.1016/j.bbi.2012.09.003

99. Skaper SD, Giusti P, Facci L. Microglia and mast cells: two tracks on the road to neuroinflammation. *FASEB J Off Publ Fed Am Soc Exp Biol*. 2012;26(8):3103-3117. doi:10.1096/fj.11-197194

100. Paolicelli RC, Sierra A, Stevens B, et al. Microglia states and nomenclature: A field at its crossroads. *Neuron*. 2022;110(21):3458-3483. doi:10.1016/j.neuron.2022.10.020

101. Walton NM, Sutter BM, Laywell ED, et al. Microglia instruct subventricular zone neurogenesis. *Glia*. 2006;54(8):815-825. doi:10.1002/glia.20419

102. Sierra A, Paolicelli RC, Kettenmann H. Cien Años de Microglía: Milestones in a Century of Microglial Research. *Trends Neurosci*. 2019;42(11):778-792. doi:10.1016/j.tins.2019.09.004

103. Corredor RG, Goldberg JL. Electrical activity enhances neuronal survival and regeneration. *J Neural Eng*. 2009;6(5):055001. doi:10.1088/1741-2560/6/5/055001

104. Zhang SJ, Zou M, Lu L, et al. Nuclear Calcium Signaling Controls Expression of a Large Gene Pool: Identification of a Gene Program for Acquired Neuroprotection Induced by Synaptic Activity. *PLOS Genet*. 2009;5(8):e1000604. doi:10.1371/journal.pgen.1000604

105. Golbs A, Nimmervoll B, Sun JJ, Sava IE, Luhmann HJ. Control of programmed cell death by distinct electrical activity patterns. *Cereb Cortex N Y N 1991*. 2011;21(5):1192-1202. doi:10.1093/cercor/bhq200

106. Borzello M, Ramirez S, Treves A, et al. Assessments of dentate gyrus function: discoveries and debates. *Nat Rev Neurosci*. 2023;24(8):502-517. doi:10.1038/s41583-023-00710-z

107. van Dijk MT, Fenton AA. On How the Dentate Gyrus Contributes to Memory Discrimination. *Neuron*. 2018;98(4):832-845.e5. doi:10.1016/j.neuron.2018.04.018

108. Matsubara S, Matsuda T, Nakashima K. Regulation of Adult Mammalian Neural Stem Cells and Neurogenesis by Cell Extrinsic and Intrinsic Factors. *Cells*. 2021;10(5):1145. doi:10.3390/cells10051145

109. Myers CE, Scharfman HE. Pattern separation in the dentate gyrus: a role for the CA3 backprojection. *Hippocampus*. 2011;21(11):1190-1215. doi:10.1002/hipo.20828

110. Boulanger-Weill J, Sumbre G. Functional Integration of Newborn Neurons in the Zebrafish Optic Tectum. *Front Cell Dev Biol*. 2019;7:57. doi:10.3389/fcell.2019.00057

111. Zhang LI, Poo MM. Electrical activity and development of neural circuits. *Nat Neurosci*. 2001;4 Suppl:1207-1214. doi:10.1038/nn753

112. Spitzer NC. Electrical activity in early neuronal development. *Nature*. 2006;444(7120):707-712. doi:10.1038/nature05300

113. Basu SK, Pradhan S, du Plessis AJ, Ben-Ari Y, Limperopoulos C. GABA and glutamate in the preterm neonatal brain: In-vivo measurement by magnetic resonance spectroscopy. *NeuroImage*. 2021;238:118215. doi:10.1016/j.neuroimage.2021.118215

114. Andreae LC, Burrone J. Spontaneous Neurotransmitter Release Shapes Dendritic Arbors via Long-Range Activation of NMDA Receptors. *Cell Rep*. 2015;10(6):873-882. doi:10.1016/j.celrep.2015.01.032

115. Goldberg JL. Role of Electrical Activity in Promoting Neural Repair. *Neurosci Lett*. 2012;519(2):134-137. doi:10.1016/j.neulet.2012.02.003

116. Nelson PG, Brenneman DE. Electrical activity of neurons and development of the brain. *Trends Neurosci*. 1982;5:229-232. doi:10.1016/0166-2236(82)90133-3

117. Sultan S, Li L, Moss J, et al. Synaptic Integration of Adult-Born Hippocampal Neurons Is Locally Controlled by Astrocytes. *Neuron*. 2015;88(5):957-972. doi:10.1016/j.neuron.2015.10.037

118. Vivar C, Potter MC, Choi J, et al. Monosynaptic inputs to new neurons in the dentate gyrus. *Nat Commun*. 2012;3(1):1107. doi:10.1038/ncomms2101

119. Bressan C, Saghatelyan A. Intrinsic Mechanisms Regulating Neuronal Migration in the Postnatal Brain. *Front Cell Neurosci*. 2020;14:620379. doi:10.3389/fncel.2020.620379

120. Ge S, Sailor KA, Ming G li, Song H. Synaptic integration and plasticity of new neurons in the adult hippocampus. *J Physiol*. 2008;586(Pt 16):3759-3765. doi:10.1113/jphysiol.2008.155655

121. Brown J, Cooper-Kuhn CM, Kempermann G, et al. Enriched environment and physical activity stimulate hippocampal but not olfactory bulb neurogenesis. *Eur J Neurosci*. 2003;17(10):2042-2046. doi:10.1046/j.1460-9568.2003.02647.x

122. Han Y, Yuan M, Guo YS, Shen XY, Gao ZK, Bi X. The role of enriched environment in neural development and repair. *Front Cell Neurosci*. 2022;16:890666. doi:10.3389/fncel.2022.890666

123. Nithianantharajah J, Hannan AJ. Enriched environments, experience-dependent plasticity and disorders of the nervous system. *Nat Rev Neurosci*. 2006;7(9):697-709. doi:10.1038/nrn1970

124. Schoenfeld T, Gould E. Stress, Stress Hormones, and Adult Neurogenesis. *Exp Neurol*. 2012;233(1):12-21. doi:10.1016/j.expneurol.2011.01.008

125. Leschik J, Lutz B, Gentile A. Stress-Related Dysfunction of Adult Hippocampal Neurogenesis—An Attempt for Understanding Resilience? *Int J Mol Sci*. 2021;22(14):7339. doi:10.3390/ijms22147339

126. Fulda S, Gorman AM, Hori O, Samali A. Cellular Stress Responses: Cell Survival and Cell Death. *Int J Cell Biol*. 2010;2010:214074. doi:10.1155/2010/214074

127. Bachis A, Cruz MI, Nosheny RL, Mocchetti I. Chronic Unpredictable Stress Promotes Neuronal Apoptosis in the Cerebral Cortex. *Neurosci Lett*. 2008;442(2):104-108. doi:10.1016/j.neulet.2008.06.081

128. Woo H, Hong CJ, Jung S, Choe S, Yu SW. Chronic restraint stress induces hippocampal memory deficits by impairing insulin signaling. *Mol Brain*. 2018;11(1):37. doi:10.1186/s13041-018-0381-8

129. Yuan M, Guo YS, Han Y, Gao ZK, Shen XY, Bi X. Effectiveness and mechanisms of enriched environment in post-stroke cognitive impairment. *Behav Brain Res*. 2021;410:113357. doi:10.1016/j.bbr.2021.113357

130. Miguel PM, Pereira LO, Silveira PP, Meaney MJ. Early environmental influences on the development of children's brain structure and function. *Dev Med Child Neurol*. 2019;61(10):1127-1133. doi:10.1111/dmcn.14182

131. Tooley UA, Bassett DS, Mackey AP. Environmental influences on the pace of brain development. *Nat Rev Neurosci*. 2021;22(6):372-384. doi:10.1038/s41583-021-00457-5

132. O'Callaghan JP, Miller DB. Neuroinflammation Disorders Exacerbated by Environmental Stressors. *Metabolism*. 2019;100 Suppl:153951. doi:10.1016/j.metabol.2019.153951

133. Ávila-Villanueva M, Gómez-Ramírez J, Maestú F, Venero C, Ávila J, Fernández-Blázquez MA. The Role of Chronic Stress as a Trigger for the Alzheimer Disease Continuum. *Front Aging Neurosci*. 2020;12:561504. doi:10.3389/fnagi.2020.561504

134. Ngugi AK, Bottomley C, Kleinschmidt I, Sander JW, Newton CR. Estimation of the burden of active and life-time epilepsy: a meta-analytic approach. *Epilepsia*. 2010;51(5):883-890. doi:10.1111/j.1528-1167.2009.02481.x

135. Gaitatzis A, Carroll K, Majeed A, W Sander J. The epidemiology of the comorbidity of epilepsy in the general population. *Epilepsia*. 2004;45(12):1613-1622. doi:10.1111/j.0013-9580.2004.17504.x

136. McCormick DA. GABA as an inhibitory neurotransmitter in human cerebral cortex. *J Neurophysiol*. 1989;62(5):1018-1027. doi:10.1152/jn.1989.62.5.1018

137. Wittner L, Huberfeld G, Clémenceau S, et al. The epileptic human hippocampal cornu ammonis 2 region generates spontaneous interictal-like activity in vitro. *Brain J Neurol*. 2009;132(Pt 11):3032-3046. doi:10.1093/brain/awp238

138. Köhling R, Lücke A, Straub H, et al. Spontaneous sharp waves in human neocortical slices excised from epileptic patients. *Brain J Neurol*. 1998;121 (Pt 6):1073-1087. doi:10.1093/brain/121.6.1073

139. Stöber TM, Batulin D, Triesch J, Narayanan R, Jedlicka P. Degeneracy in epilepsy: multiple routes to hyperexcitable brain circuits and their repair. *Commun Biol*. 2023;6:479. doi:10.1038/s42003-023-04823-0

140. Ahl M, Avdic U, Skoug C, et al. Immune response in the eye following epileptic seizures. *J Neuroinflammation*. 2016;13(1):155. doi:10.1186/s12974-016-0618-3

141. Wahab A. Difficulties in Treatment and Management of Epilepsy and Challenges in New Drug Development. *Pharmaceuticals*. 2010;3(7):2090-2110. doi:10.3390/ph3072090

142. Schuele SU, Lüders HO. Intractable epilepsy: management and therapeutic alternatives. *Lancet Neurol*. 2008;7(6):514-524. doi:10.1016/S1474-4422(08)70108-X

143. Coppler PJ, Elmer J. Status Epilepticus: A Neurologic Emergency. *Crit Care Clin*. 2023;39(1):87-102. doi:10.1016/j.ccc.2022.07.006

144. Macdonald RL, Kelly KM. Antiepileptic Drug Mechanisms of Action. *Epilepsia*. 1995;36(s2):S2-S12. doi:10.1111/j.1528-1157.1995.tb05996.x

145. Engel J, Pitkänen A. Biomarkers for epileptogenesis and its treatment. *Neuropharmacology*. 2020;167:107735. doi:10.1016/j.neuropharm.2019.107735

146. Savage N. Epidemiology: The complexities of epilepsy. *Nature*. 2014;511(7508):S2-S3. doi:10.1038/511S2a

147. Scharfman HE. The neurobiology of epilepsy. *Curr Neurol Neurosci Rep*. 2007;7(4):348-354. doi:10.1007/s11910-007-0053-z

148. Fujikawa DG. The temporal evolution of neuronal damage from pilocarpine-induced status epilepticus - PubMed. Published 1996. Accessed February 6, 2023. https://pubmed.ncbi.nlm.nih.gov/8828581/

149. Fisher RS, Cross JH, French JA, et al. Operational classification of seizure types by the International League Against Epilepsy: Position Paper of the ILAE Commission for Classification and Terminology. *Epilepsia*. 2017;58(4):522-530. doi:10.1111/epi.13670

150. Müller CJ, Bankstahl M, Gröticke I, Löscher W. Pilocarpine vs. lithium-pilocarpine for induction of status epilepticus in mice: development of spontaneous seizures, behavioral alterations and neuronal damage. *Eur J Pharmacol*. 2009;619(1-3):15-24. doi:10.1016/j.ejphar.2009.07.020

151. Murphy GG. Spatial Learning and Memory—What's TLE Got To Do With It? *Epilepsy Curr*. 2013;13(1):26-29. doi:10.5698/1535-7511-13.1.26

152. Inostroza M, Cid E, Brotons-Mas J, et al. Hippocampal-dependent spatial memory in the water maze is preserved in an experimental model of temporal lobe epilepsy in rats. *PloS One*. 2011;6(7):e22372. doi:10.1371/journal.pone.0022372

153. Javidan M. Electroencephalography in Mesial Temporal Lobe Epilepsy: A Review. *Epilepsy Res Treat*. 2012;2012:637430. doi:10.1155/2012/637430

154. Herweg NA, Solomon EA, Kahana MJ. Theta oscillations in human memory. *Trends Cogn Sci*. 2020;24(3):208-227. doi:10.1016/j.tics.2019.12.006

155. Inostroza M, Brotons-Mas JR, Laurent F, Cid E, de la Prida LM. Specific impairment of "what-where-when" episodic-like memory in experimental models of temporal lobe epilepsy. *J*

Neurosci Off J Soc Neurosci. 2013;33(45):17749-17762. doi:10.1523/JNEUROSCI.0957-13.2013

156. Chauvière L, Rafrafi N, Thinus-Blanc C, Bartolomei F, Esclapez M, Bernard C. Early deficits in spatial memory and theta rhythm in experimental temporal lobe epilepsy. *J Neurosci Off J Soc Neurosci*. 2009;29(17):5402-5410. doi:10.1523/JNEUROSCI.4699-08.2009

157. Shuman T, Amendolara B, Golshani P. Theta Rhythmopathy as a Cause of Cognitive Disability in TLE. *Epilepsy Curr*. 2017;17(2):107-111. doi:10.5698/1535-7511.17.2.107

158. Laurent F, Brotons-Mas JR, Cid E, et al. Proximodistal structure of theta coordination in the dorsal hippocampus of epileptic rats. *J Neurosci Off J Soc Neurosci*. 2015;35(11):4760-4775. doi:10.1523/JNEUROSCI.4297-14.2015

159. McNaughton N, Ruan M, Woodnorth MA. Restoring theta-like rhythmicity in rats restores initial learning in the Morris water maze. *Hippocampus*. 2006;16(12):1102-1110. doi:10.1002/hipo.20235

160. Schlesiger MI, Cannova CC, Boublil BL, et al. The medial entorhinal cortex is necessary for temporal organization of hippocampal neuronal activity. *Nat Neurosci*. 2015;18(8):1123-1132. doi:10.1038/nn.4056

161. Cantero JL, Atienza M, Salas RM. Human alpha oscillations in wakefulness, drowsiness period, and REM sleep: different electroencephalographic phenomena within the alpha band. *Neurophysiol Clin Clin Neurophysiol*. 2002;32(1):54-71. doi:10.1016/s0987-7053(01)00289-1

162. Tang D, Hu L, Lei Y, Li H, Chen A. Frontal and occipital-parietal alpha oscillations distinguish between stimulus conflict and response conflict. *Front Hum Neurosci*. 2015;9. Accessed December 4, 2023. https://www.frontiersin.org/articles/10.3389/fnhum.2015.00433

163. Pyrzowski J, Siemiński M, Sarnowska A, Jedrzejczak J, Nyka WM. Interval analysis of interictal EEG: pathology of the alpha rhythm in focal epilepsy. *Sci Rep*. 2015;5(1):16230. doi:10.1038/srep16230

164. Larsson PG, Eeg-Olofsson O, Lantz G. Alpha frequency estimation in patients with epilepsy. *Clin EEG Neurosci*. 2012;43(2):97-104. doi:10.1177/1550059411433611

165. Li Z, Huang J, Wei W, et al. EEG Oscillatory Networks in Peri-Ictal Period of Absence Epilepsy. *Front Neurol*. 2022;13:825225. doi:10.3389/fneur.2022.825225

166. Gola M, Kamiński J, Brzezicka A, Wrobel A. Beta band oscillations as a correlate of alertness - Changes in aging. *Int J Psychophysiol Off J Int Organ Psychophysiol*. 2011;85:62-67. doi:10.1016/j.ijpsycho.2011.09.001

167. Davis NJ, Tomlinson SP, Morgan HM. The Role of Beta-Frequency Neural Oscillations in Motor Control. *J Neurosci*. 2012;32(2):403-404. doi:10.1523/JNEUROSCI.5106-11.2012

168. Fisher RS, Scharfman HE, deCurtis M. How Can We Identify Ictal and Interictal Abnormal Activity? *Adv Exp Med Biol*. 2014;813:3-23. doi:10.1007/978-94-017-8914-1_1

169. Barone J, Rossiter HE. Understanding the Role of Sensorimotor Beta Oscillations. *Front Syst Neurosci*. 2021;15:655886. doi:10.3389/fnsys.2021.655886

170. Kucewicz MT, Cimbalnik J, Matsumoto JY, et al. High frequency oscillations are associated with cognitive processing in human recognition memory. *Brain J Neurol*. 2014;137(Pt 8):2231-2244. doi:10.1093/brain/awu149

171. Guan A, Wang S, Huang A, et al. The role of gamma oscillations in central nervous system diseases: Mechanism and treatment. *Front Cell Neurosci*. 2022;16:962957. doi:10.3389/fncel.2022.962957

172. Catanese J, Carmichael JE, van der Meer MAA. Low- and high-gamma oscillations deviate in opposite directions from zero-phase synchrony in the limbic corticostriatal loop. *J Neurophysiol*. 2016;116(1):5-17. doi:10.1152/jn.00914.2015

173. Han C, Wang T, Yang Y, et al. Multiple gamma rhythms carry distinct spatial frequency information in primary visual cortex. *PLoS Biol*. 2021;19(12):e3001466. doi:10.1371/journal.pbio.3001466

174. van Vugt MK, Schulze-Bonhage A, Litt B, Brandt A, Kahana MJ. Hippocampal Gamma Oscillations Increase with Memory Load. *J Neurosci*. 2010;30(7):2694-2699. doi:10.1523/JNEUROSCI.0567-09.2010

175. Fernandez-Ruiz A, Sirota A, Lopes-dos-Santos V, Dupret D. Over and above frequency: Gamma oscillations as units of neural circuit operations. *Neuron*. 2023;111(7):936-953. doi:10.1016/j.neuron.2023.02.026

176. Medvedev AV, Murro AM, Meador KJ. Abnormal interictal gamma activity may manifest a seizure onset zone in temporal lobe epilepsy. *Int J Neural Syst*. 2011;21(2):103-114. doi:10.1142/S0129065711002699

177. Ren L, Kucewicz MT, Cimbalnik J, et al. Gamma oscillations precede interictal epileptiform spikes in the seizure onset zone. *Neurology*. 2015;84(6):602-608. doi:10.1212/WNL.0000000000001234

178. Aleman-Zapata A, van der Meij J, Genzel L. Disrupting ripples: Methods, results, and caveats in closed-loop approaches in rodents. *J Sleep Res*. 2022;31(6):e13532. doi:10.1111/jsr.13532

179. Worrell GA, Gardner AB, Stead SM, et al. High-frequency oscillations in human temporal lobe: simultaneous microwire and clinical macroelectrode recordings. *Brain J Neurol*. 2008;131(Pt 4):928-937. doi:10.1093/brain/awn006

180. Engel Jr J, Bragin A, Staba R, Mody I. High-frequency oscillations: What is normal and what is not? *Epilepsia*. 2009;50(4):598-604. doi:10.1111/j.1528-1167.2008.01917.x

181. Schönberger J, Huber C, Lachner-Piza D, et al. Interictal Fast Ripples Are Associated With the Seizure-Generating Lesion in Patients With Dual Pathology. *Front Neurol*. 2020;11. Accessed December 18, 2023. https://www.frontiersin.org/articles/10.3389/fneur.2020.573975

182. Ge S, Pradhan DA, Ming GL, Song H. GABA sets the tempo for activity-dependent adult neurogenesis. *Trends Neurosci*. 2007;30(1):1-8. doi:10.1016/j.tins.2006.11.001

183. Wieser HG, ILAE Commission on Neurosurgery of Epilepsy. ILAE Commission Report. Mesial temporal lobe epilepsy with hippocampal sclerosis. *Epilepsia*. 2004;45(6):695-714. doi:10.1111/j.0013-9580.2004.09004.x

184. Sierra A, Martín-Suárez S, Valcárcel-Martín R, et al. Neuronal Hyperactivity Accelerates Depletion of Neural Stem Cells and Impairs Hippocampal Neurogenesis. *Cell Stem Cell*. 2015;16(5):488-503. doi:10.1016/j.stem.2015.04.003

185. Hüttmann K, Sadgrove M, Wallraff A, et al. Seizures preferentially stimulate proliferation of radial glia-like astrocytes in the adult dentate gyrus: functional and immunocytochemical analysis. *Eur J Neurosci*. 2003;18(10):2769-2778. doi:10.1111/j.1460-9568.2003.03002.x

186. Segi-Nishida E, Warner-Schmidt JL, Duman RS. Electroconvulsive seizure and VEGF increase the proliferation of neural stem-like cells in rat hippocampus. *Proc Natl Acad Sci U S A*. 2008;105(32):11352-11357. doi:10.1073/pnas.0710858105

187. Pilz GA, Bottes S, Betizeau M, et al. Live imaging of neurogenesis in the adult mouse hippocampus. *Science*. 2018;359(6376):658-662. doi:10.1126/science.aao5056

188. Ammothumkandy A, Ravina K, Wolseley V, et al. Altered adult neurogenesis and gliogenesis in patients with mesial temporal lobe epilepsy. *Nat Neurosci*. 2022;25(4):493-503. doi:10.1038/s41593-022-01044-2

189. Muro-García T, Martín-Suárez S, Espinosa N, et al. Reactive Disruption of the Hippocampal Neurogenic Niche After Induction of Seizures by Injection of Kainic Acid in the Amygdala. *Front Cell Dev Biol*. 2019;7. Accessed February 6, 2023. https://www.frontiersin.org/articles/10.3389/fcell.2019.00158

190. Valcárcel-Martín R, Martín-Suárez S, Muro-García T, et al. Lysophosphatidic Acid Receptor 1 Specifically Labels Seizure-Induced Hippocampal Reactive Neural Stem Cells and Regulates Their Division. *Front Neurosci*. 2020;14:811. doi:10.3389/fnins.2020.00811

191. Abbracchio MP, Burnstock G, Verkhratsky A, Zimmermann H. Purinergic signalling in the nervous system: an overview. *Trends Neurosci*. 2009;32(1):19-29. doi:10.1016/j.tins.2008.10.001

192. Valero J, Mastrella G, Neiva I, SÃ¡nchez S, Malva JO. Long-term effects of an acute and systemic administration of LPS on adult neurogenesis and spatial memory. *Front Neurosci*. 2014;8. doi:10.3389/fnins.2014.00083

193. Wang S, Bolós M, Clark R, et al. Amyloid β precursor protein regulates neuron survival and maturation in the adult mouse brain. *Mol Cell Neurosci*. 2016;77:21-33. doi:10.1016/j.mcn.2016.09.002

194. Schouten M, Bielefeld P, Garcia-Corzo L, et al. Circadian glucocorticoid oscillations preserve a population of adult hippocampal neural stem cells in the aging brain. *Mol Psychiatry*. 2020;25(7):1382-1405. doi:10.1038/s41380-019-0440-2

195. Fitzsimons CP, van Hooijdonk LWA, Schouten M, et al. Knockdown of the glucocorticoid receptor alters functional integration of newborn neurons in the adult hippocampus and impairs fear-motivated behavior. *Mol Psychiatry*. 2013;18(9):993-1005. doi:10.1038/mp.2012.123

196. Duan X, Chang JH, Ge S, et al. Disrupted-In-Schizophrenia 1 regulates integration of newly generated neurons in the adult brain. *Cell*. 2007;130(6):1146-1158. doi:10.1016/j.cell.2007.07.010

197. Kerloch T, Farrugia F, Maître M, et al. The atypical Rho GTPase Rnd2 is critical for dentate granule neuron development and anxiety-like behavior during adult but not neonatal neurogenesis. Published online September 10, 2020:2020.09.10.290866. doi:10.1101/2020.09.10.290866

198. Llorens-Martín M, Fuster-Matanzo A, Teixeira CM, et al. GSK-3β overexpression causes reversible alterations on postsynaptic densities and dendritic morphology of hippocampal granule neurons in vivo. *Mol Psychiatry*. 2013;18(4):451-460. doi:10.1038/mp.2013.4

199. Parent JM, Yu TW, Leibowitz RT, Geschwind DH, Sloviter RS, Lowenstein DH. Dentate Granule Cell Neurogenesis Is Increased by Seizures and Contributes to Aberrant Network Reorganization in the Adult Rat Hippocampus. *J Neurosci*. 1997;17(10):3727-3738. doi:10.1523/JNEUROSCI.17-10-03727.1997

200. Wang. Selective neuronal vulnerability to oxidative stress in the brain. *Front Aging Neurosci*. Published online 2010. doi:10.3389/fnagi.2010.00012

201. Cho KO, Lybrand ZR, Ito N, et al. Aberrant hippocampal neurogenesis contributes to epilepsy and associated cognitive decline. *Nat Commun*. 2015;6(1):6606. doi:10.1038/ncomms7606

202. Parent JM, Elliott RC, Pleasure SJ, Barbaro NM, Lowenstein DH. Aberrant seizure-induced neurogenesis in experimental temporal lobe epilepsy. *Ann Neurol*. 2006;59(1):81-91. doi:10.1002/ana.20699

203. Varma P, Brulet R, Zhang L, Hsieh J. Targeting Seizure-Induced Neurogenesis in a Clinically Relevant Time Period Leads to Transient But Not Persistent Seizure Reduction. *J Neurosci*. 2019;39(35):7019-7028. doi:10.1523/JNEUROSCI.0920-19.2019

204. Lybrand ZR, Goswami S, Zhu J, et al. A critical period of neuronal activity results in aberrant neurogenesis rewiring hippocampal circuitry in a mouse model of epilepsy. *Nat Commun*. 2021;12(1):1423. doi:10.1038/s41467-021-21649-8

205. Jessberger S, Zhao C, Toni N, Clemenson GD, Li Y, Gage FH. Seizure-associated, aberrant neurogenesis in adult rats characterized with retrovirus-mediated cell labeling. *J Neurosci Off J Soc Neurosci*. 2007;27(35):9400-9407. doi:10.1523/JNEUROSCI.2002-07.2007

206. Mathern GW, Leiphart JL, De Vera A, et al. Seizures decrease postnatal neurogenesis and granule cell development in the human fascia dentata. *Epilepsia*. 2002;43 Suppl 5:68-73. doi:10.1046/j.1528-1157.43.s.5.28.x

207. Hattiangady B, Rao MS, Shetty AK. Chronic temporal lobe epilepsy is associated with severely declined dentate neurogenesis in the adult hippocampus. *Neurobiol Dis*. 2004;17(3):473-490. doi:10.1016/j.nbd.2004.08.008

208. Martín-Suárez S, Abiega O, Ricobaraza A, Hernandez-Alcoceba R, Encinas JM. Alterations of the Hippocampal Neurogenic Niche in a Mouse Model of Dravet Syndrome. *Front Cell Dev Biol*. 2020;8:654. doi:10.3389/fcell.2020.00654

209. Ibrahim S, Hu W, Wang X, Gao X, He C, Chen J. Traumatic Brain Injury Causes Aberrant Migration of Adult-Born Neurons in the Hippocampus. *Sci Rep*. 2016;6:21793. doi:10.1038/srep21793

210. Mohapel P, Ekdahl CT, Lindvall O. Status epilepticus severity influences the long-term outcome of neurogenesis in the adult dentate gyrus. *Neurobiol Dis*. 2004;15(2):196-205. doi:10.1016/j.nbd.2003.11.010

211. Kasahara Y, Nakashima H, Nakashima K. Seizure-induced hilar ectopic granule cells in the adult dentate gyrus. *Front Neurosci*. 2023;17. Accessed July 20, 2023. https://www.frontiersin.org/articles/10.3389/fnins.2023.1150283

212. Singh SP, LaSarge CL, An A, McAuliffe JJ, Danzer SC. Clonal Analysis of Newborn Hippocampal Dentate Granule Cell Proliferation and Development in Temporal Lobe Epilepsy. *eNeuro*. 2015;2(6). doi:10.1523/ENEURO.0087-15.2015

213. Overstreet-Wadiche LS, Bromberg DA, Bensen AL, Westbrook GL. Seizures Accelerate Functional Integration of Adult-Generated Granule Cells. *J Neurosci*. 2006;26(15):4095-4103. doi:10.1523/JNEUROSCI.5508-05.2006

214. Zhou QG, Nemes AD, Lee D, et al. Chemogenetic silencing of hippocampal neurons suppresses epileptic neural circuits. *J Clin Invest*. 2019;129(1):310-323. doi:10.1172/JCI95731

215. McCormick DA, Contreras D. On the cellular and network bases of epileptic seizures. *Annu Rev Physiol*. 2001;63:815-846. doi:10.1146/annurev.physiol.63.1.815

216. Teleanu RI, Niculescu AG, Roza E, Vladâcenco O, Grumezescu AM, Teleanu DM. Neurotransmitters—Key Factors in Neurological and Neurodegenerative Disorders of the Central Nervous System. *Int J Mol Sci*. 2022;23(11):5954. doi:10.3390/ijms23115954

217. Aromolaran KA, Goldstein PA. Ion channels and neuronal hyperexcitability in chemotherapy-induced peripheral neuropathy. *Mol Pain*. 2017;13:1744806917714693. doi:10.1177/1744806917714693

218. Tóth K, Hofer KT, Kandrács Á, et al. Hyperexcitability of the network contributes to synchronization processes in the human epileptic neocortex. *J Physiol*. 2018;596(2):317-342. doi:10.1113/JP275413

219. Sharma AK, Reams RY, Jordan WH, Miller MA, Thacker HL, Snyder PW. Mesial temporal lobe epilepsy: pathogenesis, induced rodent models and lesions. *Toxicol Pathol*. 2007;35(7):984-999. doi:10.1080/01926230701748305

220. Dudek FE. Loss of GABAergic Interneurons in Seizure-Induced Epileptogenesis—Two Decades Later and in a More Complex World. *Epilepsy Curr*. 2020;20(6 Suppl):70S-72S. doi:10.1177/1535759720960464

221. Bonfoco E, Krainc D, Ankarcrona M, Nicotera P, Lipton SA. Apoptosis and necrosis: two distinct events induced, respectively, by mild and intense insults with N-methyl-D-aspartate or nitric oxide/superoxide in cortical cell cultures. *Proc Natl Acad Sci U S A*. 1995;92(16):7162-7166.

222. Galván EJ, Gutiérrez R. Target-Dependent Compartmentalization of the Corelease of Glutamate and GABA from the Mossy Fibers. *J Neurosci*. 2017;37(3):701-714. doi:10.1523/JNEUROSCI.1915-16.2016

223. Rossi DJ, Oshima T, Attwell D. Glutamate release in severe brain ischaemia is mainly by reversed uptake. *Nature*. 2000;403(6767):316-321. doi:10.1038/35002090

224. Jaiswal MK, Keller BU. Cu/Zn superoxide dismutase typical for familial amyotrophic lateral sclerosis increases the vulnerability of mitochondria and perturbs Ca2+ homeostasis in SOD1G93A mice. *Mol Pharmacol*. 2009;75(3):478-489. doi:10.1124/mol.108.050831

225. Orrenius S, Zhivotovsky B, Nicotera P. Regulation of cell death: the calcium-apoptosis link. *Nat Rev Mol Cell Biol*. 2003;4(7):552-565. doi:10.1038/nrm1150

226. Gaoni Y, Chapman AG, Parvez N, Pook PC, Jane DE, Watkins JC. Synthesis, NMDA receptor antagonist activity, and anticonvulsant action of 1-aminocyclobutanecarboxylic acid derivatives. *J Med Chem*. 1994;37(25):4288-4296. doi:10.1021/jm00051a005

227. Gu N, Jackson J, Goutagny R, Lowe G, Manseau F, Williams S. NMDA-dependent phase synchronization between septal and temporal CA3 hippocampal networks. *J Neurosci Off J Soc Neurosci*. 2013;33(19):8276-8287. doi:10.1523/JNEUROSCI.0179-13.2013

228. Engel T, Brennan GP, Sanz-Rodriguez A, et al. A calcium-sensitive feed-forward loop regulating the expression of the ATP-gated purinergic P2X7 receptor via specificity protein 1 and microRNA-22. *Biochim Biophys Acta BBA - Mol Cell Res*. 2017;1864(2):255-266. doi:10.1016/j.bbamcr.2016.11.007

229. Khachaturian ZS. The role of calcium regulation in brain aging: reexamination of a hypothesis. *Aging Milan Italy*. 1989;1(1):17-34. doi:10.1007/BF03323872

230. Lukasiuk K, Becker AJ. Molecular biomarkers of epileptogenesis. *Neurother J Am Soc Exp Neurother*. 2014;11(2):319-323. doi:10.1007/s13311-014-0261-6

231. Sarkisian MR. Overview of the Current Animal Models for Human Seizure and Epileptic Disorders. *Epilepsy Behav EB*. 2001;2(3):201-216. doi:10.1006/ebeh.2001.0193

232. Williams PA, White AM, Clark S, et al. Development of spontaneous recurrent seizures after kainate-induced status epilepticus. *J Neurosci Off J Soc Neurosci*. 2009;29(7):2103-2112. doi:10.1523/JNEUROSCI.0980-08.2009

233. Löscher W. Animal models of epilepsy for the development of antiepileptogenic and disease-modifying drugs. A comparison of the pharmacology of kindling and post-status epilepticus models of temporal lobe epilepsy. *Epilepsy Res*. 2002;50(1-2):105-123. doi:10.1016/s0920-1211(02)00073-6

234. Humpel C. Organotypic brain slice cultures: A review. *Neuroscience*. 2015;305:86-98. doi:10.1016/j.neuroscience.2015.07.086

235. Gähwiler BH, Capogna M, Debanne D, McKinney RA, Thompson SM. Organotypic slice cultures: a technique has come of age. *Trends Neurosci*. 1997;20(10):471-477. doi:10.1016/s0166-2236(97)01122-3

236. Gilbride CJ. The hyperexcitability of dentate granule neurons in organotypic hippocampal slice cultures is due to reorganization of synaptic inputs in vitro. *Physiol Rep*. 2016;4(19):e12889. doi:10.14814/phy2.12889

237. De Simoni A, Griesinger CB, Edwards FA. Development of rat CA1 neurones in acute Versus organotypic slices: role of experience in synaptic morphology and activity. *J Physiol*. 2003;550(Pt 1):135-147. doi:10.1113/jphysiol.2003.039099

238. Noraberg J, Poulsen FR, Blaabjerg M, et al. Organotypic hippocampal slice cultures for studies of brain damage, neuroprotection and neurorepair. *Curr Drug Targets CNS Neurol Disord*. 2005;4(4):435-452. doi:10.2174/1568007054546108

239. Cho S, Wood A, Bowlby MR. Brain slices as models for neurodegenerative disease and screening platforms to identify novel therapeutics. *Curr Neuropharmacol*. 2007;5(1):19-33. doi:10.2174/157015907780077105

240. Trinka E, Höfler J, Zerbs A. Causes of status epilepticus. *Epilepsia*. 2012;53 Suppl 4:127-138. doi:10.1111/j.1528-1167.2012.03622.x

241. Brophy GM, Bell R, Claassen J, et al. Guidelines for the evaluation and management of status epilepticus. *Neurocrit Care*. 2012;17(1):3-23. doi:10.1007/s12028-012-9695-z

242. Wasterlain CG, Liu H, Naylor DE, et al. Molecular basis of self-sustaining seizures and pharmacoresistance during status epilepticus: The receptor trafficking hypothesis revisited. *Epilepsia*. 2009;50 Suppl 12:16-18. doi:10.1111/j.1528-1167.2009.02375.x

243. Martenson JS, Yamasaki T, Chaudhury NH, Albrecht D, Tomita S. Assembly rules for GABAA receptor complexes in the brain. *eLife*. 2017;6:e27443. doi:10.7554/eLife.27443

244. Sun MY, Ziolkowski L, Mennerick S. δ subunit-containing GABAA IPSCs are driven by both synaptic and diffusional GABA in mouse dentate granule neurons. *J Physiol*. 2020;598(6):1205-1221. doi:10.1113/JP279317

245. Ochoa JG, Dougherty M, Papanastassiou A, Gidal B, Mohamed I, Vossler DG. Treatment of Super-Refractory Status Epilepticus: A Review. *Epilepsy Curr*. 2021;21(6):405-415. doi:10.1177/1535759721999670

246. Heinemann U, Kann O, Schuchmann S. CHAPTER 4 - An Overview of In Vitro Seizure Models in Acute and Organotypic Slices. In: Pitkänen A, Schwartzkroin PA, Moshé SL, eds. *Models of Seizures and Epilepsy*. Academic Press; 2006:35-44. doi:10.1016/B978-012088554-1/50006-2

247. Malouf AT, Robbins CA, Schwartzkroin PA. Epileptiform activity in hippocampal slice cultures with normal inhibitory synaptic drive. *Neurosci Lett*. 1990;108(1-2):76-80. doi:10.1016/0304-3940(90)90709-i

248. Magalhães DM, Pereira N, Rombo DM, Beltrão-Cavacas C, Sebastião AM, Valente CA. Ex vivo model of epilepsy in organotypic slices—a new tool for drug screening. *J Neuroinflammation*. 2018;15(1):203. doi:10.1186/s12974-018-1225-2

249. Bausch S. Organotypic Hippocampal Slice Cultures as a Model of Limbic Epileptogenesis. In: *Neuromethods*. Vol 40. ; 2009:183-201. doi:10.1007/978-1-60327-263-6_11

250. Dyhrfjeld-Johnsen J, Berdichevsky Y, Swiercz W, Sabolek H, Staley KJ. Interictal spikes precede ictal discharges in an organotypic hippocampal slice culture model of epileptogenesis. *J Clin Neurophysiol Off Publ Am Electroencephalogr Soc*. 2010;27(6):418-424. doi:10.1097/WNP.0b013e3181fe0709

251. Albus K, Heinemann U, Kovács R. Network activity in hippocampal slice cultures revealed by long-term in vitro recordings. *J Neurosci Methods*. 2013;217(1-2):1-8. doi:10.1016/j.jneumeth.2013.04.014

252. Zipser B, Crain SM, Bornstein MB. Directly evoked paroxysmal' depolarizations of mouse hippocampal neurons in synaptically organized explants in long-term culture. *Brain Res*. 1973;60(2):489-495. doi:10.1016/0006-8993(73)90809-3

253. Schwartzkroin PA, Prince DA. Penicillin-induced epileptiform activity in the hippocampal in vitro prepatation. *Ann Neurol*. 1977;1(5):463-469. doi:10.1002/ana.410010510

254. Müller M, Gähwiler BH, Rietschin L, Thompson SM. Reversible loss of dendritic spines and altered excitability after chronic epilepsy in hippocampal slice cultures. *Proc Natl Acad Sci U S A*. 1993;90(1):257-261.

255. Thompson SM, Fortunato C, McKinney RA, Müller M, Gähwiler BH. Mechanisms underlying the neuropathological consequences of epileptic activity in the rat hippocampus in vitro. *J Comp Neurol*. 1996;372(4):515-528. doi:10.1002/(SICI)1096-9861(19960902)372:4<515::AID-CNE2>3.0.CO;2-7

256. Routbort MJ, Bausch SB, McNamara JO. Seizures, cell death, and mossy fiber sprouting in kainic acid-treated organotypic hippocampal cultures. *Neuroscience*. 1999;94(3):755-765. doi:10.1016/s0306-4522(99)00358-9

257. Drexel M, Romanov RA, Wood J, et al. Selective silencing of hippocampal parvalbumin interneurons induces development of recurrent spontaneous limbic seizures in mice. *J Neurosci*. 2017;37(34):8166-8179. doi:10.1523/jneurosci.3456-16.2017

258. Olsen RW. Picrotoxin-like channel blockers of GABAA receptors. *Proc Natl Acad Sci U S A*. 2006;103(16):6081-6082. doi:10.1073/pnas.0601121103

259. Cabezas C, Irinopoulou T, Cauli B, Poncer JC. Molecular and functional characterization of GAD67-expressing, newborn granule cells in mouse dentate gyrus. *Front Neural Circuits*. 2013;7. Accessed April 11, 2023. https://www.frontiersin.org/articles/10.3389/fncir.2013.00060

260. Rama S, Jensen TP, Rusakov DA. Glutamate Imaging Reveals Multiple Sites of Stochastic Release in the CA3 Giant Mossy Fiber Boutons. *Front Cell Neurosci*. 2019;13:243. doi:10.3389/fncel.2019.00243

261. Wu C, Sun D. GABA receptors in brain development, function, and injury. *Metab Brain Dis*. 2015;30(2):367-379. doi:10.1007/s11011-014-9560-1

262. Wang DD, Kriegstein AR. Defining the role of GABA in cortical development. *J Physiol*. 2009;587(Pt 9):1873-1879. doi:10.1113/jphysiol.2008.167635

263. Pelkey KA, Chittajallu R, Craig MT, Tricoire L, Wester JC, McBain CJ. Hippocampal GABAergic Inhibitory Interneurons. *Physiol Rev*. 2017;97(4):1619-1747. doi:10.1152/physrev.00007.2017

264. Wei D, Yang F, Wang Y, et al. Degeneration and regeneration of GABAergic interneurons in the dentate gyrus of adult mice in experimental models of epilepsy. *CNS Neurosci Ther*. 2015;21(1):52-60. doi:10.1111/cns.12330

265. Dudek FE, Shao LR. Loss of GABAergic Interneurons in Seizure-induced Epileptogenesis. *Epilepsy Curr*. 2003;3(5):159-161. doi:10.1046/j.1535-7597.2003.03503.x

266. Elahian B, Lado NE, Mankin E, et al. Low-voltage fast seizures in humans begin with increased interneuron firing. *Ann Neurol*. 2018;84(4):588-600. doi:10.1002/ana.25325

267. Trevelyan AJ, Sussillo D, Watson BO, Yuste R. Modular propagation of epileptiform activity: evidence for an inhibitory veto in neocortex. *J Neurosci Off J Soc Neurosci*. 2006;26(48):12447-12455. doi:10.1523/JNEUROSCI.2787-06.2006

268. Schevon CA, Weiss SA, McKhann G, et al. Evidence of an inhibitory restraint of seizure activity in humans. *Nat Commun*. 2012;3:1060. doi:10.1038/ncomms2056

269. Cardin JA. Inhibitory interneurons regulate temporal precision and correlations in cortical circuits. *Trends Neurosci*. 2018;41(10):689-700. doi:10.1016/j.tins.2018.07.015

270. Löscher W. Critical review of current animal models of seizures and epilepsy used in the discovery and development of new antiepileptic drugs. *Seizure*. 2011;20(5):359-368. doi:10.1016/j.seizure.2011.01.003

271. Avoli M, de Curtis M. GABAergic synchronization in the limbic system and its role in the generation of epileptiform activity. *Prog Neurobiol*. 2011;95(2):104-132. doi:10.1016/j.pneurobio.2011.07.003

272. Chang M, Dian JA, Dufour S, et al. Brief activation of GABAergic interneurons initiates the transition to ictal events through post-inhibitory rebound excitation. *Neurobiol Dis*. 2018;109(Pt A):102-116. doi:10.1016/j.nbd.2017.10.007

273. Huberfeld G, Menendez de la Prida L, Pallud J, et al. Glutamatergic pre-ictal discharges emerge at the transition to seizure in human epilepsy. *Nat Neurosci*. 2011;14(5):627-634. doi:10.1038/nn.2790

274. Tremblay R, Lee S, Rudy B. GABAergic interneurons in the neocortex: From cellular properties to circuits. *Neuron*. 2016;91(2):260-292. doi:10.1016/j.neuron.2016.06.033

275. Godoy LD, Prizon T, Rossignoli MT, Leite JP, Liberato JL. Parvalbumin Role in Epilepsy and Psychiatric Comorbidities: From Mechanism to Intervention. *Front Integr Neurosci*. 2022;16:765324. doi:10.3389/fnint.2022.765324

276. Dong HW, Hayar A, Ennis M. Activation of Group I Metabotropic Glutamate Receptors on Main Olfactory Bulb Granule Cells and Periglomerular Cells Enhances Synaptic Inhibition of Mitral Cells. *J Neurosci*. 2007;27(21):5654-5663. doi:10.1523/JNEUROSCI.5495-06.2007

277. Coulter DA, Carlson GC. Functional regulation of the dentate gyrus by GABA-mediated inhibition. *Prog Brain Res*. 2007;163:235-243. doi:10.1016/S0079-6123(07)63014-3

278. Frotscher M. Mossy fiber synapses on glutamate decarboxylase-immunoreactive neurons: evidence for feed-forward inhibition in the CA3 region of the hippocampus. *Exp Brain Res*. 1989;75(2):441-445. doi:10.1007/BF00247950

279. Sloviter RS, Dichter MA, Rachinsky TL, et al. Basal expression and induction of glutamate decarboxylase GABA in excitatory granule cells of the rat and monkey hippocampal dentate gyrus. *J Comp Neurol*. 1996;373(4):593-618. doi:10.1002/(SICI)1096-9861(19960930)373:4<593::AID-CNE8>3.0.CO;2-X

280. Gutiérrez R. The GABAergic phenotype of the "glutamatergic" granule cells of the dentate gyrus. *Prog Neurobiol*. 2003;71(5):337-358. doi:10.1016/j.pneurobio.2003.11.004

281. Gutiérrez R. The dual glutamatergic–GABAergic phenotype of hippocampal granule cells. *Trends Neurosci*. 2005;28(6):297-303. doi:10.1016/j.tins.2005.04.005

282. Altman J, Bayer SA. Migration and distribution of two populations of hippocampal granule cell precursors during the perinatal and postnatal periods. *J Comp Neurol*. 1990;301(3):365-381. doi:10.1002/cne.903010304

283. Crawford IL, Connor JD. Localization and release of glutamic acid in relation to the hippocampal mossy fibre pathway. *Nature*. 1973;244(5416):442-443. doi:10.1038/244442a0

284. Chabrol FP, Arenz A, Wiechert MT, Margrie TW, DiGregorio DA. Synaptic diversity enables temporal coding of coincident multi-sensory inputs in single neurons. *Nat Neurosci*. 2015;18(5):718-727. doi:10.1038/nn.3974

285. Malva JO, Silva AP, Cunha RA. Presynaptic Modulation Controlling Neuronal Excitability and Epileptogenesis: Role of Kainate, Adenosine and Neuropeptide Y Receptors. *Neurochem Res*. 2003;28(10):1501-1515. doi:10.1023/A:1025618324593

286. Koizumi S, Fujishita K, Inoue K. Regulation of cell-to-cell communication mediated by astrocytic ATP in the CNS. *Purinergic Signal*. 2005;1(3):211-217. doi:10.1007/s11302-005-6321-y

287. Zimmermann H. Extracellular ATP and other nucleotides-ubiquitous triggers of intercellular messenger release. *Purinergic Signal*. 2016;12(1):25-57. doi:10.1007/s11302-015-9483-2

288. Burnstock G. The past, present and future of purine nucleotides as signalling molecules. *Neuropharmacology*. 1997;36(9):1127-1139. doi:10.1016/s0028-3908(97)00125-1

289. Burnstock G, Verkhratsky A. Long-term (trophic) purinergic signalling: purinoceptors control cell proliferation, differentiation and death. *Cell Death Dis*. 2010;1(1):e9. doi:10.1038/cddis.2009.11

290. Abbracchio MP, Ceruti S, Langfelder R, Cattabeni F, Saffrey MJ, Burnstock G. Effects of ATP analogues and basic fibroblast growth factor on astroglial cell differentiation in primary

cultures of rat striatum. *Int J Dev Neurosci Off J Int Soc Dev Neurosci*. 1995;13(7):685-693. doi:10.1016/0736-5748(95)00064-x

291. Neary JT, Kang Y, Willoughby KA, Ellis EF. Activation of extracellular signal-regulated kinase by stretch-induced injury in astrocytes involves extracellular ATP and P2 purinergic receptors. *J Neurosci Off J Soc Neurosci*. 2003;23(6):2348-2356. doi:10.1523/JNEUROSCI.23-06-02348.2003

292. Franke H, Krügel U, Illes P. P2 receptors and neuronal injury. *Pflüg Arch*. 2006;452(5):622-644. doi:10.1007/s00424-006-0071-8

293. Choi DW. Glutamate neurotoxicity and diseases of the nervous system. *Neuron*. 1988;1(8):623-634. doi:10.1016/0896-6273(88)90162-6

294. Rodrigues RJ, Tomé AR, Cunha RA. ATP as a multi-target danger signal in the brain. *Front Neurosci*. 2015;9:148. doi:10.3389/fnins.2015.00148

295. Dunwiddie T v., Hoffer B j. ADENINE NUCLEOTIDES AND SYNAPTIC TRANSMISSION IN THE in vitro RAT HIPPOCAMPUS. *Br J Pharmacol*. 1980;69(1):59-68. doi:10.1111/j.1476-5381.1980.tb10883.x

296. Dragunow M, Goddard GV. Adenosine modulation of amygdala kindling. *Exp Neurol*. 1984;84(3):654-665. doi:10.1016/0014-4886(84)90212-7

297. Engel T, Gomez-Villafuertes R, Tanaka K, et al. Seizure suppression and neuroprotection by targeting the purinergic P2X7 receptor during status epilepticus in mice. *FASEB J*. 2012;26(4):1616-1628. doi:10.1096/fj.11-196089

298. Beamer E, Conte G, Engel T. ATP release during seizures – A critical evaluation of the evidence. *Brain Res Bull*. 2019;151:65-73. doi:10.1016/j.brainresbull.2018.12.021

299. Dossi E, Blauwblomme T, Moulard J, et al. Pannexin-1 channels contribute to seizure generation in human epileptic brain tissue and in a mouse model of epilepsy. *Sci Transl Med*. 2018;10(443):eaar3796. doi:10.1126/scitranslmed.aar3796

300. Wieraszko A, Seyfried TN. Increased amount of extracellular ATP in stimulated hippocampal slices of seizure prone mice. *Neurosci Lett*. 1989;106(3):287-293. doi:10.1016/0304-3940(89)90178-X

301. Sebastián-Serrano Á, Engel T, de Diego-García L, et al. Neurodevelopmental alterations and seizures developed by mouse model of infantile hypophosphatasia are associated with purinergic signalling deregulation. *Hum Mol Genet*. 2016;25(19):4143-4156. doi:10.1093/hmg/ddw248

302. Lutz PL, Kabler S. Release of adenosine and ATP in the brain of the freshwater turtle (Trachemys scripta) during long-term anoxia. *Brain Res*. 1997;769(2):281-286. doi:10.1016/s0006-8993(97)00719-1

303. Suadicani SO, Brosnan CF, Scemes E. P2X7 receptors mediate ATP release and amplification of astrocytic intercellular Ca2+ signaling. *J Neurosci*. 2006;26(5):1378-1385. doi:10.1523/JNEUROSCI.3902-05.2006

304. Burnstock G. An introduction to the roles of purinergic signalling in neurodegeneration, neuroprotection and neuroregeneration. *Neuropharmacology*. 2016;104:4-17. doi:10.1016/j.neuropharm.2015.05.031

305. Hattori M, Gouaux E. Molecular mechanism of ATP binding and ion channel activation in P2X receptors. *Nature*. 2012;485(7397):207-212. doi:10.1038/nature11010

306. Burnstock G. Purinergic signalling: Its unpopular beginning, its acceptance and its exciting future. *BioEssays News Rev Mol Cell Dev Biol*. 2012;34(3):218-225. doi:10.1002/bies.201100130

307. Hu Y, Gao Z. The role of purinergic signaling in microglial responses. *Stress Brain*. 2021;1(1):46-58. doi:10.26599/SAB.2020.9060005

308. Illes P, Khan TM, Rubini P. Neuronal P2X7 receptors revisited: Do they really exist? *J Neurosci*. 2017;37(30):7049-7062. doi:10.1523/JNEUROSCI.3103-16.2017

309. Miras-Portugal MT, Sebastián-Serrano Á, García L de D, Díaz-Hernández M. Neuronal P2X7 Receptor: Involvement in Neuronal Physiology and Pathology. *J Neurosci*. 2017;37(30):7063-7072. doi:10.1523/JNEUROSCI.3104-16.2017

310. Kaczmarek-Hajek K, Zhang J, Kopp R, et al. Re-evaluation of neuronal P2X7 expression using novel mouse models and a P2X7-specific nanobody. Swartz KJ, Aldrich R, eds. *eLife*. 2018;7:e36217. doi:10.7554/eLife.36217

311. Rozmer K, Gao P, Araújo MGL, et al. Pilocarpine-Induced Status Epilepticus Increases the Sensitivity of P2X7 and P2Y1 Receptors to Nucleotides at Neural Progenitor Cells of the Juvenile Rodent Hippocampus. *Cereb Cortex*. 2017;27(7):3568-3585. doi:10.1093/cercor/bhw178

312. Sperlágh B, Vizi ES, Wirkner K, Illes P. P2X7 receptors in the nervous system. *Prog Neurobiol*. 2006;78(6):327-346. doi:10.1016/j.pneurobio.2006.03.007

313. Leeson HC, Chan-Ling T, Lovelace MD, Brownlie JC, Gu BJ, Weible MW. P2X7 receptor signaling during adult hippocampal neurogenesis. *Neural Regen Res*. 2019;14(10):1684-1694. doi:10.4103/1673-5374.257510

314. Jimenez-Pacheco A, Mesuret G, Sanz-Rodriguez A, et al. Increased neocortical expression of the P2X7 receptor after status epilepticus and anticonvulsant effect of P2X7 receptor antagonist A-438079. *Epilepsia*. 2013;54(9):1551-1561. doi:10.1111/epi.12257

315. Barros-Barbosa AR, Fonseca AL, Guerra-Gomes S, et al. Up-regulation of P2X7 receptor–mediated inhibition of GABA uptake by nerve terminals of the human epileptic neocortex. *Epilepsia*. 2016;57(1):99-110. doi:10.1111/epi.13263

316. Solle M, Labasi J, Perregaux DG, et al. Altered Cytokine Production in Mice Lacking P2X7Receptors*. *J Biol Chem*. 2001;276(1):125-132. doi:10.1074/jbc.M006781200

317. Beamer E, Fischer W, Engel T. The ATP-gated P2X7 receptor as a target for the treatment of drug-resistant epilepsy. *Front Neurosci*. 2017;11(FEB). doi:10.3389/fnins.2017.00021

318. Arribas-Blázquez M, Olivos-Oré LA, Barahona MV, et al. Overexpression of P2X3 and P2X7 Receptors and TRPV1 Channels in Adrenomedullary Chromaffin Cells in a Rat Model of Neuropathic Pain. *Int J Mol Sci*. 2019;20(1):155. doi:10.3390/ijms20010155

319. Zhang PA, Sun Q, Li YC, et al. Overexpression of Purinergic P2X4 Receptors in Hippocampus Rescues Memory Impairment in Rats with Type 2 Diabetes. *Neurosci Bull*. 2020;36(7):719-732. doi:10.1007/s12264-020-00478-7

320. Territo PR, Zarrinmayeh H. P2X7 Receptors in Neurodegeneration: Potential Therapeutic Applications From Basic to Clinical Approaches. *Front Cell Neurosci*. 2021;15:617036. doi:10.3389/fncel.2021.617036

321. Boada-Romero E, Martinez J, Heckmann BL, Green DR. Mechanisms and physiology of the clearance of dead cells by efferocytosis. *Nat Rev Mol Cell Biol*. 2020;21(7):398-414. doi:10.1038/s41580-020-0232-1

322. Whitney NP, Eidem TM, Peng H, Huang Y, Zheng JC. Inflammation mediates varying effects in neurogenesis: relevance to the pathogenesis of brain injury and neurodegenerative disorders. *J Neurochem*. 2009;108(6):1343-1359. doi:10.1111/j.1471-4159.2009.05886.x

323. Hickey WF. Leukocyte traffic in the central nervous system: the participants and their roles. *Semin Immunol*. 1999;11(2):125-137. doi:10.1006/smim.1999.0168

324. Sefiani A, Geoffroy CG. The Potential Role of Inflammation in Modulating Endogenous Hippocampal Neurogenesis After Spinal Cord Injury. *Front Neurosci*. 2021;15:682259. doi:10.3389/fnins.2021.682259

325. Chugh D, Ali I, Bakochi A, Bahonjic E, Etholm L, Ekdahl CT. Alterations in Brain Inflammation, Synaptic Proteins, and Adult Hippocampal Neurogenesis during Epileptogenesis in Mice Lacking Synapsin2. *PloS One*. 2015;10(7):e0132366. doi:10.1371/journal.pone.0132366

326. Zonis S, Ljubimov VA, Mahgerefteh M, Pechnick RN, Wawrowsky K, Chesnokova V. p21Cip restrains hippocampal neurogenesis and protects neuronal progenitors from apoptosis during acute systemic inflammation. *Hippocampus*. 2013;23(12):1383-1394. doi:10.1002/hipo.22192

327. Ben-Hur T, Ben-Menachem O, Furer V, Einstein O, Mizrachi-Kol R, Grigoriadis N. Effects of proinflammatory cytokines on the growth, fate, and motility of multipotential neural precursor cells. *Mol Cell Neurosci*. 2003;24(3):623-631. doi:10.1016/s1044-7431(03)00218-5

328. Riley PA. Free radicals in biology: oxidative stress and the effects of ionizing radiation. *Int J Radiat Biol*. 1994;65(1):27-33. doi:10.1080/09553009414550041

329. del Río LA, Sandalio LM, Corpas FJ, Palma JM, Barroso JB. Reactive oxygen species and reactive nitrogen species in peroxisomes. Production, scavenging, and role in cell signaling. *Plant Physiol*. 2006;141(2):330-335. doi:10.1104/pp.106.078204

330. Accardi MV, Daniels BA, Brown PMGE, Fritschy JM, Tyagarajan SK, Bowie D. Mitochondrial reactive oxygen species regulate the strength of inhibitory GABA-mediated synaptic transmission. *Nat Commun*. 2014;5(1):3168. doi:10.1038/ncomms4168

331. Crane FL, Low H. Reactive oxygen species generation at the plasma membrane for antibody control. *Autoimmun Rev*. 2008;7(7):518-522. doi:10.1016/j.autrev.2008.04.004

332. Sharifi-Rad M, Anil Kumar NV, Zucca P, et al. Lifestyle, Oxidative Stress, and Antioxidants: Back and Forth in the Pathophysiology of Chronic Diseases. *Front Physiol*. 2020;11:694. doi:10.3389/fphys.2020.00694

333. Foyer CH, Lopez-Delgado H, Dat JF, Scott IM. Hydrogen peroxide- and glutathione-associated mechanisms of acclimatory stress tolerance and signalling. *Physiol Plant*. 1997;100(2):241-254. doi:10.1111/j.1399-3054.1997.tb04780.x

334. Bello-Medina PC, González-Franco DA, Vargas-Rodríguez I, Díaz-Cintra S. Oxidative stress, the immune response, synaptic plasticity, and cognition in transgenic models of Alzheimer disease. *Neurol Engl Ed*. 2022;37(8):682-690. doi:10.1016/j.nrleng.2019.06.008

335. Singh A, Kukreti R, Saso L, Kukreti S. Oxidative Stress: A Key Modulator in Neurodegenerative Diseases. *Mol Basel Switz*. 2019;24(8):1583. doi:10.3390/molecules24081583

336. Nimse SB, Pal D. Free radicals, natural antioxidants, and their reaction mechanisms. *RSC Adv*. 2015;5(35):27986-28006. doi:10.1039/C4RA13315C

337. Rock RB, Gekker G, Hu S, et al. Role of microglia in central nervous system infections. *Clin Microbiol Rev*. 2004;17(4):942-964, table of contents. doi:10.1128/CMR.17.4.942-964.2004

338. Biswas K, Alexander K, Francis MM. Reactive Oxygen Species: Angels and Demons in the Life of a Neuron. *NeuroSci*. 2022;3(1):130-145. doi:10.3390/neurosci3010011

339. Ray PD, Huang BW, Tsuji Y. Reactive oxygen species (ROS) homeostasis and redox regulation in cellular signaling. *Cell Signal*. 2012;24(5):981-990. doi:10.1016/j.cellsig.2012.01.008

340. Matarredona ER, Murillo-Carretero M, Moreno-López B, Estrada C. Role of nitric oxide in subventricular zone neurogenesis. *Brain Res Brain Res Rev*. 2005;49(2):355-366. doi:10.1016/j.brainresrev.2005.01.001

341. Matarredona ER, Murillo-Carretero M, Moreno-López B, Estrada C. Nitric oxide synthesis inhibition increases proliferation of neural precursors isolated from the postnatal mouse subventricular zone. *Brain Res*. 2004;995(2):274-284. doi:10.1016/j.brainres.2003.10.010

342. Heckert E, Karakoti A, Seal S, Self WT. The role of cerium redox state in the SOD mimetic activity of nanoceria. *Biomaterials*. 2008;29(18):2705-2709. doi:10.1016/j.biomaterials.2008.03.014

343. Esch F, Fabris S, Zhou L, et al. Electron Localization Determines Defect Formation on Ceria Substrates. *Science*. 2005;309(5735):752-755. doi:10.1126/science.1111568

344. DeCoteau W, Heckman KL, Estevez AY, et al. Cerium oxide nanoparticles with antioxidant properties ameliorate strength and prolong life in mouse model of amyotrophic lateral sclerosis. *Nanomedicine Nanotechnol Biol Med*. 2016;12(8):2311-2320. doi:10.1016/j.nano.2016.06.009

345. Hirst SM, Karakoti AS, Tyler RD, Sriranganathan N, Seal S, Reilly CM. Anti-inflammatory properties of cerium oxide nanoparticles. *Small Weinh Bergstr Ger*. 2009;5(24):2848-2856. doi:10.1002/smll.200901048

346. Karakoti AS, Monteiro-Riviere NA, Aggarwal R, et al. Nanoceria as Antioxidant: Synthesis and Biomedical Applications. *JOM Warrendale Pa 1989*. 2008;60(3):33-37. doi:10.1007/s11837-008-0029-8

347. Dowding JM, Dosani T, Kumar A, Seal S, Self WT. Cerium oxide nanoparticles scavenge nitric oxide radical (˙NO). *Chem Commun Camb Engl*. 2012;48(40):4896-4898. doi:10.1039/c2cc30485f

348. Estevez AY, Pritchard S, Harper K, et al. Neuroprotective mechanisms of cerium oxide nanoparticles in a mouse hippocampal brain slice model of ischemia. *Free Radic Biol Med*. 2011;51(6):1155-1163. doi:10.1016/j.freeradbiomed.2011.06.006

349. Song G, Cheng N, Zhang J, et al. Nanoscale Cerium Oxide: Synthesis, Biocatalytic Mechanism, and Applications. *Catalysts*. 2021;11(9):1123. doi:10.3390/catal11091123

350. Korsvik C, Patil S, Seal S, Self WT. Superoxide dismutase mimetic properties exhibited by vacancy engineered ceria nanoparticles. *Chem Commun Camb Engl*. 2007;(10):1056-1058. doi:10.1039/b615134e

351. Pirmohamed T, Dowding JM, Singh S, et al. Nanoceria exhibit redox state-dependent catalase mimetic activity. *Chem Commun Camb Engl*. 2010;46(16):2736-2738. doi:10.1039/b922024k

352. Gao L, Zhuang J, Nie L, et al. Intrinsic peroxidase-like activity of ferromagnetic nanoparticles. *Nat Nanotechnol*. 2007;2(9):577-583. doi:10.1038/nnano.2007.260

353. Zhang B, Huyan Y, Wang J, Wang W, Zhang Q, Zhang H. Synthesis of CeO2 nanoparticles with different morphologies and their properties as peroxidase mimic. *J Am Ceram Soc*. 2019;102(4):2218-2227. doi:10.1111/jace.16071

354. Niu J, Azfer A, Rogers LM, Wang X, Kolattukudy PE. Cardioprotective effects of cerium oxide nanoparticles in a transgenic murine model of cardiomyopathy. *Cardiovasc Res*. 2007;73(3):549-559. doi:10.1016/j.cardiores.2006.11.031

355. Asati A, Santra S, Kaittanis C, Perez JM. Surface-charge-dependent cell localization and cytotoxicity of cerium oxide nanoparticles. *ACS Nano*. 2010;4(9):5321-5331. doi:10.1021/nn100816s

356. Li M, Shi P, Xu C, Ren J, Qu X. Cerium oxide caged metal chelator: anti-aggregation and anti-oxidation integrated H2O2-responsive controlled drug release for potential Alzheimer's disease treatment. *Chem Sci*. 2013;4(6):2536-2542. doi:10.1039/C3SC50697E

357. Waldbaum S, Patel M. Mitochondrial dysfunction and oxidative stress: a contributing link to acquired epilepsy? *J Bioenerg Biomembr*. 2010;42(6):449-455. doi:10.1007/s10863-010-9320-9

358. Borowicz-Reutt KK, Czuczwar SJ. Role of oxidative stress in epileptogenesis and potential implications for therapy. *Pharmacol Rep*. 2020;72(5):1218-1226. doi:10.1007/s43440-020-00143-w

359. Folbergrová J, Kunz WS. Mitochondrial dysfunction in epilepsy. *Mitochondrion*. 2012;12(1):35-40. doi:10.1016/j.mito.2011.04.004

360. Beamer E, Kuchukulla M, Boison D, Engel T. ATP and adenosine—Two players in the control of seizures and epilepsy development. *Prog Neurobiol*. 2021;204:102105. doi:10.1016/j.pneurobio.2021.102105

361. Casals E, Gusta MF, Piella J, Casals G, Jiménez W, Puntes V. Intrinsic and Extrinsic Properties Affecting Innate Immune Responses to Nanoparticles: The Case of Cerium Oxide. *Front Immunol*. 2017;8:970. doi:10.3389/fimmu.2017.00970

362. Ernst L, Casals E, Italiani P, Boraschi D, Puntes V. The Interactions between Nanoparticles and the Innate Immune System from a Nanotechnologist Perspective. *Nanomaterials*. 2021;11(11):2991. doi:10.3390/nano11112991

363. Frantseva MV, Velazquez JLP, Hwang PA, Carlen PL. Free radical production correlates with cell death in an in vitro model of epilepsy: free radicals and neurodegeneration in seizures. *Eur J Neurosci*. 2000;12(4):1431-1439. doi:10.1046/j.1460-9568.2000.00016.x

364. Pestana RRF, Kinjo ER, Hernandes MS, Britto LRG. Reactive oxygen species generated by NADPH oxidase are involved in neurodegeneration in the pilocarpine model of temporal lobe epilepsy. *Neurosci Lett*. 2010;484(3):187-191. doi:10.1016/j.neulet.2010.08.049

365. Olowe R, Sandouka S, Saadi A, Shekh-Ahmad T. Approaches for Reactive Oxygen Species and Oxidative Stress Quantification in Epilepsy. *Antioxidants*. 2020;9(10):990. doi:10.3390/antiox9100990

366. Mignone JL, Kukekov V, Chiang AS, Steindler D, Enikolopov G. Neural stem and progenitor cells in nestin-GFP transgenic mice. *J Comp Neurol*. 2004;469(3):311-324. doi:10.1002/cne.10964

367. Tønnesen J, Sørensen AT, Deisseroth K, Lundberg C, Kokaia M. Optogenetic control of epileptiform activity. *Proc Natl Acad Sci U S A*. 2009;106(29):12162-12167. doi:10.1073/pnas.0901915106

368. Rytter A, Cronberg T, Asztély F, Nemali S, Wieloch T. Mouse Hippocampal Organotypic Tissue Cultures Exposed to In Vitro "Ischemia" Show Selective and Delayed CA1 Damage that is Aggravated by Glucose. *J Cereb Blood Flow Metab*. 2003;23(1):23-33. doi:10.1097/01.WCB.0000034361.37277.1B

369. Stoppini L, Buchs PA, Muller D. A simple method for organotypic cultures of nervous tissue. *J Neurosci Methods*. 1991;37(2):173-182. doi:10.1016/0165-0270(91)90128-M

370. Stoppini L, Buchs PA, Muller D. A simple method for organotypic cultures of nervous tissue. *J Neurosci Methods*. 1991;37(2):173-182. doi:10.1016/0165-0270(91)90128-m

371. Cronberg T, Rytter A, Asztély F, Söder A, Wieloch T. Glucose but not lactate in combination with acidosis aggravates ischemic neuronal death in vitro. *Stroke*. 2004;35(3):753-757. doi:10.1161/01.STR.0000117576.09512.32

372. Martín-Suárez S, Cortes JM, Bonifazi P. Blockage of STAT3 during epileptogenesis prevents GABAergic loss and imprinting of the epileptic state. *Brain J Neurol*. Published online February 24, 2023:awad055. doi:10.1093/brain/awad055

373. Encinas JM, Enikolopov G. Identifying and quantitating neural stem and progenitor cells in the adult brain. *Methods Cell Biol*. 2008;85:243-272. doi:10.1016/S0091-679X(08)85011-X

374. Schindelin J, Arganda-Carreras I, Frise E, et al. Fiji: an open-source platform for biological-image analysis. *Nat Methods*. 2012;9(7):676-682. doi:10.1038/nmeth.2019

375. Levet F, Tønnesen J, Nägerl UV, Sibarita JB. SpineJ: A software tool for quantitative analysis of nanoscale spine morphology. *Methods*. 2020;174:49-55. doi:10.1016/j.ymeth.2020.01.020

376. Dana H, Sun Y, Mohar B, et al. High-performance calcium sensors for imaging activity in neuronal populations and microcompartments. *Nat Methods*. 2019;16(7):649-657. doi:10.1038/s41592-019-0435-6

377. Kanner S, Goldin M, Galron R, Ben Jacob E, Bonifazi P, Barzilai A. Astrocytes restore connectivity and synchronization in dysfunctional cerebellar networks. *Proc Natl Acad Sci*. 2018;115(31):8025-8030. doi:10.1073/pnas.1718582115

378. Friedrich J, Paninski L. Fast Active Set Methods for Online Spike Inference from Calcium Imaging. In: *Advances in Neural Information Processing Systems*. Vol 29. Curran Associates, Inc.; 2016. Accessed February 9, 2023. https://papers.nips.cc/paper/2016/hash/fc2c7c47b918d0c2d792a719dfb602ef-Abstract.html

379. Huuskonen J, Suuronen T, Miettinen R, van Groen T, Salminen A. A refined in vitro model to study inflammatory responses in organotypic membrane culture of postnatal rat hippocampal slices. *J Neuroinflammation*. 2005;2(1):25. doi:10.1186/1742-2094-2-25

380. Köhr G, Heinemann U. Anticonvulsant effects of tetronic acid derivatives on picrotoxin induced epileptiform activity in rat hippocampal slices. *Neurosci Lett*. 1990;112(1):43-47. doi:10.1016/0304-3940(90)90319-5

381. Radley E, Akram A, Grubb BD, Gibson CL. Investigation of the mechanisms of progesterone protection following oxygen-glucose deprivation in organotypic hippocampal slice cultures. *Neurosci Lett*. 2012;506(1):131-135. doi:10.1016/j.neulet.2011.10.065

382. Kaneko K, Currin CB, Goff KM, et al. Developmentally regulated impairment of parvalbumin interneuron synaptic transmission in an experimental model of Dravet syndrome. *Cell Rep*. 2022;38(13):110580. doi:10.1016/j.celrep.2022.110580

383. Khan AA, Shekh-Ahmad T, Khalil A, Walker MC, Ali AB. Cannabidiol exerts antiepileptic effects by restoring hippocampal interneuron functions in a temporal lobe epilepsy model. *Br J Pharmacol*. 2018;175(11):2097-2115. doi:10.1111/bph.14202

384. Fuentes-Santamaría V, Cantos R, Alvarado JC, García-Atarés N, López DE. Morphologic and neurochemical abnormalities in the auditory brainstem of the genetically epilepsy-prone hamster (GPG/Vall). *Epilepsia*. 2005;46(7):1027-1045. doi:10.1111/j.1528-1167.2005.68104.x

385. Merlo GR, Zerega B, Paleari L, Trombino S, Mantero S, Levi G. Multiple functions of Dlx genes. *Int J Dev Biol*. 2000;44(6):619-626.

386. Musto AE, Rosencrans RF, Walker CP, et al. Dysfunctional epileptic neuronal circuits and dysmorphic dendritic spines are mitigated by platelet-activating factor receptor antagonism. *Sci Rep*. 2016;6(1):30298. doi:10.1038/srep30298

387. Swann JW, Al-Noori S, Jiang M, Lee CL. Spine loss and other dendritic abnormalities in epilepsy. *Hippocampus*. 2000;10(5):617-625. doi:10.1002/1098-1063(2000)10:5<617::AID-HIPO13>3.0.CO;2-R

388. Rossini L, De Santis D, Mauceri RR, et al. Dendritic pathology, spine loss and synaptic reorganization in human cortex from epilepsy patients. *Brain*. 2021;144(1):251-265. doi:10.1093/brain/awaa387

389. Murphy MP, Bayir H, Belousov V, et al. Guidelines for measuring reactive oxygen species and oxidative damage in cells and in vivo. *Nat Metab*. 2022;4(6):651-662. doi:10.1038/s42255-022-00591-z

390. Kalinich JF, Ramakrishnan N, McClain DE. The Antioxidant Trolox Enhances the Oxidation of 2′, 7′-Dichlorofluorescin to 2′, 7′-Dichlorofluorescein. *Free Radic Res*. 1997;26(1):37-47. doi:10.3109/10715769709097782

391. Safiulina VF, Fattorini G, Conti F, Cherubini E. GABAergic signaling at mossy fiber synapses in neonatal rat hippocampus. *J Neurosci Off J Soc Neurosci*. 2006;26(2):597-608. doi:10.1523/JNEUROSCI.4493-05.2006

392. Safiulina VF, Afzalov R, Khiroug L, Cherubini E, Giniatullin R. Reactive oxygen species mediate the potentiating effects of ATP on GABAergic synaptic transmission in the immature hippocampus. *J Biol Chem*. 2006;281(33):23464-23470. doi:10.1074/jbc.M601627200

393. Cobos I, Calcagnotto ME, Vilaythong AJ, et al. Mice lacking Dlx1 show subtype-specific loss of interneurons, reduced inhibition and epilepsy. *Nat Neurosci*. 2005;8(8):1059-1068. doi:10.1038/nn1499

394. Schonfeld-Dado E, Segal M. Activity Deprivation Induces Neuronal Cell Death: Mediation by Tissue-Type Plasminogen Activator. *PLOS ONE*. 2011;6(10):e25919. doi:10.1371/journal.pone.0025919

395. Fishbein I, Segal M. Miniature synaptic currents become neurotoxic to chronically silenced neurons. *Cereb Cortex N Y N 1991*. 2007;17(6):1292-1306. doi:10.1093/cercor/bhl037

396. Schonfeld-Dado E, Fishbein I, Segal M. Degeneration of cultured cortical neurons following prolonged inactivation: molecular mechanisms. *J Neurochem*. 2009;110(4):1203-1213. doi:10.1111/j.1471-4159.2009.06204.x

397. Schonfeld-Dado E, Segal M. Activity-dependent survival of neurons in culture: a model of slow neurodegeneration. *J Neural Transm Vienna Austria 1996*. 2009;116(11):1363-1369. doi:10.1007/s00702-009-0256-3

398. Huang ZZ, Wei JY, Ou-Yang HD, et al. mir-500-Mediated GAD67 Downregulation Contributes to Neuropathic Pain. *J Neurosci Off J Soc Neurosci*. 2016;36(23):6321-6331. doi:10.1523/JNEUROSCI.0646-16.2016

399. Couillard-Despres S, Winner B, Karl C, et al. Targeted transgene expression in neuronal precursors: watching young neurons in the old brain. *Eur J Neurosci*. 2006;24(6):1535-1545. doi:10.1111/j.1460-9568.2006.05039.x

400. Piens M, Muller M, Bodson M, Baudouin G, Plumier JC. A short upstream promoter region mediates transcriptional regulation of the mouse doublecortin gene in differentiating neurons. *BMC Neurosci*. 2010;11:64. doi:10.1186/1471-2202-11-64

401. Karl C, Couillard-Despres S, Prang P, et al. Neuronal precursor-specific activity of a human doublecortin regulatory sequence. *J Neurochem*. 2005;92(2):264-282. doi:10.1111/j.1471-4159.2004.02879.x

402. Overstreet LS, Hentges ST, Bumaschny VF, et al. A transgenic marker for newly born granule cells in dentate gyrus. *J Neurosci Off J Soc Neurosci*. 2004;24(13):3251-3259. doi:10.1523/JNEUROSCI.5173-03.2004

403. Navarro S, Soletto L, Puchol S, Rotllant J, Soengas JL, Cerdá-Reverter JM. 60 YEARS OF POMC: POMC: an evolutionary perspective. *J Mol Endocrinol*. 2016;56(4):T113-118. doi:10.1530/JME-15-0288

404. Panganiban G, Rubenstein JLR. Developmental functions of the Distal-less/Dlx homeobox genes. *Dev Camb Engl*. 2002;129(19):4371-4386. doi:10.1242/dev.129.19.4371

405. Alves S, Bode J, Bemelmans AP, von Kalle C, Cartier N, Tews B. Ultramicroscopy as a novel tool to unravel the tropism of AAV gene therapy vectors in the brain. *Sci Rep*. 2016;6:28272. doi:10.1038/srep28272

406. Danzer SC. Adult Neurogenesis in the Development of Epilepsy. *Epilepsy Curr*. 2019;19(5):316-320. doi:10.1177/1535759719868186

407. Parent JM, Yu TW, Leibowitz RT, Geschwind DH, Sloviter RS, Lowenstein DH. Dentate granule cell neurogenesis is increased by seizures and contributes to aberrant network reorganization in the adult rat hippocampus. *J Neurosci Off J Soc Neurosci*. 1997;17(10):3727-3738. doi:10.1523/JNEUROSCI.17-10-03727.1997

408. Parent JM, Janumpalli S, McNamara JO, Lowenstein DH. Increased dentate granule cell neurogenesis following amygdala kindling in the adult rat. *Neurosci Lett*. 1998;247(1):9-12. doi:10.1016/S0304-3940(98)00269-9

409. Stoppini L, Duport S, Corrèges P. A new extracellular multirecording system for electrophysiological studies: application to hippocampal organotypic cultures. *J Neurosci Methods*. 1997;72(1):23-33. doi:10.1016/S0165-0270(96)00151-3

410. Pretel S, Applegate CD, Piekut D. Apoptotic and necrotic cell death following kindling induced seizures. *Acta Histochem*. 1997;99(1):71-79. doi:10.1016/S0065-1281(97)80010-4

411. Dam AM. Epilepsy and Neuron Loss in the Hippocampus. *Epilepsia*. 1980;21(6):617-629. doi:10.1111/j.1528-1157.1980.tb04315.x

412. Henshall DC, Meldrum BS. Cell Death and Survival Mechanisms after Single and Repeated Brief Seizures. In: Noebels J, Avoli M, Rogawski M, Olsen R, Delgado-Escueta A, eds. *Jasper's Basic Mechanisms of the Epilepsies*. Oxford University Press; 2012:362-376. doi:10.1093/med/9780199746545.003.0028

413. Maher P, van Leyen K, Dey PN, Honrath B, Dolga A, Methner A. The role of Ca2+ in cell death caused by oxidative glutamate toxicity and ferroptosis. *Cell Calcium*. 2018;70:47-55. doi:10.1016/j.ceca.2017.05.007

414. Tashiro A, Sandler VM, Toni N, Zhao C, Gage FH. NMDA-receptor-mediated, cell-specific integration of new neurons in adult dentate gyrus. *Nature*. 2006;442(7105):929-933. doi:10.1038/nature05028

415. Platel JC, Dave KA, Gordon V, Lacar B, Rubio ME, Bordey A. NMDA receptors activated by subventricular zone astrocytic glutamate are critical for neuroblast survival prior to entering a synaptic network. *Neuron*. 2010;65(6):859-872. doi:10.1016/j.neuron.2010.03.009

416. Bathina S, Das UN. Brain-derived neurotrophic factor and its clinical implications. *Arch Med Sci AMS*. 2015;11(6):1164-1178. doi:10.5114/aoms.2015.56342

417. Li Y, Luikart BW, Birnbaum S, et al. TrkB regulates hippocampal neurogenesis and governs sensitivity to antidepressive treatment. *Neuron*. 2008;59(3):399-412. doi:10.1016/j.neuron.2008.06.023

418. Shetty AK, Zaman V, Shetty GA. Hippocampal neurotrophin levels in a kainate model of temporal lobe epilepsy: a lack of correlation between brain-derived neurotrophic factor content and progression of aberrant dentate mossy fiber sprouting. *J Neurochem*. 2003;87(1):147-159. doi:10.1046/j.1471-4159.2003.01979.x

419. McNamara JO, Scharfman HE. Temporal Lobe Epilepsy and the BDNF Receptor, TrkB. In: Noebels JL, Avoli M, Rogawski MA, Olsen RW, Delgado-Escueta AV, eds. *Jasper's Basic Mechanisms of the Epilepsies*. 4th ed. National Center for Biotechnology Information (US); 2012. Accessed November 22, 2023. http://www.ncbi.nlm.nih.gov/books/NBK98186/

420. Heinrich C, Lähteinen S, Suzuki F, et al. Increase in BDNF-mediated TrkB signaling promotes epileptogenesis in a mouse model of mesial temporal lobe epilepsy. *Neurobiol Dis*. 2011;42(1):35-47. doi:10.1016/j.nbd.2011.01.001

421. Kuhn HG, Dickinson-Anson H, Gage FH. Neurogenesis in the dentate gyrus of the adult rat: age-related decrease of neuronal progenitor proliferation. *J Neurosci Off J Soc Neurosci*. 1996;16(6):2027-2033. doi:10.1523/JNEUROSCI.16-06-02027.1996

422. Hattiangady B, Shetty AK. Implications of decreased hippocampal neurogenesis in chronic temporal lobe epilepsy. *Epilepsia*. 2008;49(0 5):26-41. doi:10.1111/j.1528-1167.2008.01635.x

423. Hattiangady B, Rao MS, Shetty AK. Chronic temporal lobe epilepsy is associated with severely declined dentate neurogenesis in the adult hippocampus. *Neurobiol Dis*. 2004;17(3):473-490. doi:10.1016/j.nbd.2004.08.008

424. Heinrich C, Nitta N, Flubacher A, et al. Reelin deficiency and displacement of mature neurons, but not neurogenesis, underlie the formation of granule cell dispersion in the epileptic hippocampus. *J Neurosci Off J Soc Neurosci*. 2006;26(17):4701-4713. doi:10.1523/JNEUROSCI.5516-05.2006

425. Nakagawa E, Aimi Y, Yasuhara O, et al. Enhancement of progenitor cell division in the dentate gyrus triggered by initial limbic seizures in rat models of epilepsy. *Epilepsia*. 2000;41(1):10-18. doi:10.1111/j.1528-1157.2000.tb01498.x

426. Scott BW, Wojtowicz JM, Burnham WM. Neurogenesis in the dentate gyrus of the rat following electroconvulsive shock seizures. *Exp Neurol*. 2000;165(2):231-236. doi:10.1006/exnr.2000.7458

427. Ekdahl CT, Mohapel P, Elmér E, Lindvall O. Caspase inhibitors increase short-term survival of progenitor-cell progeny in the adult rat dentate gyrus following status epilepticus. *Eur J Neurosci*. 2001;14(6):937-945. doi:10.1046/j.0953-816x.2001.01713.x

428. Scharfman HE, Sollas AL, Goodman JH. Spontaneous recurrent seizures after pilocarpine-induced status epilepticus activate calbindin-immunoreactive hilar cells of the rat dentate gyrus. *Neuroscience*. 2002;111(1):71-81. doi:10.1016/s0306-4522(01)00599-1

429. Kralic JE, Ledergerber DA, Fritschy JM. Disruption of the neurogenic potential of the dentate gyrus in a mouse model of temporal lobe epilepsy with focal seizures. *Eur J Neurosci*. 2005;22(8):1916-1927. doi:10.1111/j.1460-9568.2005.04386.x

430. Wasterlain CG. Developmental brain damage after chemically induced epileptic seizures. *Eur Neurol*. 1975;13(6):495-498. doi:10.1159/000114705

431. Shi XY, Wang JW, Lei GF, Sun RP. Morphological and behavioral consequences of recurrent seizures in neonatal rats are associated with glucocorticoid levels. *Neurosci Bull*. 2007;23(2):83-91. doi:10.1007/s12264-007-0012-3

432. Porter BE. Neurogenesis and epilepsy in the developing brain. *Epilepsia*. 2008;49(s5):50-54. doi:10.1111/j.1528-1167.2008.01637.x

433. Ekdahl CT, Zhu C, Bonde S, Bahr BA, Blomgren K, Lindvall O. Death mechanisms in status epilepticus-generated neurons and effects of additional seizures on their survival. *Neurobiol Dis*. 2003;14(3):513-523. doi:10.1016/j.nbd.2003.08.022

434. Uemori T, Toda K, Seki T. Seizure severity-dependent selective vulnerability of the granule cell layer and aberrant neurogenesis in the rat hippocampus. *Hippocampus*. 2017;27(10):1054-1068. doi:10.1002/hipo.22752

435. Schwarcz R, Witter MP. Memory impairment in temporal lobe epilepsy: the role of entorhinal lesions. *Epilepsy Res*. 2002;50(1-2):161-177. doi:10.1016/s0920-1211(02)00077-3

436. Kondziella D, Alvestad S, Vaaler A, Sonnewald U. Which clinical and experimental data link temporal lobe epilepsy with depression? *J Neurochem*. 2007;103(6):2136-2152. doi:10.1111/j.1471-4159.2007.04926.x

437. Rao MS, Hattiangady B, Reddy DS, Shetty AK. Hippocampal neurodegeneration, spontaneous seizures, and mossy fiber sprouting in the F344 rat model of temporal lobe epilepsy. *J Neurosci Res*. 2006;83(6):1088-1105. doi:10.1002/jnr.20802

438. Nishimura M, Owens J, Swann JW. Effects of chronic network hyperexcitability on the growth of hippocampal dendrites. *Neurobiol Dis*. 2008;29(2):267-277. doi:10.1016/j.nbd.2007.08.018

439. Casanova JR, Nishimura M, Le J, Lam TT, Swann JW. Rapid hippocampal network adaptation to recurring synchronous activity - a role for calcineurin. *Eur J Neurosci*. 2013;38(8):3115-3127. doi:10.1111/ejn.12315

440. Gupta J, Bromwich M, Radell J, et al. Restrained Dendritic Growth of Adult-Born Granule Cells Innervated by Transplanted Fetal GABAergic Interneurons in Mice with Temporal Lobe Epilepsy. *eneuro*. 2019;6(2):ENEURO.0110-18.2019. doi:10.1523/ENEURO.0110-18.2019

441. Zha X ming, Green SH, Dailey ME. Regulation of hippocampal synapse remodeling by epileptiform activity. *Mol Cell Neurosci*. 2005;29(4):494-506. doi:10.1016/j.mcn.2005.04.007

442. Freiman TM, Eismann-Schweimler J, Frotscher M. Granule cell dispersion in temporal lobe epilepsy is associated with changes in dendritic orientation and spine distribution. *Exp Neurol*. 2011;229(2):332-338. doi:10.1016/j.expneurol.2011.02.017

443. Chen P, Chen F, Wu Y, Zhou B. New Insights Into the Role of Aberrant Hippocampal Neurogenesis in Epilepsy. *Front Neurol*. 2021;12:727065. doi:10.3389/fneur.2021.727065

444. Thut G, Miniussi C, Gross J. The Functional Importance of Rhythmic Activity in the Brain. *Curr Biol*. 2012;22(16):R658-R663. doi:10.1016/j.cub.2012.06.061

445. Başar E. Brain oscillations in neuropsychiatric disease. *Dialogues Clin Neurosci*. 2013;15(3):291-300.

446. Park CJ, Hong SB. High Frequency Oscillations in Epilepsy: Detection Methods and Considerations in Clinical Application. *J Epilepsy Res*. 2019;9(1):1-13. doi:10.14581/jer.19001

447. Weiss SA, Fried I, Engel J Jr, et al. Fast ripples reflect increased excitability that primes epileptiform spikes. *Brain Commun*. 2023;5(5):fcad242. doi:10.1093/braincomms/fcad242

448. Burnstock G, Dale N. Purinergic signalling during development and ageing. *Purinergic Signal*. 2015;11(3):277-305. doi:10.1007/s11302-015-9452-9

449. Trautmann A. Extracellular ATP in the immune system: more than just a “danger signal.” *Sci Signal*. 2009;2(56):pe6. doi:10.1126/scisignal.256pe6

450. Myrtek D, Idzko M. Chemotactic activity of extracellular nucleotideson human immune cells. *Purinergic Signal*. 2007;3(1-2):5-11. doi:10.1007/s11302-006-9032-0

451. Sáez-Orellana F, Godoy PA, Bastidas CY, et al. ATP leakage induces P2XR activation and contributes to acute synaptic excitotoxicity induced by soluble oligomers of β-amyloid peptide in hippocampal neurons. *Neuropharmacology*. 2015;100. doi:10.1016/j.neuropharm.2015.04.005

452. Delarasse C, Gonnord P, Galante M, et al. Neural progenitor cell death is induced by extracellular ATP via ligation of P2X7 receptor. *J Neurochem*. 2009;109(3):846-857. doi:10.1111/j.1471-4159.2009.06008.x

453. Ohishi A, Keno Y, Marumiya A, et al. Expression level of P2X7 receptor is a determinant of ATP-induced death of mouse cultured neurons. *Neuroscience*. 2016;319:35-45. doi:10.1016/j.neuroscience.2016.01.048

454. Ruiz-Clavijo L, Martín-Suárez S. The differential response to neuronal hyperexcitation and neuroinflammation of the hippocampal neurogenic niche. *Front Neurosci*. 2023;17. Accessed December 19, 2023. https://www.frontiersin.org/articles/10.3389/fnins.2023.1186256

455. Di Virgilio F, Vultaggio-Poma V, Falzoni S, Giuliani AL. Extracellular ATP: A powerful inflammatory mediator in the central nervous system. *Neuropharmacology*. 2023;224:109333. doi:10.1016/j.neuropharm.2022.109333

456. Badimon A, Strasburger HJ, Ayata P, et al. Negative feedback control of neuronal activity by microglia. *Nature*. 2020;586(7829):417-423. doi:10.1038/s41586-020-2777-8

457. Lin SS, Tang Y, Illes P, Verkhratsky A. The Safeguarding Microglia: Central Role for P2Y12 Receptors. *Front Pharmacol*. 2021;11:627760. doi:10.3389/fphar.2020.627760

458. Eyo UB, Wu LJ. Bidirectional Microglia-Neuron Communication in the Healthy Brain. *Neural Plast*. 2013;2013:456857. doi:10.1155/2013/456857

459. Kondo S, Kohsaka S, Okabe S. Long-term changes of spine dynamics and microglia after transient peripheral immune response triggered by LPS in vivo. *Mol Brain*. 2011;4:27. doi:10.1186/1756-6606-4-27

460. Bitzer-Quintero OK, González-Burgos I. Immune System in the Brain: A Modulatory Role on Dendritic Spine Morphophysiology? *Neural Plast*. 2012;2012. doi:10.1155/2012/348642

461. Fiebich BL, Akter S, Akundi RS. The two-hit hypothesis for neuroinflammation: role of exogenous ATP in modulating inflammation in the brain. *Front Cell Neurosci*. 2014;8:260. doi:10.3389/fncel.2014.00260

462. Surprenant A, Rassendren F, Kawashima E, North RA, Buell G. The Cytolytic P2Z Receptor for Extracellular ATP Identified as a P2X Receptor (P2X7). *Science*. 1996;272(5262):735-738. doi:10.1126/science.272.5262.735

463. Srivastava P, Cronin CG, Scranton VL, Jacobson KA, Liang BT, Verma R. Neuroprotective and neuro-rehabilitative effects of acute purinergic receptor P2X4 (P2X4R) blockade after ischemic stroke. *Exp Neurol*. 2020;329:113308. doi:10.1016/j.expneurol.2020.113308

464. Kim JE, Kwak SE, Jo SM, Kang TC. Blockade of P2X receptor prevents astroglial death in the dentate gyrus following pilocarpine-induced status epilepticus. *Neurol Res*. 2009;31(9):982-988. doi:10.1179/174313209X389811

465. Timmers M, Ravenstijn P, Xi L, et al. Clinical pharmacokinetics, pharmacodynamics, safety, and tolerability of JNJ-54175446, a brain permeable P2X7 antagonist, in a randomised single-ascending dose study in healthy participants. *J Psychopharmacol Oxf Engl*. 2018;32(12):1341-1350. doi:10.1177/0269881118800067

466. Ribeiro T, Oliveira JT, Almeida FM, et al. Blockade of ATP P2X7 receptor enhances ischiatic nerve regeneration in mice following a crush injury. *Brain Res*. 2017;1669:69-78. doi:10.1016/j.brainres.2017.05.025

467. Jimenez-Pacheco A, Diaz-Hernandez M, Arribas-Blázquez M, et al. Transient P2X7 Receptor Antagonism Produces Lasting Reductions in Spontaneous Seizures and Gliosis in Experimental Temporal Lobe Epilepsy. *J Neurosci*. 2016;36(22):5920-5932. doi:10.1523/JNEUROSCI.4009-15.2016

468. Verma R, Cronin CG, Hudobenko J, Venna VR, McCullough LD, Liang BT. Deletion of the P2X4 receptor is neuroprotective acutely, but induces a depressive phenotype during recovery from ischemic stroke. *Brain Behav Immun*. 2017;66:302-312. doi:10.1016/j.bbi.2017.07.155

469. Wang XH, Xie X, Luo XG, Shang H, He ZY. Inhibiting purinergic P2X7 receptors with the antagonist brilliant blue G is neuroprotective in an intranigral lipopolysaccharide animal model of Parkinson's disease. *Mol Med Rep*. 2017;15(2):768-776. doi:10.3892/mmr.2016.6070

470. Ryu JK, McLarnon JG. Block of purinergic P2X(7) receptor is neuroprotective in an animal model of Alzheimer's disease. *Neuroreport*. 2008;19(17):1715-1719. doi:10.1097/WNR.0b013e3283179333

471. Cavaliere F, Amadio S, Dinkel K, Reymann KG, Volonté C. P2 receptor antagonist trinitrophenyl-adenosine-triphosphate protects hippocampus from oxygen and glucose deprivation cell death. *J Pharmacol Exp Ther*. 2007;323(1):70-77. doi:10.1124/jpet.106.119024

472. Liu X, Zhao Z, Ji R, et al. Inhibition of P2X7 receptors improves outcomes after traumatic brain injury in rats. *Purinergic Signal*. 2017;13(4):529-544. doi:10.1007/s11302-017-9579-y

473. Chu K, Yin B, Wang J, et al. Inhibition of P2X7 receptor ameliorates transient global cerebral ischemia/reperfusion injury via modulating inflammatory responses in the rat hippocampus. *J Neuroinflammation*. 2012;9(1):69. doi:10.1186/1742-2094-9-69

474. Puchałowicz K, Tarnowski M, Baranowska-Bosiacka I, Chlubek D, Dziedziejko V. P2X and P2Y Receptors—Role in the Pathophysiology of the Nervous System. *Int J Mol Sci*. 2014;15(12):23672-23704. doi:10.3390/ijms151223672

475. Kalus P, Müller TJ, Zuschratter W, Senitz D. The dendritic architecture of prefrontal pyramidal neurons in schizophrenic patients. *Neuroreport*. 2000;11(16):3621-3625. doi:10.1097/00001756-200011090-00044

476. Mut-Arbona P, Huang L, Baranyi M, et al. Dual Role of the P2X7 Receptor in Dendritic Outgrowth during Physiological and Pathological Brain Development. *J Neurosci*. 2023;43(7):1125-1142. doi:10.1523/JNEUROSCI.0805-22.2022

477. Zarrinmayeh H, Territo PR. Purinergic Receptors of the Central Nervous System: Biology, PET Ligands, and Their Applications. *Mol Imaging*. 2020;19:1536012120927609. doi:10.1177/1536012120927609

478. Dietz B, Jovanovic S, Wielsch B, Nerlich J, Rübsamen R, Milenkovic I. Purinergic modulation of neuronal activity in developing auditory brainstem. *J Neurosci Off J Soc Neurosci*. 2012;32(31):10699-10712. doi:10.1523/JNEUROSCI.0372-12.2012

479. Inoue K. Nociceptive signaling of P2X receptors in chronic pain states. *Purinergic Signal*. 2021;17(1):41-47. doi:10.1007/s11302-020-09743-w

480. Garré JM, Silva HM, Lafaille JJ, Yang G. P2X7 receptor inhibition ameliorates dendritic spine pathology and social behavioral deficits in Rett syndrome mice. *Nat Commun*. 2020;11. doi:10.1038/s41467-020-15590-5

481. Rodriguez-Alvarez N, Jimenez-Mateos EM, Engel T, et al. Effects of P2X7 receptor antagonists on hypoxia-induced neonatal seizures in mice. *Neuropharmacology*. 2017;116:351-363. doi:10.1016/j.neuropharm.2017.01.005

482. Mesuret G, Engel T, Hessel EV, et al. P2X7 Receptor Inhibition Interrupts the Progression of Seizures in Immature Rats and Reduces Hippocampal Damage. *CNS Neurosci Ther*. 2014;20(6):556-564. doi:10.1111/cns.12272

483. Menéndez Méndez A, Smith J, Engel T. Neonatal Seizures and Purinergic Signalling. *Int J Mol Sci*. 2020;21(21):7832. doi:10.3390/ijms21217832

484. Armstrong JN, Brust TB, Lewis RG, MacVicar BA. Activation of Presynaptic P2X7-Like Receptors Depresses Mossy Fiber–CA3 Synaptic Transmission through p38 Mitogen-Activated Protein Kinase. *J Neurosci*. 2002;22(14):5938-5945. doi:10.1523/JNEUROSCI.22-14-05938.2002

485. Cheng RD, Ren W, Luo BY, Ye XM. The role of purinergic receptors in neural repair and regeneration after spinal cord injury. *Neural Regen Res*. 2022;18(8):1684-1690. doi:10.4103/1673-5374.363186

486. Miras-Portugal MT, Ortega F, Gómez-Villafuertes R, Gualix J, Pérez-Sen R, Delicado EG. P2X7 receptors in the central nervous system. *Biochem Pharmacol*. 2021;187:114472. doi:10.1016/j.bcp.2021.114472

487. Nardou R, Ferrari DC, Ben-Ari Y. Mechanisms and effects of seizures in the immature brain. *Semin Fetal Neonatal Med*. 2013;18(4):175-184. doi:10.1016/j.siny.2013.02.003

488. Rakhade SN, Jensen FE. Epileptogenesis in the immature brain: emerging mechanisms. *Nat Rev Neurol*. 2009;5(7):380-391. doi:10.1038/nrneurol.2009.80

489. Schubert D, Dargusch R, Raitano J, Chan SW. Cerium and yttrium oxide nanoparticles are neuroprotective. *Biochem Biophys Res Commun*. 2006;342(1):86-91. doi:10.1016/j.bbrc.2006.01.129

490. Savio LEB, de Andrade Mello P, da Silva CG, Coutinho-Silva R. The P2X7 Receptor in Inflammatory Diseases: Angel or Demon? *Front Pharmacol*. 2018;9. Accessed September 20, 2023. https://www.frontiersin.org/articles/10.3389/fphar.2018.00052

491. Cruz CM, Rinna A, Forman HJ, Ventura ALM, Persechini PM, Ojcius DM. ATP Activates a Reactive Oxygen Species-dependent Oxidative Stress Response and Secretion of Proinflammatory Cytokines in Macrophages. *J Biol Chem*. 2007;282(5):2871-2879. doi:10.1074/jbc.M608083200

492. Cao SS, Kaufman RJ. Endoplasmic Reticulum Stress and Oxidative Stress in Cell Fate Decision and Human Disease. *Antioxid Redox Signal*. 2014;21(3):396-413. doi:10.1089/ars.2014.5851

493. Juan CA, Pérez de la Lastra JM, Plou FJ, Pérez-Lebeña E. The Chemistry of Reactive Oxygen Species (ROS) Revisited: Outlining Their Role in Biological Macromolecules (DNA, Lipids and Proteins) and Induced Pathologies. *Int J Mol Sci*. 2021;22(9):4642. doi:10.3390/ijms22094642

494. Yadav DK, Kumar S, Choi EH, Chaudhary S, Kim MH. Molecular dynamic simulations of oxidized skin lipid bilayer and permeability of reactive oxygen species. *Sci Rep*. 2019;9(1):4496. doi:10.1038/s41598-019-40913-y

495. Villalpando-Rodriguez GE, Gibson SB. Reactive Oxygen Species (ROS) Regulates Different Types of Cell Death by Acting as a Rheostat. *Oxid Med Cell Longev*. 2021;2021:9912436. doi:10.1155/2021/9912436

496. Su LJ, Zhang JH, Gomez H, et al. Reactive Oxygen Species-Induced Lipid Peroxidation in Apoptosis, Autophagy, and Ferroptosis. *Oxid Med Cell Longev*. 2019;2019:5080843. doi:10.1155/2019/5080843

497. Hu C, Fan L, Cen P, Chen E, Jiang Z, Li L. Energy Metabolism Plays a Critical Role in Stem Cell Maintenance and Differentiation. *Int J Mol Sci*. 2016;17(2):253. doi:10.3390/ijms17020253

498. Huang TT, Leu D, Zou Y. Oxidative stress and redox regulation on hippocampal-dependent cognitive functions. *Arch Biochem Biophys*. 2015;576:2-7. doi:10.1016/j.abb.2015.03.014

499. Oswald MCW, Garnham N, Sweeney ST, Landgraf M. Regulation of neuronal development and function by ROS. *Febs Lett*. 2018;592(5):679-691. doi:10.1002/1873-3468.12972

500. Pardillo-Díaz R, Pérez-García P, Castro C, Nunez-Abades P, Carrascal L. Oxidative Stress as a Potential Mechanism Underlying Membrane Hyperexcitability in Neurodegenerative Diseases. *Antioxidants*. 2022;11(8):1511. doi:10.3390/antiox11081511

501. Martinc B, Grabnar I, Vovk T. The Role of Reactive Species in Epileptogenesis and Influence of Antiepileptic Drug Therapy on Oxidative Stress. *Curr Neuropharmacol*. 2012;10(4):328-343. doi:10.2174/157015912804143504

502. Scheuer T, Endesfelder S, auf dem Brinke E, Bührer C, Schmitz T. Neonatal Oxidative Stress Impairs Cortical Synapse Formation and GABA Homeostasis in Parvalbumin-Expressing Interneurons. Rauf A, ed. *Oxid Med Cell Longev*. 2022;2022:1-12. doi:10.1155/2022/8469756

503. Abbah J, Vacher CM, Goldstein EZ, et al. Oxidative Stress-Induced Damage to the Developing Hippocampus Is Mediated by GSK3β. *J Neurosci*. 2022;42(24):4812-4827. doi:10.1523/JNEUROSCI.2389-21.2022

504. Dhawan S, Myers P, Bailey DMD, Ostrovsky AD, Evers JF, Landgraf M. Reactive Oxygen Species Mediate Activity-Regulated Dendritic Plasticity Through NADPH Oxidase and Aquaporin Regulation. *Front Cell Neurosci*. 2021;15:641802. doi:10.3389/fncel.2021.641802

505. Oswald MC, Brooks PS, Zwart MF, et al. Reactive oxygen species regulate activity-dependent neuronal plasticity in Drosophila. *eLife*. 2018;7:e39393. doi:10.7554/eLife.39393

506. Wilson C, Núñez MT, González-Billault C. Contribution of NADPH-oxidase to the establishment of hippocampal neuronal polarity in culture. *J Cell Sci*. Published online January 1, 2015:jcs.168567. doi:10.1242/jcs.168567

507. Dromard Y, Arango-Lievano M, Fontanaud P, Tricaud N, Jeanneteau F. Dual imaging of dendritic spines and mitochondria in vivo reveals hotspots of plasticity and metabolic adaptation to stress. *Neurobiol Stress*. 2021;15:100402. doi:10.1016/j.ynstr.2021.100402

508. Chakraborti A, Allen A, Allen B, Rosi S, Fike JR. Cranial Irradiation Alters Dendritic Spine Density and Morphology in the Hippocampus. Tofilon PJ, ed. *PLoS ONE*. 2012;7(7):e40844. doi:10.1371/journal.pone.0040844

509. Andrioli A, Alonso-Nanclares L, Arellano JI, DeFelipe J. Quantitative analysis of parvalbumin-immunoreactive cells in the human epileptic hippocampus. *Neuroscience*. 2007;149(1):131-143. doi:10.1016/j.neuroscience.2007.07.029

510. Szabadics J, Varga C, Brunner J, Chen K, Soltesz I. Granule Cells in the CA3 Area. *J Neurosci*. 2010;30(24):8296-8307. doi:10.1523/JNEUROSCI.5602-09.2010

511. Cheng X, Li Y, Huang Y, Feng X, Feng G, Xiong ZQ. Pulse labeling and long-term tracing of newborn neurons in the adult subgranular zone. *Cell Res*. 2011;21(2):338-349. doi:10.1038/cr.2010.141

512. Tang X, Jaenisch R, Sur M. The role of GABAergic signalling in neurodevelopmental disorders. *Nat Rev Neurosci*. 2021;22(5):290-307. doi:10.1038/s41583-021-00443-x